

**Defining the Role of Nuclear Hormone Receptors in Response to Radiation Therapy:  
Targeted Therapies for Radiosensitization in Androgen Receptor-Positive and  
Estrogen Receptor-Positive Breast Cancers**

by

Anna Renee Michmerhuizen

A dissertation submitted in partial fulfillment  
of the requirements for the degree of  
Doctor of Philosophy  
(Cellular and Molecular Biology)  
in the University of Michigan  
2022

Doctoral Committee:

Associate Professor Corey W. Speers, Chair  
Associate Professor J. Chad Brenner  
Professor Celina Klerer  
Professor Mats Ljungman  
Professor Lori J. Pierce

Anna Renee Michmerhuizen

[annamich@umich.edu](mailto:annamich@umich.edu)

ORCID iD: [0000-0003-1105-287X](https://orcid.org/0000-0003-1105-287X)

© Anna R. Michmerhuizen 2022

## **Acknowledgements**

Someone once said, “You never really travel alone, the world is full of friends waiting to get to know you.” My journey over the last five years as a graduate student at the University of Michigan, if nothing else, has proven just that. Despite the challenges, changes, unknowns, and roadblocks, for so many reasons, I never really traveled alone. For that, I’m immensely grateful for all of the strangers who became mentors and friends and walked with me each step of the way.

First, one of the biggest thank yous goes to Dr. Corey Speers. When I started graduate school, I only half-jokingly told myself and my family that I had to try it for a year and then I could decide whether I wanted to stay. As the first few months finished and I contemplated the next step in joining a lab, I remember very clearly wanting to join the Speers Lab, and now, almost five years later, I still think it was one of the best decisions I could have made. So, Corey, thank you for taking a chance on me and letting me join the lab even if at times I was too quiet, drank too much water, and often took too long to make decisions – especially the important ones, like choosing ice cream flavors! In all seriousness, I am so appreciative for your mentorship and your advice on all the important things in life – including Blue Bell Ice Cream, and BBQ, as well as all things related to career planning, radiation research, and hormone receptors. You have been so generous with your time, feedback, and patience. I will always look fondly on my time as a member of the Speers Squad at Michigan both for the little things – like sprinkle donuts in lab meetings, A-team meetings on Mondays, detailed discussions and photos of Michigan sporting events, and your continuous knowledge of everyone’s overly-specific bagel and cream

cheese preferences – as well as lab outings including curling, foot-golfing, cornhole, escape rooms, water skiing, lab BBQs, Whirly Ball, Tigers games, and countless of ice cream walks. More importantly though, thank you for believing in me and pushing me to succeed when I struggled to believe in myself and in the work that I was doing. I'll always count it as an extra honor and privilege to have trained in your lab at the University of Michigan, and a simple “thank you” doesn't feel adequate for the ways that you have encouraged and guided my personal and scientific development over the last 5 years. You've been one of the most influential people in my growth as a scientist, and I am so deeply grateful for your mentorship.

Next, to my thesis committee, I am so appreciative of the feedback that you have provided on my projects as well as the ways in which you have encouraged and supported me as a PhD student and as an individual. Dr. Chad Brenner, thank you for being willing to invest in both Nicole and I during our time in grad school. Your advice and suggestions have always strengthened the work that we've done and encouraged me to ask difficult, important questions. I'm so grateful for the ways that you have guided and supported my work and experience. Dr. Celina Kleer, thank you for sharing your knowledge of breast cancer and especially for your clinical perspective on my committee. I've benefitted so much from your experience and expertise. Dr. Mats Ljungman, thank you for your enthusiasm and willingness to collaborate for so many of our sequencing projects. I've benefitted greatly from your knowledge of DNA damage repair pathways and your feedback both in committee meetings and Radiation Oncology Bagel Talks, so thank you for being so willing to share your perspective and suggestions with me. Dr. Lori Pierce, thank you for being my clinical co-mentor for the Training Program in Translational Research and sharing so many valuable clinical insights with me. Your clinical expertise and perspective on hormone receptor biology in breast cancer is invaluable, I feel so

fortunate that you've been so willing to share your time and knowledge with me throughout my time in graduate school. Together, my expression of gratitude feels inadequate, yet I am sincerely grateful for the time that each of you has spent with me at thesis committee meetings and elsewhere listening, correcting, directing, and offering advice.

To the Cellular and Molecular Biology Program, thank you for investing in me both as a scientist and as a person. Thank you to Dr. Fuller and Dr. Puthenveedu for directing the program, and Pat Ocelnik, Jessica Kijek, Lauren Perl, and Carolyn Walsh for keeping everything running so smoothly. I'm also so appreciative of the Training Program in Translational Research (TPTR), and Dr. Lieberman and Dr. Nikolovska-Coleska, as directors of the program, and Laura Labut, as administrator, for the excellent training environment that I was able to be part of as a TPTR trainee. My interest in translational research was greatly enhanced by the opportunities you provided in TPTR, and I am so grateful for that. Thank you as well, to the Department of Radiation Oncology, and Dr. Ted Lawrence in particular, for supporting me and investing in me and the science I've done over the last five years. To Dr. Jimmy Rae, thank you for always being an enthusiastic supporter of my work and development by teaching classes, and writing many letters offering support in my pursuit of fellowships and opportunities. I'm thankful for the various methods of financial support that have allowed me to pursue graduate work at the University of Michigan, including T32 training grant support from the National Institutes of General Medicine (NIGMS, T32-GM007315 and T32-GM113900), and funding from the Rackham Graduate School (Predoctoral Fellowship, Graduate Student Travel Grants, Graduate Student Research Grants). I'm also grateful for travel grants and awards that I've received from the American Association in Cancer Research (AACR), and the support our lab has received from the Breast Cancer Research Foundation.

To the current and former members of the Speers Squad, this thesis wouldn't have been completed without your support. Each of you have quickly gone from strangers to friends, and I'm so grateful that we've had the last five years together – despite any and all challenges along the way! Thank you for being willing to work on my projects and letting me have the chance to contribute to yours. It has been a privilege to come to work alongside of each of you. To Andrea Pesch, thank you for being the best lab partner I've ever had. I'm so glad that, although we had never officially met, we both joined the Speers Lab (and Party Planning Committee!) in April of 2018. From late night timepoints during our first summer collecting RPPA pellets, submitting the PARP paper on the day of your prelim, frequent Disney singalongs in cell culture, surviving the monsoon that attempted to stop us from attending the 2021 ASTRO Annual Meeting in Chicago, exploring the Riverwalk in San Antonio at the 2021 SABCS, trivia nights at Haymaker, celebrating your wedding, and everything in between, thank you for helping make Ann Arbor home for me. I could always count on you on the hard days to make lab a little more fun, and I'm really grateful for your friendship. To Kari Wilder-Romans, our fearless lab manager, thank you for all that you have done to keep the lab afloat and the mice alive. Thanks for helping us stay out of trouble and get into it, in the perfect ratio. Thanks for letting me interrupt your quiet mornings alone in the lab and sharing lots of gold stars for even the smallest achievements. To Benjamin Chandler and Leah Moubadder, thank you for patiently teaching me all the basics I need to know as a cell biologist in the Department of Radiation Oncology when I joined the lab, and being integral members of the Speers Squad, showing me all the ropes. To Charlie Nino, Kassidy Jungles, and Breanna McBean, thank you for helping with experiments, offering ideas, and being great lab mates and friends. To Meilan Liu, thank you for all the technical help that you provided with experiments, and the ways in which you reminded me that graduate school is

so much larger than our scientific pursuits. Thanks for calling to check in on me when we were quarantined, sharing updates about your weekend gardening and cooking endeavors, and enthusiastically asking about my family. To Bryan Wharram and Dr. Shyam Nyati, thank you for your suggestions, advice, and support. To Lynn Lerner, thank you for working tirelessly with me to finish this thesis. The energy and excitement that you brought to the lab during my last year and a half were unmatched, and I can't wait to follow your own journey as a graduate student at UNC. Thank you to all the students I have had the opportunity to work with in the Speers Lab: Connor Ward, Yashmeet Kaur, Rachel Schwartz, Alexa Jelley, Tanner Ward, Amanda Zhang, Nicole Hirsh, Cassie Ritter, Meleah Cameron, Marlie Androsiglio, Caroline Bishop, and Maria Fields. I am so appreciative of the effort, commitment, and energy that each of you put into the work included in this thesis. You have been patient and teachable while I have learned so much from each of you, and I can't wait to see all that you accomplish. To the Speers Lab – past and present– more than your scientific contributions, though they were noteworthy, thank you for being friends who were willing to listen, offer support, share snacks, provide entertainment, and embrace the opportunity to have fun at work each day. It has been an extraordinary five years with each of you, and I'm so grateful to count you as friends.

To all the friends who have encouraged, supported, and challenged me during my time in graduate school, thank you. Thank you for rearranging your schedules during holiday breaks to get together when I was in Holland and thank you for being willing to make the trip to Ann Arbor on multiple occasions. To the friends who I have met here that have made Ann Arbor feel like home, thank you for going on walks, running through trails, making brunch, editing quarantine dance videos, organizing trips, exchanging cookies, hosting dinners, building bonfires, playing volleyball and softball, explaining board games, watching movies, eating ice

cream, and facilitating discussions. When our lives were disrupted because of COVID, thank you for pivoting online and scheduling Zoom and FaceTime calls, or sitting outside in all kinds of weather just so we could be together. I can't express my appreciation for the time that we shared, and the impact that you all have made on my life. To those who have mentored me in official or unofficial capacities – including Jan Sherard, Dianne Roeper, George and Mary Lindquist, Roger and Norma Verhey, and others at Ann Arbor Christian Reformed Church – I never imagined my time in graduate school would allow me to cross paths with such kind and wise people. Thank you for asking real, deep questions and taking the time to listen and help me process all the ups and downs of life and graduate school.

I'd be remiss not to acknowledge the ways in which my family has supported me throughout my time in graduate school. Thank you for listening to my endless stories, stressors, and struggles, and checking in when things were hard. I can't imagine doing this without your support and love. Nicole, thanks for being the best sister and resource I could have asked for during graduate school, especially as things shifted and changed and I wasn't sure how to move forward. Thanks for being patient with me, and letting me escape to your apartment, reminding me of home and the things that matter most. Seth, you have shown me the meaning of hard work, commitment, and what it looks like to not take life so seriously. Thanks for keeping me on my toes with your hilarious remarks, showing me how to use your van full of tools as you built the house at 6085 146<sup>th</sup> Street, and letting me tag along on all your adventures. Luke, I can't believe you've outgrown me now in height and skill in so many ways. Thank you for sharing your wit and fun personality with the world: it has been so special to watch you grow up. To my brothers, being your older sister is one of my greatest privileges and pleasures, and I'm ridiculously proud of the men that you are becoming. You teach me, challenge me, and inspire me in the ways that



you pursue the opportunities placed before you. To my parents – Dad, from a young age, you have taught me so many of the most important things in life, including the words to “The Victors” at my first Michigan football games, and now, I just wanted to say, it’s *still* great to be a Michigan Wolverine. Thanks for being a voice of reason and offering solutions even when I wasn’t always ready to hear them. I have learned so much from your example in the things that were said and left unsaid. You have offered invaluable advice at each stage of my life, and I’m so thankful for you. Mom, you’ve answered my phone calls at all hours of the day and listened to my stories more often than I deserve. Thank you for reminding me that everything works out when we take the time to pray about it. You are an inspiration to me in the way that you love the people around you, and I’m grateful for all the big and little ways you show up in my life. To all my family, thank you for believing in me, encouraging me, and reminding me of life outside of Ann Arbor and the home I have with you, especially on the days when I was too overwhelmed to see it for myself.

Finally, and most importantly, thank you to Jesus, who went before, walked alongside of, and brought me to the University of Michigan, and guided me through my time here. God, thank you for being for me and with me, and orchestrating my life and path to this moment in ways that I could not have begun to imagine for myself.

## Table of Contents

Acknowledgements.....	ii
List of Tables .....	xvii
List of Figures.....	xviii
Abstract.....	xxi
Chapter 1 : AR We There Yet? Understanding Androgen Receptor Signaling in Breast Cancer	1
1.1 Abstract .....	1
1.2 Introduction .....	2
1.3 Gene Expression and Hormone Receptor Function .....	3
1.4 Transcription Factor and Protein Interactions.....	4
1.4.1 AR and FOXA1 .....	4
1.4.2 AR and PTEN.....	6
1.4.3 Non-Genomic AR Functions.....	8
1.5 Cell Growth and Proliferation.....	9
1.5.1 Androgens and AR Splice Variants.....	9
1.5.2 Estrogen Influence on Androgen Signaling in Breast Cancer.....	11
1.6 DNA Damage Repair .....	16
1.7 Cell Cycle Regulation .....	17
1.8 Metastasis .....	20
1.9 Treatments targeting androgens and the androgen receptor for prostate and breast cancer	22
1.9.1 Androgen Deprivation Therapy.....	22
1.9.2 5 $\alpha$ -Reductase Inhibitors .....	22

1.9.3 CYP17-Lyase Inhibitors.....	23
1.9.4 Anti-Androgens .....	24
1.9.5 Second Generation Anti-Androgens.....	25
1.9.6 Novel Compounds .....	27
1.10 Combination Therapies .....	30
1.10.1 AR + Radiation Therapy .....	30
1.10.2 AR + PARP inhibitors .....	31
1.10.3 AR + CDK4/6 inhibitors .....	32
1.10.4 AR + PI3K inhibitors .....	33
1.11 Phase III Development of Anti-Androgen Treatments .....	34
1.12 Conclusion.....	34
1.13 Acknowledgements .....	35
1.14 Figure .....	36
1.15 Tables .....	37
1.16 References .....	45
Chapter 2 : Seviteronel a Novel CYP17 Lyase Inhibitor and Androgen Receptor Antagonist, Radiosensitizes AR-Positive Triple Negative Breast Cancer Cells.....	59
2.1 Abstract .....	59
2.2 Introduction .....	60
2.3 Materials and Methods .....	63
2.3.1 Cell Culture .....	63
2.3.2 Immunoblotting .....	64
2.3.3 Viability Assays.....	64
2.3.4 Clonogenic Survival Assays.....	65
2.3.5 $\gamma$ H2AX Immunofluorescence .....	65
2.3.6 Xenograft Study.....	66

2.3.7 Drug Information.....	66
2.3.8 ChIP-qPCR.....	66
2.3.9 Reverse Transcription and qPCR .....	67
2.3.10 siRNA and Transfections .....	67
2.3.11 Radiation.....	68
2.3.12 Statistical Analyses.....	68
2.4 Results .....	68
2.4.1 AR Inhibition Alone Does Not Affect Viability of AR+ TNBC Cells .....	68
2.4.2 AR knockdown and seviteronel treatment radiosensitizes AR+ TNBC cells in vitro .	69
2.4.3 Differential effects on AR targets with enzalutamide- or seviteronel-mediated inhibition.....	71
2.4.4 AR inhibition results in persistence of dsDNA breaks after radiation .....	72
2.4.5 Seviteronel treatment in combination with radiation delays growth of xenograft tumors .....	73
2.4.6 AR binding at DNA damage response genes is enhanced with RT and seviteronel-mediated AR inhibition .....	73
2.5 Discussion .....	75
2.6 Acknowledgements .....	77
2.7 Figures.....	78
2.8 Tables .....	87
2.9 References .....	89
Chapter 3 : Multiomics Analysis to Uncover the Mechanism of Radiosensitization of Androgen Receptor-Positive Triple Negative Breast Cancers With AR Inhibition .....	93
3.1 Abstract .....	93
3.2 Introduction .....	94
3.3 Methods.....	96
3.3.1 Cell Culture .....	96

3.3.2 Proteomic Analysis.....	96
3.3.3 Western Blotting.....	97
3.3.4 RNA-sequencing .....	98
3.3.5 Drugs .....	99
3.3.6 Irradiation .....	99
3.4 Results .....	99
3.4.1 Nuclear localization of AR is blocked with pharmacologic AR inhibitors.....	99
3.4.2 AR localizes to the nucleus following radiation treatment .....	100
3.4.3 Transcriptomic Analyses in AR+ TNBC cell lines .....	101
3.4.4 Proteomic Analyses in AR+ TNBC cell lines .....	103
3.4.5 Validation of transcriptomic and proteomic findings in AR+ TNBC cells.....	106
3.5 Discussion .....	107
3.6 Acknowledgements .....	109
3.7 Figures.....	111
3.8 Tables .....	124
3.9 References .....	129
Chapter 4 : Estrogen Receptor Inhibition Mediates Radiosensitization of ER-Positive Breast Cancer Models .....	132
4.1 Abstract .....	132
4.2 Introduction.....	133
4.3 Results .....	135
4.3.1 Short term ER inhibition or degradation radiosensitizes ER+ breast cancer cells.....	135
4.3.2 ER-targeting therapies inhibit dsDNA break repair through NHEJ.....	138
4.3.3 Cell-cycle arrest is induced with radiation or short-term endocrine therapy treatment .....	140
4.3.4 Apoptosis is not induced with endocrine therapies in combination with radiation....	142

4.3.5 Endocrine therapies induce senescence alone and in combination with radiation therapy .....	143
4.3.6 Tamoxifen is synergistic with radiation in an in vivo xenograft model.....	144
4.4 Discussion .....	145
4.5 Methods.....	149
4.5.1 Cell Lines.....	149
4.5.2 Clonogenic Survival Assay .....	150
4.5.3 Neutral Comet Assay.....	150
4.5.4 NHEJ Reporter Assay.....	151
4.5.5 Immunofluorescence .....	152
4.5.6 HR Reporter Assay.....	152
4.5.7 Western Blotting.....	153
4.5.8 Flow Cytometry.....	153
4.5.9 Drug Information.....	154
4.5.10 Animal Experiments.....	154
4.5.11 Irradiation .....	155
4.5.12 Statistical Analyses.....	155
4.6 Acknowledgements .....	156
4.7 Figures.....	157
4.8 References .....	169
Chapter 5 : Androgen and Estrogen Receptor Co-Expression Determines Efficacy of Hormone Receptor-Mediated Radiosensitization in Breast Cancer .....	173
5.1 Abstract .....	173
5.2 Introduction .....	174
5.3 Materials and Methods .....	177
5.3.1 Cell Culture .....	177

5.3.2 Gene Expression Knockout .....	178
5.3.3 Proliferation Assays.....	178
5.3.4 Clonogenic Survival Assays.....	179
5.3.5 Western Blotting.....	179
5.3.6 Reverse Transcription and qPCR .....	180
5.3.7 Drug Information.....	181
5.3.8 Irradiation .....	181
5.3.9 Statistical Analyses.....	181
5.4 Results .....	181
5.4.1 Validation of AR+/ER+ breast cancer cell lines in vitro.....	181
5.4.2 AR inhibition with second generation anti-androgens does not radiosensitize AR+/ER+ breast cancer cell lines in vitro .....	183
5.4.3 PROTAC-mediated AR degradation in AR+/ER+ breast cancer cells .....	185
5.4.4 Dual inhibition of AR and ER together does not radiosensitize AR+/ER+ cell lines	186
5.4.5 AR knockout in combination with ER antagonists does not radiosensitize AR+/ER+ cells.....	188
5.5 Discussion .....	189
5.6 Acknowledgements .....	194
5.7 Figures.....	195
5.8 References .....	206
Chapter 6 : Summary and Perspectives .....	212
6.1 Summary .....	212
6.2 Future Directions.....	212
6.2.1 AR+/ER- Breast Cancer .....	212
6.2.2 AR-/ER+ Breast Cancer .....	215
6.2.3 AR+/ER+ Breast Cancer .....	218

6.3 Final Remarks .....	220
6.4 Figure .....	223
6.5 References .....	224
Appendix A : PARP1 Inhibition Radiosensitizes Models of Inflammatory Breast Cancer to Ionizing Radiation.....	228
A.1 Abstract: .....	228
A.2 Introduction .....	229
A.3 Methods .....	231
A.3.1 Cell Culture.....	231
A.3.2 Proliferation Assays.....	232
A.3.3 Clonogenic Survival Assays.....	232
A.3.4 Immunofluorescence .....	232
A.3.5 Immunoblotting .....	233
A.3.6 Xenograft Models .....	233
A.3.7 Irradiation .....	234
A.3.8 Immunohistochemistry .....	234
A.3.9 Comet Assay.....	235
A.3.10 Statistical Analyses.....	235
A.4 Results .....	235
A.4.1 Single agent PARPi does not significantly affect proliferation of IBC cell lines in vitro .....	235
A.4.2 PARPi leads to radiosensitization of IBC cell lines in vitro.....	236
A.4.3 PARP1 inhibition and radiation leads to delayed repair of DNA double strand breaks compared to radiation alone .....	237
A.4.4 Olaparib effectively inhibits PAR formation in IBC cell lines .....	238
A.4.5 PARP1 inhibition significantly inhibits growth of SUM-190 xenografts in vivo.....	238



A.5 Discussion .....	240
A.6 Acknowledgements .....	244
A.7 Figures .....	245
A.8 Tables .....	252
A.9 References .....	253

## List of Tables

Table 1-1: Current clinical trials in women with breast cancer assessing the safety and/or efficacy of androgen receptor inhibition.....	37
Table 1-2: Results from completed and ongoing clinical trials investigating the use of androgen receptor inhibition in women with breast cancer.....	39
Table 2-1: Plating Densities for Clonogenic Survival Assays.....	87
Table 2-2: qPCR primers .....	88
Table 3-1: Pathway Analysis in ACC-422 cells (NT vs R1881).....	124
Table 3-2: Pathway Analysis in MDA-MB-453 cells (NT vs R1881) .....	124
Table 3-3: Pathway Analysis in ACC-422 cells (NT vs R1881+RT).....	125
Table 3-4: Pathway Analysis in MDA-MB-453 cells (NT vs R881+RT).....	126
Table 3-5: Pathway Analysis in ACC-422 cells (RT vs R1881+RT).....	127
Table 3-6: Pathway Analysis in MDA-MB-453 cells (RT vs R1881+RT) .....	128
Table A-1: Extended methods for immunohistochemistry.....	252
Table A-2: Enhancement ratios and toxicity for IBC clonogenic survival assays .....	252

## List of Figures

Figure 1-1: Therapeutic strategies used to inhibit AR signaling .....	36
Figure 2-1: Cell viability is not affected by AR inhibition with enzalutamide or seviteronel.....	78
Figure 2-2: Cell viability with treatment of AR inhibitors .....	79
Figure 2-3 AR inhibition via genetic knockdown or seviteronel treatment in combination with radiation decreases clonogenic survival in AR+ TNBC cell lines.....	80
Figure 2-4: Differential effects on AR and AR targets with enzalutamide and seviteronel treatment. ....	81
Figure 2-5: Differential effects on AR and AR targets with enzalutamide and seviteronel in ACC-422 cells.....	82
Figure 2-6: Quantification of DNAPKcs and AR Protein Expression in MDA-MB-453 cells....	83
Figure 2-7: Combination treatment results in increased levels of $\gamma$ H2AX foci and delayed resolution of dsDNA breaks.....	84
Figure 2-8: Seviteronel and radiation is more effective than seviteronel or radiation alone in MDA-MB-453 xenograft model <i>in vivo</i> . ....	85
Figure 2-9: Seviteronel with radiation increases AR recruitment compared to monotherapy treatment of enzalutamide with radiation. ....	86
Figure 3-1: Pharmacologic AR inhibitors block AR nuclear translocation in AR+ TNBC cell lines. ....	111
Figure 3-2: AR localizes to the nucleus following ionizing radiation.....	112
Figure 3-3: Analysis of differentially expressed genes and pathway changes in ACC-422 and MDA-MB-453 cells with R1881 treatment.....	113
Figure 3-4: Analysis of differentially expressed genes and pathway changes in ACC-422 and MDA-MB-453 cells following treatment with ionizing radiation.....	114
Figure 3-5: Differentially expressed genes and pathway analysis in ACC-422 and MDA-MB-453 cells relative to RT or R1881 treatment.....	115

Figure 3-6: Reverse Phase Protein Array (RPPA) Analysis of global proteomic changes in MDA-MB-453 cells.....	116
Figure 3-7: RPPA Analysis of global proteomic changes in ACC-422 cells. ....	118
Figure 3-8: Proteomic Changes in DNA Damage and Repair in AR+ TNBC cell lines.....	119
Figure 3-9: Proteomic Changes related to the MAPK signaling pathway in AR+ TNBC cell lines. .....	120
Figure 3-10: Validation of a role for AR in regulating MAPK signaling in AR+ TNBC.....	122
Figure 3-11: Mechanistic overview of AR and MAPK signaling in response to ionizing radiation. .....	123
Figure 4-1: Radiosensitization of ER+ breast cancer cell lines with anti-estrogen therapies.....	157
Figure 4-2: Radiosensitization of MCF-7 cells with variable treatment times.....	158
Figure 4-3: Radiosensitization with anti-estrogen therapies.....	159
Figure 4-4: Tamoxifen inhibits double strand DNA break repair and NHEJ efficiency in MCF-7 cells. ....	160
Figure 4-5: Tamoxifen does not inhibit homologous recombination efficiency. ....	161
Figure 4-6: Representatives images of Rad51 foci from immunofluorescence.....	162
Figure 4-7: Radiation treatment promotes cell cycle arrest in ER+ MCF-7 and T47D cells. ....	163
Figure 4-8: Endocrine therapy treatment with radiation does not induce apoptosis in ER+ cells. .....	164
Figure 4-9: Endocrine therapies in combination with radiation induce senescence.....	165
Figure 4-10: Tamoxifen in combination with radiation is more effective than radiation alone in an MCF-7 xenograft model.....	166
Figure 4-11: Representative gating for PI staining of cell cycle by flow cytometry.....	167
Figure 4-12: Representative gating for AnnexinV/PI staining of apoptosis by flow cytometry.	168
Figure 5-1: Validation of AR function in AR+ breast cancer models.....	195
Figure 5-2: Expression of AR and ER target genes was assessed in AR+/ER+ breast cancer cell lines. ....	197
Figure 5-3: AR inhibition with enzalutamide does not affect radiosensitivity of AR+/ER+ breast cancer cell lines in vitro. ....	198

Figure 5-4: Inhibition with apalutamide, darolutamide, or seviteronel does not affect radiosensitivity of AR+/ER+ breast cancer cell lines <i>in vitro</i> .	199
Figure 5-5: AR degradation with ARD-61 decreases cell viability but does not sensitize CAMA-1 cells to ionizing radiation.	201
Figure 5-6: ER inhibition ± AR inhibition with enzalutamide is not sufficient to radiosensitize AR+/ER+ breast cancer cells <i>in vitro</i> .	202
Figure 5-7: Combined treatment of tamoxifen with enzalutamide does not radiosensitize AR+/ER+ breast cancer cell lines.	204
Figure 5-8: Knockout of AR by CRISPR/Cas9 is not sufficient to provide radiosensitization to AR+/ER+ cells alone or in combination with ER inhibitors.	205
Figure 6-1: Summary of hormone receptor expression and AR and ER mediated radiosensitization phenotypes in AR+ and ER+ breast cancers	223
Figure A-1: PARP1 inhibition does not affect proliferation of IBC cell lines	245
Figure A-2: Clonogenic survival of IBC cell lines decreases with olaparib treatment	246
Figure A-3: Radiation in combination with the PARP1 inhibition leads to persistence of DNA damage in IBC cell lines	247
Figure A-4: PARP1 inhibition increases dsDNA breaks and significantly decreases PAR formation in IBC cell lines.	248
Figure A-5: PARP1 inhibition with radiation is more effective than radiation alone in a SUM-190 xenograft model	249
Figure A-6: Ki67 and p16 levels are decreased in tumors from animals treated with radiation and combination PARP-inhibitor and radiation	250
Figure A-7: Total PARP1 levels do not change with treatment but PAR levels are decreased by PARPi	251

## Abstract

Breast cancer is the most common form of invasive cancer diagnosed in women, and despite advances in therapeutic strategies, approximately 10% of women with breast tumors will experience locoregional recurrence. Therefore, we have identified the presence of nuclear hormone receptors, including the androgen and estrogen receptors, as potential therapeutic targets that may be aiding in the response to ionizing radiation. While the androgen receptor (AR) and the estrogen receptor (ER) are expressed both alone and together in breast cancer, the potential roles of AR or ER alone or in tandem have not been investigated. Previous work demonstrated that AR may be a mediator of radioresistance in AR-positive, ER-negative models of breast cancer, but little is known about the underlying mechanism of radiosensitization.

First, we demonstrate that in AR<sup>+</sup> triple negative breast cancer (TNBC) models, AR inhibition with the novel AR inhibitor and CYP17 lyase inhibitor, seviteronel, or AR knockdown results in radiosensitization through a delay in dsDNA break repair following treatment with radiation therapy (RT). While seviteronel is sufficient to radiosensitize AR<sup>+</sup> TNBC cells, seviteronel appears to have a different mechanism of radiosensitization in comparison to the second-generation anti-androgen, enzalutamide.

To further investigate the mechanism of radiosensitization with AR inhibition, we transcriptomic and proteomic data to nominate the MAPK/ERK signaling pathway as a mediator of radioresistance in AR<sup>+</sup> TNBC models. Our data demonstrates an increase in p-ERK1/2 signaling in response to AR activation using synthetic androgens. This work suggests that AR

may be activating the MAPK/ERK signaling cascade to promote DNA repair following RT, and inhibition of AR may be sufficient to block this phenotype.

ER-positive (ER+) breast cancers account for 67-80% of all breast cancer diagnoses, and women with breast cancer receive multimodal therapies including surgery, radiation therapy, and endocrine therapies targeting estrogens and ER signaling. We have shown that combination treatment of endocrine therapies with RT results in an increase in radiosensitivity in AR-negative (AR-)/ER+ breast cancer models. This radiosensitization is due to a decrease in non-homologous end joining efficiency resulting in a delay in dsDNA break repair with endocrine therapy treatment.

Co-expression of ER and AR has been observed in 70-90% of all ER+ breast cancers, and we sought to understand whether AR and ER had independent roles when co-expressed together in AR+/ER+ breast cancers. Abrogation of AR alone in AR+/ER+ breast cancer models, using pharmacologic or genetic approaches, had no effect on radiosensitivity, while targeting the ER had a limited effect on radiosensitization in some models. To understand whether there may be a compensation mechanism between AR and ER signaling, we assessed radiosensitization in AR+/ER+ models, seeing no added benefit from combined abrogation of AR and ER compared to monotherapy alone, suggesting that the role of AR in response to RT may be dependent on co-expression of other proteins, most notably, the estrogen receptor.

Collectively, our data begin to uncover the nuances of nuclear hormone receptor signaling in response to ionizing radiation in breast cancer models, suggesting that AR and ER may play independent roles when expressed alone or in tandem. Together these findings will inform clinical trial design for patients with breast cancer, increasing the translational relevance of our work.

# **Chapter 1 : ARe We There Yet? Understanding Androgen Receptor Signaling in Breast Cancer<sup>1</sup>**

## **1.1 Abstract**

The role of androgen receptor (AR) activation and expression is well understood in prostate cancer. In breast cancer, expression and activation of AR is increasingly recognized for its role in cancer development and its importance in promoting cell growth in the presence or absence of estrogen. As both prostate and breast cancers often share a reliance on nuclear hormone signaling, there is increasing appreciation of the overlap between activated cellular pathways in these cancers in response to androgen signaling. Targeting of the androgen receptor as a monotherapy or in combination with other conventional therapies has proven to be an effective clinical strategy for the treatment of patients with prostate cancer, and these therapeutic strategies are increasingly being investigated in breast cancer. This overlap suggests that targeting androgens and AR signaling in other cancer types may also be effective. This manuscript will review the role of AR in various cellular processes that promote tumorigenesis and metastasis, first in prostate cancer and then in breast cancer, as well as discuss ongoing efforts to target AR for the more effective treatment and prevention of cancer, especially breast cancer.

---

<sup>1</sup> This chapter was published in *NPJ Breast Cancer* and completed in collaboration with the following authors: Daniel E. Spratt, Lori J. Pierce, Corey W. Speers.



## 1.2 Introduction

Androgens are expressed at different levels in men and women, and while they are important for proper development, they can also drive tumor growth. Most notably, the role of the androgen receptor (AR) in prostate cancer has been extensively studied. Recent data suggest that AR signaling may also be important in breast cancer, glioblastoma, and additional tumor types with AR expression<sup>1</sup>. In order to develop effective treatment strategies for patients with each of these cancer types, it is important to understand how AR is functioning similarly and differently to drive tumor growth.

AR belongs to the Type I class of nuclear hormone transcription factors along with the estrogen receptor (ER), progesterone receptor (PR), and glucocorticoid receptor (GR)<sup>2</sup>. As is characteristic to this type of receptor, inactive forms of AR are located in the cytoplasm, bound to heat shock proteins (HSPs)<sup>3</sup>. The HSPs are responsible for proper protein folding, prevention of misfolding and maintaining the 3D protein structure during events of cellular stress<sup>4,5</sup>. AR, like other receptors in this family, is activated by the binding of androgen molecules to its ligand binding domain (LBD). Androgen binding results in AR homodimerization and translocation into the nucleus, where AR binds to androgen response elements (AREs) resulting in activation and transcription of a variety of downstream genes. Binding of AR results in the activation of diverse signaling pathways, including multiple signaling pathways that have been implicated in cancer, including the PI3K/AKT pathway<sup>6</sup>. AR also contributes to cell growth and proliferation differently in the context or absence of ER, and AR has an influence on cell cycle and DNA damage repair. Further, AR has non-genomic functions that can influence cell growth, migration, metastasis, and apoptosis. Due to its many downstream effects, anti-androgen therapies have

long been of therapeutic interest along with combining AR antagonism with conventional chemotherapy or radiation therapy.

### **1.3 Gene Expression and Hormone Receptor Function**

The AR has been well characterized as a key driver for the growth of prostate cancer in men. In this context, castration or androgen deprivation therapy (ADT) is a first line of therapy for men with metastatic prostate cancer. Despite the efficacy of ADT, resistance is near-universal. In some men, resistance can be mediated by AR amplification<sup>7</sup>, and others develop mutations in the LBD of AR in response to anti-androgen treatment<sup>8</sup>. These mutations can render cells refractory to androgen deprivation as there is constitutive AR activation, even in the absence of androgens. This results in activation of AR including AR binding to AREs and constitutive AR-regulated gene expression. More recently, a role for the androgen receptor in the progression of breast cancer has been described. While AR's function has not been fully characterized in breast cancer, work done in prostate cancer informs the potential function of AR in breast cancer.

Similar to the role that AR plays in prostate cancer development and progression, the estrogen receptor (ER) has been recognized for the integral role that it plays in driving the development of the majority of breast cancers<sup>9</sup>. Breast cancers that express the estrogen receptor (ER+) grow in response to the presence of estrogen and are more responsive to endocrine ablation<sup>10,11</sup>. This understanding led to some of the first “molecularly targeted therapies” that established the use of aromatase inhibitors (AIs) or selective estrogen receptor modulators (SERMs), which block the production and signaling of estrogen<sup>12</sup>. AIs and SERMs have been used as effective therapies for women with tumors that express ER<sup>13,14</sup>. Despite having identified the presence of AR expression in breast cancer many years ago<sup>15</sup>, little is known about the role of

androgen signaling in breast cancer, though its importance as a potentially effective therapeutic target is increasingly appreciated and will be discussed herein. We begin with a review of the various processes known to be mediated by AR signaling, as recent studies have shed light on the role of AR with other pathways known to be abrogated in cancer.

## **1.4 Transcription Factor and Protein Interactions**

### ***1.4.1 AR and FOXA1***

#### *Prostate Cancer*

FOXA1 is a transcription factor which plays an important role in aiding the binding of hormone receptors to their target DNA<sup>16</sup>. More recently, three distinct classes of alterations in FOXA1 have been described in prostate cancer, each with unique structural and phenotypic consequences<sup>17</sup>. The Class-1 activating mutations originate in early prostate cancer without alterations in ETS or SPOP and are found in the wing-2 region of the DNA-binding forkhead domain. Functionally these mutations allow for enhanced chromatin mobility and binding frequency and strongly transactivate a luminal AR program. The second class of activating mutations are found in metastatic prostate cancer and are characterized by a truncated C-terminal domain. These mutations increase FOXA1 DNA affinity and promote metastasis by activating the Wnt pathway through TLE3 inactivation. The final class of FOXA1 genomic rearrangements are characterized by duplications and translocations within the FOXA1 locus that reconfigure regulatory elements (FOXA1 mastermind elements) to drive overexpression of FOXA1. This third class of alterations is found primarily in metastatic prostate cancer and further underscores the interaction and significance of AR and FOXA1 protein interactions<sup>17</sup>. Similar classes of alterations also been observed in breast cancer<sup>1</sup>. In prostate cancer, FOXA1 also influences the

ability of AR to bind DNA and control cell cycle progression. FOXA1 binds to genes necessary for growth of castration-resistant prostate cancer (CRPC), suggesting that FOXA1 is responsible for driving cell cycle progression in CRPC both from G1 to S and G2 to M<sup>18</sup>. FOXA1 also facilitates cell cycle progression from G2 to M by acting as a cofactor for AR<sup>18</sup>. Unsurprisingly, there is also significant overlap between genomic binding sites occupied by AR and FOXA1<sup>19</sup>. While AR binds to many DNA regions independent of FOXA1, DNA binding sites often require the presence of FOXA1 for AR recruitment<sup>19</sup>. Therefore, loss of FOXA1 results in the inability of AR to bind many DNA loci<sup>19</sup>. Using H3K4me2 ChIP analyses, Sahu *et al.* found that there were H3K4me2 marks at approximately 70% of sites shared by AR and FOXA1<sup>19</sup>. Furthermore, staining of FOXA1 has been shown to correlate with disease outcomes in prostate cancer patients, where even with high AR staining, low FOXA1 is associated with good prognoses, and strong FOXA1 staining correlates with poor prognoses<sup>19</sup>, indicating that FOXA1 may have an important effect on AR signaling and tumor progression. Levels of FOXA1 are also elevated in prostate tumors and metastases, and overexpression of FOXA1 in prostate cancer cell lines results in increased AR binding at novel sites that have high chromatin accessibility<sup>20</sup>. These results suggest that increased levels of FOXA1 enhance AR binding to novel sites in order to facilitate cancer cell growth<sup>20</sup> and implicate the importance of FOXA1 on AR function and tumor progression.

### *Breast Cancer*

FOXA1 is also essential for the growth of ER+ breast cancer cell lines<sup>21</sup>. Similar to prostate cancer, ChIP-seq studies have shown that there is extensive overlap between locations of AR and FOXA1 binding in breast cancer cells<sup>22</sup>. The function of AR in breast cancer is also dependent upon FOXA1, as silencing of FOXA1 inhibits AR binding of target DNA as well as

cell growth<sup>22</sup>. In addition, FOXA1 functions as a transcription factor, playing an important role in aiding binding of hormone receptors, including ER and AR, to their target DNA<sup>16,23</sup>. When expressed with AR, FOXA1 may direct AR binding at sites of ER binding in luminal tumors<sup>24</sup>. Notably, coexpression of AR and FOXA1 was observed by IHC in ~15% of triple negative breast cancer (TNBC) patients<sup>24</sup>, and AR-positive (AR+), FOXA1-positive (FOXA1+) patients had a significant decrease in recurrence-free survival and overall survival compared to TNBC patients<sup>25</sup>. These findings suggest that when co-expressed in TNBC, AR and FOXA1 may be mediating an estrogen-like gene signature similar to those expressed in luminal breast cancers. FOXA1 has been studied extensively in the context of ER chromatin binding, and ER binding is dependent on FOXA1 in the presence or absence of ligand<sup>23</sup>. Further, similar to findings in prostate cancer, 1.8% of breast cancers harbor mutations in FOXA1, and amplifications of the FOXA1 gene locus have been observed in breast and prostate cancers<sup>26</sup>. Notably most identified mutations are in the forkhead domain of FOXA1, and tumors in this study were exclusively ER+. The implications of these mutation, however, is still under investigation in breast cancer. Interestingly, differences exist between the function of FOXA1 in directing AR binding in breast versus prostate cancers, and future studies may investigate the varied roles of FOXA1 in directing AR binding in TNBC and prostate cancer, in addition to investigating the role of AR when co-expressed with ER. Current literature suggests, however, that regardless of tumor type, FOXA1 is an important cofactor for directing the transcriptional activity of AR.

#### ***1.4.2 AR and PTEN***

##### *Prostate Cancer*

Expression of AR with PTEN has also been investigated in prostate cancer. In prostate cancer patients, high AR expression with low PTEN expression is associated with poor clinical

outcomes<sup>27</sup>. In prostate tumors, with loss of *PTEN*, there are decreased levels of AR signaling<sup>28</sup>. Inhibition of PI3K in these tumors results in increased levels of AR signaling through loss of HER2 mediated feedback inhibition of AR<sup>28</sup>. A direct physical interaction between AR and PTEN in low passage LNCaP cells has been shown to inhibit nuclear translocation of AR resulting in an increase in degradation of AR protein<sup>29</sup>. A pilot study suggested that high expression of both AR and PTEN in patients with advanced prostate cancer was associated with a higher risk of relapse at 30 months after surgery (85.7% of high PTEN and AR expressing patients verses 16.6% in patients with low AR and PTEN expression)<sup>30</sup>. Further, combination therapy with both anti-androgen (bicalutamide) and PTEN induction was shown to reduce PSA promoter activity compared to PTEN alone<sup>31</sup>. Sequencing of metastatic-CRPC (mCRPC) patients revealed that *AR* and *PTEN* are among the most commonly aberrant genes, along with the ETS family and *TP53*<sup>32</sup>. Therefore, these data suggest that both AR and PTEN may influence prostate tumor growth and progression.

### *Breast Cancer*

There are opposing findings when comparing AR and PTEN transcript expression in prostate verses breast cancer. In breast cancer, there is an AR-binding motif located in the *PTEN* promoter, and there is a positive correlation between AR and PTEN transcript levels<sup>27</sup>. In addition, high expression of AR and PTEN is correlated with better clinical outcomes for breast cancer patients<sup>27</sup>. Interestingly, in AR+ TNBC, AR interacts at an ARE located in the promoter of ER $\beta$ <sup>33</sup>, and ER $\beta$  also plays a role in regulation of PTEN expression to control tumor growth<sup>34</sup>. The interaction between AR and PTEN may be context specific and important for predicting outcomes for patients with AR+ disease: where AR expression is associated with disease progression in prostate cancer<sup>7</sup>, PTEN loss is also correlated with poor outcomes<sup>35,36,27</sup>. In breast

cancer, however, loss of PTEN is also correlated with negative estrogen and progesterone receptor status, and PTEN loss is associated with breast tumor progression<sup>37</sup>. Therefore, these results suggest that the function of PTEN may be context specific and understanding the nuances in situational signaling of AR may help elucidate the role for PTEN in AR+ disease progression.

### ***1.4.3 Non-Genomic AR Functions***

#### *Prostate Cancer*

Prostate cancer cells exhibit rapid proliferation responses in response to androgen stimulation, suggesting non-genomic AR signaling. Upon activation with androgens or estrogens, cytoplasmic AR can activate MAPK/ERK signaling through an association with Src<sup>38</sup>. The activation of the Src/ERK pathway is dependent on androgen concentration (0.1-10 nM) and is inhibited at high concentrations (100 nM)<sup>39</sup>. Treatment with DHT also induces rapid ERK1/2 phosphorylation; however, MAPK activation can be blocked pharmacologically using a MEK inhibitor, suggesting AR is activating the Raf1-MEK pathway resulting in MAPK activation<sup>40</sup>. Further, AR can also activate the phosphatidylinositol 3-kinase (PI3K)/Akt pathway leading to activation of mammalian target of rapamycin (mTOR)<sup>41</sup>. In addition, androgens can interact at the plasma membrane which is associated with the modulation of intracellular calcium and cAMP levels<sup>42,41</sup>. Many membrane-bound G-protein coupled receptors (GPCRs) are also responsive to androgen treatment, leading to an increase in apoptosis<sup>43</sup>, phosphorylation of ERK<sup>44</sup>, or reduced cell migration and metastasis<sup>45</sup>. Together, these findings suggest that AR may also function within the cytoplasm or at the membrane to activate non-genomic functions.

## *Breast Cancer*

Similar to non-genomic AR functions in prostate cancer, the cytoplasmic roles of AR have also been investigated in breast cancer. Chia *et al.* demonstrated that AR is necessary and sufficient for ERK phosphorylation following DHT stimulation in MDA-MB-453 and HCC-1954 cells<sup>46</sup>. Further, inhibition of AR resulted in decreased levels of phospho-Elk1, phospho-RSK, and c-FOS in xenograft tumors and in patient tumors, corresponding to a decrease in ERK target proteins<sup>46</sup>. In TNBC, AR inhibition has also been shown to modulate the activity of the Ca<sup>2+</sup>-activated K<sup>+</sup> channel, K<sub>Ca</sub>1.1, which is associated with breast cancer invasion and metastasis<sup>47,48</sup>. Multiple groups have also studied the role of cytoplasmic AR phosphorylation<sup>49,50</sup>; however, additional work is required to understand how AR modifications influence cellular function and localization. At the membrane, many receptors mediate rapid responses to androgen signaling, representing novel membrane-ARs<sup>51,52</sup>. These signals, however, are complex as agonistic versus antagonistic effects are dependent on receptor stoichiometry<sup>52</sup>. Furthermore, AR is expressed in fibrosarcoma cells; however, a significant portion of AR is transcriptionally incompetent and does not bind to AREs upon activation. Rather, there is crosstalk between EGFR and AR, and treatment with bicalutamide decreases xenograft tumor growth<sup>53</sup>. Together these data from multiple cancer models suggest that AR has non-genomic functions affecting tumor growth both in prostate and breast cancer which warrant further investigation.

### **1.5 Cell Growth and Proliferation**

#### ***1.5.1 Androgens and AR Splice Variants***



## *Prostate Cancer*

A number of AR splice variants have been identified, and they play an important role in the development of CRPC. The gene encoding AR is located on the X chromosome, encoding nine exons that produce the full length AR transcript<sup>54</sup>. Aberrant splicing of AR pre-mRNA, however, can result in the production of AR isoforms that are constitutively active. These isoforms can drive an AR transcriptional program even in the absence of androgen signaling, resulting in androgen independent tumor growth<sup>55,56</sup>. AR variants (ARVs) are present both in prostate cancer and breast cancer, and these variants commonly are truncated or have mutations in the AR LBD<sup>57</sup>. In addition, AR transcripts can have aberrant splicing, resulting in skipped exons<sup>58</sup>. ChIP studies have demonstrated that splice variants, including AR-V7, are able to bind ARE DNA sequences as well as unique regions of additional genes<sup>58</sup>. AR splice variants have been shown to require expression of full-length AR (AR-FL) suggesting that a balance between ARV and AR-FL expression is required for resistance in prostate cancer models<sup>59</sup>.

The most common splice variant, AR-V7, lacks a ligand binding domain<sup>60</sup>. Clinically, in a cohort of prostate cancer patients treated with enzalutamide or abiraterone acetate, 39 patients (19%) had detectable levels of AR-V7 in circulating tumor cells (CTC)<sup>61</sup>. Patients who had AR-V7 expression had lower PSA response rates and worse survival compared to AR-V7 negative patients<sup>61</sup>. In addition to reliance on AR-splice variants, resistance to ADT is also mediated through signaling of additional hormone receptors. The glucocorticoid receptor (GR) has been shown to be increasingly present in androgen-deprived prostate cancer patients (78% vs. 38% of untreated patients)<sup>62</sup>, and expression of GR is increased in xenografts that are resistant to ARN-509 (apalutamide)<sup>63</sup>. In addition, there is overlap between AR and GR binding at classic response elements as well as regulation by both DHT and dexamethasone, a GR agonist<sup>63</sup>. In prostate

cancer cells, stimulation with dexamethasone in the presence of enzalutamide resulted in expression of AR target genes<sup>63</sup>, providing further evidence that GR signaling could compensate for AR in the presence of AR-antagonists.

### *Breast Cancer*

There are significantly fewer AR mutations observed in TNBC compared to CRPC; however, AR splice variants are still common. In breast cancer, AR-V7 is most highly expressed splice variant in basal tumors compared to other tumor types, with the lowest expression in luminal tumors<sup>60</sup>. Little is known about how AR-V7 may be contributing to anti-androgen resistance in AR+ TNBC or if it is functioning similarly to its observed role in CRPC<sup>64</sup>. In HER2-enriched patients, however, high AR-V7 expression is associated with significantly higher metastasis free survival and disease-specific survival<sup>60</sup>. Therefore, the ability of a tumor to produce its own androgens, as well as its reliance on splice variants may also play an important role in understanding how AR is functioning to drive tumor growth in the context of ADT or anti-androgen therapies.

Importantly, differences also exist in preclinical cell lines used to study AR+ breast cancers. While common cell lines, including MDA-MB-453, MDA-MB-231, ZR-75-1, MFM-223, MCF-7 and T47D, have varying levels of AR-FL expression, ARV expression also varies widely among cell lines – both in total ARV expression and expression of specific AR variants<sup>65</sup>. Notably, MDA-MB-453 cells contain the AR-Q865H variant which harbors a mutation in the AR LBD<sup>66</sup>, demonstrating the importance of considering the influence of ARV expression in laboratory studies. Furthermore, understanding the similarities and differences of how ARVs may be influencing AR expression and contributing to breast tumorigenesis will be important.

#### ***1.5.2 Estrogen Influence on Androgen Signaling in Breast Cancer***

### *AR+, ER+ Cancers*

Breast tumors that are ER+ are more likely to be AR+ compared to tumors that are ER-<sup>67</sup>, and AR status is related to ER and PR status but independent of the status of human epidermal growth factor receptor 2 (HER2)<sup>68</sup>. Interestingly, patients with AR:ER ratios  $\geq 2$  have worse disease free survival compared to patients with lower AR:ER ratios in the presence of anti-estrogen therapies or chemotherapy treatment<sup>69</sup>. Defining expression of AR and ER, however, is challenging, and results vary widely depending on the assays (including immunohistochemistry [IHC], radioimmunoassay, and reverse-phase protein array<sup>67</sup>) and cut-offs used to define positivity. Clinically, ER expression is measured by IHC, and ER+ tumors are defined as those with  $>1\%$  of tumor cells with positive nuclei<sup>70</sup>. AR positivity, however, has been defined with varying cut-off levels from 1% to 75%<sup>67,71</sup>. The prognostic role of AR in breast cancer remains unclear. A recent study has demonstrated that  $>78\%$  AR positivity is required to accurately assess the prognostic role of AR in ER+ cancers, with ER+ patients that have  $\geq 78\%$  AR-positivity having the best survival outcomes<sup>72</sup>. In other studies, however, breast cancer patients with AR+ tumors have better overall survival at both three and five years compared to patients with AR- tumors, regardless of ER expression<sup>67</sup>. These data suggest that the role of AR in driving breast cancer growth may differ in the presence or absence of ER and that antagonizing AR may have different effects depending on the level of AR expression.

Androgen receptor expression in ER+ breast cancers antagonizes the signaling of mitogenic ER $\alpha$ , and AR expression leads to the upregulation of ER $\beta$ <sup>33</sup>. In ER+ breast cancer, AR binds at an ARE located in the promoter of the ER $\beta$  gene, resulting in increased ER $\beta$  expression<sup>33</sup>. Interestingly, the presence of ER $\beta$  has been shown to inhibit transcriptional activity of ER $\alpha$ <sup>73</sup>, therefore, suggesting that AR-regulated increased activity of ER $\beta$  may indirectly

influence ER $\alpha$  activity. Similarly, in prostate tissue, ER $\beta$  is thought to play an antagonistic role to AR, resulting in the suppression of cellular proliferation and the promotion of apoptosis<sup>74</sup>. ER $\beta$  is also important for the control of cell cycle progression and arrest<sup>75,76</sup>, indicating that increasing ER $\beta$  expression may be a therapeutic strategy in prostate cancer<sup>77</sup>.

In contrast to early studies suggesting high AR expression is associated with improved outcomes, recent data suggest high AR expression may be associated with therapy resistance, including endocrine therapy resistance. Indeed, De Amicis *et al.* first reported the positive correlation between high AR expression and tamoxifen resistance, suggesting that tumors with a high AR:ER ratio are more likely to be resistant to anti-estrogen therapies, which are common first line of therapy for ER+ tumors<sup>78</sup>. Patients resistant to tamoxifen with AR:ER $\alpha$  ratios  $\geq 2$  have worse disease free survival, and disease specific survival<sup>79</sup>. Interestingly, in tamoxifen-resistant MCF-7 cells, loss of AR signaling by AR knockdown, but not treatment with enzalutamide, restored sensitivity to tamoxifen<sup>80</sup>. These results suggest that AR expression may be a mechanism of hormone therapy resistance, and therefore a therapeutic target in resistant hormone receptor positive breast cancers.

Anti-AR therapy is of increasing clinical interest. AR inhibition may be an effective strategy for growth inhibition of AR+, ER+ breast tumors. AR inhibition with enzalutamide has been shown to be synergistic with tamoxifen- or fulvestrant-mediated ER inhibition, in addition to controlling growth of tamoxifen-resistant MCF-7 cells *in vitro* and *in vivo* in an AR+, ER+ patient derived xenograft (PDX) model<sup>81</sup>. Enzalutamide has been shown to be effective in AR+ breast tumors, including ER+ (MCF-7) cells and ER- (MDA-MB-453) cells<sup>82</sup>. ChIP analyses demonstrate that there is extensive overlap between AR and ER binding sites after E2 stimulation in MCF-7 cells<sup>81</sup>. Interestingly, however, AR binding was different based on

stimulation with DHT or E2 in MCF-7 cells suggesting that AR may regulate a unique transcriptional program in the absence of estrogen signaling, providing additional evidence for synergism between anti-estrogen and anti-androgen therapies<sup>81</sup>. These results indicate that targeting AR in combination with anti-ER therapies may be an effective therapeutic strategy for patients with AR+, ER+ breast cancers.

Functionally, AR and ER share many similarities in their signaling pathways, including the mechanism of receptor activation, as both receptors are activated through ligand binding<sup>83</sup>. ER and AR recognize similar sequences of DNA: where ER binds to 5'-AGGTCA-3', AR recognizes the 5'-AGAACA-3' sequence<sup>83,84</sup>. Further, in breast cancer, both AR and ER require similar cofactors for the activation of common signaling pathways<sup>83</sup>. Binding of AR or ER can activate MAPK signaling, among other pathways<sup>83</sup>, and due to their similar structure and signaling function, both hormone receptors are in competition within the cell for the binding of scaffold proteins and cofactors<sup>83</sup>. While AR and ER share many similarities, there may be important differences determining their role in driving tumor growth.

#### *AR+, ER- Cancer*

The function of AR in breast cancer appears to be dependent upon its co-expression with ER, as there is evidence for varying effects of AR on the growth of breast cancer cells in the presence or absence of ER. Indeed, while AR is co-expressed with ER in 70-90% of breast tumors, AR is only expressed in 15-30% of ER-negative breast tumors<sup>85</sup>. Breast cancers that do not express ER, PR, and HER2 have been traditionally described as triple negative breast cancers (TNBC). Recently, however, a subtype of TNBC has been established which is characterized by luminal AR expression<sup>86,87</sup>. In studies with AR+ human breast cancer cell lines, androgens had both proliferative and anti-proliferative effects depending on the cell line of interest<sup>88</sup>. More

recently, however, multiple groups have demonstrated that targeting AR in AR+ TNBC is an effective treatment strategy both *in vitro* and *in vivo*<sup>82,89,90</sup>. Interestingly, in AR+ TNBC, approximately 30% of patients have expression of ER $\beta$ <sup>91</sup>, and ER $\beta$  expression has been shown to increase the efficacy of anti-androgens in AR+ TNBC cells<sup>92</sup>. Together these data demonstrate the importance of AR in driving growth of AR+ TNBCs.

While AR expression has been increasingly recognized in AR+, ER- breast cancers, the specific role of AR signaling is not well understood. Some studies suggest an important role for AR in signaling in the absence of ER<sup>93</sup>. In an analysis of AR+, ER- MDA-MB-453 cells, the AR cistrome was found to be more similar to that of ER in MCF-7 (AR-/ER+) cells compared to the AR cistrome in LNCaP prostate cancer cells<sup>22</sup>. Therefore, AR may function in place of ER in AR+, ER- breast cancer<sup>22</sup>, having a distinct role in AR+ TNBC compared to prostate cancer. AR may also be important for promoting the cancer stem cell-like (CSC-like) population in TNBC, in addition to reducing the levels of detachment-induced apoptosis in cells grown in forced suspension compared to attachment conditions<sup>94</sup>. These results suggest that AR blockade may be effective in combination with paclitaxel to target CSC-like cells and reduce tumor recurrence compared to paclitaxel treatment alone<sup>94</sup>. In addition, AR is commonly enriched in breast cancers overexpressing HER2, indicating a role for AR in activation of HER2 and Wnt signaling<sup>89,95</sup>. Therefore, AR expression may be an important target for directing treatments for patients with ER- breast cancer.

## 1.6 DNA Damage Repair

### *Prostate Cancer*

While the mechanism of the AR in response to DNA damage is just beginning to be uncovered in breast cancer, the mechanistic role of AR in DNA damage repair has been more extensively characterized in prostate cancer. Goodwin *et al.* found that AR is activated in response to reactive oxygen species (ROS) and DNA damage<sup>96</sup>. Additionally, in response to ionizing radiation, CRPC cells have enhanced DNA repair and decreased DNA damage<sup>97</sup>. AR activation results in the expression of DNA damage repair genes including *PRKDC*, encoding DNA-dependent protein kinase catalytic subunit (DNA-PKcs), an essential protein necessary for non-homologous end joining (NHEJ) repair of double-stranded DNA (dsDNA) breaks<sup>96</sup>. In addition, treatment with radiation and androgens results in the upregulation of *XRCC2* and *XRCC3*, two genes important for homologous recombination (HR)<sup>96</sup>. Conversely, anti-androgen treatment results in decreased DNA repair in cells and increased levels of dsDNA breaks<sup>97</sup>. The same group also showed that treatment with AR inhibitors results in increased radiosensitivity and decreased NHEJ-mediated recombination suggesting that AR is involved in NHEJ-mediated repair of dsDNA breaks<sup>97</sup>. DNA-PKcs has been shown to function in complex with Ku70 and Ku80 to respond to DNA damage. Interestingly, DNA-PKcs physically interacts with AR; however, this interaction does not require the presence of DNA<sup>98</sup>. This suggests that AR regulation of the DNA damage response may not be completely dependent on AR-mediated transcriptional regulation of DNA damage response genes. Following androgen stimulation in prostate cancer cells, AR is recruited to enhancer elements, along with DNA-PKcs, coregulator p300, and RNA Pol II suggesting that the interaction of AR and DNA-PKcs may be important for the regulation of specific transcriptional programming<sup>98</sup>. Therefore, an interaction between

AR and DNA-PKcs may also be important for AR's role in the repair of DNA damage. In patient tissue, castration resulted in the downregulation of Ku70 protein levels, impairing NHEJ<sup>99</sup>. AR regulates Ku70 levels in prostate tissue, and due to the critical role of Ku70 in effective NHEJ, downregulation of this protein abrogates NHEJ-mediated repair<sup>99</sup>. Collectively these data suggest that AR signaling plays an important role in the repair of dsDNA breaks, at least in part through interactions with Ku70/Ku80 and DNA-PKcs, members of the NHEJ repair pathway.

### *Breast Cancer*

Recent data in breast cancer suggests that loss of AR signaling through knockdown or pharmacologic inhibition with enzalutamide or seviteronel results in increased sensitivity to ionizing radiation<sup>100,101</sup>. In addition, AR mRNA levels correlate with survival following radiation treatment, and AR is important for regulating the DNA damage response in AR+ breast cancer cell lines<sup>102</sup>. Pharmacologic AR inhibition results in delayed repair of dsDNA breaks following ionizing radiation, suggesting that AR is influencing dsDNA damage repair. Additionally AR inhibition with enzalutamide decreases levels of phosphorylated DNA-PKcs following radiation, indicating that NHEJ may be important for the repair of radiation-induced dsDNA breaks in breast cancer<sup>100</sup>. Although some similarities exist between the DNA damage repair interaction with AR in prostate and breast cancers, a full characterization of the similarities and differences is still ongoing.

## **1.7 Cell Cycle Regulation**

### *Prostate Cancer*

Cell cycle progression is driven by the rising and falling of cyclins and cyclin dependent kinase (CDKs) protein levels, in addition to their activation<sup>103</sup>. In prostate cancer, AR is



regulated in a cell-cycle dependent manner<sup>104</sup>. Nuclear transactivation of AR is highest in G1 and decreases in S-phase, while the same changes occur in AR phosphorylation and cellular localization<sup>104</sup>. Further, CDK1 has been shown to phosphorylate AR on S308 in response to ligand binding<sup>104</sup>. The phosphorylation results in changes in AR chromatin localization<sup>104</sup>. AR signaling is responsible for the activation of genes controlling the G1-S transition<sup>105</sup>. Specifically, AR is responsible for G1 CDK activation and the phosphorylation of retinoblastoma (pRb), which is necessary for the activation of CDKs that will drive the G1-S phase progression<sup>105</sup>. In the absence of androgen signaling, prostate cancer cells will arrest in early G1 phase as they do not have expression of the necessary CDK and cyclin proteins<sup>106,107</sup>. AR and pRb have also been shown to interact, and an overexpression of pRb increases the transcriptional activity of AR<sup>108,109</sup>.

AR signaling is also important for the regulation of other cell cycle related genes, including the regulation of *CCND1* expression<sup>110</sup>. Importantly, *CCND1* encodes cyclin D1 which has an interaction with pRb that is necessary for cell cycle progression. AR binds to androgen responsive elements (ARE) that are located ~570-556 base pairs upstream of the transcription start site of the proximal promoter of *CCND1*, suggesting that AR plays a regulatory role to influence *CCND1* expression<sup>110</sup>. In prostate cancer cells, following treatment with androgens, there is induction of expression of CDK inhibitors p21 and p27<sup>111</sup>. Expression of p21 is controlled at the transcriptional level through the presence of an ARE in the promoter region, ~200 base pairs upstream of the proximal promoter<sup>112</sup>. AR signaling has been shown to be important for control of cell-cycle related gene expression, resulting in growth implications in tumor cells.

Additionally, in prostate cancer cells, the synthetic androgen mibolerone inhibited proliferation and reduced levels of c-MYC transcripts, suggesting that AR is important for regulating c-MYC levels<sup>113</sup>. AR expression is also regulated by AREs as well as MYC binding at the consensus site<sup>114</sup>. Thus, in addition to its role cell growth and the DNA damage response, AR expression and activation is itself regulated in a cell cycle-dependent manner which then influences expression of CDK and transcription factors to regulate progression through the cell cycle.

### *Breast Cancer*

In addition to interactions with cyclins and CDKs, AR also interacts with many other important proteins, including well characterized oncogenes and tumor suppressors. In AR+ TNBC, DHT has been shown to increase levels of cyclin D1, while decreasing p73 and p21 expression<sup>115</sup>. Conversely, treatment with bicalutamide resulted in a decrease in cyclin D1 expression, while increasing p73 and p21 levels, implicating a role for AR in the control of cell cycle progression in AR+ TNBC models<sup>115</sup>. The expression of AR and pRb in breast cancer is also significantly correlated, and AR has been shown to interact with other transcription factors, including MYC, which are important for cell cycle control<sup>116</sup>. In breast tumors, high AR expression is negatively correlated with MYC overexpression<sup>116</sup>. MYC expression has been linked to cell proliferation, and inactivation of MYC impairs cell cycle progression as MYC targets cell cycle regulators like cyclins, CDKs, and E2F transcription factors<sup>117</sup>. Additionally, in breast cancer models, the presence of an ARE -383 to -377 base pairs upstream of the ER $\beta$  promoter region results in enhanced control of ER $\beta$  expression as a result of AR signaling<sup>33</sup>. ER $\beta$  has been shown to negatively regulate transcription of c-MYC, cyclin D1, and cyclin A, while also increasing transcription of CDK inhibitors like p21 and p27<sup>33</sup>. In ER+ breast cancer

models, DHT-mediated activation of AR has been shown to inhibit ER $\alpha$  signaling and cell cycle progression through a reduction in cyclin D1 transcription<sup>118</sup>. Further, AR and ER both require the steroid receptor coactivator AIB1<sup>118</sup> which is commonly expressed in breast cancers<sup>119,120</sup>, and high AIB1 expression is correlated with poor mortality<sup>121</sup>. Therefore, through direct or indirect mechanisms, AR signaling likely also plays an important role in controlling cell cycle progression in breast cancer.

## **1.8 Metastasis**

### *Prostate Cancer*

AR has been shown to contribute to the formation of metastases. The AR pathway and AR splice variants have been implicated in metastatic phenotypes in prostate cancer<sup>122</sup>. Gene array and IHC data of both primary and metastatic tumors demonstrate that AR mRNA and protein expression are significantly higher in metastases compared to primary prostate lesions<sup>123</sup>. *In vitro*, increased AR expression in prostate tumors also led to the formation of metastases and induction of the epithelial to mesenchymal transition (EMT)<sup>123</sup>, the process by which cells lose their polarity and gain the ability to migrate and become invasive. In addition, during prostate cancer development, the presence of fibroblasts provides important structural and functional changes that regulate the extracellular matrix<sup>124</sup>. Expression of nuclear receptors has been shown to be important in squamous cell carcinoma cancer-associated fibroblasts (CAFs) compared to normal-associated fibroblasts, with nuclear receptors influencing many cellular functions including invasiveness<sup>125</sup>. Additionally, AR expression in prostate CAFs has been shown to promote growth and invasion<sup>126</sup>. AR activation in the stroma has been shown to be essential for prostate cancer progression and metastasis<sup>127</sup>. Interestingly, the AR cistrome in prostate CAFs is

distinct from the AR cistrome in epithelial cells suggesting a novel role for AR in the microenvironment<sup>128</sup>. Notably, AR relies on AP-1 in the stroma, rather than FOXA1 as observed in epithelial cells<sup>128</sup>.

Furthermore, the regulatory role of AR in gene expression has been shown to be important for the regulation of prostate cancer metastases. In this context, AR negatively regulates expression of ZBTB46, a tumor promoter through miR-1<sup>129</sup>. Therefore, disruption of AR signaling can result in overexpression of ZBTB46 resulting in an increase in transcriptional regulation of SNAI1, a driver of EMT, resulting in metastasis formation<sup>129</sup>. Further, AR inhibition with enzalutamide has been shown to increase metastases by decreasing EPHB6 suppression leading to JNK signaling resulting in cell invasion<sup>130</sup>. These findings suggest that AR plays an important role in controlling metastatic progression of prostate tumors, demonstrating the importance of future work in this area.

### *Breast Cancer*

In patients with breast cancer, metastases are likely to have multiple drivers of disease progression. In preclinical models, AR has also been shown to contribute to invasiveness and migration of TNBC cells through activation of the Src complex<sup>131</sup>. When MCF-7 cells were treated with DHT, there was also an increase in invasion and migration, as well as a decrease in epithelial markers and an increase in mesenchymal markers<sup>132</sup>. DHT treatment also induced other markers of EMT suggesting that AR activation may promote EMT in MCF-7 cells<sup>132</sup>.

As with prostate cancer, previous data from breast cancer patients demonstrates that AR expression is conserved from the primary tumor into metastases<sup>133,134</sup>. One study suggests that there is 78.6% agreement in AR status in primary tumor and lymph node metastases<sup>135</sup>. In the discordant cases, 60/72 had AR- primary tumors, and AR+ lymph node metastases<sup>135</sup>. Further,

IHC analyses in tumors and metastases showed greater than 60% agreement between the expression of AR in primary tumor and metastases<sup>136</sup>.

## **1.9 Treatments targeting androgens and the androgen receptor for prostate and breast cancer**

Pharmacological agents have been developed to inhibit AR binding to androgens and AR activation due to its role in driving cancer development and progression (**Figure 1**). Many of these agents have been effective in the treatment of prostate cancer, and the clinical applications have been expanded to women with AR+ breast cancers. Here we explore these various agents, their mechanisms of action, and the data that exist in the treatment with women with breast cancer, including the ongoing clinical trials assessing these agents in women with AR-positive breast cancer and the emerging results from these trials (**Tables 1 & 2**).

### ***1.9.1 Androgen Deprivation Therapy***

The use of androgen deprivation therapy (ADT) is universally accepted as a first line therapy for metastatic prostate cancer<sup>137</sup>. This treatment attempts to lower levels of serum testosterone in men with prostate cancer to prevent tumor growth<sup>138</sup>. This is done chemically with the use of luteinizing hormone-releasing hormone (LHRH) or gonadotrophin-releasing hormone (GnRH) antagonists, like Degarelix, Goserelin, and Leuprolide, which are used to suppress the production of androgens<sup>137</sup>. Many clinical trials also are assessing the efficacy of ADT in combination with other treatment strategies in an attempt to improve ADT efficacy, especially in cases where AR mutations cause castration to be ineffective at controlling disease progression.

### ***1.9.2 5 $\alpha$ -Reductase Inhibitors***

5 $\alpha$ -dihydrotestosterone (DHT) is produced from testosterone in specific tissues, including the prostate, through the enzymatic activity of 5 $\alpha$ -reductase. Compared to testosterone, DHT has a slower dissociation rate from AR, suggesting that AR-DHT is a more stable complex, making DHT the preferred AR ligand<sup>139,140</sup>. Competitive inhibitors of 5 $\alpha$ -reductase, like finasteride or dutasteride, can be used to lower levels of serum and prostate DHT<sup>141,142,143,144</sup>. The effects of these 5 $\alpha$ -reductase inhibitors, however, are complex as they may not exclusively target the enzymatic activity of 5 $\alpha$ -reductase and likely have additional off-target AR inhibitory effects as well<sup>145</sup>.

### ***1.9.3 CYP17-Lyase Inhibitors***

Abiraterone acetate is a selective inhibitor of cytochrome P450 17 $\alpha$ -hydroxylase/17,20-lyase (CYP17), which, through its function, decreases the adrenal and tumor synthesis of androgens<sup>146</sup>. CYP17 lyase inhibitors lower androgen availability to reduce the activation of androgen signaling. Trials in men with chemotherapy-naïve CRPC concluded that treatment with abiraterone acetate and prednisone prolongs overall survival compared to treatment with prednisone alone (NCT00887198)<sup>147</sup>. In a phase II trial for women with triple negative, AR+ locally advanced or metastatic breast cancer (NCT01842321), treatment with abiraterone acetate and prednisone also provided benefit for some patients<sup>148</sup>. Of 138 patients assessed for the trial, 53 (37.6%) had AR+ TNBC: 34 of these patients were included. This trial assessed the clinical benefit rate (CBR) for 30 of the patients at 6 months with a CBR of 20.0% (95% CI: 7.7-38.6%) including one patient who had a complete response (CR) and 5 patients with stable disease (SD) at  $\geq$  6 months<sup>148</sup>. Secondary outcomes included objective response rate (6.7%, 95% CI: 0.8-22.1%), and progression free survival (median time: 2.8 months, 95% CI

1.7-5.4)<sup>148</sup>. These studies suggest that treatment with abiraterone acetate may be a beneficial treatment strategy for both men with CRPC and women with molecular apocrine breast cancer.

Other CYP17-lyase inhibitors include galeterone (TOK-001) and orteronel (TAK-700)<sup>149</sup>. Galeterone has been shown to be effective in reduction of prostate specific antigen (PSA) levels and was well tolerated in patients in early clinical trials<sup>150</sup>. Orteronel treatment is effective at suppressing testosterone levels and shrinking the androgen-dependent organs including the prostate gland<sup>151</sup>. Phase III clinical trials found that orteronel and prednisone treatment verses placebo and prednisone gave patients longer progression free survival (PFS); however, men with orteronel and prednisone treatment did not have extended overall survival<sup>152</sup>. In breast cancer, there are currently phase I and II clinical trials assessing the use of orteronel in patients with metastatic breast cancer expressing the androgen receptor (NCT01808040, NCT01990209). NCT01808040 assesses the safety of orteronel use for the treatment of postmenopausal women with hormone receptor positive metastatic breast cancer in addition to measuring the estradiol levels in these patients following treatment<sup>153</sup>. NCT01990209 is a phase II trial for male or female patients with metastatic AR+ BC (TNBC or ER+ and/or PR+ BC) with primary outcome measures of response and disease control rates. This trial will also assess safety, PFS, OS, and serum hormone levels in addition to screening tumors for PTEN expression and PIK3CA mutations. Due to failure in phase III clinical trials in men with prostate cancer, orteronel was taken out of development in 2014<sup>154</sup>.

#### ***1.9.4 Anti-Androgens***

Anti-androgens are a class of agents which act as nonsteroidal competitive inhibitors of the androgen receptor<sup>155</sup>. Flutamide and bicalutamide are two such agents that have been used to block androgen binding and abrogate nuclear AR signaling. Although AR targeting has been a

strategy for over 30 years, original phase II clinical trials with flutamide suggested it did not have anti-tumor activity which delayed the initiation of further trials with the drug<sup>156</sup>. Recent studies, however, have shown that flutamide treatment is effective and well-tolerated for treating PSA recurrence following prostatectomy, radiation therapy, or cryotherapy for patients with prostate cancer<sup>157</sup>. In addition, in breast cancer, bicalutamide has been shown to have a clinical benefit rate of 19% in patients with AR+, ER-, PR- metastatic breast cancer where 12% of tumors were AR+<sup>158</sup>. These results suggest that anti-androgen therapies are effective for the treatment of patients with traditionally hormone receptor-negative breast cancers. Unfortunately, in prostate cancer, it has been shown that exposure to anti-androgens can augment frequency of AR mutations and variants<sup>159</sup>, and metabolites of anti-androgens can result in stimulation of prostate cancer cell growth as flutamide metabolites function as an AR agonist<sup>160</sup>. There are additional ongoing clinical trials that are assessing the use of flutamide as a second line treatment of patients with CRPC who have relapsed after ADT and bicalutamide treatment (NCT02918968) or using flutamide treatment to prevent prostate cancer in patients with neoplasia of the prostate (NCT00006214). In addition, NCT02910050 is investigating the use of bicalutamide with aromatase inhibitors in AR+, ER+ breast cancers<sup>161</sup>.

### ***1.9.5 Second Generation Anti-Androgens***

Four FDA-approved second-generation anti-androgens, abiraterone acetate, apalutamide, darolutamide, and enzalutamide, improve upon the first-generation anti-androgens. Enzalutamide is able to inhibit the growth of both ER+ and ER- breast tumors by inhibiting AR nuclear translocation<sup>146</sup>. In addition to growth inhibition, enzalutamide also can inhibit tumor cell migration and invasion<sup>162</sup>. In mCRPC patients who had previously received chemotherapy treatment, treatment with enzalutamide also contributed to prolonged survival



(NCT00974311)<sup>163</sup>. In breast cancer, a Phase II trial (NCT01889238) for women with advanced, AR+ TNBC tested the use of enzalutamide for improving outcomes and clinical benefit rate for patients at 16 weeks (CBR16) as well as assessing clinical benefit at 24 weeks (CBR24), PFS, response rates, and safety of enzalutamide treatment<sup>164</sup>. This study also found that 47% of the 118 enrolled patients had an AR related gene signature, and clinical outcomes were better for patients with AR+ disease<sup>164</sup>. No new side effects were reported from enzalutamide treatment in this trial, indicating its potential use as a therapeutic for women with TNBC<sup>164</sup>.

Apalutamide (ARN-509) is a second generation AR antagonist similar to enzalutamide that binds to the LBD of AR to inhibit nuclear translocation and ARE binding<sup>149</sup>. Apalutamide has a seven- to ten-fold increased binding affinity to AR compared to bicalutamide<sup>165</sup>. In preclinical studies, apalutamide had anti-tumor activity in a castration-sensitive model of prostate cancer<sup>166</sup>. There were also lower levels of apalutamide in mouse steady-state plasma and brain levels compared to enzalutamide treatment, which could indicate lower frequency of seizures with apalutamide<sup>166</sup>. In preclinical studies, apalutamide also had antitumor and growth inhibitory effects in AR+ TNBC cells<sup>166</sup>. Results from the SPARTAN trial, a Phase III clinical trial (NCT01946204) for men with non-metastatic castration-resistant prostate cancer (nmCRPC), demonstrated improved metastasis free survival in patients treated with apalutamide compared to placebo<sup>167</sup>. Following this trial, apalutamide was approved by the FDA for treatment of nmCRPC<sup>165</sup>. To date, there have been no trials with apalutamide in patients with AR+ breast cancer.

Darolutamide (ODM-201) is an AR inhibitor that binds wild-type AR with a higher affinity than enzalutamide to block AR nuclear translocation<sup>149</sup>. In addition, darolutamide can be effective against mutant AR variants which can develop with resistance to enzalutamide and

apalutamide therapy<sup>168</sup>. In prostate models, darolutamide has low brain-penetrance and treatment does not produce an increase in mouse serum testosterone levels<sup>168</sup>. Recently, results from the ARAMIS trial (NCT02200614), a phase III trial for nmCRPC patients, demonstrate that darolutamide provides better metastasis-free survival compared to placebo<sup>169</sup>. The START trial is a phase II trial for women with AR+ TNBC comparing darolutamide treatment with capecitabine, an anti-metabolite chemotherapeutic (NCT03383679). This trial investigates CBR16 as a primary objective, and CBR24, response rates, overall survival, PFS, and safety as secondary objectives for women with locally recurrent or metastatic AR+ TNBC.

### ***1.9.6 Novel Compounds***

A number of novel compounds have also been developed to block or abrogate androgen signaling. Seviteronel (VT-464) is a nonsteroidal selective CYP17 lyase inhibitor and AR antagonist that both blocks testosterone and estrogen production and inhibits AR activation<sup>170</sup>, rendering it a potentially effective alternative to agents which either inhibit androgen production or AR activation. Clinical trials for patients with ER+ or TNBC indicated that seviteronel was well-tolerated in women, with the majority of adverse events (AEs) being Grade 1/2, in addition to four Grade 3/4 AEs that may be related to seviteronel treatment<sup>171</sup>. Phase I trials in CRPC patients suggest that seviteronel may be an effective treatment alternative for men who are not responsive on other therapies with most reported AEs being Grade 1/2<sup>172</sup>. Preclinical work in AR+ TNBC demonstrates that seviteronel inhibits cell proliferation and growth on soft agar<sup>173</sup>. ChIP-seq and RNA-seq analyses demonstrate that AR regulated genes are increased with DHT stimulation and decreased in mice treated with seviteronel<sup>173</sup>. Trials with seviteronel continue to be ongoing for patients with CRPC, AR+ TNBC, or men with ER+ breast cancer, who had previously been treated with enzalutamide (NCT02130700, NCT02012920, NCT02580448,

NCT03600467). The CLARITY-01 trial (NCT02580448) is assessing the CBR at 16 or 24 weeks for women with ER+ or TNBC or men with locally advanced or metastatic breast cancer who are receiving seviteronel treatment<sup>174</sup>. Of the patients enrolled for stage 1, CBR16 for TNBC patients was 2 of 6, and CBR24 for ER+ patients was 2 of 11<sup>174</sup>. Of patients with CTCs, 7 of 10 had a CTC decline at C2D1<sup>174</sup>. Patients receiving seviteronel also had a decline from baseline in concentrations of estradiol and testosterone<sup>175</sup>. The most common adverse events were tremor, pain, fatigue and dyspnea, nausea, AST increase, ALT increase and abdominal pain, suggesting that seviteronel was well tolerated<sup>175</sup>. These results indicate that seviteronel may be a potential therapeutic option for the treatment of AR+ disease.

CR1447 (4-hydroxytestosterone [4-OHT]) is a novel AR inhibitor that acts both as a steroidal aromatase inhibitor (AI) as well as an AR-antagonist by binding to AR<sup>176</sup>. When injected, 4-OHT is converted to 4-hydroxyandrostenedione (4-OHA), a previously used form of AI that was injected for the treatment of breast cancer<sup>176</sup>. Both 4-OHT and 4-OHA are unable to be made into estrogens *in vivo*<sup>176</sup>. Preclinically, CR1447 has been shown to inhibit growth of AR+ BC cell lines, but not AR knockout cell lines, or those with siRNA mediated AR knockdown<sup>176</sup>. Results from a Phase I clinical trial (NCT02067741) indicate that, when topically administered, CR1447 was well-tolerated with grade 1/2 AEs and no dose-limiting toxicities (DLTs) in 12 patients with ER+/HER2- breast cancer<sup>176</sup>. Two patients (17%) had stable disease after 12 weeks of treatment<sup>176</sup>. Therefore, CR1447 may also be viable treatment option.

Enobosarm is a selective androgen receptor modulator (SARM) that was originally tested in Phase I, II, and III clinical trials for its use in improving lean body mass and treating cachexia<sup>177</sup>. Enobosarm has tissue specific activity, with anabolic activity in muscles and bone without affecting growth of hair in women and prostate in men<sup>178</sup>. It has been well-tolerated by

both men and women; additionally, in patients with advanced cancer, treatment with enobosarm leads to an increase in lean body mass<sup>179</sup>. Enobosarm has also been well-tolerated as an androgen agonist in women with AR+ metastatic breast cancer<sup>180</sup>. Androgen-based AR agonists have previously been shown to be effective for the treatment of breast cancer<sup>181</sup>, and enobosarm similarly stimulates AR, but unlike androgens, does not have masculinizing side-effects<sup>182</sup>. A phase II trial (NCT01616758) assesses CBR, and PSA is evaluated as a biomarker of AR activity. In addition, NCT02971761 is investigating the use of pembrolizumab with enobosarm for AR+ TNBC patients<sup>183</sup>. Enobosarm may soon join the treatment armamentarium.

Antisense oligonucleotides (ASOs) have also been used to inhibit AR-driven gene expression, especially in contexts where AR is activated independent of hormone binding. ASOs bind to mRNA, causing the mRNA to be degraded, therefore reducing levels available for protein synthesis. Prostate cancer models have shown that ASOs are able to reduce AR expression, resulting in decreased cell growth<sup>184,185</sup>. In addition, ASOs used against AR mRNA were able to shut down the downstream activation of AR-mediated genes in hormone-independent conditions<sup>186</sup>. ASO administration in mouse models did not have any observed side effects and, compared to castration, did not result in shrinking of mouse prostates<sup>185</sup>. Use of ASOs may also be a method for targeting AR splice variants as two ASOs have been used to effectively silence AR-V7, but not full-length AR signaling in CRPC cell lines<sup>187</sup>. Therefore, these findings suggest that the use of ASOs may be a useful strategy for overcoming the resistance that often develops to anti-androgens in prostate cancer. In addition, ASOs may also be an effective treatment strategy for targeting mutant AR variants.

Targeted degradation of proteins with the use of Proteolysis Targeting Chimeras (PROTACs) is a novel method for the inhibition of AR signaling in prostate cancer cell models.

PROTAC-mediated degradation takes advantage of E3 ubiquitin ligase activity by linking a ligand for the target protein to a ligand for the E3 ubiquitin ligase<sup>188</sup>. Upon ligand binding to the protein of interest, the protein is ubiquitinated by the E3 ubiquitin ligase resulting in degradation by the 26S proteasome. Multiple AR degraders have been developed using PROTAC for use in prostate cancer<sup>189,190</sup>, and they have been shown to be more effective than enzalutamide in vitro and in vivo in models of enzalutamide-sensitive and resistant prostate cancer<sup>191,192</sup>. Enhanced efficacy of AR degraders in prostate cancer models may demonstrate the importance of removing AR protein as opposed to pharmacologically inhibiting AR activity for the treatment of resistant prostate cancers. In the future, pharmacologic AR degraders may be introduced clinically for the treatment of aggressive AR-driven cancers.

There are also additional compounds that have limited use in treating AR driven disease. Ketoconazole is an anti-fungal agent that is also able to competitively bind to the androgen receptor<sup>193</sup>. Ketoconazole has also been shown to inhibit enzymes important for testosterone synthesis<sup>194</sup> and is under investigation in combination with docetaxel (NCT00212095)<sup>195</sup>. In addition, TRC253, a novel competitive inhibitor of AR has been shown to be an antagonist to wild type AR as well as all tested AR mutants<sup>196</sup>, including AR F876L, a mutation occurring in the LBD of AR<sup>197</sup>.

## **1.10 Combination Therapies**

### ***1.10.1 AR + Radiation Therapy***

#### *Prostate Cancer*

Radiotherapy has been shown to induce AR expression in prostate cancer cells, and ADT sensitizes cancer cells to radiotherapy<sup>198</sup>. Treatment with enzalutamide was also shown to

radiosensitize prostate cancer cells more effectively than ADT<sup>199</sup>. Combination treatment with enzalutamide and radiation therapy resulted in a significant increase in apoptosis and senescence compared to treatment with enzalutamide or radiation alone<sup>199</sup>. In prostate cancer, radiosensitization was also observed with ARN-509<sup>97</sup>. In addition, treatment with anti-androgen therapies resulted in the downregulation of DNA repair genes, thereby promoting radiosensitivity through a decrease in NHEJ activity<sup>97</sup>.

### *Breast Cancer*

The androgen receptor has been shown to be a potential mediator of radioresistance and a target for the radiosensitization of AR+ TNBC<sup>100,101,102,200</sup>. Inhibition of AR with enzalutamide results in increased radiosensitization of AR+ breast cancer cells through the inhibition of AR-activated DNA-PKcs-mediated repair<sup>100</sup>. Similar results were observed with seviteronel, the dual CYP17 inhibitor and AR antagonist<sup>101</sup>, however the differences in the mechanisms of radiosensitization with these agents need to be further assessed.

#### ***1.10.2 AR + PARP inhibitors***

### *Prostate Cancer*

Poly ADP-ribose polymerase (PARP) is a nuclear enzyme that modifies substrates through the addition of PAR moieties<sup>201</sup>. Cancers with mutations to BRCA1 or BRCA2 have HR deficiencies, rendering them increasingly susceptible to treatment with PARP inhibitors.

Inhibition of PARP in tumors with BRCA mutations results in synthetic lethality and forces cells to rely on NHEJ for repair of DNA breaks. PARP has been shown to be recruited to sites of AR binding and promotes AR function<sup>201</sup>. When AR is inhibited, HR deficiency and BRCAness is induced<sup>202</sup>. Therefore, AR activity is important for the maintenance of HR gene expression.

Following ADT, PARP levels are elevated leading to prostate cancer cell survival<sup>203</sup>.

Combination therapy of PARP inhibition with ADT may be important for the impairment of HR before the tumors become castration resistant<sup>203</sup>.

PARP also plays an important role in the AR signaling cascade. Combination treatment with the PARP inhibitor talazoparib with enzalutamide or abiraterone acetate has significant synergy<sup>204</sup>. Anti-androgen therapies induce PARP cleavage, resulting in an increase in dsDNA breaks<sup>204</sup>. This synergy is a therapeutic target for CRPC patients with mutations in DNA damage repair. Therefore, cancer cells with DNA damage repair mutations are more sensitive to PARP inhibitors due to the role of the AR in the transcriptional regulation of DDR genes<sup>205</sup>.

### *Breast Cancer*

PARPi has been established to be an effective treatment strategy for patients with breast cancers harboring mutant BRCA1 and BRCA2<sup>206</sup>. To date, the combination therapy of PARPi with anti-AR therapy has not been tested in breast cancer; however, this combination may be an effective treatment strategy for AR+ BC patients, especially those with BRCA mutated tumors. Because many PARPi can induce PARP trapping, resulting in the formation of dsDNA lesions<sup>207</sup>, and anti-AR therapies have been demonstrated to result in a delay in dsDNA break repair in the presence of DNA damage, combining these therapies may be effective in creating deleterious lesions for tumor cells. Future work may assess PARPi in combination with anti-AR therapies for the treatment of AR+ breast cancers.

#### ***1.10.3 AR + CDK4/6 inhibitors***

## *Prostate Cancer*

AR regulates cell cycle progression through the G1-S phase transition, therefore promoting CDK activity and inducing phosphorylation for the inactivation of pRb<sup>105</sup>. Due to crosstalk of AR with CDK/pRb in promoting cell cycle progression, combined AR and CDK4/6 inhibition has also been shown to be a therapeutic strategy in prostate cancer<sup>208</sup>.

## *Breast Cancer*

Palbociclib, ribociclib, and abemaciclib are selective inhibitors of CDK4/6 and are widely used for the treatment for ER+ breast cancer. A Phase I/II clinical trial is currently assessing the use of palbociclib with bicalutamide for treatment of AR+ metastatic TNBC (NCT02605486). This trial will establish recommended doses for the combination therapy in addition to measuring PFS, and secondary outcomes including response rates, CBR, and safety<sup>209</sup>.

### **1.10.4 AR + PI3K inhibitors**

#### *Prostate and Breast Cancer*

Phosphatidylinositol 3-kinase (PI3K) is an enzyme involved in cellular functions including cell growth, proliferation, and differentiation; however, PI3K is also highly mutated in cancer. Qi et al. found that inhibition of both AR and PI3K can be synergistic as AR and PI3K signaling work through reciprocal feedback loops<sup>210</sup>. Combined inhibition of AR with the PI3K or mTOR pathway suppressed cell proliferation and resulted in an increase in apoptosis and cell cycle arrest in CRPC cells<sup>210</sup>. An ongoing trial is investigating the treatment of taselisib, a PI3K inhibitor, and enzalutamide in patients with AR+ metastatic TNBC (NCT02457910). This trial



will assess dose limiting toxicities to determine the maximum tolerated dose in addition to measuring patient response and CBR<sup>211</sup>.

### **1.11 Phase III Development of Anti-Androgen Treatments**

Many anti-androgen treatment strategies have been effectively translated from preclinical studies into clinical use through the use of clinical trials. For women with metastatic, AR+ TNBC, there is a phase III clinical trial (NCT03055312) underway comparing conventional chemotherapy to bicalutamide treatment. This trial will assess the CBR at 16 weeks as well as progression free survival at 24 months. The ENDEAR trial (NCT02929576) is a phase III trial comparing PFS for patients treated with paclitaxel chemotherapy +/- enzalutamide or enzalutamide followed by paclitaxel treatment; however, this trial was withdrawn. Finally, there is an ongoing feasibility trial (NCT02750358) of enzalutamide in women with AR+ TNBC that should report preliminary DFS and OS data in the coming year<sup>212,213</sup>. Data recently presented from this trial reported that enzalutamide treatment is feasible and well-tolerated in this patient population. Finally, phase I/II clinical trials continue to inform drug development and clinical practice, including trials of newer generation anti-androgen agents in women with AR+ breast cancer. Additional studies are needed to better understand use of anti-androgen therapies for the treatment of women with AR+ breast cancers.

### **1.12 Conclusion**

While the role of AR in prostate cancer is more completely understood, the importance of AR signaling in breast cancer is an area of increasing investigation. In order to understand the mechanism of AR signaling and to design proper therapies against AR in breast cancer, additional work needs to be done to elucidate the mechanism by which AR is activating its target

genes and contributing to tumor growth and metastasis, as well as systemic and radiation therapy resistance. Advancements in this mechanistic understanding will shed light on potential combination therapies and will allow for more effective treatment for patients with AR+ breast cancers. Further, discerning the intricacies and crosstalk between AR and ER signaling may also provide advancements for treatment of AR+, ER+ breast cancers. These outcomes would be impactful not only for the advanced understanding of the role of AR, but also for new ways in which AR signaling can be inhibited to improve outcomes for women with AR+ breast cancer.

### **1.13 Acknowledgements**

The authors thank Steve Kronenberg for his assistance in creating the figure and illustration. A.R.M. is supported by T32-GM007315. Funding for this work was generously provided in part by a grant from the Breast Cancer Research Foundation (N02600 to L.J.P.) and the University of Michigan Rogel Cancer Center Breast Strategic Fund (P30 F049977 to C.S.).

## 1.14 Figure

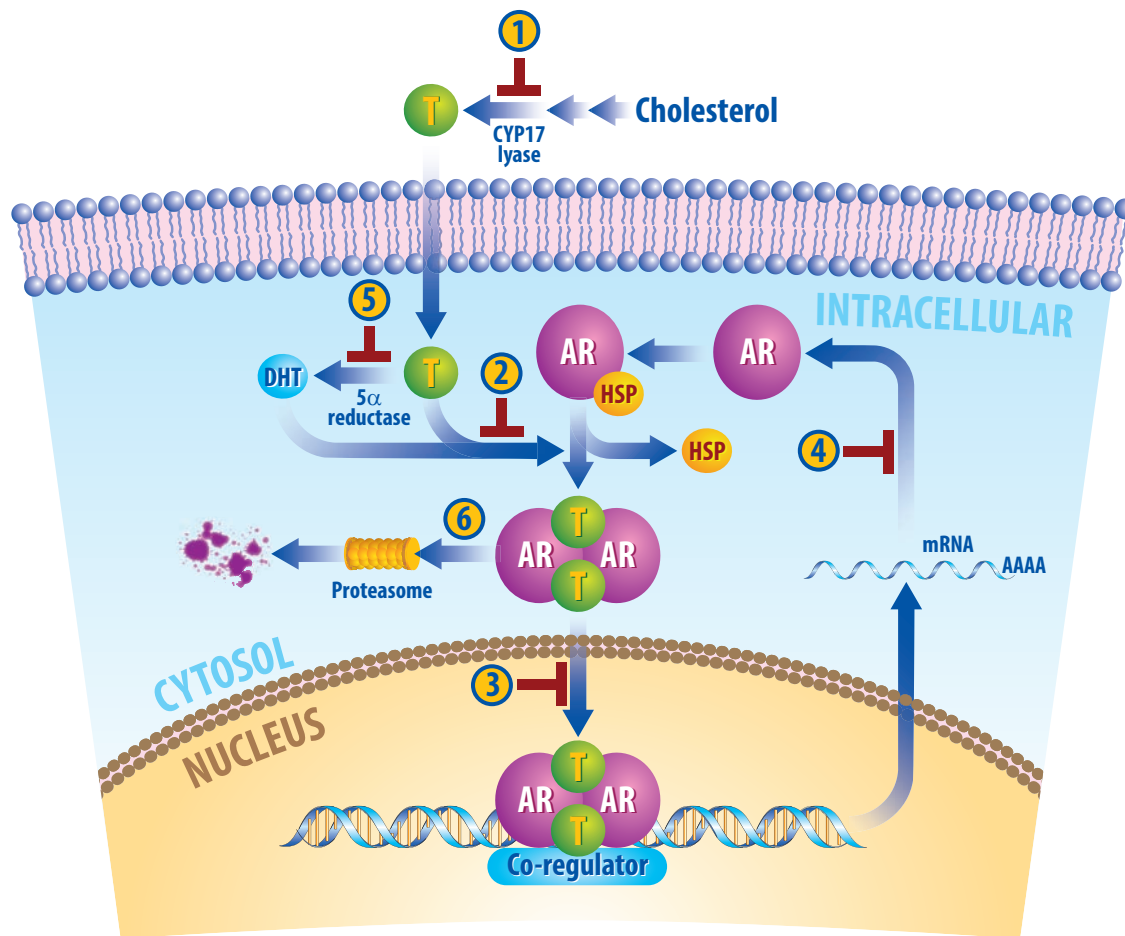


**Figure 1-1: Therapeutic strategies used to inhibit AR signaling**

Androgens like testosterone (T) are produced from cholesterol. CYP17 lyase inhibitors and aromatase inhibitors (1), including abiraterone acetate, seviteronel, CR1447, orteronel, galeterone, block the conversion of cholesterol into testosterone. Additionally, luteinizing hormone-releasing hormone (LHRH) or gonadotrophin-releasing hormone (GnRH) antagonists function to reduce levels of circulating androgens, and ketoconazole inhibits production of testosterone. When androgens enter the cell, they can be converted to DHT, a more potent AR agonist. This reaction requires 5 $\alpha$ -reductase, an enzyme that can be inhibited by finasteride and dutasteride (5). Anti-androgens (2), including flutamide, bicalutamide, enzalutamide, apalutamide, darolutamide, CR1447, seviteronel, and TRC253, block androgen binding to AR or inhibit AR function. Many anti-androgens, including enzalutamide, apalutamide and darolutamide, inhibit nuclear translation of AR, preventing DNA binding and downstream gene transcription. Anti-sense oligonucleotides bind to mRNA encoding AR, preventing protein translation (4). AR degraders (6) promote protein ubiquitination and proteasomal-mediated degradation to lower AR protein levels intracellularly.

## 1.15 Tables

**Table 1-1: Current clinical trials in women with breast cancer assessing the safety and/or efficacy of androgen receptor inhibition**

NCT Number	Title	Category	AR Agent	Additional Interventions	Phase
NCT03444025	Neoadjuvant Goserelin for Triple Negative Breast Cancer	ADT	Goserelin	Chemotherapy	Phase 2
NCT01352091	Adjuvant AI Combined With Zoladex	ADT	Goserelin	Anastrozole, Tamoxifen	Phase 3
NCT03878524	A Personalized Medicine Study for Patients With Advanced Cancer of the Breast, Prostate, Pancreas or Those With Refractory Acute Myelogenous Leukemia	CYP17 Lyase Inhibitor/anti-androgen	Abiraterone/Enzalutamide	Abiraterone, Enzalutamide, Venetoclax, Palbociclib, All-trans Retinoic Acid, Bortezomib, Cabazitaxel, Oxaliplatin, Fluorouracil, Folinic acid, Carboplatin, Panobinostat, Vorinostat, Pembrolizumab, Bevacizumab, Ipilimumab, Nivolumab, Everolimus, Sirolimus, Celecoxib, Olaparib, Afatinib, Cabozantinib, Sorafenib, Dasatinib, Erlotinib, Idelalisib, Imatinib, Lenvatinib, Pertuzumab, Ponatinib, Ruxolitinib, Sunitinib, Trametinib, Vemurafenib	Phase 1
NCT03090165	Ribociclib and Bicalutamide in AR+ TNBC	anti-androgen	Bicalutamide	Ribociclib	Phase 1/2
NCT02353988	AR-inhibitor Bicalutamide in Treating Patients With TNBC	anti-androgen	Bicalutamide	Physician's Choice	Phase 2
NCT03650894	Nivolumab, Ipilimumab, and Bicalutamide in Human Epidermal Growth Factor (HER) 2 Negative Breast Cancer Patients	anti-androgen	Bicalutamide	Nivolumab, Ipilimumab	Phase 2
NCT02299999	SAFIR02_Breast - Efficacy of Genome Analysis as a Therapeutic Decision Tool for Patients With Metastatic Breast Cancer	anti-androgen	Bicalutamide	Targeted Therapies, Chemotherapy	Phase 2

<b>NCT03055312</b>	Bicalutamide in Treatment of Androgen Receptor (AR) Positive Metastatic Triple Negative Breast Cancer	anti-androgen	Bicalutamide	TPC Chemotherapy	Phase 3
<b>NCT03383679</b>	Study on Androgen Receptor and Triple Negative Breast Cancer	anti-androgen	Darolutamide	Capecitabine	Phase 2
<b>NCT03207529</b>	Alpelisib and Enzalutamide in Treating Patients With Androgen Receptor and PTEN Positive Metastatic Breast Cancer	anti-androgen	Enzalutamide	Alpelisib	Phase 1
<b>NCT02689427</b>	Enzalutamide and Paclitaxel Before Surgery in Treating Patients With Stage I-III Androgen Receptor-Positive Triple-Negative Breast Cancer	anti-androgen	Enzalutamide	Paclitaxel, Surgery	Phase 2
<b>NCT02953860</b>	Fulvestrant Plus Enzalutamide in ER+/Her2- Advanced Breast Cancer	anti-androgen	Enzalutamide	Fulvestrant	Phase 2
<b>NCT02955394</b>	Preoperative Fulvestrant With or Without Enzalutamide in ER+/Her2- Breast Cancer	anti-androgen	Enzalutamide	Fulvestrant	Phase 2
<b>NCT02676986</b>	Short-term Preoperative Treatment With Enzalutamide, Alone or in Combination With Exemestane in Primary Breast Cancer	anti-androgen	Enzalutamide	Exemestane	Phase 2
<b>NCT00755885</b>	Abiraterone Acetate in Treating Postmenopausal Women With Advanced or Metastatic Breast Cancer	CYP17 Lyase Inhibitor	Abiraterone Acetate		Phase 1/2
<b>NCT01990209</b>	Orteronel as Monotherapy in Patients With Metastatic Breast Cancer (MBC) That Expresses the Androgen Receptor (AR)	CYP17 Lyase Inhibitor	Orteronel		Phase 2
<b>NCT01616758</b>	Phase II Study of GTx024 in Women With Metastatic Breast Cancer	SARM	Enobosarm		Phase 2
<b>NCT02463032</b>	Efficacy and Safety of GTx-024 in Patients With ER+/AR+ Breast Cancer	SARM	Enobosarm		Phase 2
<b>NCT02144051</b>	Phase I Open Label Dose Escalation Study to Investigate the Safety & Pharmacokinetics of AZD5312 in Patients With Androgen Receptor Tumors	Antisense Oligonucleotides	AZD5312		Phase 1

**Table 1-2: Results from completed and ongoing clinical trials investigating the use of androgen receptor inhibition in women with breast cancer**

NCT Number	Title	Phase	Treatments Tested	Actual or Planned Patients	Primary Endpoint	Secondary Endpoints	Three Most Common Adverse Events
NCT00186121	Estradiol Suppression for the Treatment of Metastatic Breast Cancer in Premenopausal Women	Phase II single arm	Anastrozole + Goserelin	35 pts	ORR: 37.5% (95% CI: 21-56%)	CBR: 71.9% (95% CI: 53-86%) Response Rate: CR: 1 pt (3%), PR: 11 pts (34%), SD: 11 pts (34%) TTP: 8.3 (2.1 to NA)* OS: NA (11.1 to NA) <sup>†</sup> SAE: 0 Estradiol Suppression at baseline: 7.47 pg/mL; 1 month: 20.8 pg/mL; 3 months: 18.7 pg/mL; 6 months: 14.8 pg/mL	Hot flush (60%) Arthralgia (53%) Fatigue (50%)
NCT02067741	CR1447 in Endocrine Responsive-HER2neg and AR+ TNBC	Phase I/II	CR1447	29 pts	MTD: 400 mg/day	DC at 24 weeks: 0 pts (0%) SD at 12 weeks: 2 pts (14%) PD at 12 weeks: 11 pts (79%) 4-OHT $T_{max}$ : 16 hr (range: 1.0-72.0) 4-OHT $C_{max}$ : 0.63 ng/mL (range: 0.0-1.88) median AUC0-72: 27.2 h*ng/mL (range: 0.0-69.8)	Elevated Triglycerides (57%) Anemia (50%) Elevated AST (29%) Elevated AP (29%) High creatinine (29%)
NCT00468715	Bicalutamide in Treating Patients With Metastatic Breast Cancer	Phase II	Bicalutamide	28 pts	CBR (6 mo): 19% (95% CI: 7-39%) CBR (6 mo, ITT): 18% (95% CI: 6-37%)	Median PFS: 12 weeks (95% CI: 11-22 weeks)	Elevated AST (25%) Fatigue (21%) Hot Flashes (21%) Limb Edema (21%)
NCT02910050	Bicalutamide Plus Aromatase Inhibitors in ER(+)/AR(+)/HER2(-) Metastatic Breast Cancer	Phase II Single arm	Bicalutamide + Aromatase Inhibitors	58 pts	CBR (6 mo): 16.7% CR: 0 pts (0%) PR: 0 pts (0%) SD: 3 pts (17%) PD: 15 pts (83%)	PFS: 2.7 mo (95% CI: 2.2-3.8 mo)	Tumor Pain (17%) Alopecia (6%) Hot Flashes (6%) Peripheral sensory neuropathy (6%) Insomnia (6%) Hypertension (6%)
NCT02605486	Palbociclib in Combination With	Phase I/II	Bicalutamide + Palbociclib	51 pts	The MTD was 150 mg Bicalutamide		Neutropenia (33%) Leukopenia (27%)

	Bicalutamide for the Treatment of AR(+) Metastatic Breast Cancer (MBC)				daily and 125 mg Palbociclib daily for 21 days in a 28 day cycle.		Lymphocytopenia (20%)
<b>NCT02457910</b>	Taselisib and Enzalutamide in Treating Patients With Androgen Receptor Positive Triple-Negative Metastatic Breast Cancer	Phase I/II	Enzalutamide + Taselisib	73 pts	MTD was not reached: 160 mg enzalutamide with 4 mg taselisib had manageable toxicities.  CBR (16 weeks, evaluable population): 35.7%	PFS (evaluable population): 3.4 mo	Phase I: Metabolism and Nutrition (25%), Rash maculopapular (25%), Rash acneiform (8%), Elevated alkaline phosphatase (8%)  Phase II: Rash maculopapular (29%), Rash acneiform (12%), Fatigue (12%)
<b>NCT01597193</b>	Safety Study of Enzalutamide (MDV3100) in Patients With Incurable Breast Cancer	Phase I	Enzalutamide ± Aromatase Inhibitors/SER D	101 pts	MTD not yet reported. 160 mg Enzalutamide: 22 patients, 3 AE 160 mg Enzalutamide + 1 mg Anastrozole: 20 patients, 1 AE 160 mg Enzalutamide + 50 mg Exemestane: 23 patients, 3 AEs 160 mg Enzalutamide + 500 mg Fulvestrant: 11 patients, 2 AEs	Enzalutamide: 4 pts with ≥ Grade 3 AE; 1 pt discontinued treatment due to AEs Enzalutamide + Anastrozole: 6 pts with ≥ Grade 3 AE; 1 pt discontinued treatment due to AEs Enzalutamide + Exemestane: 9 pts with ≥ Grade 3 AE; 3 pts discontinued treatment due to AEs Enzalutamide + Fulvestrant: 4 pts with ≥ Grade 3 AE  Maximum Plasma Concentration (C <sub>max</sub> ) of Enzalutamide and Metabolites after single dosing (Enzalutamide 160 mg) [□g/mL]: Enzalutamide: 4.01 (2.09); M1 (Carboxylic Acid): 0.0707 (0.0379); M2 (N-desmethyl): 0.184 (0.0689) AUC 24hr after single dosing (Enzalutamide 160 mg) [□g*hr/mL]: Enzalutamide: 41.6 (8.19); M1: 1.20 (0.648); M2: 2.76 (1.00)	Enzalutamide: Nausea (50%), Fatigue (45%), Back Pain (27%), Cough (27%)  Enzalutamide + Anastrozole: Fatigue (60%), Decreased Appetite (50%), Nausea (45%)  Enzalutamide + Exemestane: Fatigue (52%), Nausea (52%), Vomiting (30%)  Enzalutamide + Fulvestrant: Fatigue (73%),

						Terminal Elimination Half Life after Single Dosing (Enzalutamide 160 mg): 198 hrs (105)	Nausea (73%), Back Pain (55%)
<b>NCT02091960</b>	A Study to Assess the Efficacy and Safety of Enzalutamide With Trastuzumab in Patients With Human Epidermal Growth Factor Receptor 2 Positive (HER2+), Androgen Receptor Positive (AR+) Metastatic or Locally Advanced Breast Cancer	Phase II single arm	Enzalutamide + Trastuzumab	103 pts	CBR: 23.6% (95% CI: 15.2-33.8%)	ORR at Week 24: 3.4% (95% CI: 0.7-9.5) Best ORR: 4.5% (95% 1.2-11.1) PFS: 105 days (95% CI: 61-116) TTP: 108 days (95% CI: 61-116) Duration of Response: NA <sup>#</sup> Time to Response: 57 days (95% CI: 57-222) Patients with AEs: 94% (related to enzalutamide 73%, related to trastuzumab 38%)	Fatigue (34%) Nausea (27%) Hot flush (17%)
<b>NCT02007512</b>	Efficacy and Safety Study of Enzalutamide in Combination With Exemestane in Patients With Advanced Breast Cancer	Phase II	Enzalutamide + exemestane vs. placebo + exemestane	247 pts	Enzalutamide + Exemestane: PFS (ITT): 11.8 mo (7.3-15.9); PFS (DX+): 16.5 mo (11.0-NA <sup>§</sup> ) Enzalutamide: PFS (ITT): 5.8 mo (3.5-10.9); PFS (DX+): 4.3 mo (1.9-10.9) HT + Enzalutamide + Exemestane: PFS (ITT): 3.6 mo (1.9-5.5); PFS (DX+): 6.0 mo (2.3-26.7) HT + Enzalutamide: PFS (ITT): 3.9 mo (2.6-5.4); PFS (DX+): 5.3 mo (1.8-6.7)	Enzalutamide + Exemestane: CBR 24 weeks: 62% (49-74%); Best Objective Response Rate: 31% (17-48%); Duration of Objective Response: 14.0 mo (5.6-NA <sup>§</sup> ); Time to Response: 12.9 mo (7.3-NA <sup>§</sup> ); Time to Progression: 11.8 mo (7.3-15.9); PFS at 6 mo: 67% (53-77%) Enzalutamide: CBR 24 weeks: 45% (33-58%); Best Objective Response Rate: 19% (9-34%); Duration of Objective Response: 9.1 mo (3.2-10.2 <sup>§</sup> ); Time to Response: 14.0 mo (7.4-NA <sup>§</sup> ); Time to Progression: 7.4 mo (3.5-13.5); PFS at 6 mo: 50% (37-62%) HT + Enzalutamide + Exemestane: CBR 24 weeks: 20% (11-32%); Best Objective Response Rate: 10% (3-23%); Duration of Objective Response: 18.3 mo (3.3-23.1); Time to Response: NA (3.9-NA <sup>§</sup> ); Time to Progression: 3.6 mo (1.9-5.6); PFS at 6 mo: 32% (20-44%)	Combined from all arms: Fatigue (32%) Nausea (26%) Hot Flush (23%)



						HT + Enzalutamide: CBR 24 weeks: 32% (20-45%); Best Objective Response Rate: 5% (0.6-16%); Duration of Objective Response: 4.6 mo (1.9-7.4); Time to Response: NA (NA-NA <sup>§</sup> ); Time to Progression: 3.9 mo (2.6-5.4); PFS at 6 mo: 33% (22-46%)	
<b>NCT01889238</b>	Safety and Efficacy Study of Enzalutamide in Patients With Advanced, Androgen Receptor-Positive, Triple Negative Breast Cancer	Phase II single arm	Enzalutamide	118 pts	CBR (16 weeks, evaluable population): 33% (95% CI: 26-42%) CBR (16 weeks, ITT): 25% (95% CI: 19-31%)	CBR (24 weeks, evaluable population): 28% (95% CI: 21-36%) CBR (24 weeks, ITT): 20% (95% CI: 15-26%) Best Objective Response (evaluable population): 8.5% (95% CI: 3-12%) Best Objective Response (ITT): 6% (95% CI: 3-9%) PFS (evaluable population): 14.3 weeks (95% CI: 8.3-16.1) PFS (ITT): 12.6 weeks (95% CI: 8.1-15.1)	Fatigue (42%) Nausea (34%) Decreased Appetite (19%)
<b>NCT02750358</b>	Feasibility Study of Adjuvant Enzalutamide for the Treatment of Early Stage AR (+) Triple Negative Breast Cancer	Phase III	Enzalutamide	50 pts	As of 6/27/19, 34 pts (68%) completed 1 year of treatment, and 15 pts (30%) were off treatment.		Fatigue (48%) Hot Flashes (22%) Headache (18%) Hyperglycemia (18%) Nausea (18%)
<b>NCT03004534</b>	A Study to Evaluate Changes in Human Breast Cancer Tissue Following Short-Term Use of Darolutamide	Early Phase I single arm	Darolutamide	36 pts	Presurgical Molecular Assessment: AR up (7 pts, 20.6%) AR unchanged (12 pts, 35.3%) AR down (15 pts, 44.1%)	26 pts with TEAE (72%) 10 pts with no TEAE (28%)	Fatigue (22%) Constipation (8%) Diarrhea (8%) Nausea (8%)
<b>NCT02580448</b>	CYP17 Lyase and Androgen Receptor Inhibitor Treatment With Seviteronel Trial (CLARITY-01)	Phase I/II	Seviteronel	175 pts	CBR (16 weeks, TNBC): 2 pts (33%) <sup>‡</sup> CBR (24 weeks, ER+ BC): 2 pts (18%) <sup>‡</sup>	Change in CTC at C2D1: -94.3% (range: -27.5,-100) <sup>‡</sup>	Fatigue (50%) Nausea (43%) Decreased Appetite (33%)

NCT01842321	Abiraterone Acetate in Molecular Apocrine Breast Cancer	Phase II single arm	Abiraterone Acetate + Prednisone	31 pts	<p>CBR (6 mo): 20.0% (95% CI: 8-39%).</p> <p>CR (6 mo): 1 pt (3%)</p> <p>PR (6 mo): 0 pt (0%)</p> <p>SD (6 mo): 5 pts (17%)</p> <p>Progression at 6 mo: (23 pts (77%))</p> <p>Treatment stopped for toxicity before 6 mo evaluation: 1 pt (3%)</p>	<p>ORR: 6.7% (95% CI 0.8-22%)</p> <p>DoR: CR: 23.4 mo; PR: 5.6 mo</p> <p>PFS: 2.8 mo (95% CI: 1.7-5.4)</p>	<p>Fatigue (18%)</p> <p>Hypertension (12%)</p> <p>Hypokalaemia (9%)</p>
NCT00212095	Docetaxel Combined With Ketoconazole in Treatment of Breast Cancer	Phase II	Ketoconazole + Docetaxel	30 pts	<p>Cycles of Docetaxel: 4 (Ketoconazole); 6 (Conventional)</p> <p>Ketoconazole-dosed Docetaxel: 52% of pts had reduction in tumor dimension; CR: 9.7%; PR: 54.8%; ORR: 64.5; SD: 4.1%; PD: 77.6%</p> <p>Conventional-dosed Docetaxel (Doxirubicin): 55% of pts had reduction in tumor dimension; CR: 4.1%; PR: 77.6%; ORR: 81.7%; SD: 16.3%; PD: 2.0%</p>	<p>AUC (mg/l*h): ketoconazole-modulated docetaxel: <math>3.93 \pm 2.77</math>; conventional-dosed docetaxel: <math>3.77 \pm 2.70</math> [p-value = 0.794]</p> <p>Clearance (l/h): ketoconazole-modulated docetaxel: <math>22.05 \pm 8.29</math>; conventional-dosed docetaxel: <math>36.52 \pm 13.39</math> [p-value &lt; 0.001]</p> <p>Half-life (h): ketoconazole-modulated docetaxel: <math>13.46 \pm 5.05</math>; conventional-based docetaxel: <math>12.25 \pm 3.47</math> [p-value = 0.206]</p> <p><math>C_{max}</math> (mg/l): ketoconazole-modulated docetaxel: <math>2.53 \pm 1.14</math>; conventional-based docetaxel: <math>2.68 \pm 1.09</math> [p-value = 0.568]</p>	<p>Fatigue (81%)</p> <p>Diarrhea (58%)</p> <p>Myalgia (36%)</p>
NCT01808040	A Phase 1b Study of TAK-700 in Postmenopausal Women With Hormone-receptor Positive Metastatic Breast Cancer	Phase Ib	Orteronel	8 pts	<p>MTD not yet reported.</p> <p>Dose level 1: 300 mg (4 pts, 1 not evaluated)</p> <p>Dose level 2: 400 mg (3 pts)</p>	<p>1 patient with SD &gt; 6 mo</p> <p>1 patient with SD for 3 mo</p>	<p>Hot Flashes (28%)</p> <p>Nausea (28%)</p> <p>Hypokalemia (28%)</p> <p>Elevated AST (28%)</p>
NCT02971761	Pembrolizumab and Enobosarm in Treating Patients With Androgen Receptor Positive	Phase II	Enobosarm + Pembrolizumab	29 pts	<p>PR: 2 pts (13%)</p> <p>SD at 18 &amp; 19 weeks: 2 pts (13%)</p> <p>PD: 11 pts (69%)</p>		<p>Elevated Liver Function (19%)</p> <p>Diarrhea (13%)</p>

	Metastatic Triple Negative Breast Cancer						6% of the following: adrenal insufficiency, dry skin, headache, hot flashes, hyperhidrosis, hyperthyroidism, or palpitation
--	--	--	--	--	--	--	--

AE: adverse events; CBR: clinical benefit rate; CI: confidence interval; CR: complete response; CTC: circulating tumor cells; DC: disease control; DLT: dose limiting toxicities; DoR: Duration of Overall Response; DX+: diagnostic positive; HT: prior hormone therapy treatment; ITT: intent to treat; MTD: maximum tolerated dose; ORR: objective response rate; PD: progressive disease; PFS: progression free survival; PR: partial response; SAE: serious adverse events; SD: stable disease; TEAE: treatment-related adverse events; TTP: time to progression; \*Upper limit of TTP range was not determined/reached; †The median and upper limit of the range for OS were not reached / not determined. The upper limit exceeded 63 months; #Could not be estimated due to low number of events; §Upper limit of 95% confidence interval or median was not reached due to insufficient number of events at the time of data cutoff; ‡Only Phase 2 Stage 1 results have been reported

## 1.16 References

1. Schweizer, M. T. & Yu, E. Y. AR-Signaling in Human Malignancies: Prostate Cancer and Beyond. *Cancers* **9**, (2017).
2. Hollenberg, S. M. *et al.* Primary structure and expression of a functional human glucocorticoid receptor cDNA. *Nature* **318**, 635–641 (1985).
3. Sullivan, W. P. *et al.* Isolation of steroid receptor binding protein from chicken oviduct and production of monoclonal antibodies. *Biochemistry* **24**, 4214–4222 (1985).
4. Lindquist, S. & Craig, E. A. The Heat-Shock Proteins. *Annu. Rev. Genet.* **22**, 631–677 (1988).
5. Jäättelä, M. Heat shock proteins as cellular lifeguards. *Ann. Med.* **31**, 261–271 (1999).
6. Sarker, D., Reid, A. H. M., Yap, T. A. & Bono, J. S. de. Targeting the PI3K/AKT Pathway for the Treatment of Prostate Cancer. *Clin. Cancer Res.* **15**, 4799–4805 (2009).
7. Visakorpi, T. *et al.* In vivo amplification of the androgen receptor gene and progression of human prostate cancer. *Nat. Genet.* **9**, 401–406 (1995).
8. Gottlieb, B., Beitel, L. K., Nadarajah, A., Paliouras, M. & Trifiro, M. The androgen receptor gene mutations database: 2012 update. *Hum. Mutat.* **33**, 887–894 (2012).
9. Jensen, E. V. & Jordan, V. C. The Estrogen Receptor: A Model for Molecular Medicine. *Clin. Cancer Res.* **9**, 1980–1989 (2003).
10. Jensen, E. V., Block, G. E., Smith, S., Kyser, K. & DeSombre, E. R. Estrogen receptors and breast cancer response to adrenalectomy. *J. Natl. Cancer Inst. Monogr.* **34**, 55–70 (1971).
11. McGuire, W. L., Carbone, P. P. & Vollmer, E. P. Estrogen receptors in human breast cancer. *Raven Press New York* (1975).
12. Lumachi, F., Brunello, A., Maruzzo, M., Basso, U. & Basso, S. M. M. Treatment of estrogen receptor-positive breast cancer. *Curr. Med. Chem.* **20**, 596–604 (2013).
13. Goss, P. E. *et al.* A Randomized Trial of Letrozole in Postmenopausal Women after Five Years of Tamoxifen Therapy for Early-Stage Breast Cancer. *N. Engl. J. Med.* **349**, 1793–1802 (2003).
14. Early Breast Cancer Trialists' Collaborative Group. Tamoxifen for early breast cancer: an overview of the randomised trials. *The Lancet* **351**, 1451–1467 (1998).
15. Heuson, J. C. *et al.* Androgen Dependence of Breast Cancers. *The Lancet* **302**, 203–204 (1973).
16. Augello, M. A., Hickey, T. E. & Knudsen, K. E. FOXA1: master of steroid receptor function in cancer. *EMBO J.* **30**, 3885–3894 (2011).
17. Parolia, A. *et al.* Distinct structural classes of activating FOXA1 alterations in advanced prostate cancer. *Nature* **571**, 413–418 (2019).

18. Zhang, C. *et al.* Definition of a FoxA1 Cistrome That Is Crucial for G1 to S-Phase Cell-Cycle Transit in Castration-Resistant Prostate Cancer. *Cancer Res.* **71**, 6738–6748 (2011).
19. Sahu, B. *et al.* Dual role of FoxA1 in androgen receptor binding to chromatin, androgen signalling and prostate cancer. *EMBO J.* **30**, 3962–3976 (2011).
20. Robinson, J. L. L. *et al.* Elevated levels of FOXA1 facilitate androgen receptor chromatin binding resulting in a CRPC-like phenotype. *Oncogene* **33**, 5666–5674 (2014).
21. Laganière, J. *et al.* Location analysis of estrogen receptor  $\alpha$  target promoters reveals that FOXA1 defines a domain of the estrogen response. *Proc. Natl. Acad. Sci.* **102**, 11651–11656 (2005).
22. Robinson, J. L. L. *et al.* Androgen receptor driven transcription in molecular apocrine breast cancer is mediated by FoxA1. *EMBO J.* **30**, 3019–3027 (2011).
23. Hurtado, A., Holmes, K. A., Ross-Innes, C. S., Schmidt, D. & Carroll, J. S. FOXA1 is a key determinant of estrogen receptor function and endocrine response. *Nat. Genet.* **43**, 27–33 (2011).
24. Guiu, S. *et al.* Coexpression of androgen receptor and FOXA1 in nonmetastatic triple-negative breast cancer: ancillary study from PACS08 trial. *Future Oncol. Lond. Engl.* **11**, 2283–2297 (2015).
25. Guiu, S. *et al.* Prognostic value of androgen receptor and FOXA1 co-expression in non-metastatic triple negative breast cancer and correlation with other biomarkers. *Br. J. Cancer* **119**, 76–79 (2018).
26. Robinson, J. L. L., Holmes, K. A. & Carroll, J. S. FOXA1 mutations in hormone-dependent cancers. *Front. Oncol.* **3**, (2013).
27. Wang, Y. *et al.* Differential regulation of *PTEN* expression by androgen receptor in prostate and breast cancers. *Oncogene* **30**, 4327–4338 (2011).
28. Carver, B. S. *et al.* Reciprocal Feedback Regulation of PI3K and Androgen Receptor Signaling in PTEN-Deficient Prostate Cancer. *Cancer Cell* **19**, 575–586 (2011).
29. Lin, H.-K., Hu, Y.-C., Lee, D. K. & Chang, C. Regulation of Androgen Receptor Signaling by PTEN (Phosphatase and Tensin Homolog Deleted on Chromosome 10) Tumor Suppressor through Distinct Mechanisms in Prostate Cancer Cells. *Mol. Endocrinol.* **18**, 2409–2423 (2004).
30. El Sheikh, S. S., Romanska, H. M., Abel, P., Domin, J. & Lalani, E.-N. Predictive Value of PTEN and AR Coexpression of Sustained Responsiveness to Hormonal Therapy in Prostate Cancer—A Pilot Study. *Neoplasia N. Y. N* **10**, 949–953 (2008).
31. Wu, Z., Conaway, M., Gioeli, D., Weber, M. J. & Theodorescu, D. Conditional expression of PTEN alters the androgen responsiveness of prostate cancer cells. *The Prostate* **66**, 1114–1123 (2006).
32. Robinson, D. *et al.* Integrative Clinical Genomics of Advanced Prostate Cancer. *Cell* **161**, 1215–1228 (2015).

33. Rizza, P. *et al.* Estrogen receptor beta as a novel target of androgen receptor action in breast cancer cell lines. *Breast Cancer Res. BCR* **16**, R21 (2014).
34. Karamouzis, M. V., Papavassiliou, K. A., Adamopoulos, C. & Papavassiliou, A. G. Targeting Androgen/Estrogen Receptors Crosstalk in Cancer. *Trends Cancer* **2**, 35–48 (2016).
35. Whang, Y. E. *et al.* Inactivation of the tumor suppressor PTEN/MMAC1 in advanced human prostate cancer through loss of expression. *Proc. Natl. Acad. Sci.* **95**, 5246–5250 (1998).
36. Bedolla, R. *et al.* Determining Risk of Biochemical Recurrence in Prostate Cancer by Immunohistochemical Detection of PTEN Expression and Akt Activation. *Clin. Cancer Res.* **13**, 3860–3867 (2007).
37. Perren, A. *et al.* Immunohistochemical Evidence of Loss of PTEN Expression in Primary Ductal Adenocarcinomas of the Breast. *Am. J. Pathol.* **155**, 1253–1260 (1999).
38. Migliaccio, A. *et al.* Steroid-induced androgen receptor–oestradiol receptor  $\beta$ –Src complex triggers prostate cancer cell proliferation. *EMBO J.* **19**, 5406–5417 (2000).
39. Leung, J. K. & Sadar, M. D. Non-Genomic Actions of the Androgen Receptor in Prostate Cancer. *Front. Endocrinol.* **8**, (2017).
40. Peterziel, H. *et al.* Rapid signalling by androgen receptor in prostate cancer cells. *Oncogene* **18**, 6322–6329 (1999).
41. Liao, R. S. *et al.* Androgen receptor-mediated non-genomic regulation of prostate cancer cell proliferation. *Transl. Androl. Urol.* **2**, 187–196 (2013).
42. Heinlein, C. A. & Chang, C. The Roles of Androgen Receptors and Androgen-Binding Proteins in Nongenomic Androgen Actions. *Mol. Endocrinol.* **16**, 2181–2187 (2002).
43. Thomas, P., Pang, Y., Dong, J. & Berg, A. H. Identification and Characterization of Membrane Androgen Receptors in the ZIP9 Zinc Transporter Subfamily: II. Role of Human ZIP9 in Testosterone-Induced Prostate and Breast Cancer Cell Apoptosis. *Endocrinology* **155**, 4250–4265 (2014).
44. Pi, M., Parrill, A. L. & Quarles, L. D. GPRC6A Mediates the Non-genomic Effects of Steroids. *J. Biol. Chem.* **285**, 39953–39964 (2010).
45. Kalyvianaki, K. *et al.* Antagonizing effects of membrane-acting androgens on the eicosanoid receptor OXER1 in prostate cancer. *Sci. Rep.* **7**, 44418 (2017).
46. Chia, K. M., Liu, J., Francis, G. D. & Naderi, A. A Feedback Loop between Androgen Receptor and ERK Signaling in Estrogen Receptor-Negative Breast Cancer. *Neoplasia N. Y. N* **13**, 154–166 (2011).
47. Bleach, R. & McIlroy, M. The Divergent Function of Androgen Receptor in Breast Cancer; Analysis of Steroid Mediators and Tumor Intracrinology. *Front. Endocrinol.* **9**, (2018).
48. Khatun, A. *et al.* Transcriptional Repression and Protein Degradation of the Ca<sup>2+</sup>-Activated K<sup>+</sup> Channel KCa1.1 by Androgen Receptor Inhibition in Human Breast Cancer Cells. *Front. Physiol.* **9**, (2018).

49. Ren, Q. *et al.* Expression of androgen receptor and its phosphorylated forms in breast cancer progression. *Cancer* **119**, 2532–2540 (2013).
50. Roseweir, A. K. *et al.* Phosphorylation of androgen receptors at serine 515 is a potential prognostic marker for triple negative breast cancer. *Oncotarget* **8**, 37172–37185 (2017).
51. Kampa, M., Pelekanou, V. & Castanas, E. Membrane-initiated steroid action in breast and prostate cancer. *Steroids* **73**, 953–960 (2008).
52. Kalyvianaki, K. *et al.* Membrane androgen receptors (OXER1, GPRC6A AND ZIP9) in prostate and breast cancer: A comparative study of their expression. *Steroids* **142**, 100–108 (2019).
53. Castoria, G. *et al.* Targeting Androgen Receptor/Src Complex Impairs the Aggressive Phenotype of Human Fibrosarcoma Cells. *PLoS ONE* **8**, (2013).
54. Tilley, W. D., Marcelli, M., Wilson, J. D. & McPhaul, M. J. Characterization and expression of a cDNA encoding the human androgen receptor. *Proc. Natl. Acad. Sci. U. S. A.* **86**, 327–331 (1989).
55. Hu, R. *et al.* Ligand-independent androgen receptor variants derived from splicing of cryptic exons signify hormone-refractory prostate cancer. *Cancer Res.* **69**, 16–22 (2009).
56. Dehm, S. M., Schmidt, L. J., Heemers, H. V., Vessella, R. L. & Tindall, D. J. Splicing of a novel AR exon generates a constitutively active androgen receptor that mediates prostate cancer therapy resistance. *Cancer Res.* **68**, 5469–5477 (2008).
57. Antonarakis, E., Armstrong, A., Dehm, S. & Luo, J. Androgen receptor variant-driven prostate cancer: clinical implications and therapeutic targeting. *Prostate Cancer Prostatic Dis.* **19**, 231–241 (2016).
58. Wadosky, K. M. & Koochekpour, S. Androgen receptor splice variants and prostate cancer: From bench to bedside. *Oncotarget* **8**, 18550–18576 (2017).
59. Watson, P. A. *et al.* Constitutively active androgen receptor splice variants expressed in castration-resistant prostate cancer require full-length androgen receptor. *Proc. Natl. Acad. Sci. U. S. A.* **107**, 16759–16765 (2010).
60. Hickey, T. E. *et al.* Expression of androgen receptor splice variants in clinical breast cancers. *Oncotarget* **6**, 44728–44744 (2015).
61. Antonarakis, E. S. *et al.* AR-V7 and Resistance to Enzalutamide and Abiraterone in Prostate Cancer. *N. Engl. J. Med.* **371**, 1028–1038 (2014).
62. Szmulewitz, R. Z. *et al.* Serum/glucocorticoid-regulated kinase 1 expression in primary human prostate cancers. *The Prostate* **72**, 157–164 (2012).
63. Arora, V. K. *et al.* Glucocorticoid Receptor Confers Resistance to Anti-Androgens by Bypassing Androgen Receptor Blockade. *Cell* **155**, 1309–1322 (2013).
64. Christenson, J. L. *et al.* Harnessing a Different Dependency: How to Identify and Target Androgen Receptor-Positive Versus Quadruple-Negative Breast Cancer. *Horm. Cancer* **9**, 82–94 (2018).
65. Hu, D. G. *et al.* Identification of androgen receptor splice variant transcripts in breast cancer cell lines and human tissues. *Horm. Cancer* **5**, 61–71 (2014).

66. Moore, N. L. *et al.* An androgen receptor mutation in the MDA-MB-453 cell line model of molecular apocrine breast cancer compromises receptor activity. *Endocr. Relat. Cancer* **19**, 599–613 (2012).
67. Vera-Badillo, F. E. *et al.* Androgen receptor expression and outcomes in early breast cancer: a systematic review and meta-analysis. *J. Natl. Cancer Inst.* **106**, djt319 (2014).
68. Ogawa, Y. *et al.* Androgen receptor expression in breast cancer: relationship with clinicopathological factors and biomarkers. *Int. J. Clin. Oncol.* **13**, 431–435 (2008).
69. Rangel, N. *et al.* The role of the AR/ER ratio in ER-positive breast cancer patients. *Endocr. Relat. Cancer* **25**, 163–172 (2018).
70. Hammond, M. E. H. *et al.* American Society of Clinical Oncology/College of American Pathologists Guideline Recommendations for Immunohistochemical Testing of Estrogen and Progesterone Receptors in Breast Cancer. *J. Clin. Oncol.* **28**, 2784–2795 (2010).
71. Peters, A. A. *et al.* Androgen Receptor Inhibits Estrogen Receptor- $\alpha$  Activity and Is Prognostic in Breast Cancer. *Cancer Res.* **69**, 6131–6140 (2009).
72. Ricciardelli, C. *et al.* The Magnitude of Androgen Receptor Positivity in Breast Cancer Is Critical for Reliable Prediction of Disease Outcome. *Clin. Cancer Res.* **24**, 2328–2341 (2018).
73. Hall, J. M. & McDonnell, D. P. The Estrogen Receptor  $\beta$ -Isoform (ER $\beta$ ) of the Human Estrogen Receptor Modulates ER $\alpha$  Transcriptional Activity and Is a Key Regulator of the Cellular Response to Estrogens and Antiestrogens. *Endocrinology* **140**, 5566–5578 (1999).
74. Cheng, J., Lee, E. J., Madison, L. D. & Lazennec, G. Expression of estrogen receptor  $\beta$  in prostate carcinoma cells inhibits invasion and proliferation and triggers apoptosis. *FEBS Lett.* **566**, 169–172 (2004).
75. Hurtado, A. *et al.* Estrogen receptor beta displays cell cycle-dependent expression and regulates the G1 phase through a non-genomic mechanism in prostate carcinoma cells. *Anal. Cell. Pathol.* **30**, 349–365 (2008).
76. Nakamura, Y. *et al.* Cyclin D1 (CCND1) expression is involved in estrogen receptor beta (ER $\beta$ ) in human prostate cancer. *The Prostate* **73**, 590–595 (2013).
77. Christoforou, P., Christopoulos, P. F. & Koutsilieris, M. The Role of Estrogen Receptor  $\beta$  in Prostate Cancer. *Mol. Med.* **20**, 427–434 (2014).
78. De Amicis, F. *et al.* Androgen receptor overexpression induces tamoxifen resistance in human breast cancer cells. *Breast Cancer Res. Treat.* **121**, 1–11 (2010).
79. Cao, L. *et al.* A high AR:ER $\alpha$  or PDEF:ER $\alpha$  ratio predicts a sub-optimal response to tamoxifen therapy in ER $\alpha$ -positive breast cancer. *Cancer Chemother. Pharmacol.* **84**, 609–620 (2019).
80. Chia, K. *et al.* Non-canonical AR activity facilitates endocrine resistance in breast cancer. *Endocr. Relat. Cancer* **26**, 251–264 (2019).
81. D’Amato, N. C. *et al.* Cooperative Dynamics of AR and ER Activity in Breast Cancer. *Mol. Cancer Res.* **14**, 1054–1067 (2016).



82. Cochrane, D. R. *et al.* Role of the androgen receptor in breast cancer and preclinical analysis of enzalutamide. *Breast Cancer Res.* **16**, R7 (2014).
83. Fioretti, F. M., Sita-Lumsden, A., Bevan, C. L. & Brooke, G. N. Revising the role of the androgen receptor in breast cancer. *J. Mol. Endocrinol.* **52**, R257-265 (2014).
84. Wilson, S., Qi, J. & Filipp, F. V. Refinement of the androgen response element based on ChIP-Seq in androgen-insensitive and androgen-responsive prostate cancer cell lines. *Sci. Rep.* **6**, 32611 (2016).
85. Collins, L. C. *et al.* Androgen receptor expression in breast cancer in relation to molecular phenotype: results from the Nurses' Health Study. *Mod. Pathol.* **24**, 924–931 (2011).
86. Lehmann, B. D. *et al.* Identification of human triple-negative breast cancer subtypes and preclinical models for selection of targeted therapies. *J. Clin. Invest.* **121**, 2750–2767 (2011).
87. Farmer, P. *et al.* Identification of molecular apocrine breast tumours by microarray analysis. *Oncogene* **24**, 4660–4671 (2005).
88. Birrell, S. N. *et al.* Androgens induce divergent proliferative responses in human breast cancer cell lines. *J. Steroid Biochem. Mol. Biol.* **52**, 459–467 (1995).
89. Ni, M. *et al.* Targeting Androgen Receptor in Estrogen Receptor-Negative Breast Cancer. *Cancer Cell* **20**, 119–131 (2011).
90. Barton, V. N. *et al.* Multiple Molecular Subtypes of Triple-Negative Breast Cancer Critically Rely on Androgen Receptor and Respond to Enzalutamide In Vivo. *Mol. Cancer Ther.* **14**, 769–778 (2015).
91. Wang, J. *et al.* ER $\beta$ 1 inversely correlates with PTEN/PI3K/AKT pathway and predicts a favorable prognosis in triple-negative breast cancer. *Breast Cancer Res. Treat.* **152**, 255–269 (2015).
92. Anestis, A. *et al.* Estrogen receptor beta increases sensitivity to enzalutamide in androgen receptor-positive triple-negative breast cancer. *J. Cancer Res. Clin. Oncol.* **145**, 1221–1233 (2019).
93. Hall, R. E., Birrell, S. N., Tilley, W. D. & Sutherland, R. L. MDA-MB-453, an androgen-responsive human breast carcinoma cell line with high level androgen receptor expression. *Eur. J. Cancer* **30**, 484–490 (1994).
94. Barton, V. N. *et al.* Androgen Receptor Supports an Anchorage-Independent, Cancer Stem Cell-like Population in Triple-Negative Breast Cancer. *Cancer Res.* **77**, 3455–3466 (2017).
95. Naderi, A. & Hughes-Davies, L. A Functionally Significant Cross-talk between Androgen Receptor and ErbB2 Pathways in Estrogen Receptor Negative Breast Cancer. *Neoplasia N. Y. N* **10**, 542–548 (2008).
96. Goodwin, J. F. *et al.* A hormone-DNA repair circuit governs the response to genotoxic insult. *Cancer Discov.* **3**, 1254–1271 (2013).

97. Polkinghorn, W. R. *et al.* Androgen receptor signaling regulates DNA repair in prostate cancers. *Cancer Discov.* **3**, 1245–1253 (2013).
98. Goodwin, J. F. *et al.* DNA-PKcs-Mediated Transcriptional Regulation Drives Prostate Cancer Progression and Metastasis. *Cancer Cell* **28**, 97–113 (2015).
99. Al-Ubaidi, F. L. T. *et al.* Castration therapy results in decreased Ku70 levels in prostate cancer. *Clin. Cancer Res. Off. J. Am. Assoc. Cancer Res.* **19**, 1547–1556 (2013).
100. Speers, C. *et al.* Androgen receptor as a mediator and biomarker of radioresistance in triple-negative breast cancer. *Npj Breast Cancer* **3**, 29 (2017).
101. Michmerhuizen, A. R. *et al.* Seviteronel, a Novel CYP17 Lyase Inhibitor and Androgen Receptor Antagonist, Radiosensitizes AR-Positive Triple Negative Breast Cancer Cells. *Front. Endocrinol.* **11**, (2020).
102. Yard, B. D. *et al.* A genetic basis for the variation in the vulnerability of cancer to DNA damage. *Nat. Commun.* **7**, 11428 (2016).
103. Sherr, C. J. & Roberts, J. M. Living with or without cyclins and cyclin-dependent kinases. *Genes Dev.* **18**, 2699–2711 (2004).
104. Koryakina, Y., Knudsen, K. E. & Gioeli, D. Cell-cycle-dependent regulation of androgen receptor function. *Endocr. Relat. Cancer* **22**, 249–264 (2015).
105. Balk, S. P. & Knudsen, K. E. AR, the cell cycle, and prostate cancer. *Nucl. Recept. Signal.* **6**, (2008).
106. Knudsen, K. E., Arden, K. C. & Cavenee, W. K. Multiple G1 Regulatory Elements Control the Androgen-dependent Proliferation of Prostatic Carcinoma Cells. *J. Biol. Chem.* **273**, 20213–20222 (1998).
107. Xu, Y., Chen, S.-Y., Ross, K. N. & Balk, S. P. Androgens Induce Prostate Cancer Cell Proliferation through Mammalian Target of Rapamycin Activation and Post-transcriptional Increases in Cyclin D Proteins. *Cancer Res.* **66**, 7783–7792 (2006).
108. Yeh, S. *et al.* Retinoblastoma, a tumor suppressor, is a coactivator for the androgen receptor in human prostate cancer DU145 cells. *Biochem. Biophys. Res. Commun.* **248**, 361–367 (1998).
109. Lu, J. & Danielsen, M. Differential Regulation of Androgen and Glucocorticoid Receptors by Retinoblastoma Protein. *J. Biol. Chem.* **273**, 31528–31533 (1998).
110. Lanzino, M. *et al.* Inhibition of cyclin D1 expression by androgen receptor in breast cancer cells—identification of a novel androgen response element. *Nucleic Acids Res.* **38**, 5351–5365 (2010).
111. Kokontis, J. M., Hay, N. & Liao, S. Progression of LNCaP Prostate Tumor Cells during Androgen Deprivation: Hormone-Independent Growth, Repression of Proliferation by Androgen, and Role for p27Kip1 in Androgen-Induced Cell Cycle Arrest. *Mol. Endocrinol.* **12**, 941–953 (1998).
112. Lu, S., Liu, M., Epner, D. E., Tsai, S. Y. & Tsai, M.-J. Androgen Regulation of the Cyclin-Dependent Kinase Inhibitor p21 Gene through an Androgen Response Element in the Proximal Promoter. *Mol. Endocrinol.* **13**, 376–384 (1999).

113. Wolf, D. A., Kohlhuber, F., Schulz, P., Fittler, F. & Eick, D. Transcriptional down-regulation of *c-myc* in human prostate carcinoma cells by the synthetic androgen mibolerone. *Br. J. Cancer* **65**, 376–382 (1992).
114. Grad, J. M., Le Dai, J., Wu, S. & Burnstein, K. L. Multiple Androgen Response Elements and a Myc Consensus Site in the Androgen Receptor (AR) Coding Region Are Involved in Androgen-Mediated Up-Regulation of AR Messenger RNA. *Mol. Endocrinol.* **13**, 1896–1911 (1999).
115. Zhu, A. *et al.* Antiproliferative Effect of Androgen Receptor Inhibition in Mesenchymal Stem-Like Triple-Negative Breast Cancer. *Cell. Physiol. Biochem.* **38**, 1003–1014 (2016).
116. Bièche, I., Parfait, B., Tozlu, S., Lidereau, R. & Vidaud, M. Quantitation of androgen receptor gene expression in sporadic breast tumors by real-time RT–PCR: evidence that MYC is an AR-regulated gene. *Carcinogenesis* **22**, 1521–1526 (2001).
117. Bretones, G., Delgado, M. D. & León, J. Myc and cell cycle control. *Biochim. Biophys. Acta BBA - Gene Regul. Mech.* **1849**, 506–516 (2015).
118. Amicis, F. D. *et al.* AIB1 sequestration by androgen receptor inhibits estrogen-dependent cyclin D1 expression in breast cancer cells. *BMC Cancer* **19**, 1–11 (2019).
119. Anzick, S. L. *et al.* AIB1, a steroid receptor coactivator amplified in breast and ovarian cancer. *Science* **277**, 965–968 (1997).
120. List, H.-J., Reiter, R., Singh, B., Wellstein, A. & Riegel, A. T. Expression of the nuclear coactivator AIB1 in normal and malignant breast tissue. *Breast Cancer Res. Treat.* **68**, 21–28 (2001).
121. Narbe, U. *et al.* The estrogen receptor coactivator AIB1 is a new putative prognostic biomarker in ER-positive/HER2-negative invasive lobular carcinoma of the breast. *Breast Cancer Res. Treat.* **175**, 305–316 (2019).
122. Augello, M. A., Den, R. B. & Knudsen, K. E. AR function in promoting metastatic prostate cancer. *Cancer Metastasis Rev.* **33**, 399–411 (2014).
123. Lin, C.-Y. *et al.* Elevation of Androgen Receptor Promotes Prostate Cancer Metastasis via Induction of EMT and Reduction of KAT5. *Cancer Sci.* (2018) doi:10.1111/cas.13776.
124. Barron, D. A. & Rowley, D. R. The reactive stroma microenvironment and prostate cancer progression. *Endocr. Relat. Cancer* **19**, R187–R204 (2012).
125. Chan, J. S. K. *et al.* Targeting nuclear receptors in cancer-associated fibroblasts as concurrent therapy to inhibit development of chemoresistant tumors. *Oncogene* **37**, 160–173 (2018).
126. Yu, S. *et al.* Androgen receptor in human prostate cancer-associated fibroblasts promotes prostate cancer epithelial cell growth and invasion. *Med. Oncol.* **30**, 674 (2013).

127. Ricke, E. A. *et al.* Androgen hormone action in prostatic carcinogenesis: stromal androgen receptors mediate prostate cancer progression, malignant transformation and metastasis. *Carcinogenesis* **33**, 1391–1398 (2012).
128. Leach, D. A. *et al.* Cell-lineage specificity and role of AP-1 in the prostate fibroblast androgen receptor cistrome. *Mol. Cell. Endocrinol.* **439**, 261–272 (2017).
129. Chen, W.-Y. *et al.* Inhibition of the androgen receptor induces a novel tumor promoter, ZBTB46, for prostate cancer metastasis. *Oncogene* **36**, 6213–6224 (2017).
130. Chen, J. *et al.* Androgen-deprivation therapy with enzalutamide enhances prostate cancer metastasis via decreasing the EPHB6 suppressor expression. *Cancer Lett.* **408**, 155–163 (2017).
131. Giovannelli, P., Donato, M. D., Auricchio, F., Castoria, G. & Migliaccio, A. Androgens Induce Invasiveness of Triple Negative Breast Cancer Cells Through AR/Src/PI3-K Complex Assembly. *Sci. Rep.* **9**, 1–14 (2019).
132. Feng, J. *et al.* Androgen and AR contribute to breast cancer development and metastasis: an insight of mechanisms. *Oncogene* **36**, 2775–2790 (2017).
133. Grogg, A. *et al.* Androgen receptor status is highly conserved during tumor progression of breast cancer. *BMC Cancer* **15**, (2015).
134. Gasparini, P. *et al.* Androgen receptor status is a prognostic marker in non-basal triple negative breast cancers and determines novel therapeutic options. *PloS One* **9**, e88525 (2014).
135. Kraby, M. R. *et al.* The prognostic value of androgen receptors in breast cancer subtypes. *Breast Cancer Res. Treat.* (2018) doi:10.1007/s10549-018-4904-x.
136. Bronte, G. *et al.* Androgen Receptor Expression in Breast Cancer: What Differences Between Primary Tumor and Metastases? *Transl. Oncol.* **11**, 950–956 (2018).
137. Perlmutter, M. A. & Lepor, H. Androgen Deprivation Therapy in the Treatment of Advanced Prostate Cancer. *Rev. Urol.* **9**, S3–S8 (2007).
138. Huggins, C., Stevens, R. E. & Hodges, C. V. Studies on Prostate Cancer: II. The Effects of Castration on Advanced Carcinoma of the Prostate Gland. *Arch. Surg.* **43**, 209–223 (1941).
139. Wilson, E. M. & French, F. S. Binding properties of androgen receptors. Evidence for identical receptors in rat testis, epididymis, and prostate. *J. Biol. Chem.* **251**, 5620–5629 (1976).
140. Askew, E. B., Gampe, R. T., Stanley, T. B., Faggart, J. L. & Wilson, E. M. Modulation of Androgen Receptor Activation Function 2 by Testosterone and Dihydrotestosterone. *J. Biol. Chem.* **282**, 25801–25816 (2007).
141. Andriole, G. L. *et al.* Effect of the dual 5alpha-reductase inhibitor dutasteride on markers of tumor regression in prostate cancer. *J. Urol.* **172**, 915–919 (2004).
142. Clark, R. V. *et al.* Marked suppression of dihydrotestosterone in men with benign prostatic hyperplasia by dutasteride, a dual 5alpha-reductase inhibitor. *J. Clin. Endocrinol. Metab.* **89**, 2179–2184 (2004).

143. McConnell, J. D. *et al.* Finasteride, an inhibitor of 5 alpha-reductase, suppresses prostatic dihydrotestosterone in men with benign prostatic hyperplasia. *J. Clin. Endocrinol. Metab.* **74**, 505–508 (1992).
144. Span, P. N. *et al.* Selectivity of finasteride as an in vivo inhibitor of 5alpha-reductase isozyme enzymatic activity in the human prostate. *J. Urol.* **161**, 332–337 (1999).
145. Wu, Y. *et al.* Prostate Cancer Cells Differ in Testosterone Accumulation, Dihydrotestosterone Conversion, and Androgen Receptor Signaling Response to Steroid 5 $\alpha$ -Reductase Inhibitors. *The Prostate* **73**, 1470–1482 (2013).
146. Mina, A., Yoder, R. & Sharma, P. Targeting the androgen receptor in triple-negative breast cancer: current perspectives. *Oncotargets Ther.* **10**, 4675–4685 (2017).
147. Ryan, C. J. *et al.* Abiraterone acetate plus prednisone versus placebo plus prednisone in chemotherapy-naïve men with metastatic castration-resistant prostate cancer (COU-AA-302): final overall survival analysis of a randomised, double-blind, placebo-controlled phase 3 study. *Lancet Oncol.* **16**, 152–160 (2015).
148. Bonnefoi, H. *et al.* A phase II trial of abiraterone acetate plus prednisone in patients with triple-negative androgen receptor positive locally advanced or metastatic breast cancer (UCBG 12-1). *Ann. Oncol.* **27**, 812–818 (2016).
149. Proverbs-Singh, T., Feldman, J. L., Morris, M. J., Autio, K. A. & Traina, T. A. Targeting the androgen receptor in prostate and breast cancer: several new agents in development. *Endocr. Relat. Cancer* **22**, R87–R106 (2015).
150. Montgomery, R. B. *et al.* Phase I clinical trial of galeterone (TOK-001), a multifunctional antiandrogen and CYP17 inhibitor in castration resistant prostate cancer (CRPC). *J. Clin. Oncol.* **30**, 4665–4665 (2012).
151. Hook, K. V., Huang, T. & Alumkal, J. J. Orteronel for the treatment of prostate cancer. *Future Oncol.* **10**, 803–811 (2014).
152. Fizazi, K. *et al.* Phase III, Randomized, Double-Blind, Multicenter Trial Comparing Orteronel (TAK-700) Plus Prednisone With Placebo Plus Prednisone in Patients With Metastatic Castration-Resistant Prostate Cancer That Has Progressed During or After Docetaxel-Based Therapy: ELM-PC 5. *J. Clin. Oncol.* **33**, 723–731 (2015).
153. Rampurwala, M. M. *et al.* Phase 1b study of orteronel in postmenopausal women with hormone-receptor positive (HR+) metastatic breast cancer. *J. Clin. Oncol.* **32**, 538–538 (2014).
154. Takeda Announces Termination of Orteronel (TAK-700) Development for Prostate Cancer in Japan, U.S.A. and Europe. *Takeda*  
<https://www.takeda.com/newsroom/newsreleases/2014/takeda-announces-termination-of-orteronel-tak-700-development-for--prostate-cancer-in-japan-u.s.a.-and-europe/>  
 (2014).
155. Gucalp, A. & Traina, T. A. Targeting the androgen receptor in triple-negative breast cancer. *Curr. Probl. Cancer* **40**, 141–150 (2016).

156. Perrault, D. J. *et al.* Phase II study of flutamide in patients with metastatic breast cancer. A National Cancer Institute of Canada Clinical Trials Group study. *Invest. New Drugs* **6**, 207–210 (1988).
157. Barqawi, A., Akduman, B., Abouelfadel, Z., Robischon, M. & Crawford, E. D. The use of flutamide as a single antiandrogen treatment for hormone-refractory prostate cancer. *BJU Int.* **92**, 695–698 (2003).
158. Gucalp, A. *et al.* Phase II Trial of Bicalutamide in Patients with Androgen Receptor–Positive, Estrogen Receptor–Negative Metastatic Breast Cancer. *Clin. Cancer Res.* **19**, 5505–5512 (2013).
159. Veldscholte, J. *et al.* A mutation in the ligand binding domain of the androgen receptor of human INCaP cells affects steroid binding characteristics and response to anti-androgens. *Biochem. Biophys. Res. Commun.* **173**, 534–540 (1990).
160. Yeh, S., Miyamoto, H. & Chang, C. Hydroxyflutamide may not always be a pure antiandrogen. *The Lancet* **349**, 852–853 (1997).
161. Lu, Q. *et al.* Bicalutamide plus Aromatase Inhibitor in Patients with Estrogen Receptor-Positive/Androgen Receptor-Positive Advanced Breast Cancer. *Oncologist* **21**, 21-e15 (2020).
162. Caiazza, F. *et al.* Preclinical evaluation of the AR inhibitor enzalutamide in triple-negative breast cancer cells. *Endocr. Relat. Cancer* **23**, 323–334 (2016).
163. Scher, H. I. *et al.* Increased Survival with Enzalutamide in Prostate Cancer after Chemotherapy. <http://dx.doi.org/10.1056/NEJMoa1207506>  
[https://www.nejm.org/doi/10.1056/NEJMoa1207506?url\\_ver=Z39.88-2003&rfr\\_id=ori%3Arid%3Acrossref.org&rfr\\_dat=cr\\_pub%3Dwww.ncbi.nlm.nih.gov](https://www.nejm.org/doi/10.1056/NEJMoa1207506?url_ver=Z39.88-2003&rfr_id=ori%3Arid%3Acrossref.org&rfr_dat=cr_pub%3Dwww.ncbi.nlm.nih.gov)  
 (2012) doi:10.1056/NEJMoa1207506.
164. Traina, T. A. *et al.* Results from a phase 2 study of enzalutamide (ENZA), an androgen receptor (AR) inhibitor, in advanced AR+ triple-negative breast cancer (TNBC). *J. Clin. Oncol.* **33**, 1003–1003 (2015).
165. Chong, J. T., Oh, W. K. & Liaw, B. C. Profile of apalutamide in the treatment of metastatic castration-resistant prostate cancer: evidence to date. *OncoTargets and Therapy* <https://www.dovepress.com/profile-of-apalutamide-in-the-treatment-of-metastatic-castration-resis-peer-reviewed-article-OTT> (2018)  
 doi:10.2147/OTT.S147168.
166. Clegg, N. J. *et al.* ARN-509: a novel anti-androgen for prostate cancer treatment. *Cancer Res.* **72**, 1494–1503 (2012).
167. Smith, M. R. *et al.* Apalutamide Treatment and Metastasis-free Survival in Prostate Cancer. *N. Engl. J. Med.* **378**, 1408–1418 (2018).
168. Moilanen, A.-M. *et al.* Discovery of ODM-201, a new-generation androgen receptor inhibitor targeting resistance mechanisms to androgen signaling-directed prostate cancer therapies. *Sci. Rep.* **5**, 12007 (2015).
169. Fizazi, K. *et al.* Darolutamide in Nonmetastatic, Castration-Resistant Prostate Cancer. *N. Engl. J. Med.* **380**, 1235–1246 (2019).

170. Christenson, J. L. *et al.* Harnessing a Different Dependency: How to Identify and Target Androgen Receptor-Positive Versus Quadruple-Negative Breast Cancer. *Horm. Cancer* **9**, 82–94 (2018).
171. Bardia, A. *et al.* Phase 1 study of seviteronel, a selective CYP17 lyase and androgen receptor inhibitor, in women with estrogen receptor-positive or triple-negative breast cancer. *Breast Cancer Res. Treat.* 1–10 (2018) doi:10.1007/s10549-018-4813-z.
172. Gupta, S. *et al.* Phase 1 Study of Seviteronel, a Selective CYP17 Lyase and Androgen Receptor Inhibitor, in Men with Castration-Resistant Prostate Cancer. *Clin. Cancer Res. clincanres.0564.2018* (2018) doi:10.1158/1078-0432.CCR-18-0564.
173. Reese, J. M. *et al.* Abstract P5-05-05: Targeting the androgen receptor with seviteronel, a CYP17 lyase and AR inhibitor, in triple negative breast cancer. *Cancer Res.* **79**, P5-05-05-P5-05–05 (2019).
174. Gucalp, A. *et al.* Phase (Ph) 2 stage 1 clinical activity of seviteronel, a selective CYP17-lyase and androgen receptor (AR) inhibitor, in women with advanced AR+ triple-negative breast cancer (TNBC) or estrogen receptor (ER)+ BC: CLARITY-01. *J. Clin. Oncol.* **35**, 1102–1102 (2017).
175. Gucalp, A. *et al.* Abstract P2-08-04: Phase 1/2 study of oral seviteronel (VT-464), a dual CYP17-lyase inhibitor and androgen receptor (AR) antagonist, in patients with advanced AR positive triple negative (TNBC) or estrogen receptor (ER) positive breast cancer (BC). *Cancer Res.* **77**, P2-08-04-P2-08–04 (2017).
176. Zweifel, M. *et al.* Phase I trial of the androgen receptor modulator CR1447 in breast cancer patients. *Endocr. Connect.* **6**, 549–556 (2017).
177. Srinath, R. & Dobs, A. Enobosarm (GTx-024, S-22): a potential treatment for cachexia. *Future Oncol* **10**, 187–194 (2014).
178. Dalton, J. T. *et al.* The selective androgen receptor modulator GTx-024 (enobosarm) improves lean body mass and physical function in healthy elderly men and postmenopausal women: results of a double-blind, placebo-controlled phase II trial. *J. Cachexia Sarcopenia Muscle* **2**, 153–161 (2011).
179. Dobs, A. S. *et al.* Effects of enobosarm on muscle wasting and physical function in patients with cancer: a double-blind, randomised controlled phase 2 trial. *Lancet Oncol.* **14**, 335–345 (2013).
180. Overmoyer, B. *et al.* Enobosarm: A targeted therapy for metastatic, androgen receptor positive, breast cancer. *J. Clin. Oncol.* **32**, 568–568 (2014).
181. Testosterone Propionate Therapy in Breast Cancer. *JAMA* **188**, 1069–1072 (1964).
182. Lim, E. *et al.* Pushing estrogen receptor around in breast cancer. *Endocr. Relat. Cancer* **23**, T227–T241 (2016).
183. Lee-Bitar, J. S. *et al.* A phase II clinical trial of pembrolizumab and selective androgen receptor modulator GTx-024 in patients with advanced androgen receptor-positive triple-negative breast cancer. *J. Clin. Oncol.* **37**, 1069–1069 (2019).

184. Eder, I. E. *et al.* Inhibition of LNCaP prostate cancer cells by means of androgen receptor antisense oligonucleotides. *Cancer Gene Ther.* **7**, 997–1007 (2000).
185. Eder, I. E. *et al.* Inhibition of LNCaP prostate tumor growth *in vivo* by an antisense oligonucleotide directed against the human androgen receptor. *Cancer Gene Ther.* **9**, 117–125 (2002).
186. Hamy, F. *et al.* Specific block of androgen receptor activity by antisense oligonucleotides. *Prostate Cancer Prostatic Dis.* **6**, 27–33 (2003).
187. Velez, M. V. L., Verhaegh, G. W., Smit, F., Sedelaar, J. P. M. & Schalken, J. A. Suppression of prostate tumor cell survival by antisense oligonucleotide-mediated inhibition of AR-V7 mRNA synthesis. *Oncogene* **1** (2019) doi:10.1038/s41388-019-0696-7.
188. Zou, Y., Ma, D. & Wang, Y. The PROTAC technology in drug development. *Cell Biochem. Funct.* **37**, 21–30 (2019).
189. Han, X. *et al.* Discovery of ARD-69 as a Highly Potent Proteolysis Targeting Chimera (PROTAC) Degradator of Androgen Receptor (AR) for the Treatment of Prostate Cancer. *J. Med. Chem.* **62**, 941–964 (2019).
190. Han, X. *et al.* Discovery of Highly Potent and Efficient PROTAC Degradators of Androgen Receptor (AR) by Employing Weak Binding Affinity VHL E3 Ligase Ligands. *J. Med. Chem.* **62**, 11218–11231 (2019).
191. Kregel, S. *et al.* Androgen receptor degraders overcome common resistance mechanisms developed during prostate cancer treatment. *Neoplasia N. Y. N* **22**, 111–119 (2020).
192. Salami, J. *et al.* Androgen receptor degradation by the proteolysis-targeting chimera ARCC-4 outperforms enzalutamide in cellular models of prostate cancer drug resistance. *Commun. Biol.* **1**, 1–9 (2018).
193. Eil, C. Ketoconazole binds to the human androgen receptor. *Horm. Metab. Res. Horm. Stoffwechselforschung Horm. Metab.* **24**, 367–370 (1992).
194. Zhang, S. *et al.* Endocrine disruptors of inhibiting testicular 3 $\beta$ -hydroxysteroid dehydrogenase. *Chem. Biol. Interact.* (2019) doi:10.1016/j.cbi.2019.02.027.
195. Lim, Y.-W. *et al.* Pharmacokinetics and pharmacodynamics of docetaxel with or without ketoconazole modulation in chemo-naïve breast cancer patients. *Ann. Oncol.* **21**, 2175–2182 (2010).
196. Bignan, G. *et al.* Development of a Small Molecule Inhibitor Targeting Androgen Receptor (AR) Mutations Associated with Resistance to Current AR Antagonists. (2018).
197. Joseph, J. D. *et al.* A Clinically Relevant Androgen Receptor Mutation Confers Resistance to Second-Generation Antiandrogens Enzalutamide and ARN-509. *Cancer Discov.* **3**, 1020–1029 (2013).
198. Spratt, D. E. *et al.* Androgen Receptor Upregulation Mediates Radioresistance after Ionizing Radiation. *Cancer Res.* **75**, 4688–4696 (2015).



199. Ghashghaei, M. *et al.* Enhanced radiosensitization of enzalutamide via schedule dependent administration to androgen-sensitive prostate cancer cells. *The Prostate* **78**, 64–75 (2018).
200. Manem, V. S. *et al.* Modeling cellular response in large-scale radiogenomic databases to advance precision radiotherapy. *Cancer Res.* (2019) doi:10.1158/0008-5472.CAN-19-0179.
201. Schiewer, M. J. *et al.* Dual Roles of PARP-1 Promote Cancer Growth and Progression. *Cancer Discov.* **2**, 1134–1149 (2012).
202. Li, L. *et al.* Androgen receptor inhibitor–induced “BRCAness” and PARP inhibition are synthetically lethal for castration-resistant prostate cancer. *Sci Signal* **10**, eaam7479 (2017).
203. Asim, M. *et al.* Synthetic lethality between androgen receptor signalling and the PARP pathway in prostate cancer. *Nat. Commun.* **8**, 374 (2017).
204. Pamarthy, S. *et al.* Abstract 1114: Combining anti-androgen therapy and PARP inhibition results in synergistic cytotoxicity of metastatic castration-resistant prostate cancer (mCRPC) cells. *Cancer Res.* **77**, 1114–1114 (2017).
205. Karanika, S., Karantanos, T., Li, L., Corn, P. G. & Thompson, T. C. DNA damage response and prostate cancer: defects, regulation and therapeutic implications. *Oncogene* **34**, 2815–2822 (2015).
206. Comen, E. & Robson, M. Poly(ADP-Ribose) Polymerase Inhibitors in Triple-Negative Breast Cancer. *Cancer J.* **16**, 48–52 (2010).
207. Murai, J. *et al.* Trapping of PARP1 and PARP2 by Clinical PARP Inhibitors. *Cancer Res.* **72**, 5588–5599 (2012).
208. Comstock, C. E. S. *et al.* Targeting cell cycle and hormone receptor pathways in cancer. *Oncogene* **32**, 5481–5491 (2013).
209. Gucalp, A. *et al.* Abstract P3-11-04: Phase I/II trial of palbociclib in combination with bicalutamide for the treatment of androgen receptor (AR)+ metastatic breast cancer (MBC). *Cancer Res.* **78**, P3-11-04-P3-11-04 (2018).
210. Qi, W. *et al.* Reciprocal feedback inhibition of the androgen receptor and PI3K as a novel therapy for castrate-sensitive and -resistant prostate cancer. *Oncotarget* **6**, 41976–41987 (2015).
211. Lehmann, B. D. *et al.* TBCRC 032 IB/II Multicenter Study: Molecular Insights to AR Antagonist and PI3K Inhibitor Efficacy in Patients with AR+ Metastatic Triple-Negative Breast Cancer. *Clin. Cancer Res.* **26**, 2111–2123 (2020).
212. Traina, T. A. *et al.* Adjuvant enzalutamide for the treatment of early-stage androgen receptor-positive (AR+) TNBC. *J. Clin. Oncol.* **37**, 546–546 (2019).
213. Traina, T. A. *et al.* Abstract P5-12-09: Patient-reported outcomes (PROs) during one year of adjuvant enzalutamide for the treatment of early stage androgen receptor positive (AR+) triple negative breast cancer. *Cancer Res.* **80**, P5-12-09-P5-12-09 (2020).

## **Chapter 2 : Seviteronel a Novel CYP17 Lyase Inhibitor and Androgen Receptor Antagonist, Radiosensitizes AR-Positive Triple Negative Breast Cancer Cells<sup>2</sup>**

### **2.1 Abstract**

Increased rates of locoregional recurrence (LR) have been observed in triple negative breast cancer (TNBC) despite multimodality therapy, including radiation (RT). Recent data suggest inhibiting the androgen receptor (AR) may be an effective radiosensitizing strategy, and AR is expressed in 15-35% of TNBC tumors. The aim of this study was to determine whether seviteronel (INO-464), a novel CYP17 lyase inhibitor and AR antagonist, is able to radiosensitize AR-positive (AR+) TNBC models. In cell viability assays, seviteronel and enzalutamide exhibited limited effect as a single agent ( $IC_{50} > 10 \mu M$ ). Using clonogenic survival assays, however, AR knockdown and AR inhibition with seviteronel were effective at radiosensitizing cells with radiation enhancement ratios of 1.20-1.89 in models of TNBC with high AR expression. AR-negative (AR-) models, regardless of their estrogen receptor expression, were not radiosensitized with seviteronel treatment at concentrations up to 5  $\mu M$ . Radiosensitization of AR+ TNBC models was at least partially dependent on impaired dsDNA break repair with significant delays in repair at 6, 16, and 24 h as measured by immunofluorescent staining of  $\gamma H2AX$  foci. Similar effects were observed in an *in vivo* AR+

---

<sup>2</sup> This chapter was published in *Frontiers in Endocrinology* and completed in collaboration with the following authors: Benjamin C. Chandler, Eric Olsen, Kari Wilder-Romans, Leah Moubadder, Meilan Liu, Andrea M. Pesch, Amanda Zhang, Cassandra Ritter, S. Tanner Ward, Alyssa Santola, Shyam Nyati, James M. Rae, Daniel Hayes, Felix Y. Feng, Daniel Spratt, Daniel Wahl, Joel Eisner, Lori J. Pierce, and Corey W. Speers.

TNBC xenograft model where there was a significant reduction in tumor volume and a delay to tumor doubling and tripling times in mice treated with seviteronel and radiation. Following combination treatment with seviteronel and radiation, increased binding of AR occurred at DNA damage response genes, including genes involved both in homologous recombination and non-homologous end joining. This trend was not observed with combination treatment of enzalutamide and RT, suggesting that seviteronel may have a different mechanism of radiosensitization compared to other AR inhibitors. Enzalutamide and seviteronel treatment also had different effects on AR and AR target genes as measured by immunoblot and qPCR. These results implicate AR as a mediator of radioresistance in AR+ TNBC models and support the use of seviteronel as a radiosensitizing agent in AR+ TNBC.

## **2.2 Introduction**

Each year, it is estimated that over 250,000 women will be diagnosed with invasive breast cancer<sup>1</sup>, 15-30% of whom will be diagnosed with triple negative breast cancer (TNBC). This subtype of breast cancer is defined by the lack of estrogen receptor (ER), progesterone receptor, or HER2/*neu* expression and is unresponsive to anti-ER or human epidermal growth factor receptor 2 (HER2) targeting agents. Most patients with TNBC receive multimodal therapy, including surgery, chemotherapy, and radiation therapy (RT), yet TNBC patients still experience the highest rates of locoregional recurrence of any breast cancer subtype. Due to the lack of molecular targeted therapies available for these patients, as well as their intrinsic insensitivity to radiation therapy<sup>2</sup>, there is a clinical need for the development of new radiosensitization strategies.

The heterogeneity of TNBC tumors adds to the difficulty of treating this cancer subtype<sup>3,4</sup>. In order to improve response to treatment, it is important to understand the molecular drivers underlying the growth of TNBCs<sup>5</sup>. Current molecular therapies for breast cancer patients target the estrogen receptor or HER2; however, these therapies are ineffective against TNBC due to the lack of ER and HER2 expression<sup>3,5</sup>. Previous studies have established a subgroup of TNBCs which express the androgen receptor (AR)<sup>6</sup>, and studies have shown that AR is expressed in 15-35% of all TNBCs<sup>7</sup>, rendering AR signaling as a potential target for treatment. Previous work has also suggested an oncogenic role for AR in driving growth of AR-positive (AR+) TNBC<sup>8,9,10</sup> as well as contributing to invasiveness and migration of TNBC cells<sup>11</sup>. Indeed, AR may play multiple roles in breast cancer, both in ER-positive (ER+) and ER-negative tumors, and these results have demonstrated that AR may be an effective target for the clinical treatment of patients with AR+ TNBC<sup>12</sup>. Ongoing and completed clinical trials continue to assess the efficacy of AR blockade as a monotherapy for patients with AR+ breast cancers (NCT01889238, NCT01842321, NCT00755885, NCT01808040, NCT01990209, NCT02580448, NCT03383679, NCT02348281, NCT02130700, NCT02067741).

Efforts to target androgen receptor signaling have largely focused on decreasing circulating androgens (CYP17 inhibition) or blocking the binding of androgens to their cognate receptor (AR inhibition)<sup>13,14,15,16,17</sup>. Production of androgens is dependent upon the activity of cytochrome P450 17 $\alpha$ -hydroxylase/17,20-lyase (CYP17 lyase)<sup>18</sup>. Inhibitors of CYP17 lyase have been developed as a strategy for blocking the production of androgens<sup>19</sup>. These inhibitors, including the most commonly used CYP17 lyase inhibitor, abiraterone acetate, are used to lower levels of intra-prostatic androgens to treat prostate cancer patients<sup>20,21,22</sup>. Enzalutamide (MDV3100) is a well-characterized second generation anti-androgen which competitively

inhibits androgen binding to AR and prevents AR nuclear translocation to block AR binding to DNA<sup>23,24</sup>. In this way, enzalutamide inhibits AR-mediated transcriptional regulation<sup>23</sup>. In contrast, seviteronel (INO-464) is a novel inhibitor of both CYP17 lyase and AR. Seviteronel has been shown to be more effective than abiraterone acetate at inhibiting CYP17 lyase<sup>25</sup>, and seviteronel also possesses some antagonistic effects against AR, potentially rendering it a dual-AR inhibitor. In phase I studies, seviteronel has been well-tolerated both in men with castration-resistant prostate cancer (CRPC)<sup>26</sup> and in women with ER+ breast cancer or TNBC<sup>27</sup>. There is hope that these novel agents, including seviteronel, will be effective in patients with AR+ cancers, including TNBC.

Beyond the role of the androgen receptor in driving cancer cell proliferation, previous work in prostate cancer and breast cancer has demonstrated the role of AR in mediating DNA repair and in the DNA damage response following radiation therapy<sup>28,29,30,31</sup>. These studies suggest that pharmacologic abrogation of AR both in prostate cancer (darolutamide and enzalutamide) and in AR+ TNBC (enzalutamide) may be a viable treatment strategy for the radiosensitization of aggressive tumors, as AR inhibition may inhibit DNA repair. In addition, following radiation, AR activity increases the expression and phosphorylation of DNAPKcs<sup>28,30</sup>. Therefore, AR inhibition may render cells more sensitive to radiation treatment by reducing activity of DNAPKcs and inhibiting non-homologous end joining (NHEJ), but not homologous recombination (HR)<sup>29</sup>. To date, newer generation agents including seviteronel have not been tested as radiosensitizing agents.

Previous work by our group has shown that AR is a mediator of radioresistance in TNBC and that enzalutamide-mediated AR inhibition is sufficient to sensitize AR+ TNBC cells to RT<sup>28</sup>. Here we report that seviteronel is able to selectively radiosensitize AR+ TNBC models *in vitro*

and *in vivo* and that radiosensitization is mediated, at least in part, through the delayed repair of dsDNA breaks. The mechanism of radiosensitization, however, appears to be different with seviteronel treatment compared to enzalutamide due to differences in AR binding to DNA damage response genes following treatment with seviteronel and radiation

## **2.3 Materials and Methods**

### **2.3.1 Cell Culture**

Cell lines were obtained from American Type Culture Collection (ATCC) and grown from frozen samples, including MDA-MB-453 and ACC-422 (AR+ TNBC), MCF-7 (AR-, ER+), and MDA-MB-231 (AR- TNBC). SUM-159 and SUM-185PE (AR+ TNBC) cells were obtained from the University of Michigan stocks generously provided by Dr. Stephen Ethier who isolated the cells while at the University of Michigan. MDA-MB-453 and MDA-MB-231 cells were grown in DMEM (Invitrogen) with 10% fetal bovine serum (FBS, Atlanta Biologicals S11550H). ACC-422 cells were grown in MEM (Gibco) supplemented with 15% FBS (Invitrogen) and 1X Insulin-Transferrin-Selenium-Ethanolamine (ITS-X, Gibco 51500-056). SUM-185 cells were grown in Ham's F-12 media (Gibco) with 5% FBS (Invitrogen), with 0.01M HEPES (Gibco #H3375), 1 µg/mL Hydrocortisone (Sigma #H4001), and 1X ITS-X (Gibco). SUM-159 cells were grown in Ham's F-12 media (Gibco) with 5% FBS (Invitrogen), 0.01M HEPES, 1 µg/mL Hydrocortisone, 1x antibiotic-antimycotic (anti-anti, Thermo Fisher 15240062), and 6 µg/mL insulin (Sigma #I9278). MCF-7 cells were grown in DMEM (Gibco) with 5% FBS (Invitrogen). MDA-MB-453, ACC-422, MCF-7, and MDA-MB-231 cells were supplemented with 1% penicillin/streptomycin (Thermo #15070063). All cell lines were grown in a 5% CO<sub>2</sub> incubator at 37°C. All cell lines were also authenticated using DNA fingerprinting by short tandem repeat (STR) profiling and routinely tested for mycoplasma (monthly).

### **2.3.2 Immunoblotting**

Cells were plated in 6-well plates in media containing FBS (MDA-MB-453:  $3.5 \times 10^5$  cells/well, ACC-422  $2.5 \times 10^5$  cells/well). The following day, cells were pretreated with charcoal stripped serum (Atlanta Biologics S11650H) for 24 h. Cells were stimulated with 10 nM dihydrotestosterone (DHT, Sigma D-073) and 5  $\mu$ M enzalutamide (MedChemExpress HY-70002) or seviteronel (Innocrin) and harvested at indicated time points following treatment. Lysis was performed using RIPA buffer (Thermo Fisher 89901) containing protease and phosphatase inhibitors (Sigma-Aldrich PHOSS-RO, CO-RO; Santa Cruz Biotechnology sc-3540, sc-24988A; Cayman Chemical 14333, 14405). Proteins were detected using antibodies for phospho-DNAPKcs (Abcam ab124918, 1:1,000), total DNAPKcs (CST 12311, 1:1,000), androgen receptor (Millipore 06-680, 1:1,000), GAPDH (CST 2118, 1:1,000), and  $\beta$ -Actin (8H10D10, Cell Signaling 12262S, 1:50,000). Secondary antibodies were obtained from Cell Signaling (HRP anti-rabbit CST 7074S, HRP anti-mouse 7076S).

### **2.3.3 Viability Assays**

Cells were plated in 96 well-plates in media containing FBS and allowed to adhere overnight. The following day the cells were treated with seviteronel or enzalutamide at concentrations ranging from 1 nM to 10  $\mu$ M. MCF-7 (2,000 cells/well) cells were grown for five days and stained with 0.5% crystal violet. SUM-159 (750 cells/well), MDA-MB-231 (3,500 cells/well), MDA-MB-453 (5,000 cells/well), SUM-185 (4,000 cells/well), and ACC-422 (4,000 cells/well) cells were grown for three days, and cell viability was assessed using Alamar Blue (Thermo Fisher DAL1100). Plates were read on a microplate reader (Cytation 3), and growth was calculated relative to the vehicle control (DMSO). IC<sub>50</sub> values for were calculated with GraphPad Prism, and results are reported as the mean  $\pm$  SEM of three independent experiments.

To model hormone deplete conditions, media contained charcoal stripped serum (CSS), without phenol-red were used for MDA-MB-453 and MDA-MB-231 (Gibco 21063-029) and ACC-422 (Gibco 51200-038) cells. Phenol-red free media for ACC-422 cells was supplemented with 2 mM L-glutamine (Sigma G7513). Cells were plated in media containing FBS and were pretreated overnight with CSS before treatment with enzalutamide or seviteronel in concentrations from 1 nM to 10  $\mu$ M.

### ***2.3.4 Clonogenic Survival Assays***

Cells were plated at single cell density in 6 well-plates and allowed to adhere overnight. Cells were then treated with seviteronel at various doses for 1 h before radiation (2–8 Gy) treatment. Cells were grown for one to four weeks before fixing with methanol/acetic acid and staining with crystal violet. Colonies of 50+ cells were counted and analyzed with the linear quadratic model. Plating densities are outlined in **Table 2-1**.

### ***2.3.5 $\gamma$ H2AX Immunofluorescence***

Cells were plated at a density of  $2.5 \times 10^5$  cells/well on coverslips in 12 well-plates and allowed to adhere overnight. The following day plates were pretreated with seviteronel (1 and 5  $\mu$ M) for 1 h before radiation treatment. Cells were fixed at designated time points after radiation using 4% paraformaldehyde. Foci were stained with an anti-phospho-histone H2AX (ser139) antibody (Millipore 05-636), and a fluorescent goat anti-mouse secondary antibody (Invitrogen A11005). Pictures were taken of >100 cells per condition, and  $\gamma$ H2AX foci were scored visually by a blinded observer. MDA-MB-453 cells containing  $\geq 15$   $\gamma$ H2AX foci were scored as positive, and ACC-422 cells with  $\geq 10$   $\gamma$ H2AX foci were scored as positive. Results were pooled for statistical analysis.



### **2.3.6 Xenograft Study**

MDA-MB-453 cells were subcutaneously injected bilaterally into the flanks of female CB17-SCID mice.  $4.0 \times 10^6$  cells were resuspended in 50% Matrigel (BD Biosciences) with PBS. In addition, one 12.5 mg 60 day release DHT pellet (Innovative Research of America) was implanted at the nape of the neck at the time of cell injections. When tumors reached  $\sim 80 \text{ mm}^3$ , mice were treated with one of the following treatment conditions: vehicle control (1% CMC, 0.1% Tween-80), seviteronel (75 mg/kg), 2 Gy of RT given once a day for 6 days, or combination of seviteronel with RT with 8 mice in each treatment group. Vehicle control and seviteronel (75 mg/kg) were both administered orally, once daily during treatment. Mice treated with both seviteronel and RT were given seviteronel for 24 h before RT. Tumor growth was measured with digital calipers using the equation:  $V = L \cdot W^2 \cdot \pi / 6$ . Body weight was measured weekly to assess weight loss and toxicity of therapy. All procedures were approved by the Institutional Animal Care and Use Committee (IACUC) at the University of Michigan and comply with regulatory standards.

### **2.3.7 Drug Information**

DHT was obtained from Sigma (D-073). Enzalutamide was obtained from MedChemExpress (HY-70002). Seviteronel was obtained directly from Innocrin Pharmaceuticals and solubilized in DMSO. Tamoxifen was obtained from MedChemExpress (HY-13757A) and solubilized in DMSO. For cellular assays including clonogenic survival and  $\gamma\text{H2AX}$  immunofluorescence assays, seviteronel was administered 1 hour before radiation treatment.

### **2.3.8 ChIP-qPCR**

Cells were plated in 10 cm dishes with  $4.0 \times 10^6$  cells/dish and allowed to adhere overnight before treatment with enzalutamide (1  $\mu$ M), seviteronel (1  $\mu$ M), or DMSO control for 18 hours before 4 Gy radiation. Cells were harvested 6 hours after radiation and crosslinked using formaldehyde (Sigma, F8775). ChIP was performed following the protocol from the HighCell# ChIP kit (Diagenode C01010062) using the anti-androgen receptor antibody (Millipore 06-680). Following immunoprecipitation, DNA was purified using the iPure kit v2 (Diagenode C03010015) and diluted 1:5 for qPCR. qPCR was performed using Fast SYBR Green Master Mix (Thermo Fisher 4385612). Percent of input is reported as the mean  $\pm$  SEM of two independent experiments. Primers for qPCR are listed in Table 2-2<sup>30</sup>.

### ***2.3.9 Reverse Transcription and qPCR***

RNA was harvested from cells using QIAzol and extracted using the miRNeasy mini kit (Qiagen 217004). Reverse transcription was performed using SuperScript III Reverse Transcriptase (ThermoFisher 18080085) with random primers (Thermo Fisher 48190011), and cDNA was diluted 1:5. Comparative qPCR was performed using Fast Sybr Green Master Mix (Thermo Fisher 4385612). Plates were read using a QuantStudio6 Flex Real Time qPCR system and analyzed using a comparative method to no treatment control. Relative expression was calculated as compared to gene expression of an untreated control and reported as the mean  $\pm$  SEM of three independent experiments. Primers for qPCR are listed in Table 2-2<sup>28</sup>.

### ***2.3.10 siRNA and Transfections***

siRNAs targeting AR were Dharmacon ON-TARGETplus siRNA individual oligos (J-003400-05-0002, J-003400-07-0002). siAR #1: GGAACUCGAUCGUAUCAUU, siAR #2: UCAAGGAACUCGAUCGUAU. Cells were transfected with siRNA using Opti-MEM

(Invitrogen 31985-062) and Lipofectamine RNAiMAX (Invitrogen 13778-150). For clonogenic survival assays, cells were transfected with siRNA and irradiated, then plated at cell densities as outlined in **Table 2-1**.

### ***2.3.11 Radiation***

Irradiation of cells and mice was performed at the University of Michigan Experimental Irradiation Core using a Philips RT250 (Kimtron Medical). In keeping with previous studies, the dose rate was approximately 2 Gy/min as previously described<sup>32,33</sup>.

### ***2.3.12 Statistical Analyses***

Statistical tests were performed in GraphPad Prism 7.0. Statistics for *in vitro* experiments were performed using a two-sided Student's *t*-test to compare gene expression between cells treated with DMSO and enzalutamide. For immunoblot comparisons, a one-way ANOVA with Dunnett's multiple comparisons test was used. For *in vivo* studies, a one-way ANOVA was used to compare tumor volume, and a log-rank test was used to compare survival curves. Synergy between seviteronel with radiation was assessed using the fractional tumor volume (FTV) method for *in vivo* experiments as previously described<sup>34,35</sup>.

## **2.4 Results**

### ***2.4.1 AR Inhibition Alone Does Not Affect Viability of AR+ TNBC Cells***

Anti-androgen therapies have been effective at inhibiting the growth of AR+ prostate cancer cells due to their reliance on AR signaling. Similarly, one strategy for inhibiting the growth of AR+ TNBC cell line models has been the use of AR inhibitors as monotherapy<sup>36,37</sup>. Here we compared two AR-antagonists, seviteronel and enzalutamide, in their ability to inhibit

viability of TNBC cells *in vitro*. Levels of AR protein were initially assessed in five TNBC cell lines and one ER<sup>+</sup> cell line (**Figure 2-1A**). Triple-negative breast cancer cell lines with the highest AR expression were selected for subsequent study, including MDA-MB-453, ACC-422, and SUM-185<sup>28</sup>. In AR<sup>+</sup> TNBC cells lines, MDA-MB-453, ACC-422, SUM-185, and SUM-159, treatment with enzalutamide or seviteronel did not cause a significant decrease in viability at concentrations up to 10  $\mu$ M (**Figure 2-1B-E**). Similar results were observed when MDA-MB-453 and ACC-422 cells were treated with enzalutamide or seviteronel in media containing CSS and lacking phenol red (**Figure 2-2A, B**). In an AR<sup>-</sup> TNBC model, MDA-MB-231 cells, treatment with seviteronel or enzalutamide did not decrease cell viability at concentrations up to 10  $\mu$ M when grown in FBS (**Figure 2-1F**) or CSS (**Figure 2-2C**).

Seviteronel has also been reported to have some anti-estrogen activity, so similar experiments were performed in an ER<sup>+</sup> cell line with low AR expression (MCF-7 cells). While the selective estrogen receptor modulator tamoxifen is able to inhibit viability of ER<sup>+</sup> MCF-7 cells in a dose-dependent manner (IC<sub>50</sub> = 1.1  $\mu$ M, **Figure 2-2D**), treatment with enzalutamide did not significantly inhibit viability (IC<sub>50</sub> > 10  $\mu$ M, **Figure 2-1G**). Seviteronel, however, also had some antagonistic effects on MCF-7 cells with an IC<sub>50</sub> ~7  $\mu$ M. This may be due to the anti-estrogenic effects of seviteronel in reducing CYP17 lyase activity, which has been previously reported<sup>27</sup>. These results suggest that AR inhibition does not affect cell viability at concentrations up to 10  $\mu$ M in AR<sup>+</sup> TNBC cell lines, and inhibition of AR alone at these concentrations may not be sufficient to inhibit viability of AR<sup>+</sup> TNBC cells *in vitro*.

#### ***2.4.2 AR knockdown and seviteronel treatment radiosensitizes AR<sup>+</sup> TNBC cells in vitro***

Initially, to determine whether AR knockdown is sufficient to confer radiosensitivity in AR<sup>+</sup> TNBC cells, clonogenic survival assays were performed with siRNA-mediated knockdown

of AR in multiple AR+ TNBC cell lines. Knockdown of AR with multiple siRNAs was performed in MDA-MB-453 cells, resulting in increased radiosensitivity with radiation enhancement ratios (rER) of 1.28-1.47. There was also a significant decrease in surviving fraction of cells at 2 Gy (**Figure 2-3A**). Comparatively, cisplatin, a well characterized radiosensitizer, provides enhancement ratios of 1.2<sup>38,39</sup>. Similar to results observed in MDA-MB-453 cells, a significant decrease in the surviving fraction at 2 Gy was observed in ACC-422 cells with siRNA-mediated AR knockdown (**Figure 2-3B**) with enhancement ratios of 1.58-1.89. siRNA knockdown of AR was verified by western blot in MDA-MB-453 and ACC-422 cells (**Figure 2-3C**).

To further address how AR is involved in the radiation response, radiosensitization was assessed via clonogenic survival assays with seviteronel-mediated AR inhibition in multiple AR+ models of TNBC. Doses of seviteronel were selected to be 10-100 fold lower than the IC50 of the drug to evaluate radiosensitizing effects independent of cytostatic or cytotoxic effects of seviteronel as a single agent. In AR+ TNBC cell lines, treatment with seviteronel provided a dose-dependent increase in radiosensitivity. In MDA-MB-453 cells, treatment with seviteronel led to significant radiosensitization with radiation enhancement ratios from 1.21-1.50 and a significant decrease in the surviving fraction of cells at 2 Gy (**Figure 2-3D**). Similarly, in SUM-185 and SUM-159 cells, the radiation enhancement ratios with seviteronel were 1.20-1.35 and 1.05-1.15, respectively (**Figure 2-3E, F**). SUM-185 cells also had a significant decrease in the surviving fraction of cells after 2 Gy radiation suggesting that seviteronel-mediated AR inhibition is effective at sensitizing TNBC cells that have high AR expression, even with low doses of RT<sup>40</sup>.

In contrast, in MDA-MB-231 cells, a TNBC model with low AR expression, seviteronel treatment did not result in significant radiosensitization (rER = 0.97-1.10) or a significant decrease in the surviving fraction of cells at 2 Gy (**Figure 2-3G**). Similar results were seen in MCF-7 cells (**Figure 2-3H**) which have high ER expression, but low AR expression (rER = 0.81-0.98). Together, these results suggest that seviteronel-mediated AR inhibition is able to radiosensitize AR+ TNBC models *in vitro*. In breast cancer cell lines that lack AR, however, treatment with seviteronel does not lead to radiosensitization (**Figure 2-3G**), suggesting the effect is mediated through the androgen receptor.

#### ***2.4.3 Differential effects on AR targets with enzalutamide- or seviteronel-mediated inhibition***

The role of the androgen receptor to signal as a transcription factor has been well-characterized in prostate cancer and is increasingly being recognized and studied in breast cancer. AR nuclear translocation results in the activation of downstream target genes including *AQP3* and *SEC14L2*<sup>41</sup>. Activation of target genes was studied in two TNBC cell lines with high AR expression: MDA-MB-453 and ACC-422 cells. Following stimulation with DHT, there is a decrease in AR transcript expression in MDA-MB-453 cells (**Figure 2-4A**). Treatment with enzalutamide and DHT, however, results in increased levels of AR mRNA in comparison to control cells also stimulated with DHT. Following DHT stimulation, AR inhibition with enzalutamide also decreases mRNA levels of target genes (*AQP3*, *SEC14L2*) in AR+ TNBC (**Figure 2-4B, C**). Seviteronel-mediated inhibition, however, results in no significant change in expression of AR target genes. Similar results were also seen in ACC-422 cells following DHT stimulation and treatment with enzalutamide or seviteronel (**Figure 2-5A-C**). In addition, AR activation has been shown to increase levels of phosphorylation of the catalytic subunit of DNA protein kinase (p-DNAPKcs) following radiation<sup>28,30</sup>. Treatment with only enzalutamide or

seviteronel following DHT stimulation in the absence of radiation does not result in changes in p-DNAPKcs levels, total levels of DNAPKcs, or AR protein in MDA-MB-453 (**Figure 2-4D**, **Figure 2-6A, B**) or ACC-422 cells (**Figure 2-6D-G**). Together these results indicate differences between enzalutamide- and seviteronel-mediated AR inhibition and the effects on downstream AR target genes.

#### ***2.4.4 AR inhibition results in persistence of dsDNA breaks after radiation***

Ionizing radiation induces single and double strand breaks in DNA that are acted upon by distinct DNA repair pathways. If unrepaired, single strand DNA breaks can be converted into dsDNA breaks at stalled replication forks; dsDNA breaks then require repair through NHEJ or HR repair pathways. Therefore, to further understand how seviteronel mediates radiosensitization *in vitro*, cells were stained for  $\gamma$ H2AX foci to assess levels of dsDNA breaks following RT in multiple models of AR+ TNBC. When AR+ TNBC cells (MDA-MB-453 and ACC-422) were treated with seviteronel alone, there was no change in levels of  $\gamma$ H2AX positive cells at 2, 6, 16 or 24 hours in MDA-MB-453 cells (**Figure 2-7A**) or at 30 minutes, 6, 16, or 24 hours in ACC-422 cells (**Figure 2-7B**), suggesting that seviteronel alone does not induce widespread dsDNA breaks. As expected, RT alone (2-4 Gy) rapidly induces dsDNA breaks that were slowly resolved over ~16-24 hours, depending on the cell line used. Differences in the p53 status of MDA-MB-453 (wild type) and ACC-422 (mutant)<sup>6</sup> cells, however, do not appear to affect dsDNA break repair<sup>42</sup>. Combination treatment with radiation and seviteronel at 1  $\mu$ M or 5  $\mu$ M led to significant delays in dsDNA break repair in both cell lines as indicated by significantly higher levels of  $\gamma$ H2AX positive cells compared to cells treated with radiation alone at the same time points. Representative images of cells at 16 hours after RT are shown for both cell lines (**Figure 2-7C, D**). These results suggest that seviteronel-mediated AR inhibition results

in accumulation of dsDNA breaks following radiation in AR+ TNBC models, including MDA-MB-453 and ACC-422 cell lines.

#### ***2.4.5 Seviteronel treatment in combination with radiation delays growth of xenograft tumors***

To further validate the *in vitro* radiosensitization findings and determine whether these occurred in intact tumors, an *in vivo* xenograft model with MDA-MB-453 cells was used. MDA-MB-453 cells were injected subcutaneously into bilateral flanks of CB17-SCID mice. When tumors reached ~80 mm<sup>3</sup>, seviteronel was administered orally each day. In order to assess true radiosensitization, seviteronel treatment was started one day prior to the beginning of radiation to achieve plasma concentrations in the 5 μM range at time of first radiation treatment (**Figure 2-8A**). In contrast to the *in vitro* viability assays, xenograft tumor growth was significantly inhibited by seviteronel alone and, as expected, was also inhibited by RT alone. The combination treatment with seviteronel and RT, however, led to a much more significant decrease in tumor volume compared to either treatment alone (**Figure 2-8B**). In addition, there was a significant delay in time to tumor doubling (7.5 days vs. 36 days) and tripling (13.5 days vs. undefined) in the mice treated with seviteronel and radiation compared to control mice (**Figure 2-8C, D**). The combination treatment seemed to be well tolerated, as there were no differences in weights or activity levels of the mice (**Figure 2-8E**). Using the fractional tumor volume (FTV) method for assessing synergy, the combination of seviteronel with radiation was found to have a synergistic effect (not just additive) with ratios greater than 1 (**Figure 2-8F**). Together these results suggest that seviteronel treatment in combination with radiation is effective at slowing tumor growth *in vivo* and that the combination treatment was more effective than either therapy alone.

#### ***2.4.6 AR binding at DNA damage response genes is enhanced with RT and seviteronel-mediated AR inhibition***



Having demonstrated that seviteronel-mediated AR inhibition is sufficient to confer radiosensitization in AR+ models of TNBC and that dsDNA breaks persist longer with combination treatment than with RT alone, we sought to better understand the mechanism by which seviteronel mediates radiosensitization. We hypothesized that AR transcriptional activity was regulating DNA damage gene expression to influence repair of DNA damage. Therefore, inhibition of AR with seviteronel or enzalutamide would decrease target gene expression and AR binding to AR-transcription factor binding sites located near or within DNA repair genes. Using ChIP-qPCR, we evaluated AR recruitment at DNA damage response genes containing AR binding regions in an effort to understand how seviteronel was influencing the DNA damage response following radiation compared to AR inhibition with enzalutamide. Previous work from our lab suggests that that AR may be important in AR+ TNBC for the repair of dsDNA breaks by activating DNAPKcs<sup>28</sup>, an important protein involved in NHEJ<sup>43</sup>. A number of DNA damage response genes have previously been reported to be controlled by AR expression in prostate cancer models, including *XRCC2*, *XRCC3*, and *PRKDC*<sup>30</sup>. *XRCC2* and *XRCC3* contain AR regulatory regions, and these genes are part of the Rad51 family, playing an important role in the repair of dsDNA breaks through HR<sup>44</sup>. *PRKDC* is the gene encoding DNAPKcs. At all three loci, AR binding is thought to influence gene expression.

To begin to understand how enzalutamide and seviteronel may be differentially affecting expression of AR-controlled genes following radiation, ChIP-qPCR experiments were performed. AR recruitment to AR-occupied regions was compared between the following treatment conditions: control (no treatment), enzalutamide only, seviteronel only, radiation alone, or the combination of enzalutamide and radiation, or seviteronel and radiation. When cells were treated with seviteronel or enzalutamide alone, AR was recruited to regulatory regions of

*XRCC2*, *XRCC3*, and *PRKDC* (Figure 2-9). When compared to cells treated with radiation alone, cells receiving both radiation and seviteronel had significantly increased AR recruitment. Similar AR binding was not observed when cells were treated with combination of enzalutamide and radiation, suggesting that this is a seviteronel-specific effect.

## 2.5 Discussion

Here we show that although seviteronel and enzalutamide exhibited limited effect as a single agent ( $IC_{50} > 10 \mu M$ ), AR knockdown and AR inhibition with seviteronel were effective at radiosensitizing AR+ TNBC models with radiation enhancement ratios of 1.20-1.89. Radiosensitization of AR+ TNBC models was at least partially dependent on impaired dsDNA break repair. Similar effects were observed *in vivo* where there was a significant reduction in tumor volume and a delay to tumor doubling and tripling times in mice with AR+ TNBC xenograft tumors treated with seviteronel and radiation. Mechanistically, we report differential binding of AR to target genes in the presence of enzalutamide and seviteronel, suggesting different mechanisms of action between the two drugs.

These findings should be taken in the broader context of anti-androgens as a therapeutic strategy in breast cancer. Other groups have investigated how AR inhibition may be a therapeutic strategy for aggressive TNBC tumors. Clinical trials with enzalutamide as monotherapy have demonstrated that AR inhibition is safe and efficacious<sup>45</sup>, and patients with AR-activated tumors who receive enzalutamide have improved metastatic progression-free survival<sup>46</sup>. Additional studies are investigating the use of CYP17 lyase inhibitors, like abiraterone acetate, which may be effective for patients with molecular apocrine tumors<sup>47</sup>. Similarly, a trial investigating treatment with seviteronel for patients with breast cancer (NCT02580448) was recently completed, and stage 1 results from the Phase II trial suggest that seviteronel provides clinical

benefit and decreased levels of circulating tumor cells when administered alone<sup>27,48</sup>. This work demonstrates additional clinical applications for AR targeting agents in the treatment of breast cancer.

There are also a number of limitations of the current study. While this study suggests that AR inhibition is an effective strategy for the radiosensitization of AR+ TNBC cells, additional studies are needed to understand the exact mechanism of radiosensitization in these models, and confirmation using additional AR+ TNBC models, including patient derived xenograft (PDX) models are still needed. Future work will also seek to understand the differences in how enzalutamide and seviteronel affect the ability of AR to bind DNA and activate the transcription of downstream target genes. Our results suggest that seviteronel has a unique mechanism of radiosensitization compared to the second-generation anti-androgen enzalutamide. Indeed, these results suggest that AR is increasingly recruited to binding sites of DNA damage response genes involved both in HR and NHEJ following treatment with seviteronel and radiation. This may suggest that AR remains bound to these regions but may not be activating transcription of these genes. This may be due to co-repressor recruitment at these sites (instead of co-activator) or stalling of the transcriptional machinery. Thus, although seviteronel is found more frequently bound to promoter regions of NHEJ and HR genes, there does not seem to be a functional improvement of DNA repair efficacy or efficiency, suggesting that the mechanism of radiosensitization with seviteronel is different than that previously reported for enzalutamide. Although the details of these mechanistic differences remain unresolved, additional studies are underway to investigate the mechanism of AR-mediated radiosensitization both with enzalutamide and seviteronel to understand how these AR inhibitors are differentially affecting the radiation response. Another limitation is the disparate findings on the effect of seviteronel *in*

*vitro* and *in vivo*. Indeed, this study demonstrates that although AR inhibition with seviteronel alone is not sufficient to inhibit the viability of AR+ TNBC cells *in vitro*, seviteronel does inhibit proliferation *in vivo* and sensitizes cells to radiation treatment both *in vitro* and *in vivo* (**Figure 2-1, Figure 2-3, Figure 2-8**). This difference may be attributed to a difference in intratumoral androgens, which would be inhibited *in vivo* but not affected in tissue culture, *ex vivo* studies. Furthermore, cytostatic effects of a drug tend to have a more significant impact *in vivo* compared to the *in vitro* cell proliferation studies performed, as these are compared to vehicle controls. Finally, seviteronel may have cancer cell extrinsic effects, including altering the tumor microenvironment and endocrine signaling within the mice that would not be observed to the same extent *in vitro*.

In summary, TNBC continues to be a clinically challenging disease entity with limited/no effective molecularly targeted therapies. With the identification of AR+ TNBC subtype, interest in targeting AR in these patients continues. The data reported herein provide the preclinical rationale for continued clinical investigation of anti-androgens as a general class of molecularly targeted therapies for the targeted treatment of AR+ TNBC and specifically for the further investigation of seviteronel as a radiosensitizing agent in women with radioresistant AR+ TNBC.

## **2.6 Acknowledgements**

SUM-159 and SUM-185PE cells were generously provided by Dr. Stephen Ethier from stocks at the University of Michigan. Seviteronel was generously provided by Innocrin Pharmaceuticals.

## 2.7 Figures

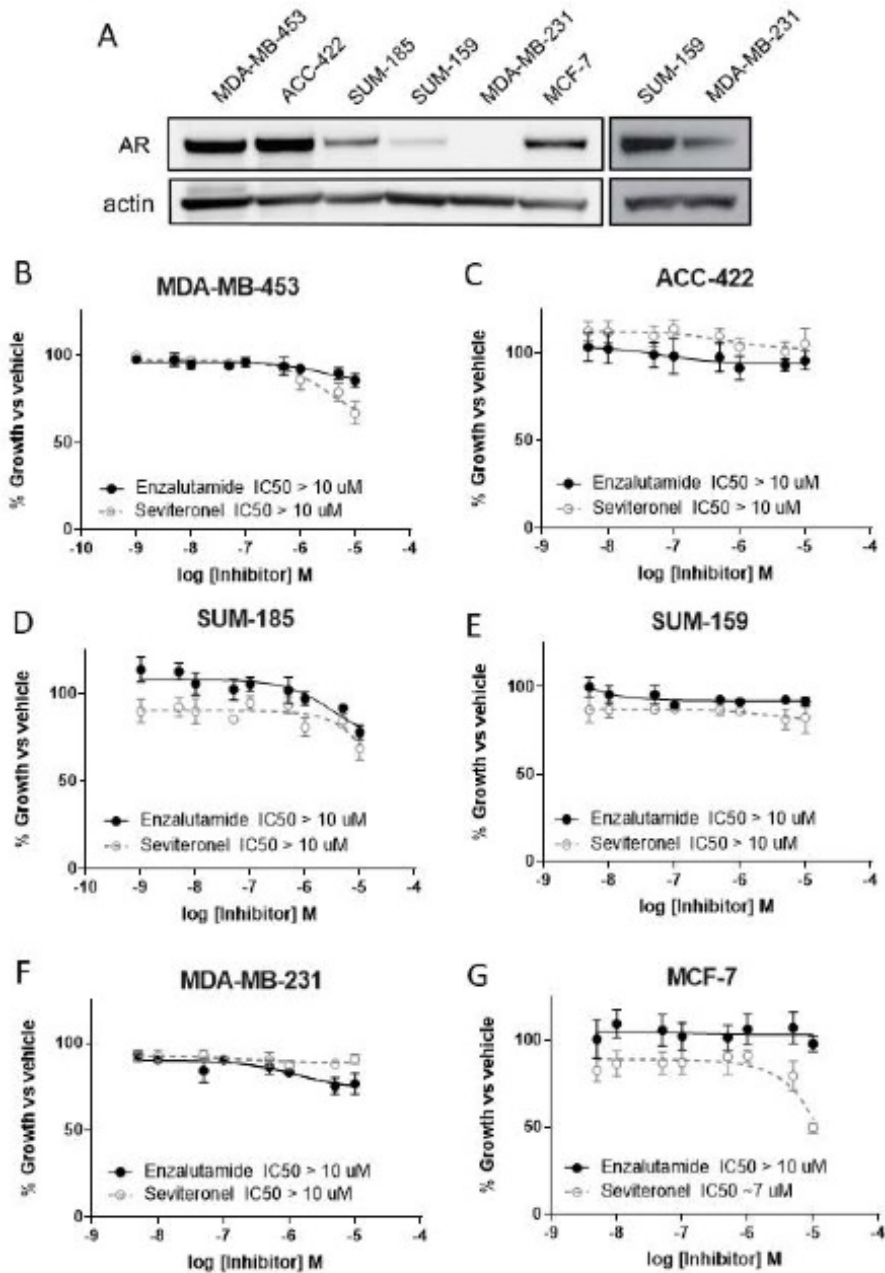


**Figure 2-1: Cell viability is not affected by AR inhibition with enzalutamide or seviteronel**

(A) AR expression was measured via immunoblot in TNBC and ER+ cell lines. Cells were treated with seviteronel or enzalutamide, and viability was assessed via metabolic activity for AR+ TNBC cells: (B) MDA-MB-453 (C) ACC-422, (D) SUM-185, (E) SUM-159, and (F) AR- TNBC MDA-MB-231 cells. Viability of AR-, ER+ MCF-7 cells was assessed with (G) enzalutamide and seviteronel treatment at concentrations up to 10  $\mu$ M. Graphs represent mean  $\pm$  SEM for three independent experiments.

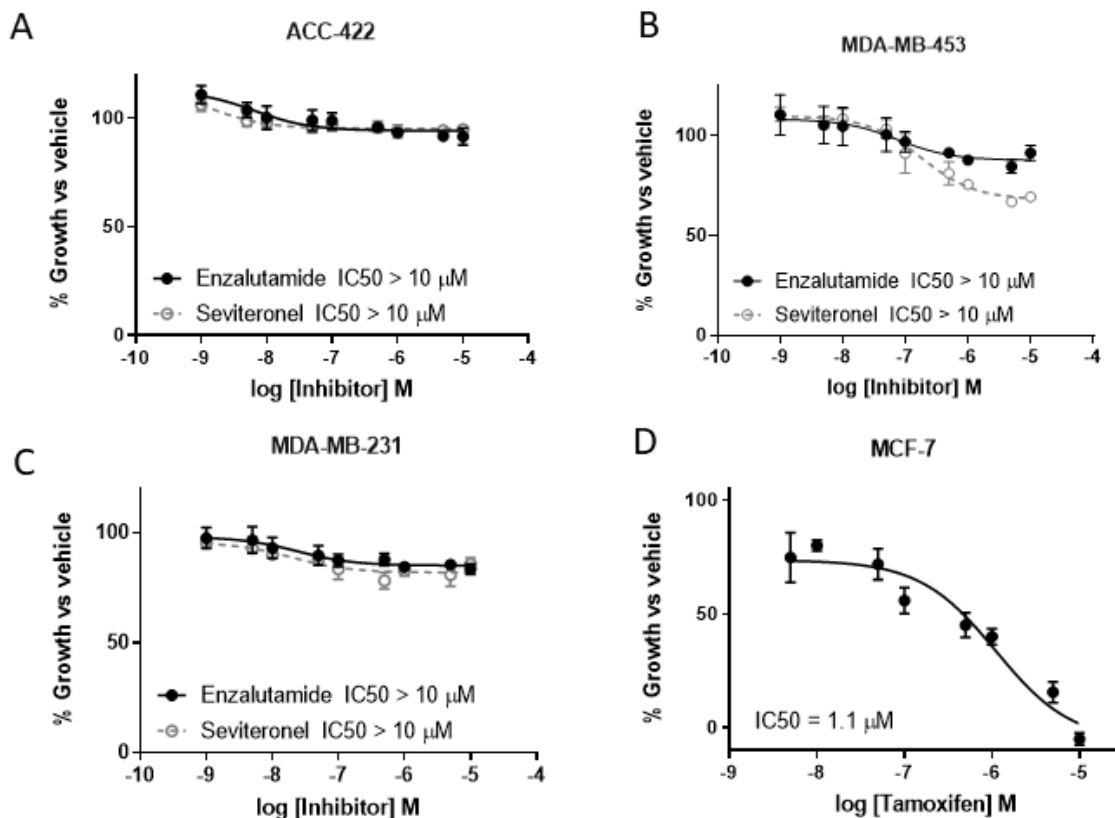


**Figure 2-2: Cell viability with treatment of AR inhibitors**

AR+ TNBC cell lines were pretreated with CSS and phenol free media overnight before treatment with enzalutamide or seviteronel. Cell viability was assessed via metabolic activity in (A) MDA-MB-453 and (B) ACC-422 cells. (C) Viability of MDA-MB-231 cells, a AR- TNBC cell line, was used as a control. (D) Viability of MCF-7 cells was inhibited with treatment of tamoxifen with an IC50 of 1.1  $\mu$ M. Graphs represent mean  $\pm$  SEM for triplicate experiments.

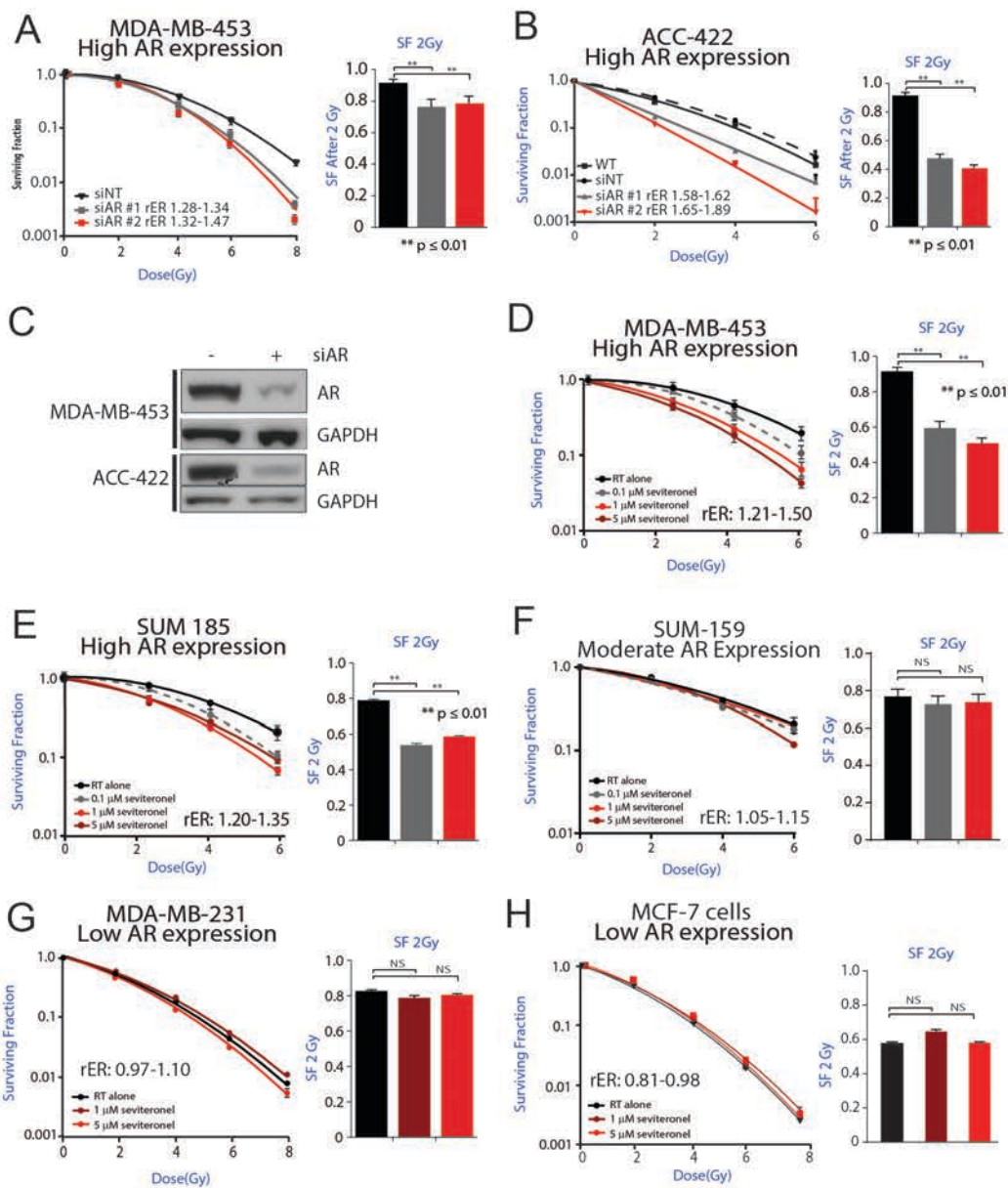


**Figure 2-3 AR inhibition via genetic knockdown or seviteronol treatment in combination with radiation decreases clonogenic survival in AR+ TNBC cell lines**

Clonogenic survival assays with siRNA targeting AR were performed in (A) MDA-MB-453 and (B) ACC-422 cells. (C) Knockdown was confirmed by immunoblot. Clonogenic survival assays with seviteronol were performed in TNBC cell lines with high AR expression including (D) MDA-MB-453, and (E) SUM-185 cells, and a moderate AR-expressing cell line (F) SUM-159. Assays were also performed in AR- TNBC (G) MDA-MB-231 cells or AR-, ER+ (H) MCF-7 cells. Representative clonogenic survival assays for each cell line are shown, while the surviving fractions of cells at 2 Gy (SF 2 Gy) are shown as the mean ± SEM of three independent experiments (NS = p is not significant, \*\* = p ≤ 0.01).

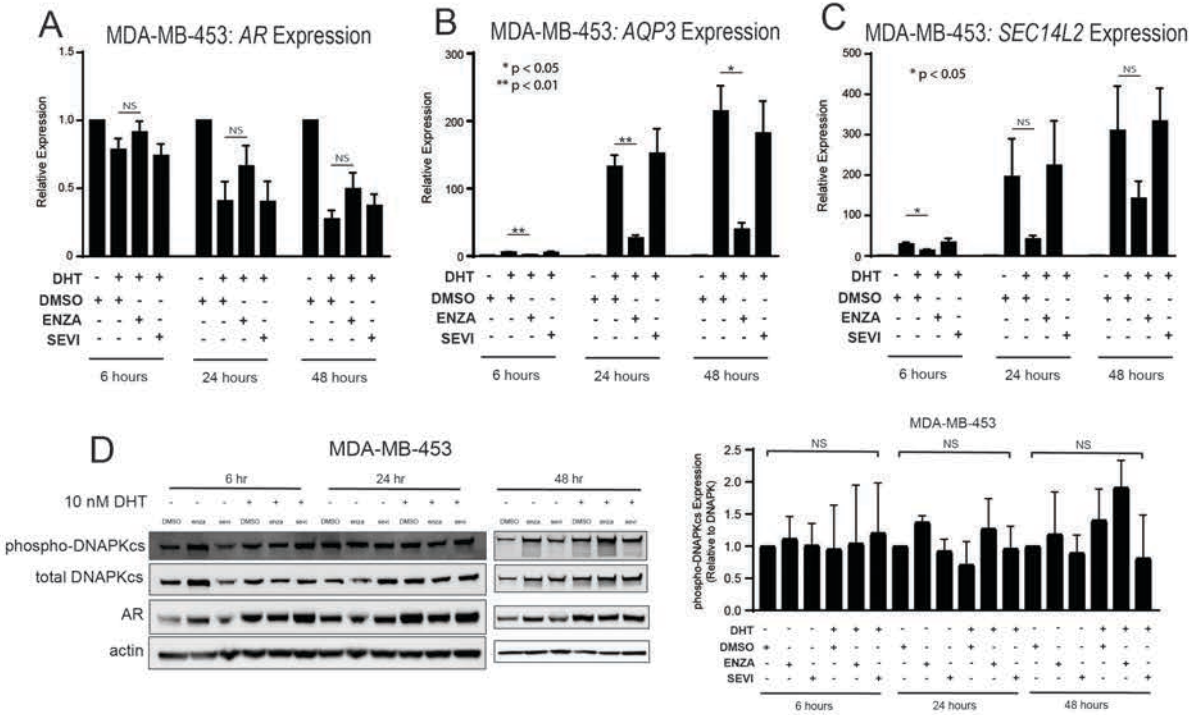


**Figure 2-4: Differential effects on AR and AR targets with enzalutamide and seviteronel treatment**

AR+ TNBC cells were treated with 5  $\mu$ M enzalutamide or seviteronel  $\pm$  10 nM DHT. RT-qPCR was used to assess mRNA expression of (A) AR, (B) AQP3, and (C) SEC14L2 in MDA-MB-453 cells. (D) Protein levels of p-DNAPKcs, total DNAPKcs, and AR were measured by immunoblot in MDA-MB-453 cells. Gene expression data represent mean  $\pm$  SEM for three independent experiments, and immunoblots are representative of triplicate experiments. (NS = p is not significant, \* =  $p < 0.05$ , \*\* =  $p < 0.01$ ).



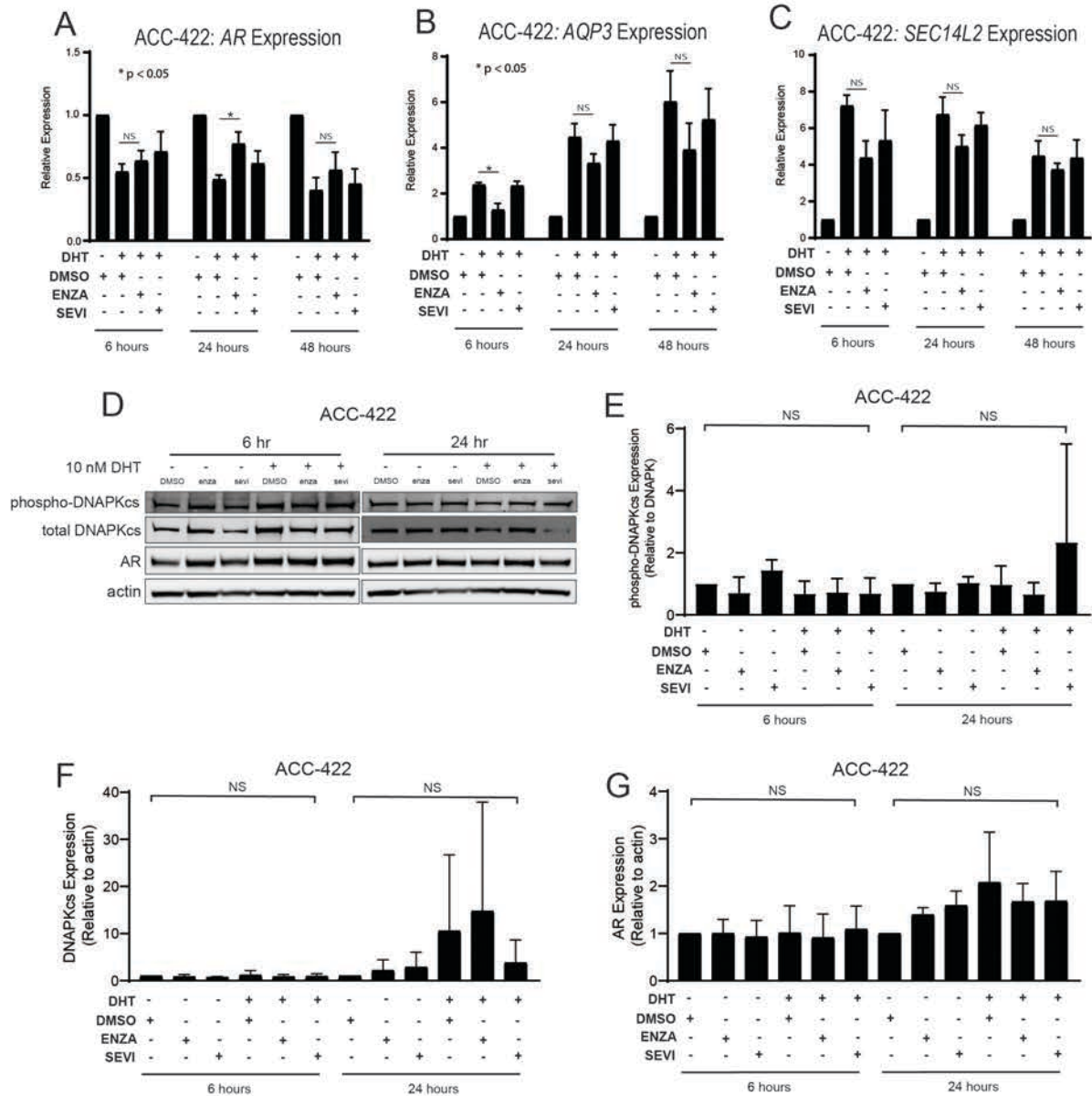


**Figure 2-5: Differential effects on AR and AR targets with enzalutamide and seviteronel in ACC-422 cells**

ACC-422, AR+ TNBC cells, were treated with 5  $\mu$ M enzalutamide or seviteronel  $\pm$  10 nM DHT. mRNA expression was assessed via qPCR for (A) *AR*, (B) *AQP3*, (C) *SEC14L2*. Expression of p-DNAPKcs, total DNAPKcs, and AR protein levels were measured by immunoblot (D) and quantified (E-G). Gene expression data represent three independent experiments and are shown as mean  $\pm$  SEM. Immunoblots are representative of triplicate experiments. (NS = p is not significant, \* = p < 0.05).

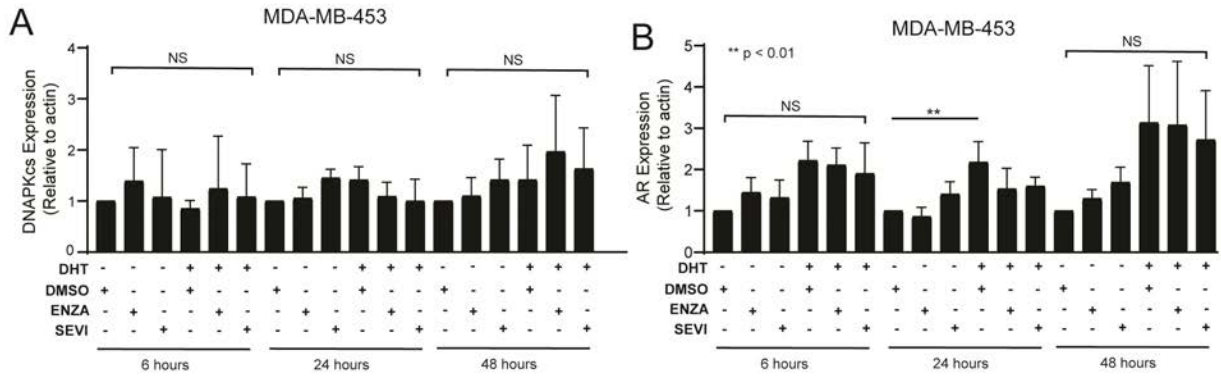


**Figure 2-6: Quantification of DNAPKcs and AR Protein Expression in MDA-MB-453 cells**

Quantification of immunoblots for (A) DNAPKcs and (B) AR expression in MDA-MB-453 cells. (NS = p is not significant, \*\* = p < 0.01).

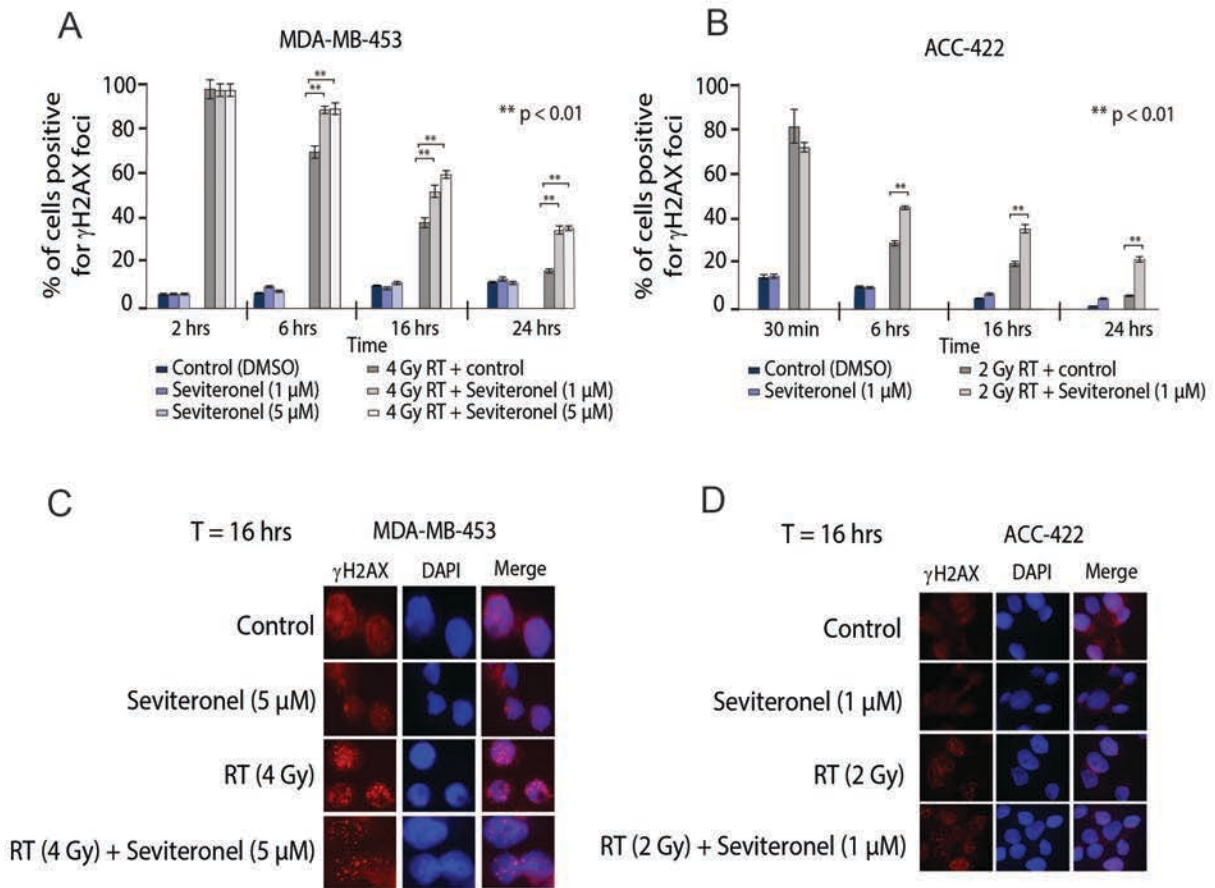


**Figure 2-7: Combination treatment results in increased levels of  $\gamma$ H2AX foci and delayed resolution of dsDNA breaks**

$\gamma$ H2AX foci in (A) MDA-MB-453 (p53 wild type) and (B) ACC-422 (p53 mutant) cells were observed using a fluorescent microscope. MDA-MB-453 cells containing  $\geq 15$  foci were counted as positive, and ACC-422 cells containing  $\geq 15$  foci were counted as positive. Representative images of  $\gamma$ H2AX foci are shown for (C) MDA-MB-453 and (D) ACC-422 cells for each treatment group. Graphs represent the mean  $\pm$  SD for three independent experiments (\*\* =  $p < 0.01$ ).

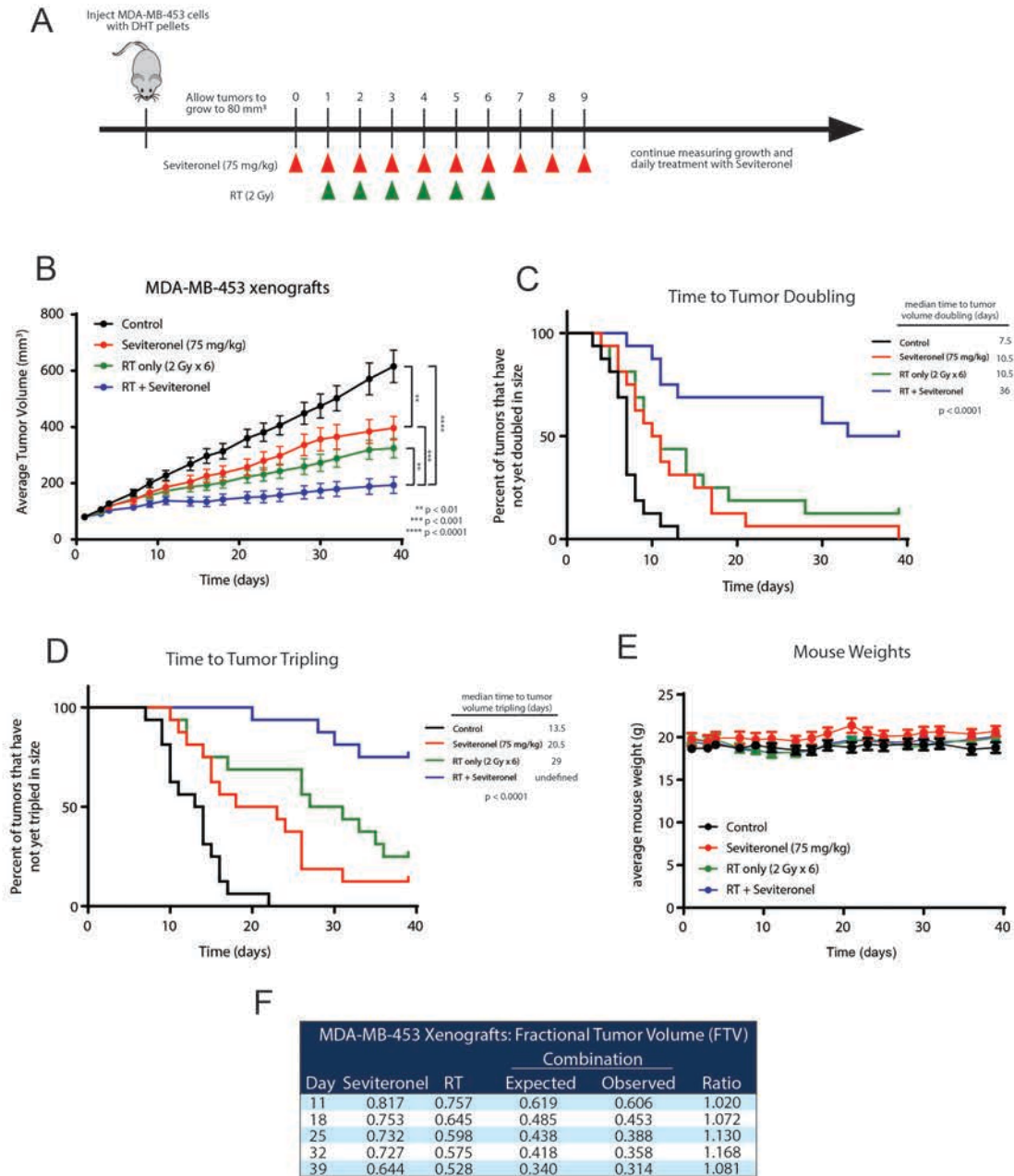


**Figure 2-8: Seviteronel and radiation is more effective than seviteronel or radiation alone in MDA-MB-453 xenograft model *in vivo***

(A) MDA-MB-453 cells were injected into CB17-SCID mice, and treatment began when tumors reached approximately 80 mm<sup>3</sup> in size. Treatment with seviteronel began one day prior to initiation of radiation treatment and continued after the completion of 6 fractions of radiation. (B) Tumor volume was measured, and (C) time to tumor doubling and (D) time to tumor tripling was assessed. (E) Toxicities were evaluated by animal weights throughout the duration of treatment and monitoring. (F) The FTV method was used to assess synergy of use of seviteronel with radiation (\*\* = p < 0.01, \*\*\* = p < 0.001, \*\*\*\* = p < 0.0001).

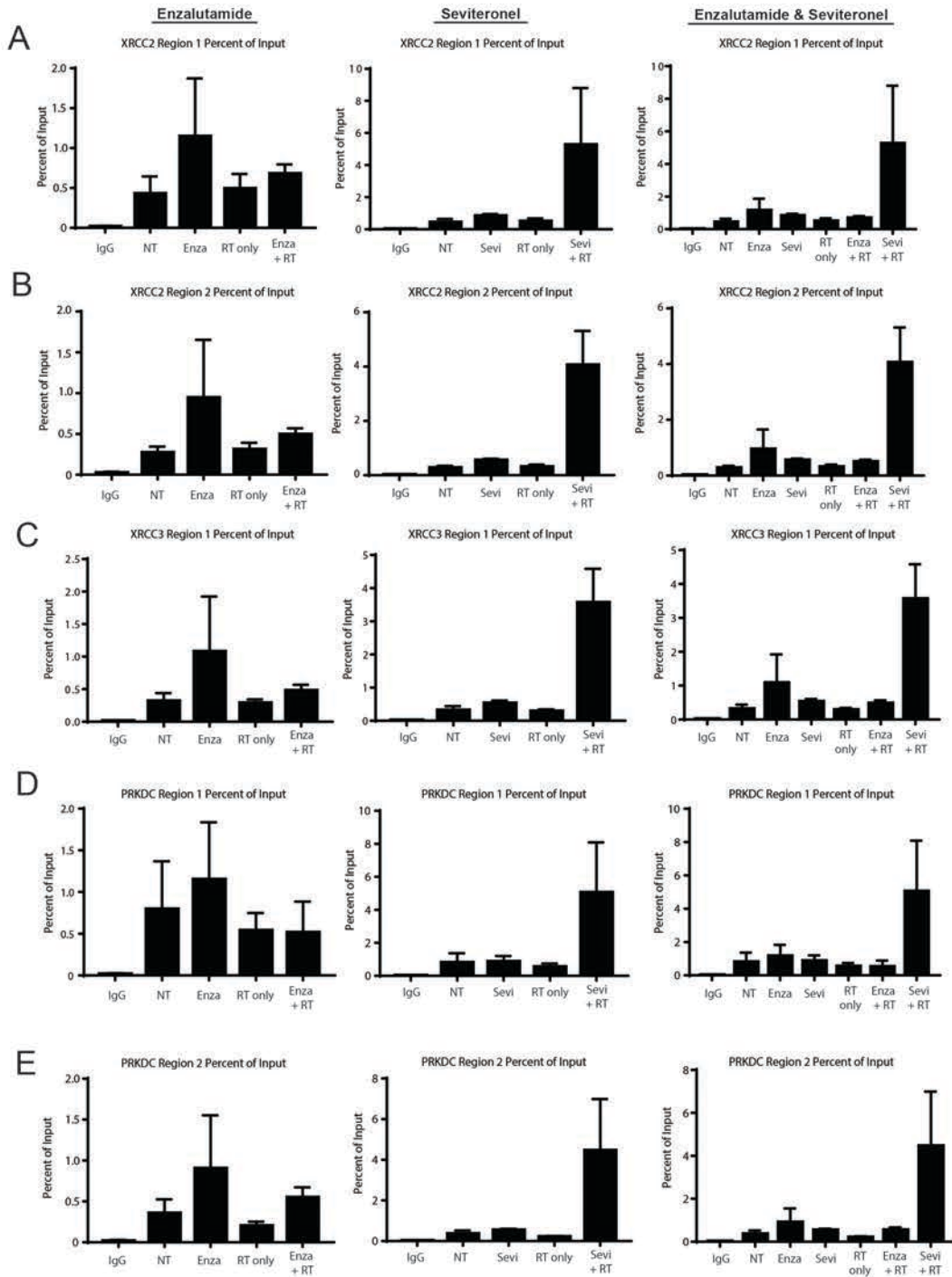


**Figure 2-9: Seviteronel with radiation increases AR recruitment compared to monotherapy treatment of enzalutamide with radiation**

AR recruitment to DNA damage response genes was measured by ChIP-qPCR experiments at AR binding to regions surrounding (A, B) *XRCC2*, (C) *XRCC3*, and (D, E) *PRKDC*. Graphs represent the mean  $\pm$  SEM for two independent experiments.

## 2.8 Tables

**Table 2-1: Plating Densities for Clonogenic Survival Assays**

	<b>MDA-MB-453</b>	<b>ACC-422</b>	<b>SUM-185</b>	<b>SUM-159</b>	<b>MDA-MB-231</b>	<b>MCF-7</b>
<b>0 Gy</b>	250	500	300	150	250	500
	500	1000				
<b>2 Gy</b>	1000	1000	600	300	500	1000
	2000	2000				
<b>4 Gy</b>	2000	10,000	1200	300	1000	5000
	4000	20,000				
<b>6 Gy</b>	2500	20,000	4500	450	2500	10,000
	5000	50,000				
<b>8 Gy</b>	5000				5000	12,500
	8000					

**Table 2-2: qPCR primers**

XRCC2_AROR1_F1	GCCTGAACAATGGAGATAAAAGAG
XRCC2_AROR1_R1	TGCCTCAGGGAACAAATAAGAC
XRCC2_AROR2_F1	AGCCAAAACACTCCCTCAAG
XRCC2_AROR2_R1	CTCAAGTCATCTTCCCACCTC
XRCC3_AROR1_F1	GCCAGCGTTTTGTAACTG
XRCC3_AROR1_R1	GGATTTGGATCTACTGGACCTG
PKRDC_AROR1_F1	GCATCGCTAGGGAACAAGG
PKRDC_AROR1_R1	CTGCGATAAACATCTTGACAGAG
PKRDC_AROR2_F1	AAGGTGTCACTTCCTGTTCAC
PKRDC_AROR2_R1	TGAGCTATGCTGATTTTACCTAGG
AR Forward	CAGTGGATGGGCTGAAAAT
AR Reverse	GGAGCTTGGTGAGCTGGTAG
AQP3 Forward	CCGTGACCTTTGCCATGTGCTT
AQP3 Reverse	TTGTGCGCGAAGTGCCAGATTG
SEC14L2 Forward	CCTGAAGACCAAGATGGGAGAG
SEC14L2 Reverse	GCTGTAGGTGTTGTCAAACCGC

## 2.9 References

1. American Cancer Society. Breast Cancer Facts & Figures 2017-2018. 44.
2. Kyndi, M. *et al.* Estrogen Receptor, Progesterone Receptor, HER-2, and Response to Postmastectomy Radiotherapy in High-Risk Breast Cancer: The Danish Breast Cancer Cooperative Group. *JCO* **26**, 1419–1426 (2008).
3. Abramson, V. G. & Mayer, I. A. Molecular Heterogeneity of Triple Negative Breast Cancer. *Curr Breast Cancer Rep* **6**, 154–158 (2014).
4. Garrido-Castro, A. C., Lin, N. U. & Polyak, K. Insights into Molecular Classifications of Triple-Negative Breast Cancer: Improving Patient Selection for Treatment. *Cancer Discov* **9**, 176–198 (2019).
5. Bareche, Y. *et al.* Unravelling triple-negative breast cancer molecular heterogeneity using an integrative multiomic analysis. *Ann. Oncol.* **29**, 895–902 (2018).
6. Lehmann, B. D. *et al.* Identification of human triple-negative breast cancer subtypes and preclinical models for selection of targeted therapies. *J Clin Invest* **121**, 2750–2767 (2011).
7. Proverbs-Singh, T., Feldman, J. L., Morris, M. J., Autio, K. A. & Traina, T. A. Targeting the androgen receptor in prostate and breast cancer: several new agents in development. *Endocr. Relat. Cancer* **22**, R87–R106 (2015).
8. Ni, M. *et al.* Targeting Androgen Receptor in Estrogen Receptor-Negative Breast Cancer. *Cancer Cell* **20**, 119–131 (2011).
9. Cochrane, D. R. *et al.* Role of the androgen receptor in breast cancer and preclinical analysis of enzalutamide. *Breast Cancer Research* **16**, R7 (2014).
10. Barton, V. N. *et al.* Multiple Molecular Subtypes of Triple-Negative Breast Cancer Critically Rely on Androgen Receptor and Respond to Enzalutamide In Vivo. *Mol Cancer Ther* **14**, 769–778 (2015).
11. Giovannelli, P., Donato, M. D., Auricchio, F., Castoria, G. & Migliaccio, A. Androgens Induce Invasiveness of Triple Negative Breast Cancer Cells Through AR/Src/PI3-K Complex Assembly. *Sci Rep* **9**, 1–14 (2019).
12. Giovannelli, P. *et al.* The Androgen Receptor in Breast Cancer. *Front Endocrinol (Lausanne)* **9**, (2018).
13. Mina, A., Yoder, R. & Sharma, P. Targeting the androgen receptor in triple-negative breast cancer: current perspectives. *Onco Targets Ther* **10**, 4675–4685 (2017).
14. Kono, M. *et al.* Androgen Receptor Function and Androgen Receptor–Targeted Therapies in Breast Cancer: A Review. *JAMA Oncol* **3**, 1266–1273 (2017).
15. Crawford, E. D. *et al.* Androgen Receptor Targeted Treatments of Prostate Cancer: 35 Years of Progress with Antiandrogens. *J. Urol.* **200**, 956–966 (2018).
16. Tesei, A. *et al.* Effect of small molecules modulating androgen receptor (SARMs) in human prostate cancer models. *PLoS ONE* **8**, e62657 (2013).



17. Varchi, G. *et al.* Nonsteroidal androgen receptor ligands: versatile syntheses and biological data. *ACS Med Chem Lett* **3**, 454–458 (2012).
18. Miller, W. L. Androgen biosynthesis from cholesterol to DHEA. *Mol. Cell. Endocrinol.* **198**, 7–14 (2002).
19. Vasaitis, T. S., Bruno, R. D. & Njar, V. C. O. CYP17 inhibitors for prostate cancer therapy. *J Steroid Biochem Mol Biol* **125**, 23–31 (2011).
20. Alex, A. B., Pal, S. K. & Agarwal, N. CYP17 inhibitors in prostate cancer: latest evidence and clinical potential. *Ther Adv Med Oncol* **8**, 267–275 (2016).
21. Vasaitis, T. S., Bruno, R. D. & Njar, V. C. O. CYP17 inhibitors for prostate cancer therapy. *J. Steroid Biochem. Mol. Biol.* **125**, 23–31 (2011).
22. Moreira, V. M., Salvador, J. a. R., Vasaitis, T. S. & Njar, V. C. O. CYP17 inhibitors for prostate cancer treatment--an update. *Curr. Med. Chem.* **15**, 868–899 (2008).
23. Tran, C. *et al.* Development of a Second-Generation Antiandrogen for Treatment of Advanced Prostate Cancer. *Science* **324**, 787–790 (2009).
24. Cochrane, D. R. *et al.* Role of the androgen receptor in breast cancer and preclinical analysis of enzalutamide. *Breast Cancer Research* **16**, R7 (2014).
25. Toren, P. J. *et al.* Anticancer Activity of a Novel Selective CYP17A1 Inhibitor in Preclinical Models of Castrate-Resistant Prostate Cancer. *Mol Cancer Ther* **14**, 59–69 (2015).
26. Gupta, S. *et al.* Phase 1 Study of Seviteronel, a Selective CYP17 Lyase and Androgen Receptor Inhibitor, in Men with Castration-Resistant Prostate Cancer. *Clin Cancer Res* clincanres.0564.2018 (2018) doi:10.1158/1078-0432.CCR-18-0564.
27. Bardia, A. *et al.* Phase 1 study of seviteronel, a selective CYP17 lyase and androgen receptor inhibitor, in women with estrogen receptor-positive or triple-negative breast cancer. *Breast Cancer Res Treat* **171**, 111–120 (2018).
28. Speers, C. *et al.* Androgen receptor as a mediator and biomarker of radioresistance in triple-negative breast cancer. *npj Breast Cancer* **3**, 29 (2017).
29. Polkinghorn, W. R. *et al.* Androgen receptor signaling regulates DNA repair in prostate cancers. *Cancer Discov* **3**, 1245–1253 (2013).
30. Goodwin, J. F. *et al.* A hormone-DNA repair circuit governs the response to genotoxic insult. *Cancer Discov* **3**, 1254–1271 (2013).
31. Yard, B. D. *et al.* A genetic basis for the variation in the vulnerability of cancer to DNA damage. *Nature Communications* **7**, 11428 (2016).
32. Speers, C. *et al.* Maternal Embryonic Leucine Zipper Kinase (MELK) as a Novel Mediator and Biomarker of Radioresistance in Human Breast Cancer. *Clin Cancer Res* **22**, 5864–5875 (2016).
33. Feng, F. Y. *et al.* Targeted radiosensitization with PARP1 inhibition: optimization of therapy and identification of biomarkers of response in breast cancer. *Breast Cancer Res Treat* **147**, 81–94 (2014).

34. Yokoyama, Y., Dhanabal, M., Griffioen, A. W., Sukhatme, V. P. & Ramakrishnan, S. Synergy between Angiostatin and Endostatin: Inhibition of Ovarian Cancer Growth. *Cancer Res* **60**, 2190–2196 (2000).
35. Matar, P. *et al.* Combined Epidermal Growth Factor Receptor Targeting with the Tyrosine Kinase Inhibitor Gefitinib (ZD1839) and the Monoclonal Antibody Cetuximab (IMC-C225): Superiority Over Single-Agent Receptor Targeting. *Clin Cancer Res* **10**, 6487–6501 (2004).
36. Caiazza, F. *et al.* Preclinical evaluation of the AR inhibitor enzalutamide in triple-negative breast cancer cells. *Endocr. Relat. Cancer* **23**, 323–334 (2016).
37. Gucalp, A. & Traina, T. A. Targeting the androgen receptor in triple-negative breast cancer. *Current Problems in Cancer* **40**, 141–150 (2016).
38. Skov, K. & Macphail, S. Interaction of platinum drugs with clinically relevant X-ray doses in mammalian cells: A comparison of cisplatin, carboplatin, iproplatin, and tetraplatin. *International Journal of Radiation Oncology\*Biophysics* **20**, 221–225 (1991).
39. Zhang, X. *et al.* In vitro and in vivo study of a nanoliposomal cisplatin as a radiosensitizer. *International Journal of Nanomedicine* <https://www.dovepress.com/in-vitro-and-in-vivo-study-of-a-nanoliposomal-cisplatin-as-a-radiosens-peer-reviewed-article-IJN> (2011) doi:10.2147/IJN.S15997.
40. Cuenca-López, M. D. *et al.* Phospho-kinase profile of triple negative breast cancer and androgen receptor signaling. *BMC Cancer* **14**, 302 (2014).
41. Bolton, E. C. *et al.* Cell- and gene-specific regulation of primary target genes by the androgen receptor. *Genes Dev* **21**, 2005–2017 (2007).
42. Moon, S.-H. *et al.* Wild-type p53-induced Phosphatase 1 Dephosphorylates Histone Variant  $\gamma$ -H2AX and Suppresses DNA Double Strand Break Repair. *J. Biol. Chem.* **285**, 12935–12947 (2010).
43. Davis, A. J. & Chen, D. J. DNA double strand break repair via non-homologous end-joining. *Transl Cancer Res* **2**, 130–143 (2013).
44. Liu, N. *et al.* XRCC2 and XRCC3, New Human Rad51-Family Members, Promote Chromosome Stability and Protect against DNA Cross-Links and Other Damages. *Molecular Cell* **1**, 783–793 (1998).
45. Traina, T. A. *et al.* Enzalutamide for the Treatment of Androgen Receptor-Expressing Triple-Negative Breast Cancer. *JCO* **36**, 884–890 (2018).
46. Traina, T. A. *et al.* Results from a phase 2 study of enzalutamide (ENZA), an androgen receptor (AR) inhibitor, in advanced AR+ triple-negative breast cancer (TNBC). *JCO* **33**, 1003–1003 (2015).
47. Bonnefoi, H. *et al.* A phase II trial of abiraterone acetate plus prednisone in patients with triple-negative androgen receptor positive locally advanced or metastatic breast cancer (UCBG 12-1). *Ann Oncol* **27**, 812–818 (2016).

48. Gucalp, A. *et al.* Phase (Ph) 2 stage 1 clinical activity of seviteronel, a selective CYP17-lyase and androgen receptor (AR) inhibitor, in women with advanced AR+ triple-negative breast cancer (TNBC) or estrogen receptor (ER)+ BC: CLARITY-01. *JCO* **35**, 1102–1102 (2017).

## **Chapter 3 : Multiomics Analysis to Uncover the Mechanism of Radiosensitization of Androgen Receptor-Positive Triple Negative Breast Cancers With AR Inhibition<sup>3</sup>**

### **3.1 Abstract**

Expression of the androgen receptor (AR) has been identified as a driver of tumor growth in triple negative breast cancers (TNBC), and previous work has nominated AR inhibition as a strategy for radiosensitization in AR+ TNBC. Despite its role in radioresistance in AR+ TNBC, the mechanistic role of AR and specifically its role in mediating DNA damage repair in response to radiation therapy (RT) remains unknown. While stimulation with R1881 is sufficient to induce nuclear translocation of AR in AR+ TNBC cells, AR inhibition with enzalutamide, apalutamide, or darolutamide blocked AR nuclear translocation under CSS or FBS growth conditions. When cells are treated with R1881+RT, AR nuclear translocation was induced at similar or greater levels compared to R1881 alone in AR+ TNBC cells. Combination treatment of RT with enzalutamide in the presence of hormones reduced AR nuclear localization (32-39% reduction) compared to RT alone. These results suggest that decreased promoter region binding, and gene expression upregulation may be a mechanism of radiosensitization with AR inhibition. Pathway analyses and proteomic changes in these models demonstrated changes in the MAPK/ERK signaling pathway, suggesting that MAPK signaling may be responsible for AR-mediated

---

<sup>3</sup>This chapter was completed in collaboration with the following authors: Benjamin C. Chandler, Andrea M. Pesch, Lynn M. Lerner, Leah Moubadder, Stephanie The, Breanna McBean, Lori J. Pierce, Corey W. Speers

radioresistance phenotype. Together our findings suggest that AR-mediated radioresistance is due, at least in part, to downstream MAPK/ERK signaling.

### 3.2 Introduction

Therapies targeting the androgen receptor (AR) have been of increasing interest for the treatment of AR-positive (AR+) breast tumors, including AR+ triple negative breast cancers (TNBC). Due to the ineffectiveness of molecular targeted therapies, patients with TNBC, which lack expression of the estrogen receptor (ER), progesterone receptor (PR), and the human epidermal growth factor receptor 2 (HER2), generally receive multimodal treatments including surgery, chemotherapy, and radiation therapy (RT). Recent work has demonstrated that therapies targeting the AR may be effective for the treatment of AR+ TNBC as monotherapy<sup>1,2,3</sup>. Additional work indicates that AR inhibitors, when combined with RT, result in significant radiosensitization in AR+ TNBC models<sup>4,5,6</sup>, but may have different effects in tumors expressing both AR and ER together<sup>7-9</sup>.

While many anti-androgen therapies have been investigated for the treatment of AR+ cancers, including AR+ breast cancer<sup>10</sup>, here we focus on the use enzalutamide (MDV3100), a second generation anti-androgen and competitive inhibitor of AR which also prevents AR nuclear translocation<sup>2,11</sup>. While AR inhibition and knockdown has previously been demonstrated to sensitize AR+ models, including prostate cancer<sup>12-14</sup>, glioblastoma<sup>15</sup>, and breast cancer<sup>4-6</sup>, to RT both *in vitro* and *in vivo*, the mechanism of radiosensitization and a role for AR in driving resistance to radiotherapy in AR+ TNBC remains understudied and of clinical importance. Notably, as AR is increasingly being investigated as a target for therapy, there remains a critical need for the development of accurate biomarkers of response to AR inhibitors to correctly identify the patient populations that will most reliably respond to AR targeted therapies.

Here we use multiomics approaches to investigate the transcriptional and proteomic effects mediated by AR in the response to ionizing radiation. Canonically, AR has been characterized as a transcription factor, and we have identified a transcriptional program driven by AR following RT. Additionally, we demonstrate that AR also plays distinct, non-canonical, roles that may warrant further investigation. To this end, we have used reverse phase protein array (RPPA) as a high-throughput, quantitative method for assessing proteomic changes occurring within cells. RPPA is also very sensitive, allowing for the detection of a range of low-abundance signaling proteins<sup>16</sup>. Antibodies used for RPPA analysis are highly validated and specific resulting in a limited number of antibodies available for use; however, proteins and phosphoproteins can be further classified into pathways, and pathway changes can be assessed.

Furthermore, we report that AR inhibition with enzalutamide is sufficient to block nuclear translocation of AR in response to hormones and in combination with radiation therapy (RT). In addition, transcriptomic and proteomic analyses have been performed to characterize the role of AR in response to radiation, and better understand how AR is mediating radioresistance in multiple AR+ breast cancer cell lines with diverse genetic backgrounds. Changes occurring at the protein or phosphoprotein level were also assessed following treatment with radiotherapy and with the combination of AR inhibition with RT. Together these results nominate the MAPK signaling pathway as being downstream of AR signaling in AR+ TNBC models suggesting that MAPK, and specifically phosphorylation of ERK1/2, is mediating the radioresistance observed in AR+ TNBC. These findings suggest that AR may be regulating the MEK/ERK signaling pathway in AR+ TNBC to promote DNA repair.

### 3.3 Methods

#### 3.3.1 Cell Culture

Cells were grown in incubator at 37°C with 5% CO<sub>2</sub>. MDA-MB-453 cells were obtained from ATCC and grown in DMEM media (ThermoFisher 11965092) containing 1% penicillin/streptomycin (pen/strep; ThermoFisher 15070063) and 10% Fetal Bovine Serum (FBS; Atlanta Biologicals S11550H). ACC-422 cells were grown in MEM media (ThermoFisher 11095080) containing 1X Insulin-Transferrin-Selenium-Ethanolamine (ITS-X; Gibco 51500056), 1% pen/strep, and 15% FBS. Cell lines were authenticated by DNA fingerprinting using short tandem repeat (STR) profiling. Cells were routinely tested for mycoplasma using the MycoAlert Mycoplasma Detection kit (Lonza LT07).

#### 3.3.2 Proteomic Analysis

Cells were seeded in 6 well plates before treatment with 1 μM enzalutamide (MDV3100; MedChem Express HY-70002), 1 μM seviteronel (Innocrin Pharmaceuticals) or vehicle control (DMSO). Drug treatment was administered 24 hours prior to radiation treatment (4 Gy). Following radiation, cells were harvested at indicated time points using cell scrapers. Cells were lysed with RIPA buffer supplemented with cOmplete Mini protease (PHOSS-RO) and phosSTOP (COEDTAF-RO). Bond-Breaker TCEP solution (Pierce Biotechnology) was added at 1/10<sup>th</sup> volume and samples were boiled at 95°C and stored at -80°C prior to analysis. A schematic of treatment is outlined in **Figure 3-6A**.

Prepared protein lysates were then serially diluted (1:2, 1:4, 1:8, 1:16), and a spot array was created for all samples with each individual antibody using the Aushon 2470 arrayer (Quanterix) on Oncyte Avid nitrocellulose-coated slides (Grace Bio-Labs) according to

manufacturer's instructions. Prepared slides were stored at -80°C until an automated slide stainer (Dako Link 48) was used for immunostaining. All antibodies (approximately 100 in total) were validated at the Royal College of Surgeons, Dublin, Ireland. MicroVigene software V.5.1 (VigeneTech) was used to analyze the scanned slides. The MicroVigene software was used to generate spot intensities where a four-parameter logistic-log model, 'SuperCurve' algorithm, was used to fit a curve to each sample<sup>17</sup>. All samples for a single antibody were normalized using global sample median normalization. Differential protein expression was measured by comparing treated samples at each timepoint to the untreated samples within a single cell line.

### ***3.3.3 Western Blotting***

Cells were seeded in 10 cm dishes and allowed to adhere overnight before cells were stripped of hormones using phenol-red free media. For ACC-422 cells, MEM media (#51200-028) was supplemented with 15% charcoal stripped serum (CSS, Atlanta Biologicals #S11650H), 1% pen/strep, 2 mM L-glutamine (Sigma G7313) and 1X ITS-X. For MDA-MB-453 cells, DMEM media (#21063-029) was supplemented with 10% CSS, 1% pen/strep. Cells were cultured in hormone deplete conditions for 48 hours before stimulation with 1 nM R1881 and harvested after 1 hour of stimulation. For experiments with cells cultured in FBS, drug treatments were administered 1 hour before harvesting cells. For experiments with radiation treatment, cells were treated with pharmacologic agent, where denoted, 1 hour before 4 Gy RT, and harvested 1 hour after radiation. To harvest cells, they were washed twice with cold PBS and harvested by scraping. Nuclear and cytoplasmic cellular fractionations were subsequently separated using NE-PER Nuclear and Cytoplasmic Extraction Reagents (Thermo Scientific 78835). Lysates were standardized using the Pierce BCA Protein Assay Kit (Thermo Scientific 23227) and RIPA buffer (Thermo Scientific 89901) containing phosphatase and protease



inhibitors (Sigma #PHOSS-RO, #CO-RO). Following standardization, samples were sonicated, reduced with 4x NU-PAGE buffer (Life Technologies NP0007) and 2%  $\beta$ -mercaptoethanol. For nuclear fractionation experiments, reduced lysates were run on gels and probed for AR (1:1000; Millipore PG-21), LaminB1 (1:1000; CST 12586), and GAPDH (1:1000; CST 2118L). An anti-rabbit secondary was used (1:10,000; CST 7074S). Antibodies for p-ERK1/2 (1:1000, CST 4370), total ERK1/2 (1:1000, CST 4695) were also used. Quantification of western blots was performed using ImageJ software.

### **3.3.4 RNA-sequencing**

MDA-MB-453 and ACC-422 cells were plated in media containing FBS and left to adhere overnight. The following day, cells were pretreated in media without phenol red containing CSS instead of FBS for 48 hours. After this pretreatment, cells were stimulated with 1 nM R1881, 2  $\mu$ M enzalutamide, or 4 Gy RT for 24 hours. Cells treated with a combination of R1881 with RT or enzalutamide with RT first received a 24-hour pretreatment with R1881, following by 4 Gy RT, and RNA was collected 24 hours post-RT (**Figure 3-3A**). For each sample, RNA was collected using TRIzol and isolated using the miRNeasy mini kit (Qiagen 217004). Poly(A) mRNA library preparation and RNA sequencing was performed by the Advanced Genomics Core at the University of Michigan using Illumina sequencing on the NovaSeq flow cell platform. Three replicates of samples were submitted for each condition. Schematic of treatment outline is shown in **Figure 3-3A**. DeSeq2 was used for normalization and comparing treatment groups. Lists of differentially expressed genes were assessed using iPathway Analysis by Advaita Bioinformatics using a  $\log_2$ (fold change) cutoff of 0.58 and an adjusted p-value cutoff of 0.05.

### **3.3.5 Drugs**

Androgen receptor inhibitors were purchased from MedChemExpress (Apalutamide: HY-16060, Darolutamide: HY-16985, Enzalutamide: HY-70002). Trametinib was purchased from Selleckchem (S2673). R1881 was provided by the lab of Arul Chinnaiyan at the University of Michigan.

### **3.3.6 Irradiation**

X-ray irradiation was performed at the University of Michigan Experimental Irradiation Core using a Kimtron IC-225. The dose rate of 2 Gy/min was used in keeping with previous studies<sup>4,5,18</sup>. For in vitro experiments, a 0.1mm Cu filter was used, and for in vivo experiments, the filter was 0.4mm Sn + 0.25mm Cu.

## **3.4 Results**

### **3.4.1 Nuclear localization of AR is blocked with pharmacologic AR inhibitors**

Having previously observed radiosensitization with AR knockdown or pharmacologic inhibition<sup>4-6</sup>, we sought to understand the mechanism of AR-inhibitor mediated radiosensitization in AR+ TNBC models. First, to determine whether pharmacologic AR inhibitors were effectively blocking AR nuclear translocation in AR+ TNBC models, western blots were performed to look at the cellular localization of AR either in the nuclear and cytosolic cellular fractions. To do this, MDA-MB-453 and ACC-422 cells were cultured in hormone deplete conditions for 48 hours and stimulated with a synthetic androgen (R1881) for one hour before cells were harvested. When stimulated for one hour with 1 nM R1881, AR translocates to the nucleus, and this is at least partially blocked with the addition of 2  $\mu$ M enzalutamide (1 hour pretreatment before R1881 stimulation) in MDA-MB-453 (16% reduction, **Figure 3-1A**) and

ACC-422 (24% reduction, **Figure 3-1B**) cells. In cells treated with FBS, which contains hormones, AR is located in the nuclear fraction. Treatment for two hours with the second-generation anti-androgens apalutamide, darolutamide, or enzalutamide blocks AR nuclear translocation in both cell lines (24-66%, **Figure 3-1A,B**). Interestingly, apalutamide and enzalutamide more efficiently blocked AR nuclear translocation in MDA-MB-453 cells compared to darolutamide, suggesting that the structural differences in these inhibitors<sup>19</sup> may affect their ability to block AR in some contexts. These findings suggest that pharmacologic inhibitors of AR are effective at blocking AR nuclear translocation resulting in some increased accumulation of AR in the cytoplasm in AR+ TNBC models *in vitro*.

### ***3.4.2 AR localizes to the nucleus following radiation treatment***

Next, to determine how radiation was affecting cellular localization of AR in the presence or absence of AR inhibition, cellular fractionation experiments were performed on AR+ TNBC cell lines treated with radiation in the context of AR stimulation or inhibition. First, cells were cultured in hormone deplete conditions for 48 hours, then stimulated with R1881 for one hour before 4 Gy RT and harvested one hour after radiation. Again, treatment with R1881 induced AR nuclear translocation, and this was sustained with radiation treatment in both MDA-MB-453 and ACC-422 cells (**Figure 3-2A, C**). In cells treated with media containing FBS, AR was again observed in the nucleus under these baseline conditions; however, AR inhibition with enzalutamide was sufficient to block AR nuclear translocation (50-58% reduction, **Figure 3-2B, D**). Notably, AR remained in the nucleus following RT, but AR accumulated in the cytoplasm when enzalutamide was given one hour prior to RT in MDA-MB-453 and ACC-422 cells (10-60% increase in cytoplasmic AR relative to NT, **Figure 3-2B, D**). These findings suggest that AR is indeed present in the nucleus immediately following radiation treatment; however,

treatment with enzalutamide is sufficient to block AR nuclear translocation and may inhibit AR's activity in its canonical role of a transcription factor. Therefore, as it has been previously reported that treatment with enzalutamide before radiation provides increased radiosensitization<sup>4-6</sup>, we sought to understand how AR may be promoting DNA repair and resistance to RT in AR+ TNBC models.

### **3.4.3 Transcriptomic Analyses in AR+ TNBC cell lines**

A canonical role for AR is to function as a transcription factor and regulate expression of target genes in response to hormone signaling. To understand how AR may be controlling transcriptional regulation in response to ionizing radiation, we performed bulk RNA-sequencing on AR+ MDA-MB-453 and ACC-422 cells. These cells were first cultured in hormone deplete conditions, treated with 1 nM R1881 or 4 Gy RT, and harvested 24 hours after treatment (**Figure 3-3A**). Sequencing was also performed on cells treated with the combination of R1881 with RT where R1881 treatment was administered 24 hours prior to RT, and cells were harvested 24 hours after RT (**Figure 3-3A**). Treatment with R1881 resulted in a large number of differentially expressed genes in both ACC-422 (669 genes, **Figure 3-3B**) and MDA-MB-453 (938 genes, **Figure 3-3C**) cells compared to control. When pathway analysis was performed on the differentially expressed gene lists, multiple pathways were found to be enriched in each cell line, including *Pathways in Cancer* in both MDA-MB-453 and ACC-422 cells treated with R1881 (**Figure 3-3D, E**), and *Transcriptional Misregulation in Cancer* in MDA-MB-453 cells. Complete pathway analyses results can be found in **Table 3-1** (ACC-422) and **Table 3-2** (MDA-MB-453).

Next, we compared cells treated with RT alone or RT in combination with R1881. In cells treated with RT alone, there were far fewer differentially expressed genes compared to

untreated (NT) control cells (ACC-422: 46 genes, MDA-MB-453: 114 genes). When untreated cells were compared to cells receiving both R1881 and RT, there were 979 differentially expressed genes in ACC-422 cells (**Figure 3-4A**), and 1119 differentially expressed genes in MDA-MB-453 cells (**Figure 3-4B**). Pathway analysis was again performed on these gene lists to identify pathways that are overrepresented with combination treatment (**Figure 3-4C, D**). Many of the pathways that were found to be overrepresented with treatment of R1881+RT were identified to be the same as those seen with treatment of R1881 alone. Notably, 16 of the 17 identified pathways with R1881 treatment were also overrepresented with combination treatment of R1881+RT in ACC-422 cells. Similarly, 7 of the 10 identified pathways following R1881 treatment were also overrepresented with combination treatment in MDA-MB-453 cells. All pathway changes can be found in **Table 3-3** (ACC-422) and **Table 3-4** (MDA-MB-453).

To identify changes that are due to R1881 treatment in the context of RT, we compared cells treated with RT alone to cells treated with R1881+RT. In this comparison, there were 1012 differentially expressed genes in ACC-422 cells (**Figure 3-5A**) and 1194 differentially expressed genes in MDA-MB-453 cells (**Figure 3-5B**). Pathway analysis was performed in both cell lines (**Figure 3-5C, D**), and complete lists of significant pathways are recorded in **Table 3-5** (ACC-422) and **Table 3-6** (MDA-MB-453). Many similar pathways were identified to be overrepresented in ACC-422 cells with R1881 treatment (NT vs R1881) compared to R1881 in the context of RT (RT vs R1881+RT). These pathways include the *Estrogen Signaling Pathway*, *Pathways in Cancer*, and the *TGF- $\beta$  Signaling Pathway*, among others. To identify changes that are due to ionizing radiation in the context of R1881 treatment, we compared cells treated with R1881 against combination treated cells (R1881+RT). Interestingly, there were 174 differentially expressed genes in MDA-MB-453 cells. Despite identifying 846 differentially expressed genes

in ACC-422 cells (**Figure 3-5E**), pathway analysis did not identify any pathways that were overrepresented in this comparison (R1881 vs R1881+RT). While there were many changed pathways across the different treatment groups and comparisons based on our transcriptomic data, we identified multiple recurring pathways including the *PI3K-Akt Signaling Pathway*, *MAPK Signaling Pathway*, and the *TGF- $\beta$  Signaling Pathway*. These pathways play important roles within the cell, specifically in the regulation of cell growth and proliferation, and therefore may be important in contributing to cellular growth following treatment with R1881 alone or in combination with RT.

#### **3.4.4 Proteomic Analyses in AR+ TNBC cell lines**

In addition to its canonical roles in regulating transcription, AR has also been shown to have non-canonical activities that can contribute to endocrine resistance in breast cancer<sup>20</sup>, and in prostate cancer, AR signaling has many non-nuclear functions<sup>21</sup> which include influencing Src<sup>22</sup>, PI3K/Akt<sup>23</sup>, immune cells<sup>24,25</sup>, and the Ras/Raf1/MEK/ERK signaling cascade<sup>26</sup>. To obtain a more complete picture of the role for AR signaling in AR+ TNBC, in addition to our transcriptional studies, we used reverse phase protein arrays (RPPA) to assess changes in approximately 100 proteins and phosphoproteins in response to treatment with enzalutamide, RT alone, or enzalutamide with RT. MDA-MB-453 or ACC-422 were pretreated with enzalutamide for 24 hours prior to RT, and cells were harvested at 1-, 12-, or 24-hours post-RT (**Figure 3-6A**). Expression of proteins or phosphoproteins for treatment conditions was assessed for untreated cells, cells treated with enzalutamide alone, RT alone, or enzalutamide with RT within each cell line.

Within each cell line, we compared the proteomic changes at each timepoint (1-, 12-, 24-hours after RT). While we observed changes in protein expression in cells treated with each

condition, we expected to see treatment specific trends in proteins or phosphoproteins where expression is decreased with enzalutamide, increased with radiation, and blunted with combination treatment. In cells that were harvested one hour after RT, we can note this trend in MDA-MB-453 cells (p-Src [Y416], p-ATM, total ATM, p53, p-Akt [S473, T308], total Akt, p-AMPK [T172], p-Chk1 [S345], total Chk1; **Figure 3-6B**) and in ACC-422 cells (HER2 [Y1248], p-Chk2 [T68], p-MEK1 [S217, S221], ERK1, ERK1/2 [S217], IGFIR; **Figure 3-7A**). Overall, these targets represent key proteins in the DNA damage repair pathways as well as the MAPK/ERK signaling pathway, suggesting that AR may be mediating signals important for DNA repair and the MAPK pathway, thus contributing to radioresistance in this context. Additional proteomic changes were observed in MDA-MB-453 and ACC-422 cells with enzalutamide, RT, or combination treatment at 12-hours post-RT (**Figure 3-6C, Figure 3-7B**) or 24-hours post-RT (**Figure 3-6D, Figure 3-7C**).

To look more directly at the proteins and phosphoproteins involved in these pathways, we analyzed the specific proteins and phosphoproteins related to DNA Damage and Repair or the MAPK signaling based on the specific genes identified to be part of these pathways using gene ontology biological processes. Using these lists of proteins and phosphoproteins included in the (1) DNA Damage and Repair and (2) MAPK Pathway, we assessed pathway specific changes with enzalutamide, RT, or combination treatment. First, we queried changes in the 15 proteins and phosphoproteins in our dataset related to DNA damage and repair. Based on the proteomic changes across treatment conditions, we observe that there are distinct groups of proteins and phosphoproteins that are up or downregulated under these conditions. Notably, with RT, there is an increase in important DNA repair proteins, including p53, p-ATM, total ATM, p-Chk1 (S345), total Chk1, p-Chk2 (T68), and XRCC1 (**Figure 3-8A**). Most of these proteins, in

addition to others, were decreased relative to cells treated with radiation following treatment of enzalutamide alone or in combination with RT. Similar results were observed in ACC-422 cells at one-hour post-RT with increases in 53bp1, p-ATM, total ATM, Chk1, p-Chk2 (S345), p-EGFR (Y1068), EGFR, p53 (**Figure 3-8D**). In addition, most proteins and phosphoproteins were decreased with enzalutamide treatment, and similar decreases were observed for most proteins and phosphoproteins with combination treatment (**Figure 3-8D**). Across multiple timepoints, combination treatment had a varied effect, with more nuanced changes in proteins following RT in cells pretreated with enzalutamide compared to cells treated with RT alone (**Figure 3-8B, C, E, F**). Overall, early responding changes in response to RT (e.g. p-ATM, total ATM) are seen after 12-24 hours post-RT when cells are pretreated with enzalutamide (**Figure 3-8**). This is concordant with phenotypes seen in breast and prostate cancer models where AR inhibition results in delays in DNA damage repair<sup>13,14,27</sup>.

Next, we assessed changes in proteins and phosphoproteins relate to the MAPK pathway under the same treatment conditions. Similar to results observed in DNA damage and repair proteins, there are subsets of proteomic changes that are opposite between cells treated with enzalutamide compared to RT alone. In these instances, enzalutamide decreases expression of proteins that are increased in response to RT, further suggesting that AR may be regulating proteomic changes of proteins and phosphoproteins that are activated following treatment with ionizing radiation. Specifically, in MDA-MB-453 cells at 1-hour post-RT, there are increases in total ERK1, p-PKC $\alpha$  (S657), AR, p-Src (Y416), p-Akt (T308), and total Akt after RT, with decreases in the same proteins after treatment with enzalutamide alone or in combination with RT (**Figure 3-9A**). While there are differences in the specific proteomic changes observed under the same treatment conditions in ACC-422 cells, p-ERK1/2 (S217), p-ERK1 (T202), total ERK1,



and p-MEK1 (S217, S221) have some of largest decreases in expression with enzalutamide and relative increases in expression with RT (**Figure 3-9B**). Similar trends were observed at 12- and 24-hours post-RT in ACC-422 and MDA-MB-453 (**Figure 3-9C-F**); however, distinct subsets of proteins and phosphoproteins are activated at later timepoints after treatment with enzalutamide and RT.

### **3.4.5 Validation of transcriptomic and proteomic findings in AR+ TNBC cells**

Large scale transcriptomic and proteomic analyses (**Figure 3-9**) in AR+ TNBC cell lines indicate that the MAPK signaling pathway may be an important part of AR-mediated radioresistance. Therefore, to validate the role of the MAPK pathway, and specifically MEK and ERK signaling in response to AR activation or inhibition *in vitro*, additional western blots were performed assessing p-ERK1/2 and total ERK1/2 protein levels. MDA-MB-453 and ACC-422 cells were pretreated for 48 hours in media without phenol red and containing CSS. Next, cells are stimulated with R1881, and western blots were performed to assess changes in p-ERK1/2 and total ERK1/2 levels as a readout of activation of the MAPK signaling pathway after AR stimulation. Stimulation with R1881 was sufficient to induce an increase in p-ERK1/2 in both cell lines (**Figure 3-10A, B**). Changes in the MAPK signaling pathway were assessed in AR+ TNBC cells treated with enzalutamide. Western blots were performed after treatment with 1  $\mu$ M enzalutamide in ACC-422 (**Figure 3-10C**) and MDA-MB-453 (**Figure 3-10D**) cells. In both cell lines, following treatment with enzalutamide, there was an increase in p-ERK1/2, suggesting an increase of the MAPK signaling pathway with AR inhibitor treatment. Because enzalutamide primarily functions to suppress AR's transcriptional activity, enzalutamide treatment still allows for accumulation of nuclear AR, allowing for modulation of p-ERK despite treatment with pharmacologic AR inhibitors.

### 3.5 Discussion

Previous work has demonstrated that AR is a mediator of radioresistance both in AR+ TNBC<sup>5,6,27</sup> and prostate cancer models<sup>12-14</sup>. Our work has demonstrated that AR inhibition or knockdown radiosensitizes AR+ TNBC cells<sup>4,5</sup>. Here we demonstrate that under baseline conditions, AR is located both in the cytoplasm and in the nucleus, and AR is responsive to stimulation with R1881, a synthetic androgen, or AR inhibition with the second-generation anti-androgens, apalutamide, darolutamide, and enzalutamide (**Figure 3-1, Figure 3-2**). While this previously has been explored in prostate cancer models, these findings confirm a canonical role for AR as a nuclear hormone transcription factor, that is responsive to both stimulation and inhibition in our AR+ TNBC cell lines. In addition, our data suggest that AR is driving a transcriptional program in response to stimulation and RT (**Figure 3-3, Figure 3-4**). Further, our proteomic data suggests a novel, non-canonical role for AR in the regulation of MAPK/ERK signaling following RT (**Figure 3-6, Figure 3-7, Figure 3-8, Figure 3-9**), suggesting that AR may be regulating changes at both the transcriptional and proteomic levels resulting in the observed AR-mediated radioresistance. This is in line with previous findings in prostate cancer, where inhibition of MEK is sufficient to modulate the radiation response in AR+ prostate models<sup>28</sup>.

Previous work by our group and others has demonstrated that inhibiting AR results in decreased phosphorylation of DNAPKcs<sup>14,27,29</sup> resulting in a delay in dsDNA break repair with AR inhibitors following RT in breast and prostate models. Our work highlights the role for the MAPK cascade in response to ionizing radiation (**Figure 3-9, Figure 3-10**) which has previously been noted in other cancers including glioma and non-small cell lung cancer<sup>30-33</sup>. This parallels with work done in prostate cancer where activation of AR has been shown to activate the Ras-

Raf-1 signaling cascade and ERK phosphorylation<sup>21,26</sup>. In addition, with radiation, targeting of MAPK signaling and specifically inhibition of MEK/ERK results in decreased ERK phosphorylation and increased radiosensitivity<sup>28</sup>. These changes in radiosensitivity are due, at least in part to a delay in dsDNA repair as a result of impaired efficiency of NHEJ and HR<sup>31,32</sup>. Therefore, taken with our findings, our working model indicates that use of AR inhibitors including enzalutamide may reduce MAPK signaling resulting in aberrations to DNA repair pathways including changes in *ATM*, *DNAPKcs*, *PARP1* (**Figure 3-11**).

There are limitations of our study that should also be considered. First, here we use cell line models that can be cultured in the presence or absence of media containing hormones. In our study, we have used multiple culture conditions to try to provide a more complete picture of what may be happening when AR inhibitors are used in combination with RT. Our studies, however, were performed using cell culture models and they have not been expanded into 3D culture systems using organoids or *in vivo* animal models. Future studies will continue to validate this work in diverse model systems. In addition, our proposed model for AR-inhibitor mediated radiosensitization may lack intermediary steps that could be involved in this phenotype. One example could include the minor spliceosome. While we demonstrate that AR regulates p-ERK signaling, transcripts in the MAPK signaling pathway are highly regulated by minor spliceosome activity<sup>34</sup>, and knockdown of the minor spliceosome results in the inhibition of DNA repair<sup>35</sup>. Therefore, AR inhibition may also be directly or indirectly influencing the minor spliceosome to promote radiosensitization. Our studies were also performed *in vitro* using models that do not account for the role of the immune system or tumor microenvironment<sup>36</sup>. In prostate cancer models, AR has been demonstrated to repress IFN $\gamma$  expression resulting in

immunotherapy resistance<sup>37</sup>. Future and ongoing studies will investigate these limitations by using immunocompetent *in vivo* models.

Our findings contribute to a larger body of literature demonstrating that use of AR inhibitors alone or in combination with radiotherapy may be an important addition to the treatment armamentarium for AR+ TNBC. Results from clinical trials demonstrate that AR inhibitors, specifically enzalutamide, are well tolerated<sup>38</sup> and have response rates of ~30%. Ongoing work is needed to understand the mechanisms by which AR is contributing to tumorigenesis in AR+ breast cancer models. Most notably, there is a critical need for biomarkers of response that can be used to effectively identify patient populations that will benefit from treatment with AR inhibitors. While AR has been identified as a biomarker of radioresistance when expressed in AR+ TNBC, additional work has demonstrated that it may play a different role in the context of AR+/ER+ breast cancers<sup>7,9</sup>. Therefore, future studies are needed to identify other biomarkers that can impact radiosensitivity in a variety of contexts in order to inform appropriate clinical strategies for women with AR+ breast tumors.

### **3.6 Acknowledgements**

The authors thank Drs. Arul Chinnaiyan and Abhijit Parolia for providing the R1881, the Advanced Genomics Core at the University of Michigan for library preparation and RNA-sequencing, and Adviaata Bioinformatics for the use of analysis software for RNA-sequencing results.

This work was supported a Breast Cancer Research Foundation (BCRF) Grant to L.J.P. (BCRF-21-128) and by a generous donation to C.W.S. by Susan and Richard Bayer. A.R.M., A.M.P., and B.M. are supported by National Institute of General Medical Sciences (NIGMS) training grants: T-32 GM113900 (A.R.M.), T32-GM007315 (A.R.M.), T32-GM007767

(A.M.P.), and T32-HG000040 (B.M.). A.R.M. is supported by the Rackham Predoctoral Fellowship Program and Rackham Graduate School Research Grants. A.M.P. is supported by a Ruth L. Kirschstein NRSA F31 award (F31CA254138).

### 3.7 Figures

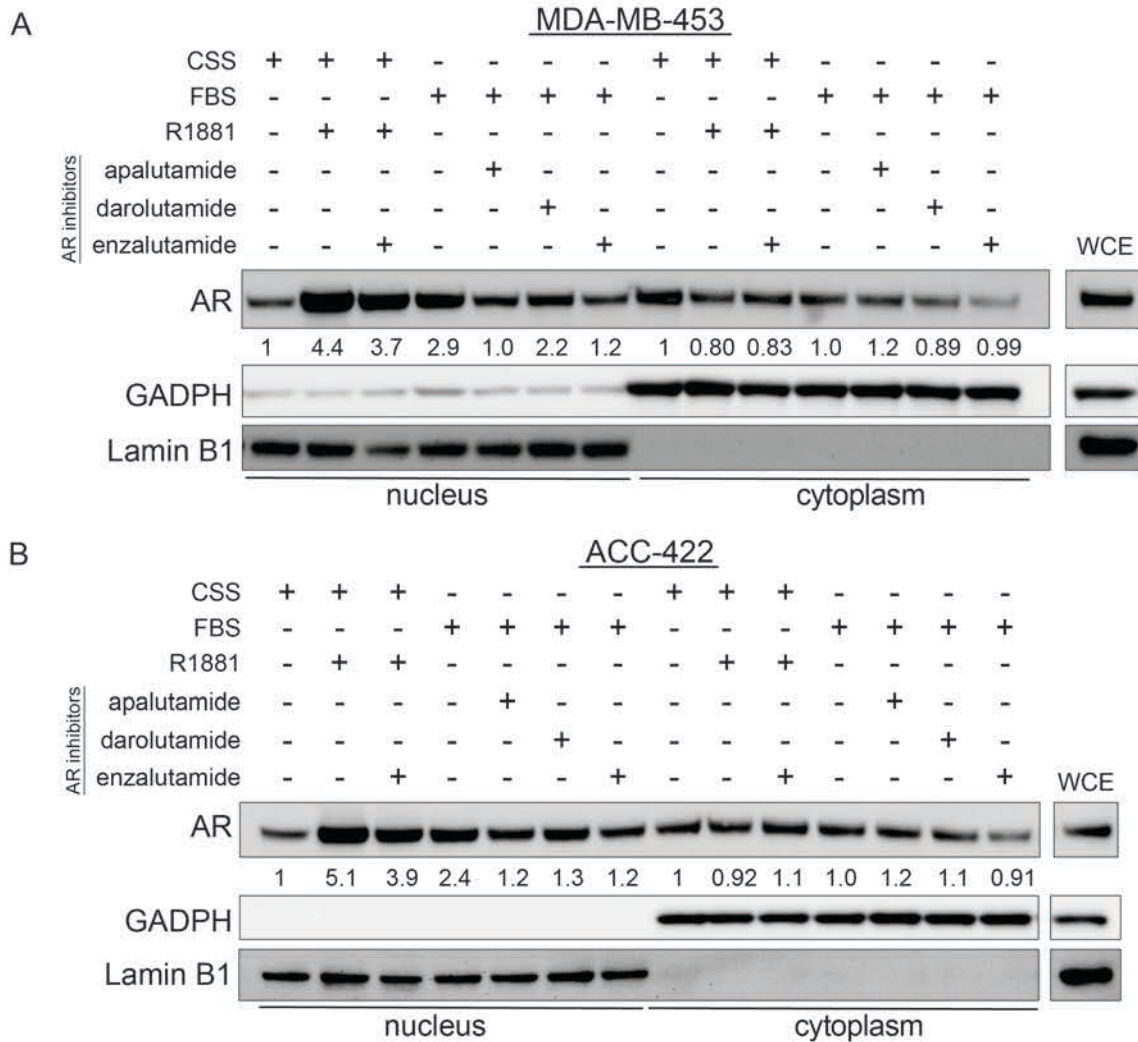


**Figure 3-1: Pharmacologic AR inhibitors block AR nuclear translocation in AR+ TNBC cell lines**

Nuclear fractionation experiments were performed in MDA-MB-453 (A) and ACC-422 (B) cells treated with 1 nM R1881, 2  $\mu$ M enzalutamide, 2  $\mu$ M apalutamide, and/or 2  $\mu$ M darolutamide cultured in media containing charcoal stripped serum (CSS) or fetal bovine serum (FBS). Experiments were performed in triplicate, and quantifications represent relative AR protein expression.

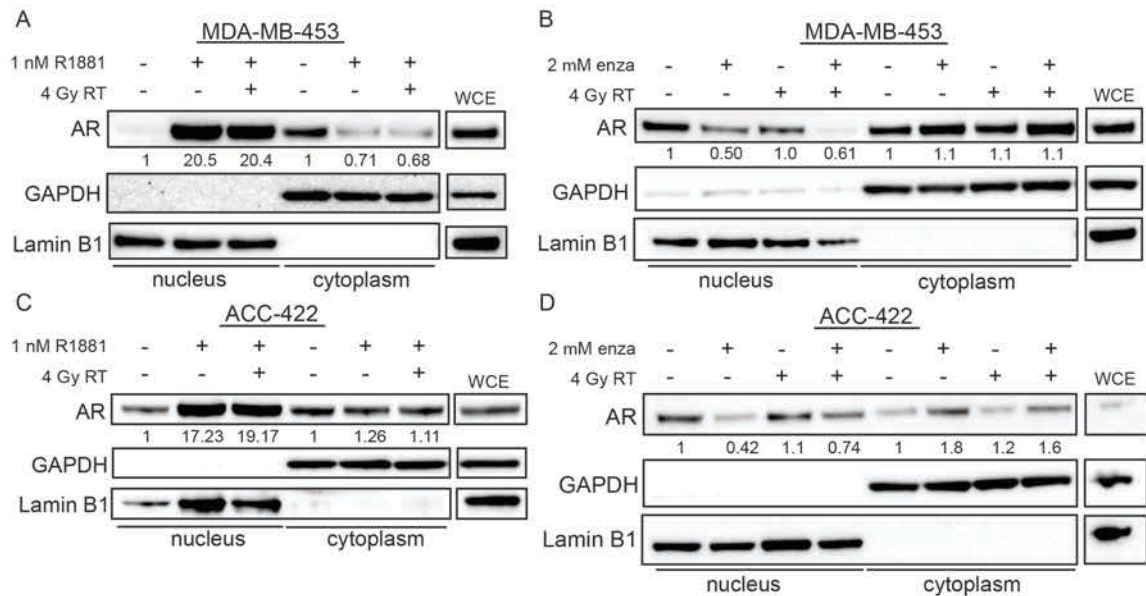


**Figure 3-2: AR localizes to the nucleus following ionizing radiation**

Nuclear fractionation experiments were performed in MDA-MB-453 (A) and ACC-422 (C) cells initially cultured in CSS, then treated with R1881, RT, or R1881+RT. R1881 was given one hour prior to RT, and cells were harvested one hour after RT. Experiments were also performed in MDA-MB-453 (B) and ACC-422 (D) cells cultured in FBS, treated with enzalutamide, RT, or enzalutamide + RT. Enzalutamide was given one hour prior to RT, and cells were harvested one hour after RT. Experiments were performed in triplicate, and quantifications represent relative AR protein expression.

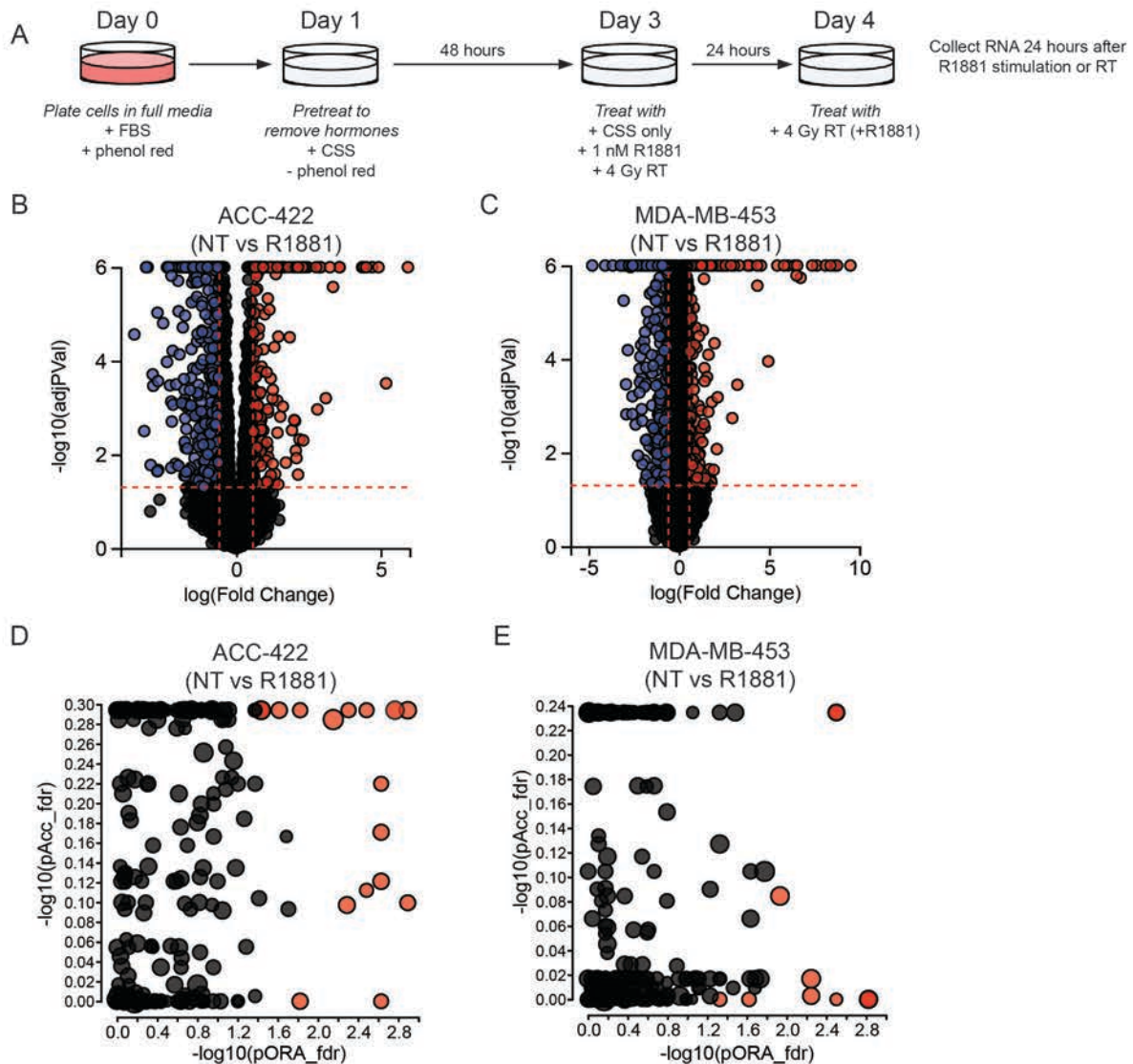


**Figure 3-3: Analysis of differentially expressed genes and pathway changes in ACC-422 and MDA-MB-453 cells with R1881 treatment**

(A) Schematic of treatment for RNA-seq samples. ACC-422 and MDA-MB-453 cells were pretreated in charcoal stripped serum (CSS) for 48 hours prior to stimulation with R1881 (24 hours), treatment with 4 Gy RT, or combination treatment (24-hour pretreatment with R1881 before RT). All cells were harvested 24 hours post-treatment. Volcano plots identified differentially expressed genes in (B) ACC-422 and (C) MDA-MB-453 cells treated with 1 nM R1881. Pathway analysis of the differentially expressed genes identified biological pathways that are overrepresented in (D) ACC-422 and (E) MDA-MB-453 cells.



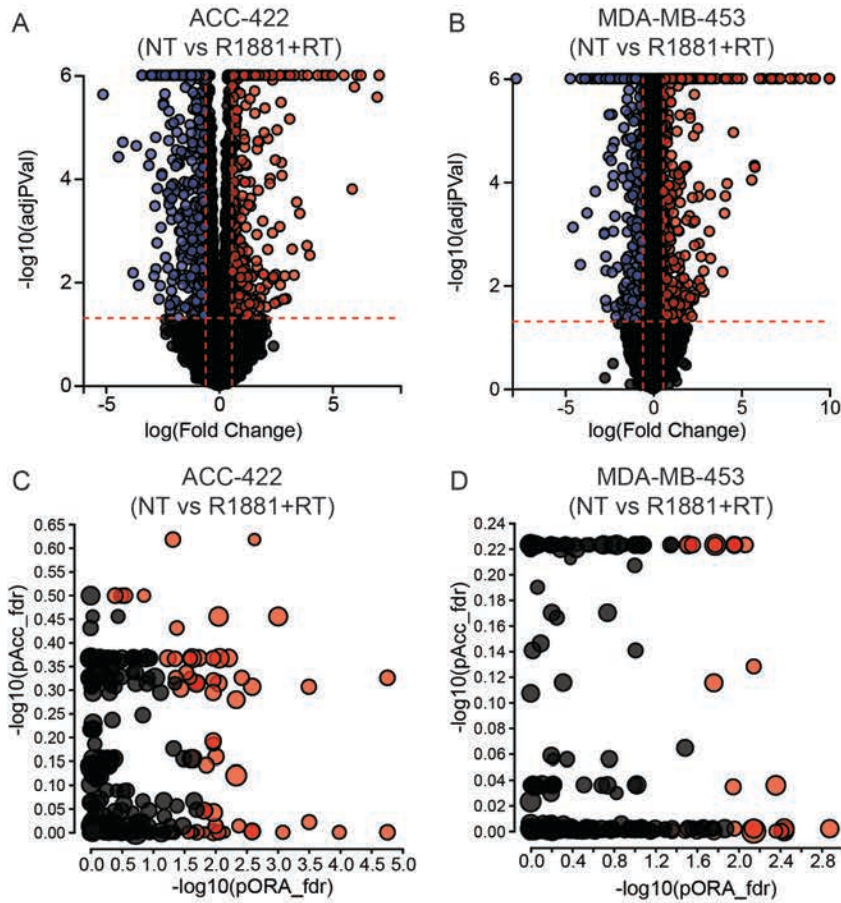


**Figure 3-4: Analysis of differentially expressed genes and pathway changes in ACC-422 and MDA-MB-453 cells following treatment with ionizing radiation**

Differentially expressed genes in (A) ACC-422 or (B) MDA-MB-453 cells treated with R1881+RT compared to untreated cells. Pathway analysis identifies pathways that are overexpressed with treatment of R1881+RT compared to untreated cells in (C) ACC-422 and (D) MDA-MB-453 cells.

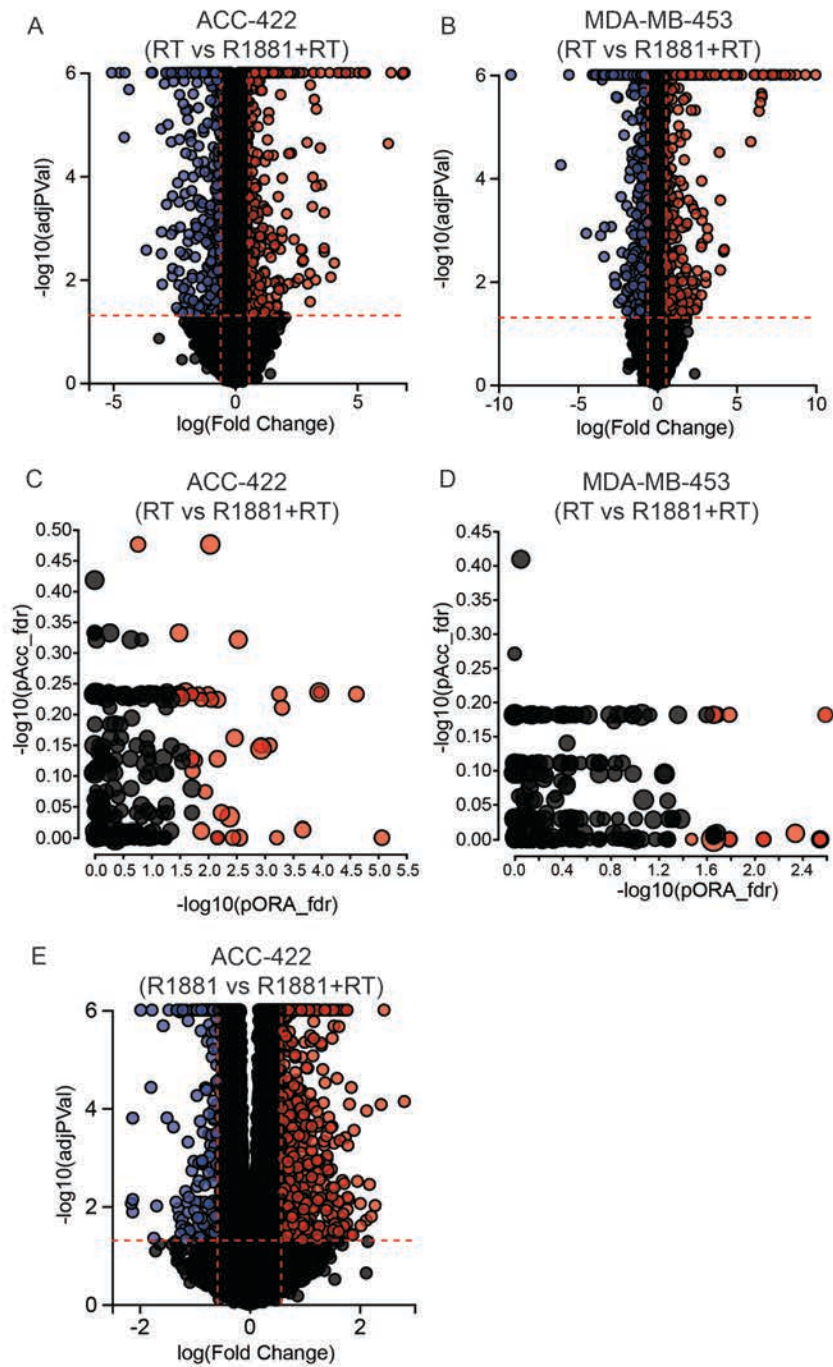


**Figure 3-5: Differentially expressed genes and pathway analysis in ACC-422 and MDA-MB-453 cells relative to RT or R1881 treatment**

Differentially expressed genes are displayed in volcano plots in (A) ACC-422 and (B) MDA-MB-453 cells with R1881+RT treatment relative to RT alone. Pathway changes were also assessed in (C) ACC-422 and (D) MDA-MB-453 cells. (E) Differentially expressed genes were also assessed for ACC-422 cells treated with R1881 compared to R1881+RT.

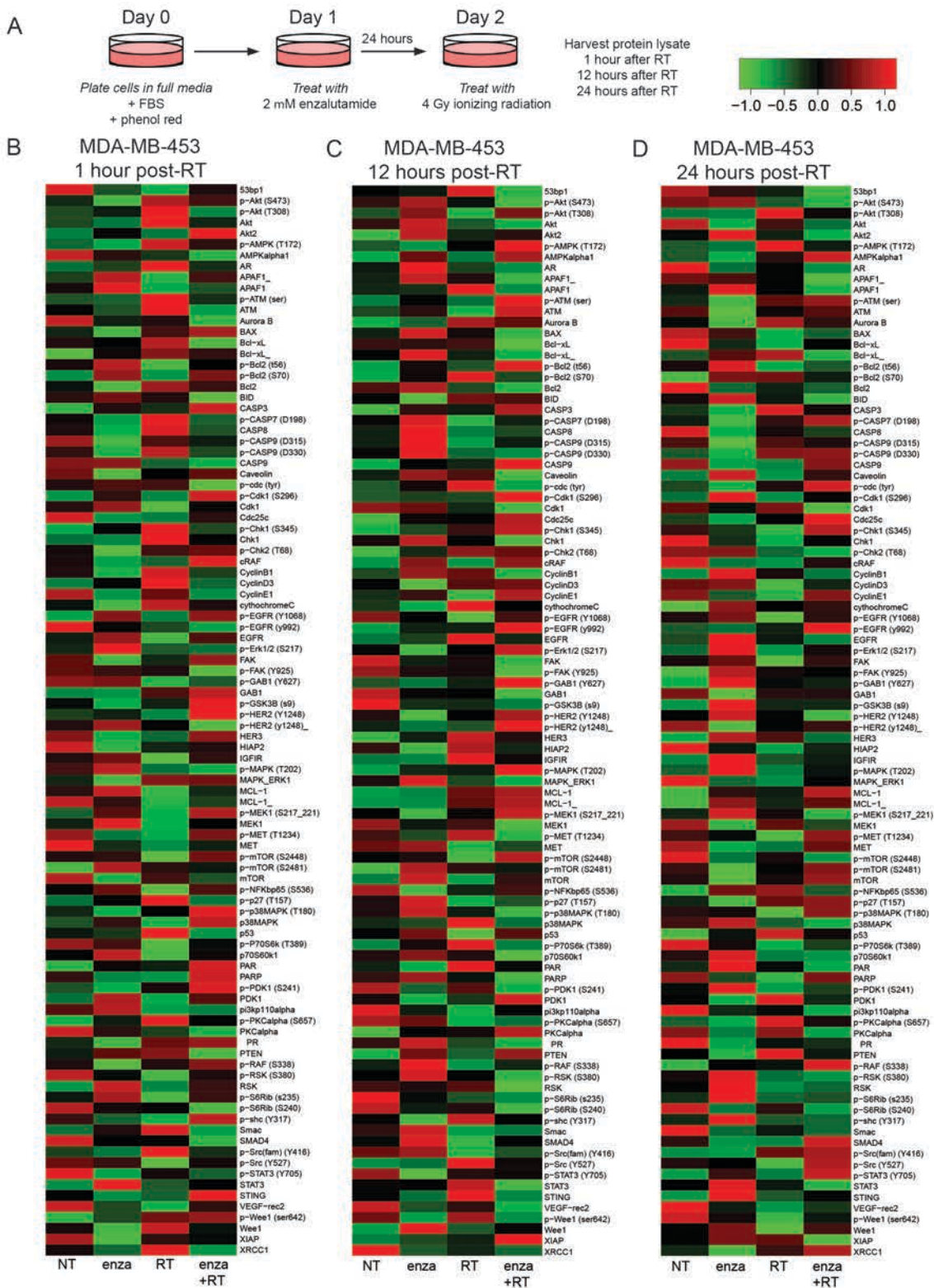


**Figure 3-6: Reverse Phase Protein Array (RPPA) Analysis of global proteomic changes in MDA-MB-453 cells**

(A) Schematic of treatment for RPPA samples. Global protein and phosphoprotein changes in cells treated with DMSO (No treatment [NT]), 1  $\mu$ M enzalutamide alone, 4 Gy RT alone, enzalutamide and RT in MDA-MB-453 cells at (B) 1 hour-post RT, (C) 12-hours post-RT, or (D) 24-hours post-RT in cells that are pretreated for 24 hours with enzalutamide prior to RT.

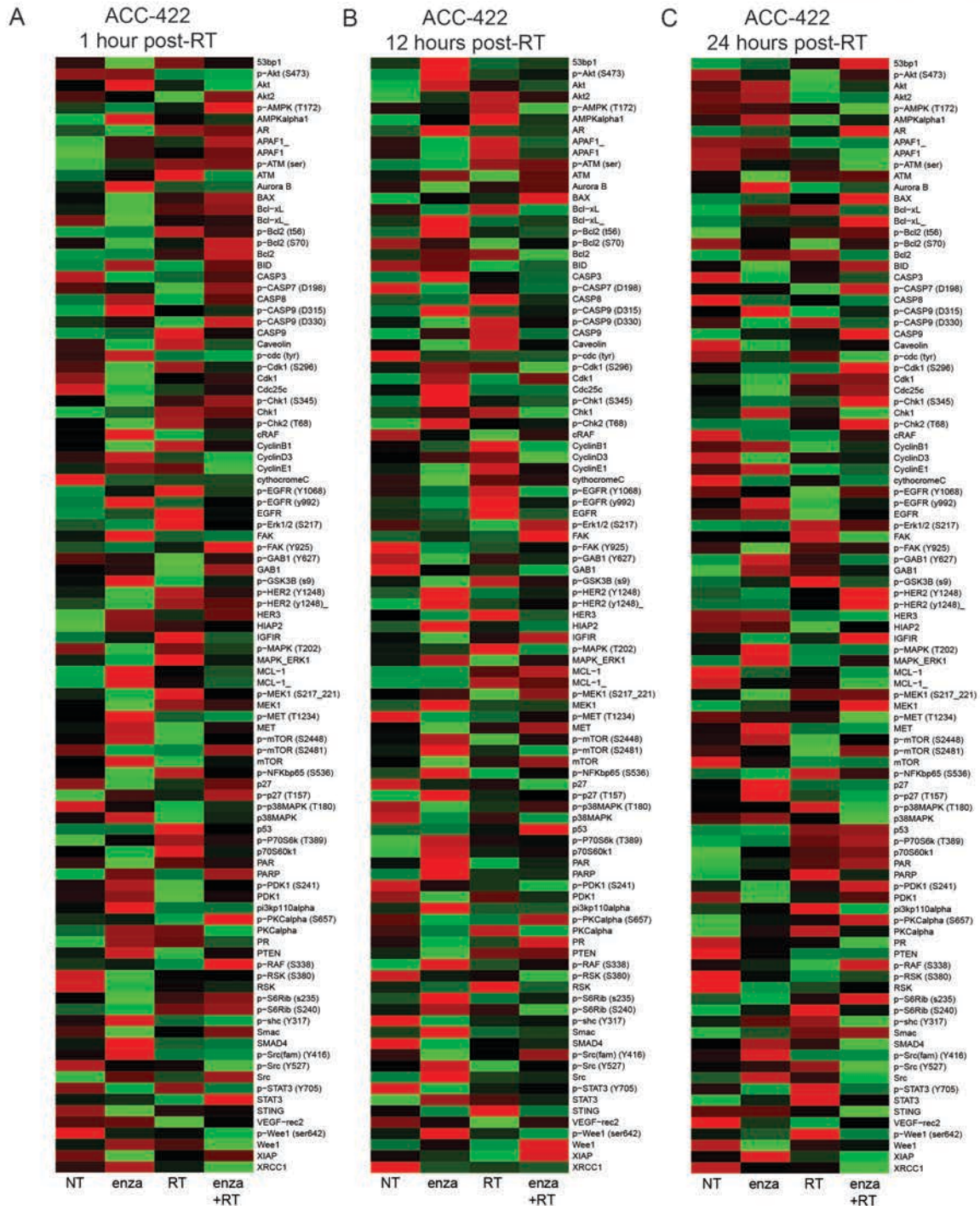


**Figure 3-7: RPPA Analysis of global proteomic changes in ACC-422 cells**

Protein and phosphoprotein changes in ACC-422 cells treated with DMSO (No treatment [NT]), 1  $\mu$ M enzalutamide alone, 4 Gy RT alone, enzalutamide and RT at (A) 1 hour-post RT, (B) 12-hours post-RT, or (C) 24-hours post-RT in cells that are pretreated for 24 hours with enzalutamide prior to RT.

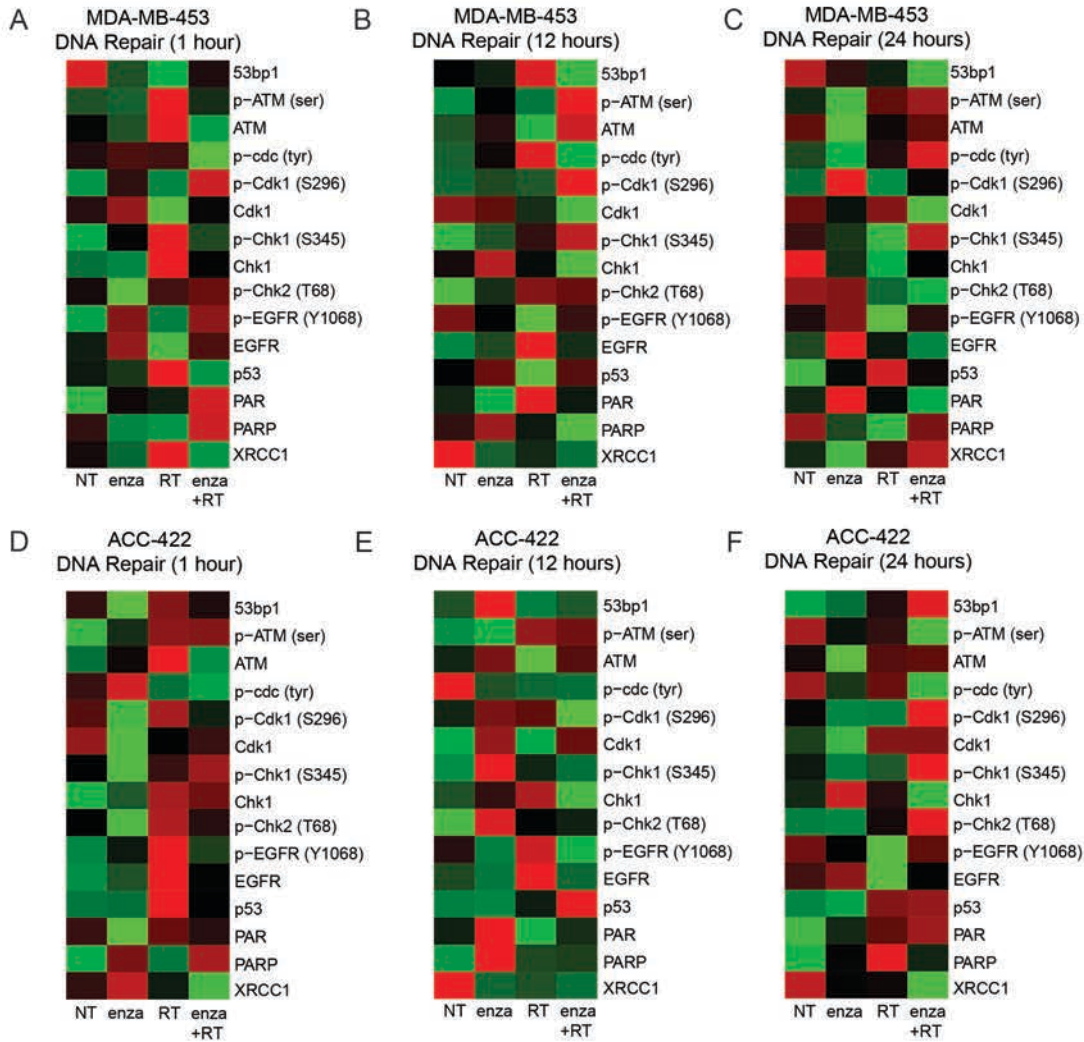


**Figure 3-8: Proteomic Changes in DNA Damage and Repair in AR+ TNBC cell lines**

Changes in proteins and phosphoproteins related to DNA Damage and DNA Repair were identified and assessed in MDA-MB-453 and ACC-422 cells at 1-hour (A, D), 12-hours (B, E), and 24-hours (C, F) post-RT.

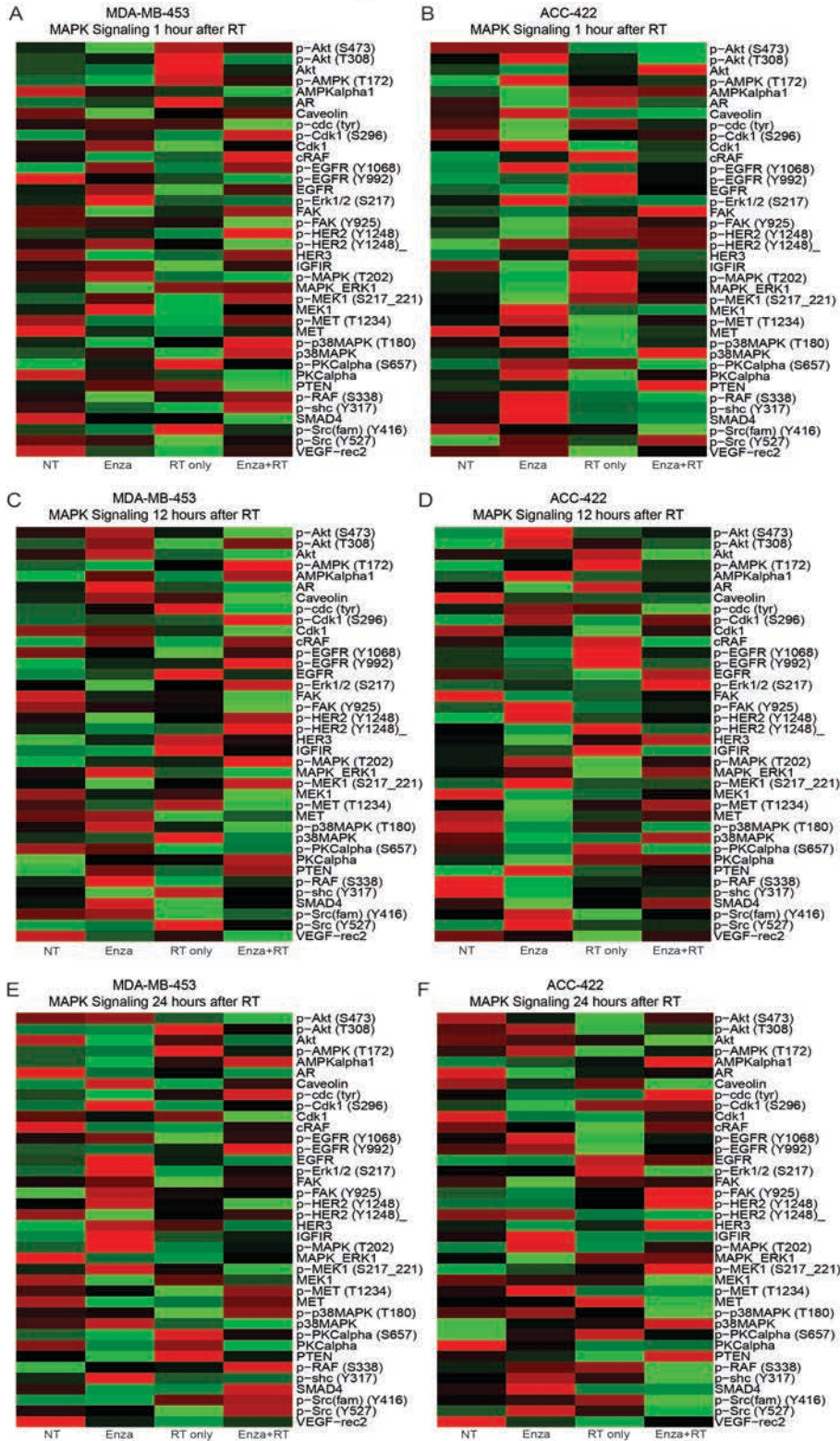


**Figure 3-9: Proteomic Changes related to the MAPK signaling pathway in AR+ TNBC cell lines**

Changes in proteins and phosphoproteins related to the MAPK signaling pathway were identified and assessed in MDA-MB-453 and ACC-422 cells at 1-hour (**A, B**), 12-hours (**C, D**), and 24-hours (**E, F**) post-RT.



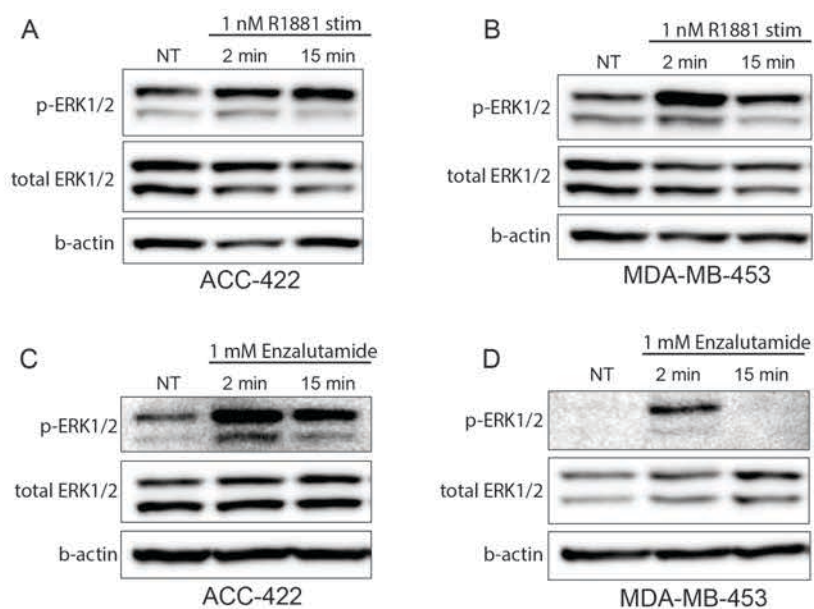


**Figure 3-10: Validation of a role for AR in regulating MAPK signaling in AR+ TNBC**

Western blots were performed to assess activation of p-ERK1/2 following stimulation with R1881 in cells pretreated with CSS in (A) ACC-422 or (B) MDA-MB-453 cells. Western blots were also performed in cells treated with 1  $\mu$ M enzalutamide in (C) ACC-422 and (D) MDA-MB-453 cells.

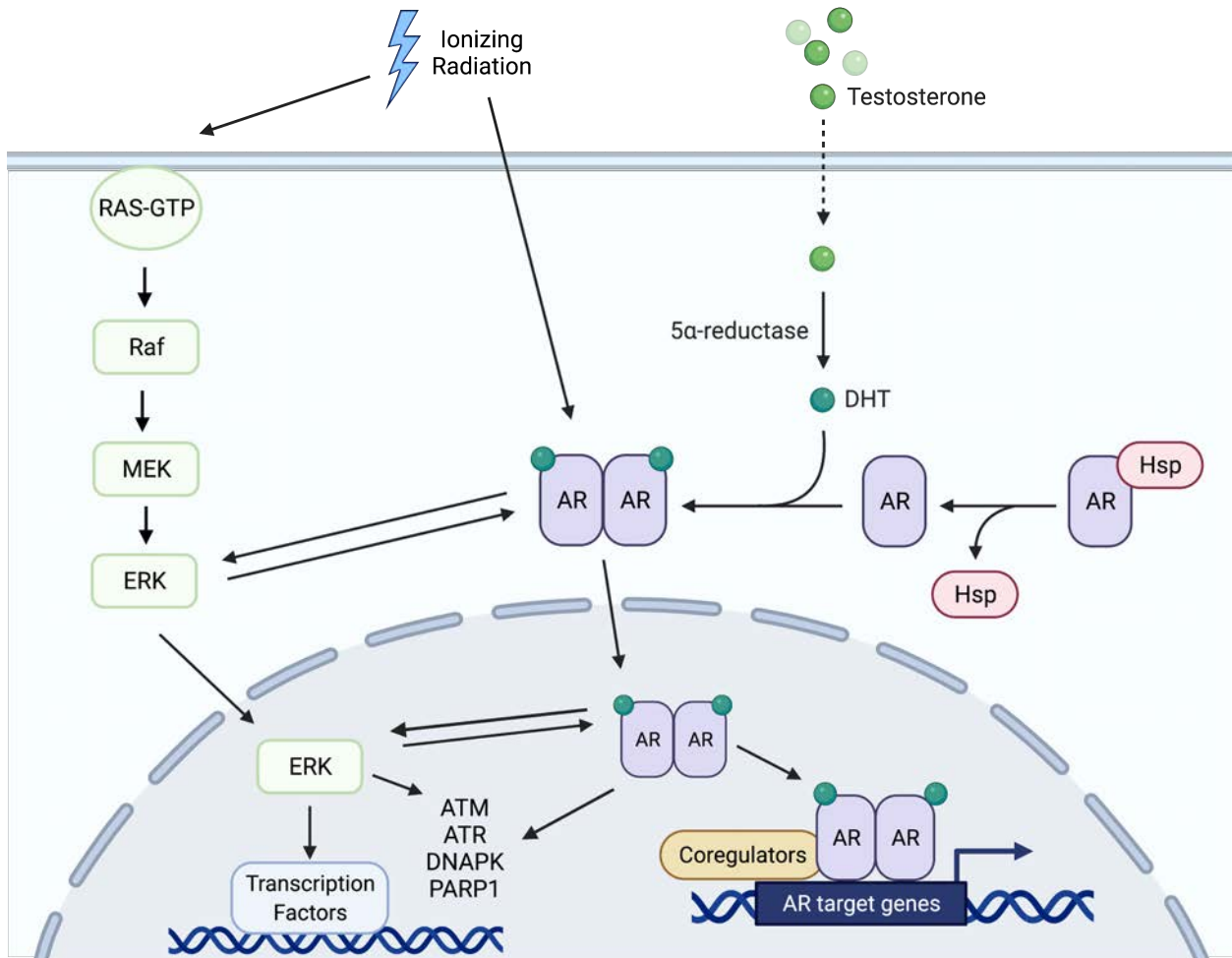


**Figure 3-11: Mechanistic overview of AR and MAPK signaling in response to ionizing radiation**

AR and MAPK signaling pathways are activated following RT, and interplay between pathways may be promoting radioresistance in AR+ TNBC models.

### 3.8 Tables

**Table 3-1: Pathway Analysis in ACC-422 cells (NT vs R1881)**

Pathway	Number of differentially expressed genes	Total genes	p-value (FDR)
Cytokine-cytokine receptor interaction	15	92	0.00118827
cAMP signaling pathway	19	130	0.00118827
Protein digestion and absorption	10	48	0.004945
Osteoclast differentiation	15	87	0.00513793
Salivary secretion	10	48	0.01056113
TGF-beta signaling pathway	12	72	0.01056113
Estrogen signaling pathway	15	101	0.01109902
Hippo signaling pathway	17	125	0.01253916
Pancreatic secretion	10	55	0.01253916
Staphylococcus aureus infection	6	18	0.01762969
Cell adhesion molecules (CAMs)	10	65	0.01762969
Pathways in cancer	33	376	0.01762969
Gastric cancer	13	109	0.02487231
Axon guidance	18	151	0.02487231
Calcium signaling pathway	12	102	0.02487231
Neuroactive ligand-receptor interaction	11	89	0.02607779
AGE-RAGE signaling pathway in diabetic complications	11	77	0.02607779

**Table 3-2: Pathway Analysis in MDA-MB-453 cells (NT vs R1881)**

Pathway	Number of differentially expressed genes	Total genes	p-value (FDR)
MicroRNAs in cancer	20	119	0.0014982
Cell adhesion molecules (CAMs)	14	67	0.00150588
ABC transporters	8	26	0.00428113
ECM-receptor interaction	10	41	0.00476728
Transcriptional misregulation in cancer	17	107	0.00627322
PI3K-Akt signaling pathway	25	206	0.04258276
Neuroactive ligand-receptor interaction	12	70	0.04258276
cAMP signaling pathway	17	115	0.04258276
Hypertrophic cardiomyopathy (HCM)	8	41	0.04258276
Pathways in cancer	34	346	0.04883725

**Table 3-3: Pathway Analysis in ACC-422 cells (NT vs R1881+RT)**

Pathway	Number of differentially expressed genes	Total genes	p-value (FDR)
Aldosterone-regulated sodium reabsorption	9	30	0.00039535
Pancreatic secretion	17	60	0.00039535
Cytokine-cytokine receptor interaction	19	104	0.00047739
Protein digestion and absorption	16	54	0.00047739
Arachidonic acid metabolism	11	30	0.00047739
Salivary secretion	14	55	0.00086227
ECM-receptor interaction	14	54	0.00201528
Retinol metabolism	10	32	0.00392811
Calcium signaling pathway	19	126	0.00423765
Neuroactive ligand-receptor interaction	16	102	0.00423765
Viral protein interaction with cytokine and cytokine receptor	5	22	0.00504354
Axon guidance	23	154	0.00629361
Dilated cardiomyopathy	12	56	0.00643494
Hypertrophic cardiomyopathy	12	53	0.01013271
PI3K-Akt signaling pathway	29	239	0.0110732
Focal adhesion	22	153	0.01224755
Gastric cancer	19	114	0.01537782
Breast cancer	16	115	0.01639264
Aldosterone synthesis and secretion	12	69	0.01768495
Pathways in cancer	44	401	0.01768495
Hippo signaling pathway	19	133	0.01768495
Basal cell carcinoma	11	49	0.02130519
Bile secretion	10	50	0.02130519
MAPK signaling pathway	26	235	0.02208858
Glioma	10	66	0.02208858
Ascorbate and aldarate metabolism	6	17	0.02218718
Osteoclast differentiation	14	88	0.02795163
FoxO signaling pathway	17	114	0.02861963
Ovarian steroidogenesis	5	31	0.02886668
Inflammatory mediator regulation of TRP channels	13	74	0.02886668
Inflammatory bowel disease	8	34	0.0295734
Thyroid hormone synthesis	9	51	0.0295734
Vascular smooth muscle contraction	14	88	0.03140008
Cell adhesion molecules	13	77	0.03593259
Gastric acid secretion	10	57	0.03656625
Arrhythmogenic right ventricular cardiomyopathy	9	48	0.03656625
cAMP signaling pathway	18	139	0.03929434
Colorectal cancer	14	83	0.03929434
Intestinal immune network for IgA production	5	18	0.03929434
Small cell lung cancer	12	82	0.03929434
Oxytocin signaling pathway	14	115	0.03999697
AGE-RAGE signaling pathway in diabetic complications	13	81	0.04114041
Staphylococcus aureus infection	8	33	0.04114041
Ras signaling pathway	22	170	0.04251244
alpha-Linolenic acid metabolism	5	15	0.04521641
Prostate cancer	12	88	0.04758495

**Table 3-4: Pathway Analysis in MDA-MB-453 cells (NT vs R881+RT)**

<b>Pathway</b>	<b>Number of differentially expressed genes</b>	<b>Total genes</b>	<b>p-value (FDR)</b>
cAMP signaling pathway	25	121	0.01623944
MicroRNAs in cancer	25	133	0.01623944
ECM-receptor interaction	11	43	0.01623944
PI3K-Akt signaling pathway	34	213	0.01623944
Steroid hormone biosynthesis	9	25	0.01623944
Peroxisome	16	70	0.01623944
Gastric cancer	19	108	0.01623944
Neuroactive ligand-receptor interaction	17	80	0.01623944
ABC transporters	9	26	0.01623944
PPAR signaling pathway	10	38	0.01743053
Adipocytokine signaling pathway	12	48	0.01743053
Staphylococcus aureus infection	8	26	0.02179902
Pathways in cancer	45	364	0.02179902
Metabolic pathways	117	1106	0.02179902
Bile secretion	9	35	0.03111319
MAPK signaling pathway	31	206	0.03485228
Prostate cancer	16	84	0.04453442
Salivary secretion	10	48	0.04858374
Calcium signaling pathway	18	106	0.04858374
p53 signaling pathway	14	67	0.0486301

**Table 3-5: Pathway Analysis in ACC-422 cells (RT vs R1881+RT)**

Pathway	Number of differentially expressed genes	Total genes	p-value (FDR)
Aldosterone-regulated sodium reabsorption	11	30	0.00023578
Cytokine-cytokine receptor interaction	22	108	0.00023578
Pancreatic secretion	17	60	0.00028949
Protein digestion and absorption	17	54	0.00056025
Bile secretion	13	50	0.00155422
Neuroactive ligand-receptor interaction	17	110	0.00155422
Salivary secretion	14	56	0.00155422
Osteoclast differentiation	19	89	0.001605
cAMP signaling pathway	22	142	0.00168049
Retinol metabolism	10	31	0.00310702
TGF-beta signaling pathway	16	76	0.00314425
Staphylococcus aureus infection	10	34	0.00442699
Pathways in cancer	48	405	0.00455356
Axon guidance	23	154	0.01206851
Cell adhesion molecules	15	77	0.01206851
Calcium signaling pathway	17	130	0.01510218
Hematopoietic cell lineage	10	40	0.01650866
Estrogen signaling pathway	17	106	0.01937239
Insulin secretion	11	56	0.01937239
MAPK signaling pathway	27	236	0.01937239
AGE-RAGE signaling pathway in diabetic complications	14	81	0.0234905
PI3K-Akt signaling pathway	31	241	0.0234905
Gastric cancer	18	115	0.02370846
Viral protein interaction with cytokine and cytokine receptor	4	23	0.02370846
Ascorbate and aldarate metabolism	6	17	0.02537829
Proximal tubule bicarbonate reclamation	6	17	0.02537829
Arachidonic acid metabolism	8	30	0.02537829
Systemic lupus erythematosus	13	67	0.02537829
Thyroid hormone synthesis	10	51	0.02544994
Inflammatory bowel disease	8	34	0.02585136
Carbohydrate digestion and absorption	7	29	0.02745822
cGMP-PKG signaling pathway	16	119	0.03208475
Oxytocin signaling pathway	15	117	0.03391241
Mineral absorption	8	37	0.03404564
Gastric acid secretion	11	57	0.04290282

**Table 3-6: Pathway Analysis in MDA-MB-453 cells (RT vs R1881+RT)**

<b>Pathway</b>	<b>Number of differentially expressed genes</b>	<b>Total genes</b>	<b>p-value (FDR)</b>
PPAR signaling pathway	13	39	0.00427509
Cell adhesion molecules	18	74	0.01730401
Fatty acid metabolism	14	49	0.01730401
ECM-receptor interaction	11	44	0.01890809
cAMP signaling pathway	24	123	0.03120092
Adipocytokine signaling pathway	12	48	0.03120092
ABC transporters	9	26	0.03120092
Retinol metabolism	8	21	0.03120092
Gastric cancer	19	107	0.03120092

### 3.9 References

1. Ni, M. *et al.* Targeting Androgen Receptor in Estrogen Receptor-Negative Breast Cancer. *Cancer Cell* **20**, 119–131 (2011).
2. Cochrane, D. R. *et al.* Role of the androgen receptor in breast cancer and preclinical analysis of enzalutamide. *Breast Cancer Res.* **16**, R7 (2014).
3. Barton, V. N. *et al.* Multiple Molecular Subtypes of Triple-Negative Breast Cancer Critically Rely on Androgen Receptor and Respond to Enzalutamide In Vivo. *Mol. Cancer Ther.* **14**, 769–778 (2015).
4. Speers, C. *et al.* Androgen receptor as a mediator and biomarker of radioresistance in triple-negative breast cancer. *Npj Breast Cancer* **3**, 29 (2017).
5. Michmerhuizen, A. R. *et al.* Seviteronel, a Novel CYP17 Lyase Inhibitor and Androgen Receptor Antagonist, Radiosensitizes AR-Positive Triple Negative Breast Cancer Cells. *Front. Endocrinol.* **11**, (2020).
6. Yard, B. D. *et al.* A genetic basis for the variation in the vulnerability of cancer to DNA damage. *Nat. Commun.* **7**, 11428 (2016).
7. Kensler, K. H. *et al.* Prognostic and predictive value of androgen receptor expression in postmenopausal women with estrogen receptor-positive breast cancer: results from the Breast International Group Trial 1–98. *Breast Cancer Res.* **21**, 30 (2019).
8. Iacopetta, D., Rechoum, Y. & Fuqua, S. A. The Role of Androgen Receptor in Breast Cancer. *Drug Discov. Today Dis. Mech.* **9**, e19–e27 (2012).
9. Michmerhuizen, A. R. *et al.* Abstract 6271: Hormone receptor inhibition as a strategy for radiosensitization of breast cancer. *Cancer Res.* **80**, 6271–6271 (2020).
10. Michmerhuizen, A. R., Spratt, D. E., Pierce, L. J. & Speers, C. W. ARE we there yet? Understanding androgen receptor signaling in breast cancer. *Npj Breast Cancer* **6**, 1–19 (2020).
11. Tran, C. *et al.* Development of a Second-Generation Antiandrogen for Treatment of Advanced Prostate Cancer. *Science* **324**, 787–790 (2009).
12. Kakouratos, C. *et al.* Apalutamide radio-sensitisation of prostate cancer. *Br. J. Cancer* 1–11 (2021) doi:10.1038/s41416-021-01528-1.
13. Polkinghorn, W. R. *et al.* Androgen receptor signaling regulates DNA repair in prostate cancers. *Cancer Discov.* **3**, 1245–1253 (2013).
14. Goodwin, J. F. *et al.* A hormone-DNA repair circuit governs the response to genotoxic insult. *Cancer Discov.* **3**, 1254–1271 (2013).
15. Werner, C. K. *et al.* Expression of the Androgen Receptor Governs Radiation Resistance in a Subset of Glioblastomas Vulnerable to Antiandrogen Therapy. *Mol. Cancer Ther.* **19**, 2163–2174 (2020).
16. Boellner, S. & Becker, K.-F. Reverse Phase Protein Arrays—Quantitative Assessment of Multiple Biomarkers in Biopsies for Clinical Use. *Microarrays* **4**, 98–114 (2015).



17. Hu, J. *et al.* Non-parametric quantification of protein lysate arrays. *Bioinforma. Oxf. Engl.* **23**, 1986–1994 (2007).
18. Chandler, B. C. *et al.* TTK inhibition radiosensitizes basal-like breast cancer through impaired homologous recombination. *J. Clin. Invest.* **130**, 958–973 (2020).
19. Rajaram, P. *et al.* Second-Generation Androgen Receptor Antagonists as Hormonal Therapeutics for Three Forms of Prostate Cancer. *Molecules* **25**, 2448 (2020).
20. Chia, K. *et al.* Non-canonical AR activity facilitates endocrine resistance in breast cancer. *Endocr. Relat. Cancer* **26**, 251–264 (2019).
21. Liao, R. S. *et al.* Androgen receptor-mediated non-genomic regulation of prostate cancer cell proliferation. *Transl. Androl. Urol.* **2**, 187–196 (2013).
22. Fizazi, K. The role of Src in prostate cancer. *Ann. Oncol. Off. J. Eur. Soc. Med. Oncol.* **18**, 1765–1773 (2007).
23. Yang, L. *et al.* Induction of androgen receptor expression by phosphatidylinositol 3-kinase/Akt downstream substrate, FOXO3a, and their roles in apoptosis of LNCaP prostate cancer cells. *J. Biol. Chem.* **280**, 33558–33565 (2005).
24. Benten, W. P. M. *et al.* Testosterone Signaling through Internalizable Surface Receptors in Androgen Receptor-free Macrophages. *Mol. Biol. Cell* **10**, 3113–3123 (1999).
25. Wunderlich, F. *et al.* Testosterone signaling in T cells and macrophages. *Steroids* **67**, 535–538 (2002).
26. Peterziel, H. *et al.* Rapid signalling by androgen receptor in prostate cancer cells. *Oncogene* **18**, 6322–6329 (1999).
27. Speers, C. *et al.* Androgen receptor as a mediator and biomarker of radioresistance in triple-negative breast cancer. *Npj Breast Cancer* **3**, 29 (2017).
28. Ciccarelli, C. *et al.* Disruption of MEK/ERK/c-Myc signaling radiosensitizes prostate cancer cells in vitro and in vivo. *J. Cancer Res. Clin. Oncol.* **144**, 1685–1699 (2018).
29. Goodwin, J. F. *et al.* DNA-PKcs-Mediated Transcriptional Regulation Drives Prostate Cancer Progression and Metastasis. *Cancer Cell* **28**, 97–113 (2015).
30. Munshi, A. & Ramesh, R. Mitogen-Activated Protein Kinases and Their Role in Radiation Response. *Genes Cancer* **4**, 401–408 (2013).
31. Golding, S. E. *et al.* Extracellular signal-related kinase positively regulates ataxia telangiectasia mutated, homologous recombination repair, and the DNA damage response. *Cancer Res.* **67**, 1046–1053 (2007).
32. Golding, S. E. *et al.* Pro-survival AKT and ERK signaling from EGFR and mutant EGFRvIII enhances DNA double-strand break repair in human glioma cells. *Cancer Biol. Ther.* **8**, 730–738 (2009).
33. Wei, F. *et al.* Inhibition of ERK activation enhances the repair of double-stranded breaks via non-homologous end joining by increasing DNA-PKcs activation. *Biochim. Biophys. Acta* **1833**, 90–100 (2013).

34. Baumgartner, M., Drake, K. & Kanadia, R. N. An Integrated Model of Minor Intron Emergence and Conservation. *Front. Genet.* **10**, (2019).
35. Tanikawa, M., Sanjiv, K., Helleday, T., Herr, P. & Mortusewicz, O. The spliceosome U2 snRNP factors promote genome stability through distinct mechanisms; transcription of repair factors and R-loop processing. *Oncogenesis* **5**, e280 (2016).
36. Lai, J.-J. *et al.* Androgen Receptor Influences on Body Defense System via Modulation of Innate and Adaptive Immune Systems. *Am. J. Pathol.* **181**, 1504–1512 (2012).
37. Guan, X. *et al.* Androgen receptor activity in T cells limits checkpoint blockade efficacy. *Nature* 1–6 (2022) doi:10.1038/s41586-022-04522-6.
38. Traina, T. A. *et al.* Enzalutamide for the Treatment of Androgen Receptor–Expressing Triple-Negative Breast Cancer. *J. Clin. Oncol.* **36**, 884–890 (2018).

## Chapter 4 : Estrogen Receptor Inhibition Mediates Radiosensitization of ER-Positive Breast Cancer Models<sup>4</sup>

### 4.1 Abstract

Endocrine therapy (ET) is an effective first-line therapy for women with estrogen receptor-positive (ER + ) breast cancers. While both ionizing radiation (RT) and ET are used for the treatment of women with ER+ breast cancer, the most effective sequencing of therapy and the effect of ET on tumor radiosensitization remains unclear. Here we sought to understand the effects of inhibiting estrogen receptor (ER) signaling in combination with RT in multiple preclinical ER+ breast cancer models. Clonogenic survival assays were performed using variable pre- and post-treatment conditions to assess radiosensitization with estradiol, estrogen deprivation, tamoxifen, fulvestrant, or AZD9496 in ER+ breast cancer cell lines. Estrogen stimulation was radioprotective (radiation enhancement ratios [rER]: 0.51–0.82). Conversely, when given one hour prior to RT, ER inhibition or estrogen depletion radiosensitized ER+ MCF-7 and T47D cells (tamoxifen rER: 1.50–1.60, fulvestrant rER: 1.76–2.81, AZD9496 rER: 1.33–1.48, estrogen depletion rER: 1.47–1.51). Combination treatment resulted in an increase in double-strand DNA (dsDNA) breaks as a result of inhibition of non-homologous end joining-mediated dsDNA break repair with no effect on homologous recombination. Treatment with

---

<sup>4</sup> This chapter was published in *NPJ Breast Cancer* and completed in collaboration with the following authors: Lynn M. Lerner, Andrea M. Pesch, Connor Ward, Rachel Schwartz, Kari Wilder-Romans, Meilan Liu, Charles Nino, Cassidy Jungles, Ruth Azaria, Alexa Jelley, Nicole Zambrana Garcia, Alexis Harold, Amanda Zhang, Bryan Wharram, Daniel F. Hayes, James M. Rae, Lori J. Pierce, and Corey W. Speers.

tamoxifen or fulvestrant in combination with RT also increased the number of senescent cells but did not affect apoptosis or cell cycle distribution. Using an MCF-7 xenograft model, concurrent treatment with tamoxifen and RT was synergistic and resulted in a significant decrease in tumor volume and a delay in time to tumor doubling without significant toxicity. These findings provide preclinical evidence that concurrent treatment with ET and RT may be an effective radiosensitization strategy.

## 4.2 Introduction

Invasive breast cancer is the leading cause of cancer deaths in women globally, accounting for 15% of all cancer-related deaths<sup>1</sup>. Breast cancer, however, is a heterogeneous disease, and treatment strategies for breast cancer patients are largely determined based on the presence of molecular drivers, including expression of the estrogen receptor (ER). ER expression is present in 70-80% of breast tumors and has been shown to be a significant driver of breast cancer pathogenesis<sup>2</sup>. Based on multiple randomized studies demonstrating its benefit for treatment and prevention, endocrine therapy (ET), which targets ER and downstream ER signaling, is the first line treatment for women with ER-positive (ER+) breast cancer<sup>3</sup>. These therapies include selective estrogen receptor modulators (SERMs), such as tamoxifen, raloxifene, and toremifene, which can act as an ER $\alpha$  partial agonist or antagonist depending on the target tissue<sup>4,5</sup>. Selective estrogen receptor degraders (SERDs), such as fulvestrant, and investigational SERDS including AZD9496, AZD9833, LY3484356, GDC-0810, GDC-0927, GDC-9545, and SAR439859, inhibit ER-mediated cellular proliferation through degradation of ER $\alpha$ <sup>6</sup>. In contrast, aromatase inhibitors (AIs), such as anastrozole, letrozole, and exemestane, are used to block the production of estrogens through inhibition of CYP19 aromatase thereby blocking downstream ER signaling<sup>7</sup>.

Ionizing radiation has also been shown to significantly increase overall survival and decrease rates of locoregional recurrence in ER+ breast cancer patients following breast conserving surgery and mastectomy<sup>8</sup>. Despite tumor heterogeneity and potential differences in the intrinsic radiation sensitivities of each tumor, all breast cancer patients receive similar scheduling and dosing of radiation without personalization based on molecular characteristics. While ER+ patients receive targeted therapies, including SERMs, SERDs, and AIs, the effects of these therapies on tumor radiosensitization remains unclear. Previous retrospective clinical studies suggest that concurrent administration of tamoxifen with RT may not be detrimental to rates of local control in patients<sup>9,10</sup> despite tamoxifen-mediated cell cycle arrest in G1, a more radioresistant phase of the cell cycle<sup>11</sup>. Although there is a lack of conclusive evidence available to support concurrent versus adjuvant administration of tamoxifen with RT, multiple studies have demonstrated an increase in local control with administration of tamoxifen and radiation therapy (RT) compared to RT alone<sup>12,13</sup>. Ongoing clinical trials, including REaCT-RETT (NCT03948568), CONSET (NCT00896155), and STARS (NCT00887380), are assessing the use of anti-estrogen therapies in combination with radiation to assess the toxicity and efficacy of sequential versus concurrent administration of treatment clinically in women with breast cancer.

In addition, the ongoing global COVID-19 pandemic has in many cases necessitated changes to the standard treatment for women with early-stage ER+ breast cancer, with neoadjuvant ET used much more frequently as a bridge to surgery<sup>14-16</sup>. These women, who initiated ET while breast surgeries were delayed, often continued their ET treatment while receiving adjuvant radiation therapy. Whether this change in practice will impact clinical outcomes for women with early-stage breast cancer remains unclear, and whether concurrent ET with RT is helpful or harmful is again of significant clinical interest. We sought to determine whether endocrine therapy

administered concurrently with radiotherapy had a radiosensitizing or radioprotective effect and evaluated whether SERMs, SERDs, estrogen-depleted, or estradiol-stimulated conditions had differential effects on radiosensitization using multiple ER<sup>+</sup> breast cancer cell lines and an *in vivo* xenograft model. Having observed radiosensitization with ER inhibition, we also sought to understand the mechanism of estrogen-mediated DNA damage repair in response to RT.

## 4.3 Results

### 4.3.1 Short term ER inhibition or degradation radiosensitizes ER<sup>+</sup> breast cancer cells

Anti-estrogen therapies, including SERMs, SERDs, and AIs, are effective single agent therapies that inhibit growth of ER<sup>+</sup> breast cancer cells reliant on estrogen signaling. The efficacy of combination therapy with ionizing radiation, however, remains unclear. To assess radiosensitization *in vitro*, clonogenic survival assays were first performed with the SERM, tamoxifen, in breast cancer cell lines. The ER<sup>+</sup> breast cancer cell lines, MCF-7 or T47D, or the ER-negative cell line, SUM-159, were treated with sub-IC<sub>50</sub> concentrations of tamoxifen for one hour prior to radiation treatment. Radiosensitization was observed with a 1-hour pretreatment of tamoxifen in MCF-7 cells with radiation enhancement ratios (rER) of 1.14-1.50 with 10-250 nM tamoxifen (**Figure 4-1A**) and rER of 1.33-1.60 with 500 nM-2.0 mM tamoxifen in T47D cells (**Figure 4-1C**). Interestingly, little radiosensitization was observed in MCF-7 cells when tamoxifen was given six hours before radiation treatment (rER: 0.99-1.10, **Figure 4-2A**) or when tamoxifen was given 24 hours before radiation (rER: 0.98-1.09, **Figure 4-2B**). In contrast to results in ER<sup>+</sup> cell lines, RT-induced cell death of ER-negative SUM-159 cells was not potentiated with the addition of tamoxifen (**Figure 4-1E**). Pretreatment for one hour with tamoxifen did not sensitize SUM-159 cells to RT as there was no observed increase in

radiosensitization (rER: 0.99-1.02) or decrease in the surviving fraction of cells at 2 Gy (SF-2Gy) with tamoxifen treatment.

Radiosensitization was also assessed after treatment with the SERD, fulvestrant, given one hour prior to RT. ER+ MCF-7 cells treated with 1-25 nM fulvestrant had rER of 1.33-1.76 (**Figure 4-1B**). Similar levels of radiosensitization were observed in T47D cells with 0.5-5 nM fulvestrant (rER: 0.97-2.81, **Figure 4-1D**), with a statistically significant decrease in the SF-2Gy in both cell lines. In contrast to results with tamoxifen, extended pretreatment with fulvestrant for 6 or 24 hours in MCF-7 cells resulted in comparable levels of radiosensitization as observed with 1-hour pretreatment (6-hour rER: 1.42-1.49, **Figure 4-2C**; 24-hour rER: 1.51-1.89, **Figure 4-2D**). These data suggest that the delayed administration of radiation following treatment with tamoxifen, but not fulvestrant, may be less effective than the shorter timeline of treatment *in vitro*. These observed differences may be explained by the kinetics of degradation of ER $\alpha$  protein in MCF-7 and T47D cells in which maximal degradation occurs 4-6 hours post-fulvestrant treatment (**Figure 4-2E, F**). Treatment with fulvestrant also did not radiosensitize ER-negative SUM-159 cells (rER: 1.0-1.03, **Figure 4-1F**).

Next, we used the investigational oral SERD, AZD9496, to assess radiosensitization in ER+ breast cancer cell lines *in vitro*. ER+ MCF-7 cells were treated with 100-500 nM AZD9496 for 1-hour prior to RT, and radiosensitization was observed (rER: 1.36-1.56, **Figure 4-3C**). T47D cells were more sensitive to AZD9496 treatment, and radiosensitization was achieved with 100 pM-1.0 nM (rER: 1.00-1.33, **Figure 4-3**). SUM-159 cells, a triple negative breast cancer (TNBC) cell line lacking ER expression, had no change in sensitivity to radiation with AZD9496 treatment (rER: 1.06-1.07, **Figure 4-3E**). Together, these results suggest that pharmacologic inhibition (tamoxifen)

or degradation (fulvestrant, AZD9496) of ER is sufficient to radiosensitize ER+ breast cancer cells but not ER-negative breast cancer cells.

We also wanted to explore whether sequencing of treatment mattered as recent data has suggested that this may be important for activity of immune agents for breast cancer cell deaths<sup>17</sup>. Clonogenic survival assays were performed in which fulvestrant treatment was administered 6 or 24 hours after RT to see if there were effects on radiosensitization or cellular survival. Treatment of MCF-7 cells first with RT, followed six hours later with fulvestrant, resulted in similar levels of radiosensitization as observed when fulvestrant was given prior to radiotherapy (rER: 1.23-1.49, **Figure 4-2G**). Treatment of MCF-7 cells with fulvestrant 24 hours after RT resulted in only a slight radiosensitization (rER: 1.03-1.25, **Figure 4-2H**), suggesting that delayed administration of fulvestrant after RT (24 hours) is not sufficient to promote the radiosensitization phenotype. Together these findings indicate that fulvestrant treatment, given prior to or shortly after radiotherapy (6 hours), is sufficient to promote radiosensitization of ER+ MCF-7 cells *in vitro*.

To further investigate the role of estrogen in promoting radioresistance, we performed clonogenic survival assays with cells treated with growth medium containing fetal bovine serum (FBS) compared to cells that were pretreated with charcoal-stripped bovine serum (CSS) to remove hormones and growth factors. These conditions mimic the use of aromatase inhibitors which are used to lower levels of estrogens. When MCF-7 cells were pretreated with CSS for one hour prior to RT, radiosensitization was observed relative to FBS-treated MCF-7 cells (rER:  $1.47 \pm 0.13$ , **Figure 4-1G**). Similarly, T47D cells pretreated with CSS for one hour prior to RT were radiosensitized relative to FBS treated T47D cells (rER:  $1.51 \pm 0.10$ , **Figure 4-3A**). Simulation with estradiol for 1-hour prior to RT was also sufficient to provide a radioprotective effect in hormone-stripped MCF-7 cells (rER: 0.75-0.82, **Figure 4-1H**) and hormone-stripped T47D cells



(rER: 0.51-0.57, **Figure 4-3B**). Therefore, restriction of estrogens in these experiments was sufficient to promote radioresistance, where stimulation with estradiol re-established the radioresistant phenotype in ER+ MCF-7 and T47D cells pretreated with CSS *in vitro*. Schematics outlining the various treatment conditions for clonogenic survival assays are shown (**Figure 4-1I**, **Figure 4-2I**, **Figure 4-3F**). Together these results suggest a role for estrogens in promoting radioresistance in ER+ breast cancer models.

#### ***4.3.2 ER-targeting therapies inhibit dsDNA break repair through NHEJ***

Ionizing radiation induces both single and double-strand DNA (dsDNA) breaks, though double strand breaks are more difficult to repair and are more likely to be lethal<sup>18</sup>. One mechanism of radiosensitization is through altered DNA damage repair in which decreased efficiency of dsDNA break repair results in increased cell death. To assess the repair of potentially lethal dsDNA breaks and distinguish dsDNA breaks from the more readily repaired single-strand DNA breaks, the neutral comet assay was performed in MCF-7 cells. Cells were treated with vehicle control (DMSO), 500 nM tamoxifen, or 25 nM fulvestrant for one hour prior to RT, then harvested six hours after treatment with 4 Gy RT and residual unrepaired dsDNA breaks were measured. The average tail moment was recorded with longer tail moments corresponding to a higher number of unresolved dsDNA breaks. As expected, treatment with radiation was sufficient to induce dsDNA breaks compared to control, with significantly longer tail moments in the RT group. Combination treatment of tamoxifen with RT or fulvestrant with RT resulted in an increase in dsDNA breaks compared to RT alone (average tail moment in control: 27.1, tamoxifen: 35.1, fulvestrant: 39.0, RT: 37.1, RT+tamoxifen: 48.2, RT+fulvestrant: 47.2, **Figure 4-4A**). Representative images of

comet tails are shown (**Figure 4-4A**). These results suggest that endocrine therapy treatment leads to increased dsDNA breaks at this timepoint when ET is given concurrently with RT.

DNA double strand breaks are primarily repaired through the NHEJ pathway or through homologous recombination (HR). To determine whether these dsDNA break repair mechanisms were altered with ER-targeting therapies, efficiency of NHEJ and HR was assessed using multiple, non-overlapping assays for NHEJ and HR. A pEYFP reporter system was first used to measure NHEJ efficiency. Cells were treated with tamoxifen or fulvestrant as well as controls including NU7441, an inhibitor of DNA-dependent protein kinase (DNAPK), an important part of the NHEJ pathway, or AZD7762, a pharmacologic inhibitor of Chk1/2, which are essential proteins for an efficient HR response. In MCF-7 cells, treatment with 1.0  $\mu$ M tamoxifen decreased NHEJ efficiency 30% compared to control (**Figure 4-4B**). Treatment with 10-25 nM fulvestrant also had a relative decrease in NHEJ efficiency (10 nM: 24%, 25 nM: 20%, **Figure 4-4C**). Taken together with the results from the comet assay, where RT with tamoxifen or fulvestrant led to an increase in unresolved dsDNA breaks, these findings suggest that the unresolved DNA breaks are a result, at least in part, of inhibited NHEJ activity after treatment with tamoxifen or fulvestrant.

HR was assessed by observing Rad51 foci as a marker for active repair. In MCF-7 cells, treatment with tamoxifen and radiation induced an increase in Rad51-positive cells at six hours post-RT (**Figure 4-5A**). There was no statistically significant difference in the percentage of Rad51-positive cells when comparing those treated with RT alone compared to the combination of tamoxifen with RT at six hours. This effect persisted with no change in Rad51-positive cells in RT versus combination treated cells even as dsDNA breaks were repaired at 16 hours post-RT. Similar results were observed in T47D cells (**Figure 4-5B**), and representative images are shown

(**Figure 4-5D**, **Figure 4-6**). In addition, no changes were observed in total Rad51 protein expression as observed by western blot at 6- or 16-hours post-RT (**Figure 4-5E**).

To further confirm these findings, a stable HR-reporter system was used to assess HR efficiency in MCF-7 cells. Cells treated with the positive control, AZD7762, had, as expected, a statistically significant decrease (46%) in HR efficiency. Cells treated with tamoxifen or the negative control, NU7441, had no change in HR efficiency or a slight increase in HR efficiency, respectively (250 nM tamoxifen: 37% increase, 500 nM tamoxifen: 20% increase, NU7441: 28% increase, **Figure 4-5C**), suggesting that HR efficiency is not altered by ER inhibition with tamoxifen in MCF-7 cells. Taken together, these data indicate that efficiency of NHEJ, but not of HR, is negatively affected by anti-estrogen therapy in ER+ models of breast cancer and may be contributing to the radiosensitization phenotype observed with concurrent administration of anti-estrogen therapy and RT.

#### ***4.3.3 Cell-cycle arrest is induced with radiation or short-term endocrine therapy treatment***

Endocrine therapies used for ER+ breast cancer treatment are known to cause G1 cell cycle arrest *in vitro*<sup>19</sup>, but the effect of concurrent endocrine therapy and radiation on the cell cycle has not been established. To determine whether cell cycle arrest was contributing to the observed radiosensitization with tamoxifen or fulvestrant treatment, cell cycle progression was assessed in MCF-7 and T47D cells following treatment. Cells were treated with tamoxifen or fulvestrant for one hour before RT, and cell cycle was assessed at 6-, 16-, and 24-hours post-RT. Changes in cell cycle distributions were not observed until 16 hours post-RT, when RT-induced G1 arrest was observed in p53 wildtype MCF-7 cells (control: 40.6% G1, RT: 70.9% G1; **Figure 4-7A**) and radiation-induced G2 arrest was observed in p53-mutant T47D cells (control: 74.5% G1, RT:

36.5% G1; **Figure 4-7B**). Treatment with tamoxifen alone or in combination with radiotherapy did not result in changes to cell cycle distribution compared to control cells or cells treated with RT alone, respectively (MCF-7: tamoxifen: 42.5% G1, RT+tamoxifen: 71.0% G1; T47D: tamoxifen: 79.7% G1, RT+tamoxifen: 40.1% G1). Similar results were observed at 16 hours post-RT with fulvestrant treatment in MCF-7 (control: 29.9% G1, fulvestrant: 36.9% G1, RT: 62.1% G1 RT+fulvestrant: 63.2%; **Figure 4-7C**) or T47D cells (control: 53.7% G1, fulvestrant: 60.1% G1, RT: 20.6% G1, RT+fulvestrant: 23.2% G1; **Figure 4-7D**). At 24 hours, there was an increase in G1 arrest in T47D cells that were treated with tamoxifen or fulvestrant alone; however, cells treated with the combination of RT with tamoxifen or RT with fulvestrant remained arrested in G1 (MCF-7) or G2 (T47D). Corroborating data were observed by western blot in which minimal changes were observed in the expression of cyclins A, B, and E in T47D cells at 6 hours post-RT, but by 16 hours post-RT there was a substantial increase in expression of cyclins A and B, suggesting arrest in G2/M (**Figure 4-7F**). Expression of cyclin A and B is increased at 24 hours but resolved by 48 hours post-RT. Increased expression of cyclins A and B was not observed in MCF-7 cells, but rather an increase in cyclin E expression, corresponding to arrest in G1 (**Figure 4-7E**), was also observed by western blot. Taken together, these data indicate that treatment with tamoxifen or fulvestrant causes arrest in G1 in both MCF-7 and T47D cells after prolonged treatment. G1 arrest, however, is achieved only after 24 hours, and not on a timeline that is relevant to explain the observed radiosensitization. Treatment with RT alone or in combination with tamoxifen or fulvestrant also results in G1 or G2 arrest in p53 wildtype or mutant cells, respectively, further suggesting that when given in combination with RT, ER-targeting therapies do not promote radiosensitization through a cell-cycle mediated mechanism.

#### ***4.3.4 Apoptosis is not induced with endocrine therapies in combination with radiation***

Induction of apoptosis is also a potential mechanism for the radiosensitization that was observed with endocrine therapies<sup>20-22</sup>. Treatment with tamoxifen has been shown to induce apoptosis<sup>20</sup> while estrogens have been shown to induce or inhibit apoptosis in different contexts<sup>21</sup>. Clinically, treatment with tamoxifen or anastrozole does not result in a change in apoptotic index over time<sup>22</sup>. To understand whether the combination of tamoxifen or fulvestrant with RT was increasing the percentage of cells undergoing apoptosis, and therefore increasing radiosensitivity, apoptosis was assessed by multiple non-overlapping assays including Annexin V/PI-based flow cytometry and cleaved PARP formation by western blotting at 48 hours post-RT. In MCF-7 cells, treatment with tamoxifen alone (500 nM), radiation alone (4 Gy), or the combination treatment did not increase the percentage of cells undergoing apoptosis as observed by flow cytometry (control: 10.2% tamoxifen: 11.2%, RT: 10.8%, RT+tamoxifen: 10.2%; **Figure 4-8A**). Similarly, in T47D cells, no statistically significant changes in the percentage of cells undergoing apoptosis were observed with treatment of tamoxifen alone (2.0  $\mu$ M), or RT alone, although there was a slight increase in apoptosis with combination treatment compared to control (control: 4.2%, tamoxifen: 4.9%, RT: 6.7%, RT+tamoxifen: 10.4%; **Figure 4-8B**). In addition, there were no changes in cleaved PARP, suggesting that the increase in radiosensitization with tamoxifen is not due to an increase in apoptosis in MCF-7 and T47D cells (**Figure 4-8C, D**). Using the flow-based approach, cells treated with fulvestrant or fulvestrant in combination with RT did not induce apoptosis compared to RT alone in MCF-7 (control: 9.4%, fulvestrant: 9.4%, RT: 10.7%, RT+fulvestrant: 15.6%; **Figure 4-8E**) or T47D (control: 6.8%, fulvestrant: 11.1%, RT: 15.3%, RT+fulvestrant: 21.2%; **Figure 4-8F**) cells. Taken together these experiments indicate that

radiosensitization was not due to apoptosis in response to the combination treatment of endocrine therapy with RT.

#### ***4.3.5 Endocrine therapies induce senescence alone and in combination with radiation therapy***

Estrogens and ER $\alpha$  signaling have also been recognized for their contributions toward inhibiting cellular senescence and promoting cellular growth<sup>23,24</sup>. Furthermore, induction of cellular senescence is a well-described phenomenon of several classes of radiosensitizing drugs<sup>25–27</sup>. Treatment with RT alone has also been shown to induce senescence<sup>28–30</sup>; however, the impact of RT on breast cancer cells specifically is not well characterized. In our models,  $\beta$ -galactosidase staining was used to determine whether treatment with tamoxifen or fulvestrant alone or in combination with RT may induce an increase in senescence *in vitro* in breast cancer cell lines. MCF-7 cells treated with tamoxifen or fulvestrant alone had a marked increase in cells positive for  $\beta$ -galactosidase staining (**Figure 4-9A**). In cells treated with the combination of tamoxifen or fulvestrant with RT, however, there was a substantial increase in  $\beta$ -galactosidase-positive cells suggesting that the combination of RT with tamoxifen or RT with fulvestrant resulted in an overall increase in senescence (control: 5.3%, tamoxifen: 8.2%, fulvestrant: 30.6%, RT: 3.6%, RT+tamoxifen: 25.9%, RT+fulvestrant: 30.6%, **Figure 4-9A**). This was confirmed visually with representative images of each treatment shown (**Figure 4-9B**). Similar results were observed in T47D cells treated with tamoxifen in combination with RT or fulvestrant in combination with RT in which there was an induction of senescence with tamoxifen or fulvestrant treatment alone, but this increase was magnified in cells treated with ET in combination with RT (control: 1.9%, tamoxifen: 13.7%, fulvestrant: 27.1%, RT: 3.9%, RT+tamoxifen: 19.0%, RT+fulvestrant: 46.7%, **Figure 4-9C, D**). These findings suggest that an induction of senescence is responsible, at least in

part, for the observed radiosensitization with combination ET and RT in preclinical ER+ breast cancer models.

#### ***4.3.6 Tamoxifen is synergistic with radiation in an *in vivo* xenograft model***

Next, to further assess radiosensitization in an *in vivo* xenograft model, MCF-7 cells were injected subcutaneously into the mammary fat pads of CB17-SCID mice. The resultant tumors were treated with tamoxifen alone (10 mg/kg), RT alone (5 x 2 Gy fractions), or tamoxifen and RT with variable timing of the RT in the combination groups (**Figure 4-10A**). To strictly assess radiosensitization, all tamoxifen treatments were stopped after the first 11 days of treatment. Tamoxifen was given concurrently with the fractions of administered radiation and discontinued so as to eliminate confounding effects as a result of single agent tamoxifen treatment. When assessing tumor volume, compared to control, there was a significant reduction in the tumor volume for mice treated with tamoxifen alone or RT alone (**Figure 4-10B**). Notably, the mice receiving both tamoxifen and RT had a statistically significant reduction in tumor volume compared to tamoxifen or radiation treatment alone, and the combination treatment resulted in a delay in time to tumor doubling (17 days for control, 40 days for tamoxifen only, 32 days for RT only, undefined for tamoxifen + RT, **Figure 4-10C**). In addition, there were no notable changes in the weights of the mice, suggesting that treatments were well-tolerated (**Figure 4-10D**). Synergy was assessed with the fractional tumor volume (FTV) method<sup>31</sup>, which demonstrated that compared to treatment with RT or tamoxifen alone, the combination of tamoxifen with RT with either a 1-day pretreatment (**Figure 4-10E**) or 6-day pretreatment (**Figure 4-10F**) of tamoxifen was synergistic and not just additive. Together, these *in vivo* data suggest that combining tamoxifen with RT is more effective than either monotherapy alone. In addition, there may not be

a significant difference in radiosensitization when comparing the 1-day versus 6-day pretreatment of the MCF-7 xenografts as there was no statistically significant change in tumor volume between mice with different pretreatments of tamoxifen.

#### 4.4 Discussion

Here we demonstrate that abrogation of ER signaling with tamoxifen, fulvestrant, or AZD9496 results in radiosensitization of ER<sup>+</sup> breast cancer cell lines (**Figure 4-1, Figure 4-2, Figure 4-3**) through the inhibition of DNA damage repair via NHEJ (**Figure 4-4**) and an induction of cellular senescence with combination treatment of ET and RT (**Figure 4-9**). Changes in HR-mediated repair, apoptosis, and cell cycle were not observed in cells treated with ET and RT compared to cells treated with RT alone (**Figure 4-5, Figure 4-6, Figure 4-7, Figure 4-8**). Estradiol stimulation resulted in radioprotection in ER<sup>+</sup> models, and estrogen depletion was radiosensitizing in these same models (**Figure 4-1, Figure 4-3**). Radiosensitization was also observed *in vivo* with concurrent tamoxifen treatment using an MCF-7 xenograft model (**Figure 4-10**). Together, these results propose that treatment with the combination of ER inhibition and RT may be more effective than ER inhibition or RT alone. These data also suggest an expanded role for ER-targeting therapies as radiosensitization agents for patients with ER<sup>+</sup> breast tumors and support the continued use of ET during RT when ET is started as a bridging strategy to surgery.

Our work demonstrates that treatment with tamoxifen, fulvestrant, or AZD9496 may radiosensitize ER<sup>+</sup> breast cancer models through induction of senescence and inhibition of NHEJ-mediated repair. These findings are consistent with previous work which has demonstrated a decrease in NHEJ efficiency in human fibroblasts undergoing senescence compared to young or presenescent cells<sup>32</sup>. Because cell cycle redistribution was not observed at early time points



following tamoxifen or fulvestrant treatment, these results suggest that changes to cell cycle assortment are not driving the radiosensitization phenotype observed with short, one hour pretreatment times in MCF-7 and T47D cells. Cell cycle arrest does occur on timescales that are relevant for the longer fulvestrant pretreatment times prior to radiation, however, similar levels of radiosensitization still occur despite cell cycle redistribution, further suggesting that the observed radiosensitization is not solely based on cell cycle changes. Together our findings do not support the clinical concern of sequential use of radiation with endocrine therapy due to radioresistance resulting from cell cycle redistribution. Rather, our work suggests that concurrent administration of RT with tamoxifen or fulvestrant results in radiosensitization despite cell cycle arrest with longer drug pretreatment times. Previous work from our lab and others demonstrated that antagonism of hormone receptors, notably the androgen receptor, results in radiosensitization of AR+ TNBC<sup>33-35</sup> and prostate cancer<sup>36-39</sup>. The observed radiosensitization is due, at least in part, to an inhibition of NHEJ through downregulation of p-DNAPK. These findings, along with our work outlined here, suggest a broader role for hormone receptors in regulation of NHEJ efficiency in hormone receptor-positive cancers following ionizing radiation treatment.

Previous studies have also demonstrated the utility of using ER-targeted therapies in combination with RT in ER+ breast cancer models. This work, performed in both *in vitro* and *in vivo* models, has been inconclusive in determining the optimal timing of administration of ET and RT for patients. In one study, rats with mammary tumors induced by 1-methyl-1-nitrosourea (MNU) benefited from treatment of tamoxifen or RT alone, while receiving similar levels of benefit from the combination treatment with no significant radiosensitization noted<sup>40</sup>. Other studies using MCF-7 cells grown in spheroids with estrogen supplementation had little change in radiosensitization compared to cells grown in monolayers; however, cells grown in estrogen-free

media had a significant decrease in radiosensitivity compared to cells treated with  $17\beta$ -estradiol<sup>41</sup>. Treatment with the aromatase inhibitor, letrozole, also had a radiosensitizing effects on MCF-7 cells *in vitro*<sup>42</sup>. In a contrasting study, a decrease in radiosensitivity was observed by Wazer *et al.* when treating MCF-7 cells with tamoxifen in combination with RT compared to treatment with RT alone when tamoxifen was given 48 hours prior to RT<sup>43</sup>. These findings are consistent with our results suggesting that prolonged tamoxifen pretreatment may be insufficient to radiosensitize MCF-7 cells *in vitro*. Treatment of MCF-7 cells with fulvestrant also resulted in significant radiosensitization through a decrease in Rad51 and DNAPKcs protein levels with sustained fulvestrant treatment<sup>44</sup>. While our results suggest that tamoxifen or fulvestrant treatment decreases efficiency of NHEJ, no changes in Rad51 protein levels were observed (**Figure 4-5E**). Differences in fulvestrant pretreatment times (4 days versus 1 hour), however, could explain differences in these results. Together our findings suggest that both SERMs and SERDs can function as radiosensitization agents in p53 wildtype and p53 mutant models of ER+ breast cancer and add to a body of literature suggesting this may be an effective clinical strategy, especially in women at high risk for locoregional disease recurrence.

Our current study uses multiple ER+ breast cancer models and suggests that treatment with tamoxifen may sensitize cell and xenograft models to RT *in vitro* through the inhibition of dsDNA repair in an NHEJ-dependent manner as well as an increase in the induction of senescence with RT in combination with ET. However, there remain limitations to these studies. There are a limited number of model systems used in this work due to the finite number of ER+ breast cancer models that grow *ex vivo* in culture. In addition, this work uses *in vitro* or immunocompromised models and therefore cannot address a potential role for the immune system in modulating the radiation response. Extensions of future work could include a more robust investigation of the impact of the

immune system using immunocompetent models. Future work will also expand this study using xenograft models with additional ER-targeting agents including additional oral SERDs, an ER $\alpha$  PROTAC degrader, and aromatase inhibitors that require estrogen depleted media and/or exogenous stable expression of aromatase in the cultured cells. These models will assess radiosensitization in an increasingly diverse set of breast cancer model systems using multiple ER-targeting therapies. This work will also investigate the transcriptional role of ER in the response to radiation to understand how ER may be promoting the transcriptional regulation of genes important for the DNA damage response through canonical ER transcription factor activity.

Importantly, previous clinical studies also raise concerns about concurrent administration of tamoxifen with RT in regard to the toxicity of treatment. While none of our experiments address this question directly, in our *in vivo* studies, we saw no evidence of increased toxicity in animals treated with tamoxifen and RT together compared to those treated with RT alone (weight loss, hair loss, dermatitis). Additionally, although previous work has demonstrated that tamoxifen is more toxic to the skin when administered in combination with RT<sup>45</sup>, other groups have shown in long term follow-up studies there are no differences in cosmesis with tamoxifen and RT<sup>46</sup>. Concurrent treatment of tamoxifen with RT has also been shown to result in increased levels of lung fibrosis compared to RT alone<sup>47</sup>. Results from the CO-HO-RT trial (NCT00208273), however, demonstrated that concurrent administration of the aromatase inhibitor, letrozole, with RT provides radiosensitization without an increase in skin toxicity<sup>42</sup>. Future clinical studies can address to what extent, if any, concurrent anti-estrogen therapies contribute to added normal tissue toxicity during and after radiation.

Together our data suggest that the administration of tamoxifen or fulvestrant or depletion of estrogens concurrently with RT may increase effectiveness of radiotherapy, demonstrating that

this could be an effective treatment intensification strategy for patients with locally advanced ER+ breast cancer at high risk for locoregional recurrence. This intensification of therapy could be considered in appropriately selected patients but should be balanced against the ongoing efforts for treatment de-escalation for women with early stage ER+ breast cancer who may appropriately choose to omit radiation therapy given their low risk of local recurrence<sup>48</sup>. Previous studies have demonstrated that concurrent treatment of tamoxifen with RT does not appear to have an adverse effect on local/systemic control compared to sequential treatment<sup>10</sup>. In addition, the REaCT-RETT trial underway is comparing sequential to concurrent administration of RT with ET and will provide further insight into this clinical question. Future studies will continue to investigate these hypotheses through clinical trials seeking to improve local control and outcomes for patients with ER+ breast cancers. This work remains of clinical importance for the treatment of breast cancer patients especially in light of the COVID-19 pandemic where patients have received endocrine therapy prior to the administration of radiotherapy.

## **4.5 Methods**

### ***4.5.1 Cell Lines***

Cells were grown in an incubator at 37°C with 5% CO<sub>2</sub>. SUM-159 cells received from Dr. Steven P. Ethier (University of Michigan, Ann Arbor, MI) were grown in HAMS F-12 media (ThermoFisher 11765054), supplemented with 6 µg/mL insulin (Sigma I9278), 0.01M HEPES (Sigma H3375), 1 µg/mL hydrocortisone (Sigma H4001), 1X antibiotic-antimycotic (anti-anti; ThermoFisher 15240062), and 5% FBS (Atlanta Biologicals S11550H). MCF-7 and T47D cells were received from ATCC and grown in DMEM media (ThermoFisher 11965092) containing 1% penicillin/streptomycin (ThermoFisher 15070063) and 10% FBS. Media containing charcoal-

stripped bovine serum (Atlanta Biologicals S11650H) was used for indicated assays. For experiments with  $\beta$ -estradiol stimulation, cells were stripped of hormones with media containing CSS for three days prior to stimulation. All cell lines were authenticated by DNA fingerprinting using short tandem repeat (STR) profiling. Cells were routinely tested for mycoplasma using the MycoAlert Mycoplasma Detection kit (Lonza LT07).

#### ***4.5.2 Clonogenic Survival Assay***

Cells were suspended in single cell suspension before plating in 6 well plates. Cells were allowed to adhere overnight before treatment with drug containing media. Drug treatment was given 1-24 hours prior to or following radiation (0-6 Gy). Colony growth was allowed for 1-2 weeks, then cells were fixed with methanol/acetic acid and stained with crystal violet. Colonies containing  $\geq 50$  cells were counted and analyzed using the linear-quadratic method. Experiments were repeated in triplicate, and SF-2Gy values are represented as the mean  $\pm$  SEM.

#### ***4.5.3 Neutral Comet Assay***

Cells were plated in 6 well plates and allowed to adhere overnight. The following morning, cells were treated with drug media one hour before radiation treatment (4 Gy). At six hours after radiation, cells were harvested with trypsin, suspended in low melting point agarose (Thermo Fisher 15-455-200), and pipetted onto a CometSlide (Trevigen 4250-050-03). When agarose had adhered to the slide, the slides were lysed overnight at 4°C using CometAssay Lysis Solution (Trevigen 4250-050-01). Following lysis, slides were immersed in TBE buffer containing 90 mM tris buffer, 90 mM boric acid, and 2 mM Na<sub>2</sub>EDTA (pH 8.0). Cells were separated using

electrophoresis, then washed, and neutralized in distilled water. Once dry, cells were stained using propidium iodide to stain for DNA. Images were then taken of at least 50 comets per treatment condition using a Nikon Fluorescent Microscope and analyzed using Comet Assay IV (software version 4.3). Results were pooled for statistical analyses, and data are shown as the mean  $\pm$  SEM for triplicate experiments.

#### ***4.5.4 NHEJ Reporter Assay***

A pEYFP plasmid (gift from Canman lab at the University of Michigan, Ann Arbor, MI) was linearized and purified as previously described<sup>49</sup>. MCF-7 cells were plated in 6 well plates, and the following morning treated with tamoxifen, NU7441, or AZD7762 for one hour before transfection. Following pretreatment, cells in each well were transfected with 1  $\mu$ g of linearized pEYFP plasmid using Lipofectamine 2000 (Invitrogen 11668) and OptiMEM media (Invitrogen 31985-062). Cells were harvested with trypsin six hours after transfection, and plasmid DNA was isolated using the QIAprep Spin Miniprep Kit (Qiagen 27106). Sybr Green (Thermo Fisher 4385612) was used to perform real-time quantitative PCR ( $\Delta\Delta$ Ct) on a QuantStudio6 Flex Real Time 384-well qPCR system. NHEJ efficiency was assessed with primers to detect GFP expression (Rejoined DNA: F: 5'-GCTGGTTTAGTGAACCGTCAG-3', R: 5'-GCTGAACTTGTGGCCGTTTA-3') relative to a plasmid internal control (Uncut DNA: F: 5'-TACATCAATGGGCGTGGATA-3', R: 5'-AAGTCCCGTTGATTTTGGTG-3'). Relative efficiency was calculated by normalizing to the Ct value of the internal control relative to a no treatment control sample.

#### ***4.5.5 Immunofluorescence***

Coverslips were sterilized in ethanol, and cells were plated on coverslips in 12-well plates. Cells were allowed to adhere overnight before treatment with drug containing media for one hour prior to RT (4 Gy). Following RT, cells were grown until designated time points and fixed using 4% paraformaldehyde (Thermo Scientific J19943K2). Cells were blocked in a solution containing goat serum (Thermo Fisher 16210064) and stained using an anti-Rad51 antibody (GeneTex GTX70230, 1:300) and a fluorescent goat anti-mouse secondary antibody (Invitrogen A11005, 1:2000). Nuclei were stained with ProLong Gold antifade reagent with DAPI (Invitrogen P36931). Pictures of >100 cells were taken using a Nikon Fluorescent Microscope. Cells with  $\geq 10$  Rad51 foci/cell were counted as positive. Results were pooled for statistical analyses, and data are shown as the mean  $\pm$  SD for three or four replicate experiments.

#### ***4.5.6 HR Reporter Assay***

As previously described<sup>49</sup>, an HR reporter DR-GFP plasmid was transfected into MCF-7 cells using Lipofectamine 2000 (Invitrogen 11668) according to manufacturer's instructions. Cells containing the plasmid were selected with Geneticin (Thermo Fisher 10131035) and validated by flow-cytometry for GFP expression. Validated clones were plated in 6-well plates and treated with tamoxifen, NU7441, or AZD7762 for one hour before the addition of SceI adenovirus to induce dsDNA breaks<sup>50</sup>. After 48 hours, cells were harvested and fixed before analysis by flow cytometry for GFP<sup>+</sup> cells at the University of Michigan Flow Cytometry Core. Relative expression was calculated in comparison to untreated control cells for each experiment.

#### **4.5.7 Western Blotting**

Cells were plated, allowed to adhere overnight, and pretreated with tamoxifen or fulvestrant one hour prior to irradiation. Cells were harvested at indicated time points and lysed using RIPA buffer (Thermo Fisher 89901) containing protease and phosphatase inhibitors (Sigma-Aldrich PHOSS-RO, CO-RO; Santa Cruz Biotechnology sc-3540, sc-24988A; Cayman Chemical 14333, 14405). Samples were separated on precast NuPAGE Bis-Tris protein gels (Thermo Fisher), transferred to PDVF membranes (Millipore IPVH00010), and blocked with blotting grade blocker (BioRad 1706404, 5% milk). Antibodies used for protein detection include ER $\alpha$  (Cell Signaling 8644S; 1:1000), Rad51 (Millipore PC130; 1:500),  $\beta$ -actin (Cell Signaling 12262S; 1:50,000), total PARP1 (Abcam ab6079; 1:1000), cleaved PARP (Cell Signaling 5625S; 1:1000), cyclin E1 (Santa Cruz sc-247; 1:1000), cyclin B (Santa Cruz sc-245; 1:1000), and cyclin A (Santa Cruz sc-271682; 1:1000). Secondary antibodies used include anti-mouse (Cell Signaling 7076S; 1:10,000) and anti-rabbit (Cell Signaling 7074S; 1:10,000). All blots are derived from single experiments and are processed in parallel. Quantification of western blots was performed with ImageJ software.

#### **4.5.8 Flow Cytometry**

Cells were plated and treated with drug for one hour before radiation treatment. Following radiation, cells were harvested at predetermined time points. For cell cycle experiments, cells were fixed in 70% ethanol at 6-, 16-, and 24-hours post-RT. Before analysis, fixed cells were resuspended in 1X PBS and stained with propidium iodide and RNase (Qiagen 19101). For analysis of apoptosis, cells were harvested by trypsinization 48 hours after radiation and stained with annexin V and propidium iodide (Roche 11858777001) immediately preceding analysis. Both



apoptosis and cell cycle samples were analyzed at the University of Michigan Flow Cytometry Core using the Bio-Rad ZE5 Cell Analyzer (**Figure 4-11, Figure 4-12**). Data are shown as mean  $\pm$  SD for triplicate experiments.

#### ***4.5.9 Drug Information***

Tamoxifen was obtained from MedChemExpress (HY-13757A). Fulvestrant was obtained from MedChemExpress (HY-13636). AZD9496 was obtained from MedChemExpress (HY-12870). NU7441, an inhibitor of DNA protein kinase catalytic subunit (DNAPKcs), was obtained from Selleckchem (Ku-57788). AZD7762, an inhibitor of Chk1/2, was purchased from Sigma (SML0350).  $\beta$ -Estradiol was obtained from MedChemExpress (HY-B0141). All compounds were solubilized in DMSO.

#### ***4.5.10 Animal Experiments***

MCF-7 cells suspended in 50% Matrigel (Thermo Fisher CB-40234) were injected into bilateral mammary fat pads of CB17-SCID mice ( $6 \times 10^6$  cells/injection). Simultaneously on the day of injection, estrogen pellets (Innovative Research of America SE-121) were subcutaneously implanted at the nape of the neck. Pellets were removed when tumors were palpable. Mice were randomized into five groups when tumors had reached 80-100 mm<sup>3</sup> with 9-12 tumors/group. Mice were then treated with one of the following treatment options (**Figure 4-10A**): vehicle (corn oil: Sigma C8267), tamoxifen only for 11 days, radiation only, or combination of tamoxifen with radiation. Treatment of tamoxifen was administered by oral gavage for 11 days at a dose of 10 mg/kg. Radiation treatment was administered in 5 fractions of 2 Gy. Mice in the first combination

group received tamoxifen one day before starting radiation therapy, then received concurrent tamoxifen with radiation for five days, followed by five days of tamoxifen therapy following the completion of radiation. Mice in the second combination group received six days of tamoxifen prior to beginning radiation therapy and received five doses of radiation with concurrent tamoxifen (**Figure 4-10A**). Tumor growth was measured 2-3 times/week, and tumor volume was calculated using the equation  $V = L*W^2*\pi/6$ . Animal protocols and procedures are approved by the Institutional Animal Care and Use Committee at the University of Michigan (Ann Arbor, MI).

#### ***4.5.11 Irradiation***

X-ray irradiation was performed at the University of Michigan Experimental Irradiation Core using a Kimtron IC-225. The dose rate of 2 Gy/min was used in keeping with previous studies<sup>49,51,52</sup>. For *in vitro* experiments, a 0.1mm Cu filter was used, and for *in vivo* experiments, the filter was 0.4mm Sn + 0.25mm Cu.

#### ***4.5.12 Statistical Analyses***

Statistical analyses were performed in GraphPad Prism 8. For *in vitro* experiments, a one-way ANOVA with Dunnett's test for multiple comparisons was used to compare SF-2Gy values, data from the NHEJ reporter, cell cycle analysis for each time point, and apoptosis with annexin V/PI. A two-sided Student's *t*-test was used to compare tail moments for the comet assay, HR reporter, Rad51 foci, and senescence data. For animal experiments, a log-rank (Mantel-Cox) test was performed to compare survival curves. P-values equal to or less than 0.05 were considered

significant. Synergy calculations were performed using fractional tumor volume (FTV) in keeping with previous studies<sup>49,51</sup>.

#### **4.6 Acknowledgements**

The authors thank Dr. Matthew Schipper for his help with statistical analyses. The authors acknowledge the University of Michigan Flow Cytometry Core for their assistance in data collection and analysis. This work was supported a Breast Cancer Research Foundation (BCRF) Grant to L.J.P. (BCRF-21-128) and by a generous donation by Susan and Richard Bayer to C.W.S. National Institute of General Medical Sciences (NIGMS) training grants provided support for A.R.M., A.M.P., K.J., and C.N.: T32-GM113900 (A.R.M.), T32-GM007315 (A.R.M.), T32-GM007767 (A.M.P. and K.J.), and T32-GM007863 (C.N.). A.M.P. is supported by a Ruth L. Kirschstein NRSA F31 award (F31-CA254138). A.R.M. is supported by the Rackham Predoctoral Fellowship Program, and K.J. is supported by the Rackham Merit Fellowship Program. A.R.M. and A.M.P. are also supported by Rackham Graduate School Research Grants. SUM-159 cells were generously provided by Dr. Stephen Ethier from University of Michigan stocks.

## 4.7 Figures

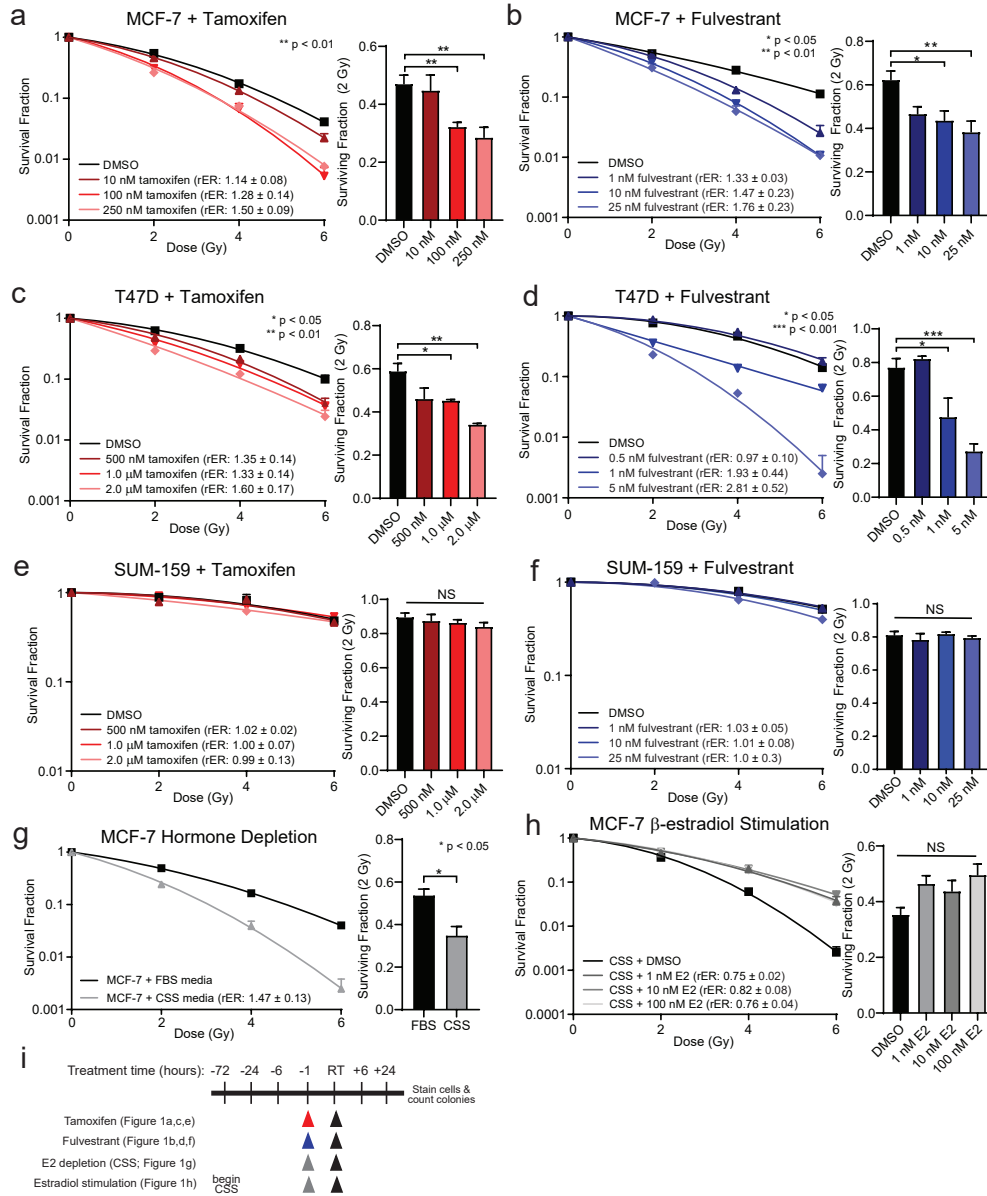


**Figure 4-1: Radiosensitization of ER+ breast cancer cell lines with anti-estrogen therapies**

Clonogenic survival assays indicate concentration-dependent radiosensitization of ER+ MCF-7 cells with tamoxifen (a) or fulvestrant (b). Radiosensitization was also observed in T47D cells with tamoxifen (c) or fulvestrant (d) treatment, but not in the ER-negative SUM-159 cells treated with tamoxifen (e) or fulvestrant (f). Clonogenic survival assays were performed in MCF-7 cells pretreated with CSS for one hour compared to FBS-treated cells (g), or MCF-7 cells pretreated for 3 days with CSS before stimulation with β-estradiol (h). Clonogenic treatment times are displayed in a schematic (i). Data from three or four replicate experiments are graphed as mean ± SEM. (\*p < 0.05; \*\*p < 0.01; \*\*\*p < 0.001; NS = not significant).

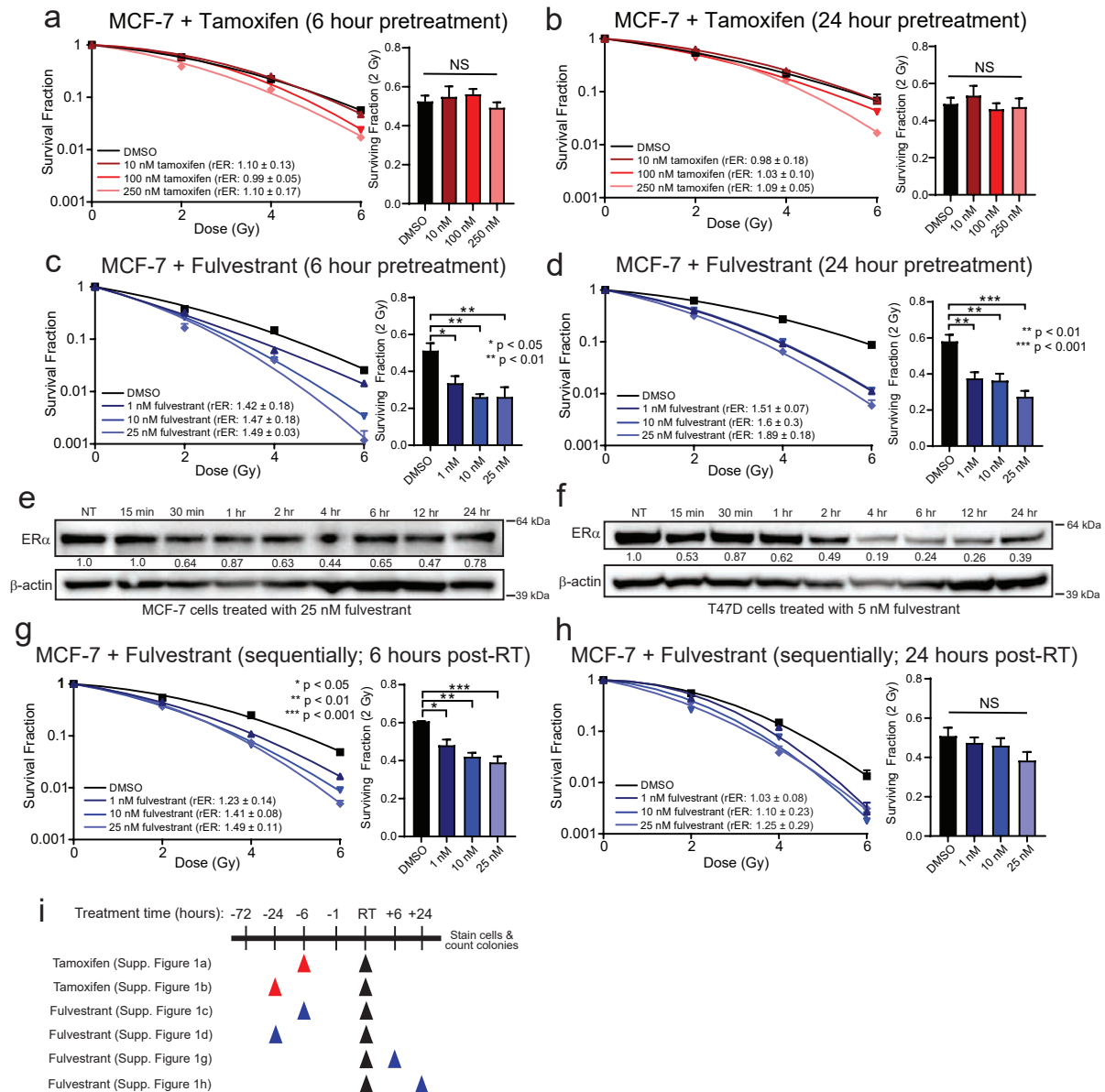


**Figure 4-2: Radiosensitization of MCF-7 cells with variable treatment times**

Clonogenic survival assays were performed with a 6- (**a**) or 24-hour (**b**) pretreatment with tamoxifen in MCF-7 cells. Similarly, clonogenic survival assays were performed with a 6- (**c**) or 24-hour (**d**) pretreatment with fulvestrant in MCF-7 cells. Western blots assessed the time course of ER $\alpha$  degradation with 25 nM fulvestrant in MCF-7 cells (**e**) or with 5 nM fulvestrant in T47D cells (**f**). Clonogenic survival assays were performed in MCF-7 cells with fulvestrant administered 6 hours (**g**) or 24 hours post-RT (**h**). A schematic of pretreatment times for clonogenic survival assays is shown (**i**). Quantification of western blots is representative of two replicates; quantification is ER $\alpha$  expression relative to no treatment (DMSO) control. Clonogenic data is from triplicate experiments and is graphed as mean  $\pm$  SEM. (\*  $p < 0.05$ ; \*\*  $p < 0.01$ ; \*\*\*  $p < 0.001$ ; NS = not significant)

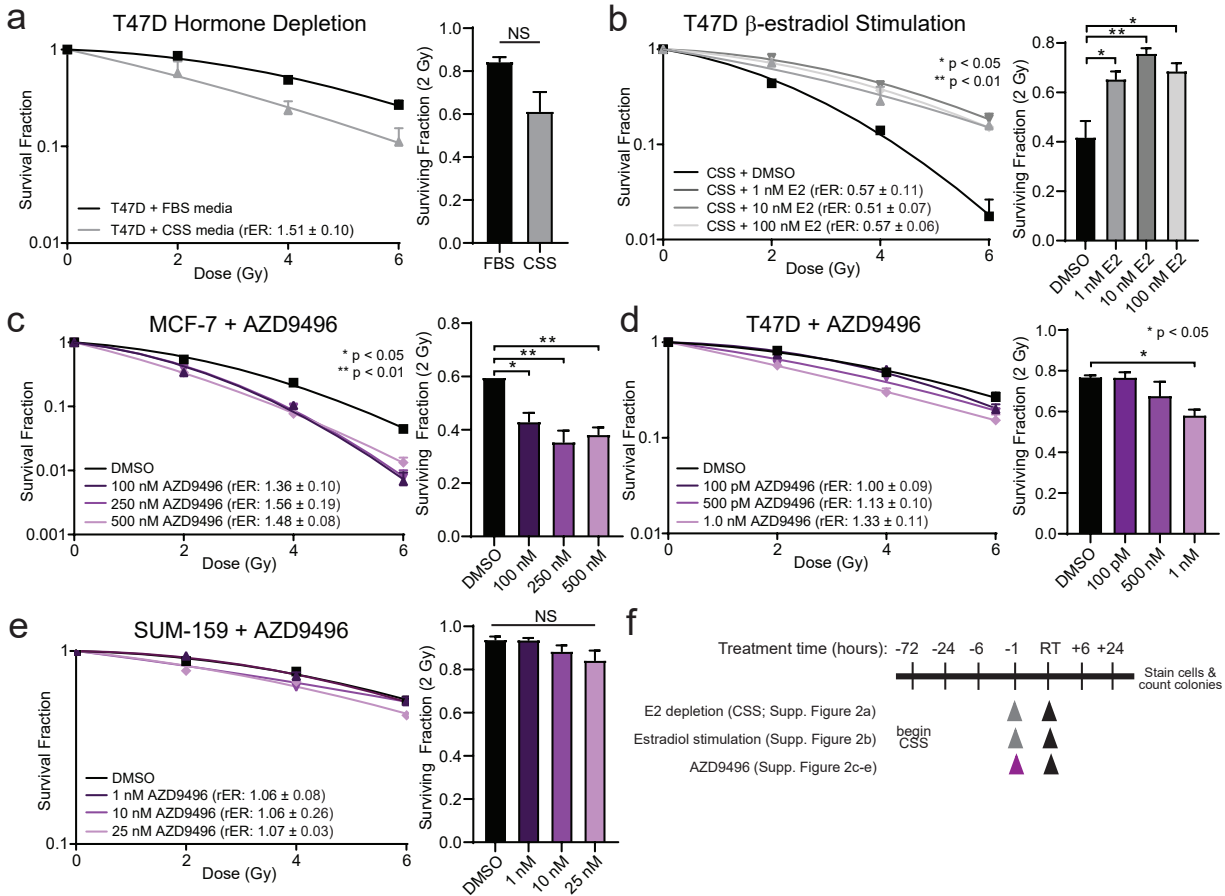


**Figure 4-3: Radiosensitization with anti-estrogen therapies**

Clonogenic survival assays were performed in T47D cells pretreated with CSS for 1-hour compared to FBS-treated cells (a), or T47D cells pretreated for 3 days with CSS before stimulation with  $\beta$ -estradiol (b). Clonogenic survival assays were performed with a 1-hour pretreatment of AZD9496 in ER+ MCF-7 (c) or T47D (d), and ER-negative SUM-159 cells (e). A schematic of pretreatment times for clonogenic survival assays is shown (f). Clonogenic data is from triplicate experiments (a, c-e) or duplicate experiments (b) and is graphed as mean  $\pm$  SEM. (\* p < 0.05; \*\* p < 0.01; NS = not significant)

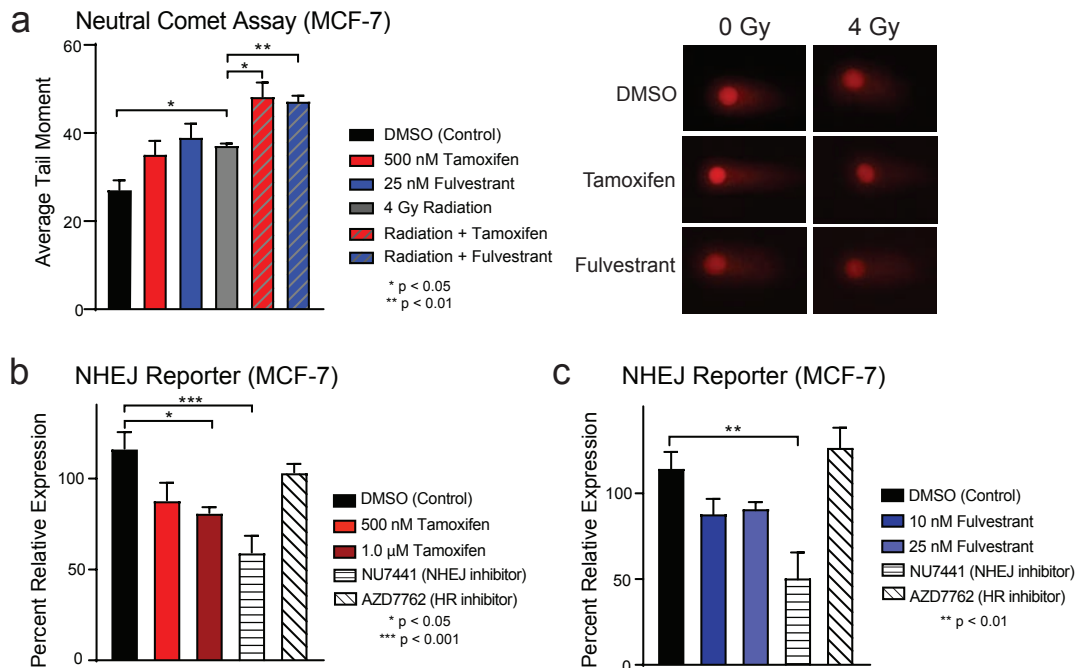


**Figure 4-4: Tamoxifen inhibits double strand DNA break repair and NHEJ efficiency in MCF-7 cells**

The neutral comet assay was used to assess dsDNA break repair in MCF-7 cells treated with  $\pm$  500 nM tamoxifen  $\pm$  25 nM fulvestrant  $\pm$  4 Gy RT (**a**). Representative images of comets are shown. NHEJ efficiency in MCF-7 cells was assessed using a transient pEYFP reporter construct. Cells were treated with tamoxifen (**b**) or fulvestrant (**c**) with AZD7762, a Chk1/2 inhibitor, used as a negative control and NU7441, a DNAPK inhibitor, used as a positive control. Data from triplicate experiments are graphed as mean  $\pm$  SEM. (\*  $p < 0.05$ ; \*\*  $p < 0.01$ ; \*\*\*  $p < 0.001$ )

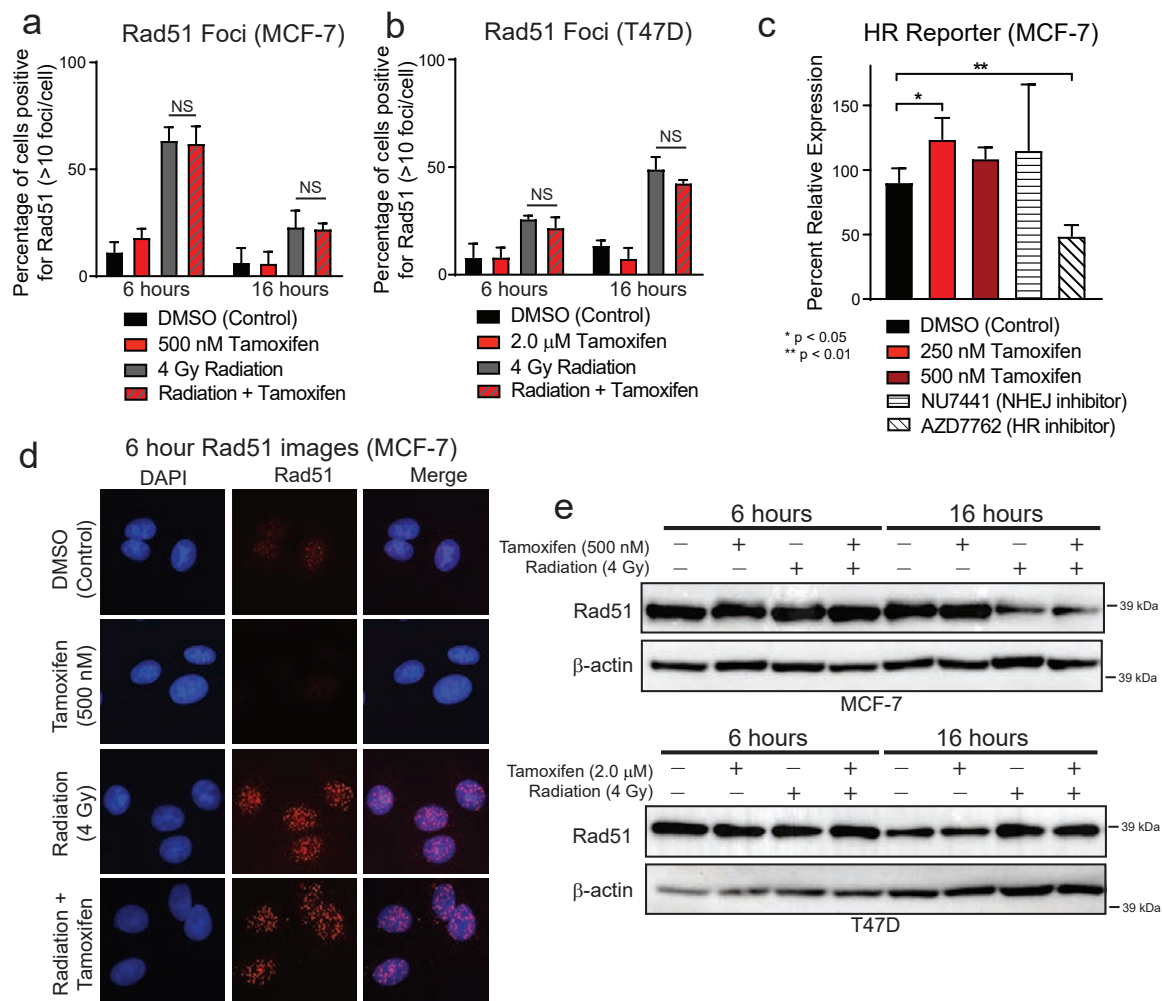


**Figure 4-5: Tamoxifen does not inhibit homologous recombination efficiency**

Immunofluorescence was used to stain Rad51 foci in MCF-7 cells treated with  $\pm$  500 nM tamoxifen  $\pm$  4 Gy RT (**a**) and in T47D cells treated  $\pm$  2.0 mM tamoxifen  $\pm$  4 Gy RT (**b**). A stable homologous recombination reporter construct was used to assess HR efficiency in MCF-7 cells treated with tamoxifen (**c**). AZD7762, a Chk1/2 inhibitor, was used as a positive control; NU7441, a DNAPK inhibitor, was used as a negative control. Representative images of MCF-7 Rad51 foci at the 6-hour timepoint are shown in (**d**). Total Rad51 protein levels were assessed by western blot in MCF-7 and T47D cells treated  $\pm$  tamoxifen  $\pm$  RT at 6- and 16-hours post-RT (**e**). Data from three or four replicate experiments are graphed as mean  $\pm$  SD. (\*  $p < 0.05$ ; \*\*  $p < 0.01$ ; NS = not significant).



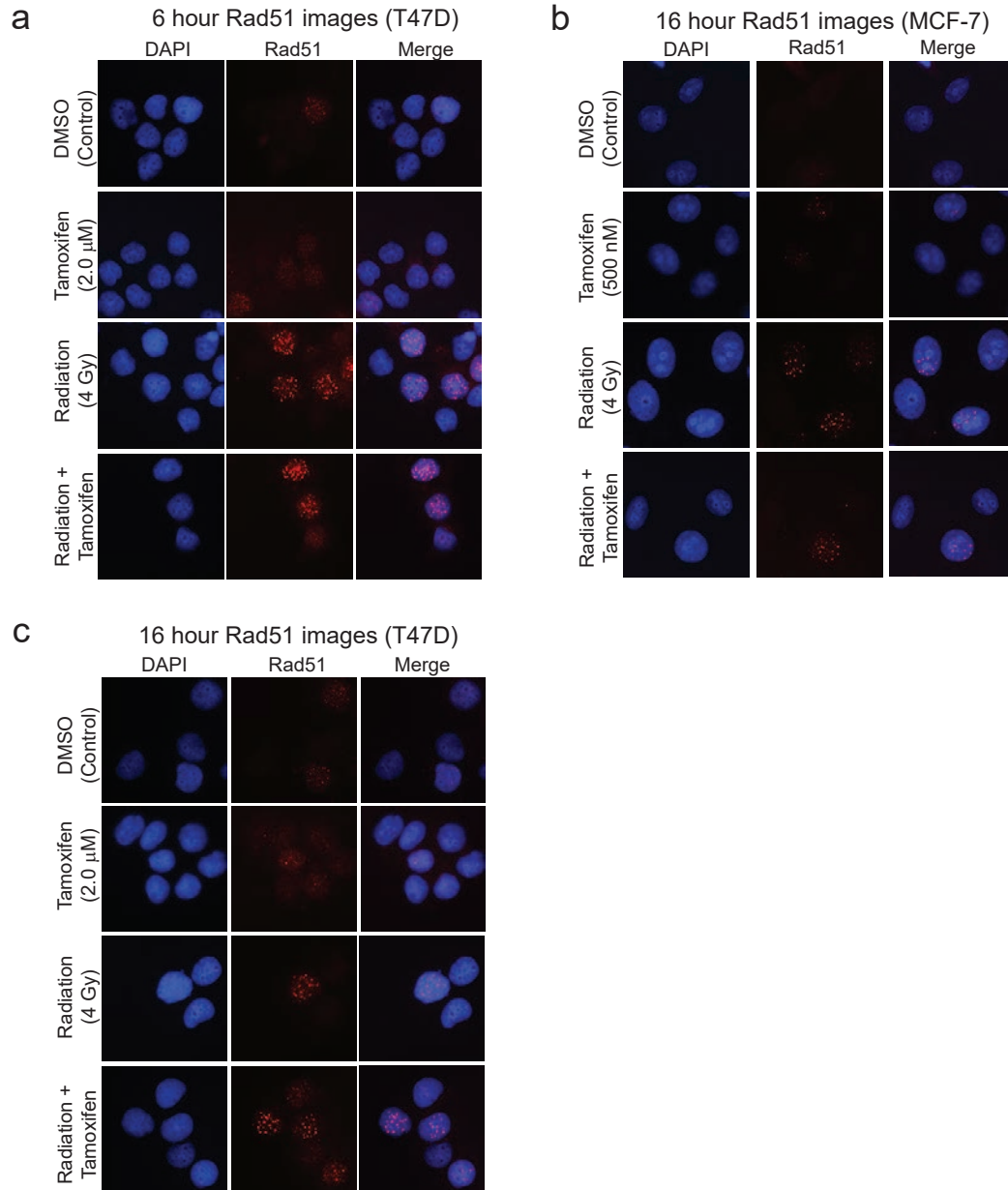


**Figure 4-6: Representatives images of Rad51 foci from immunofluorescence**

Images of T47D cells  $\pm$  tamoxifen  $\pm$  4 Gy RT at 6 hours post-RT are shown (**a**). Images for MCF-7 (**b**) or T47D (**c**) cells at 16 hours post-RT are shown for all treatment groups.

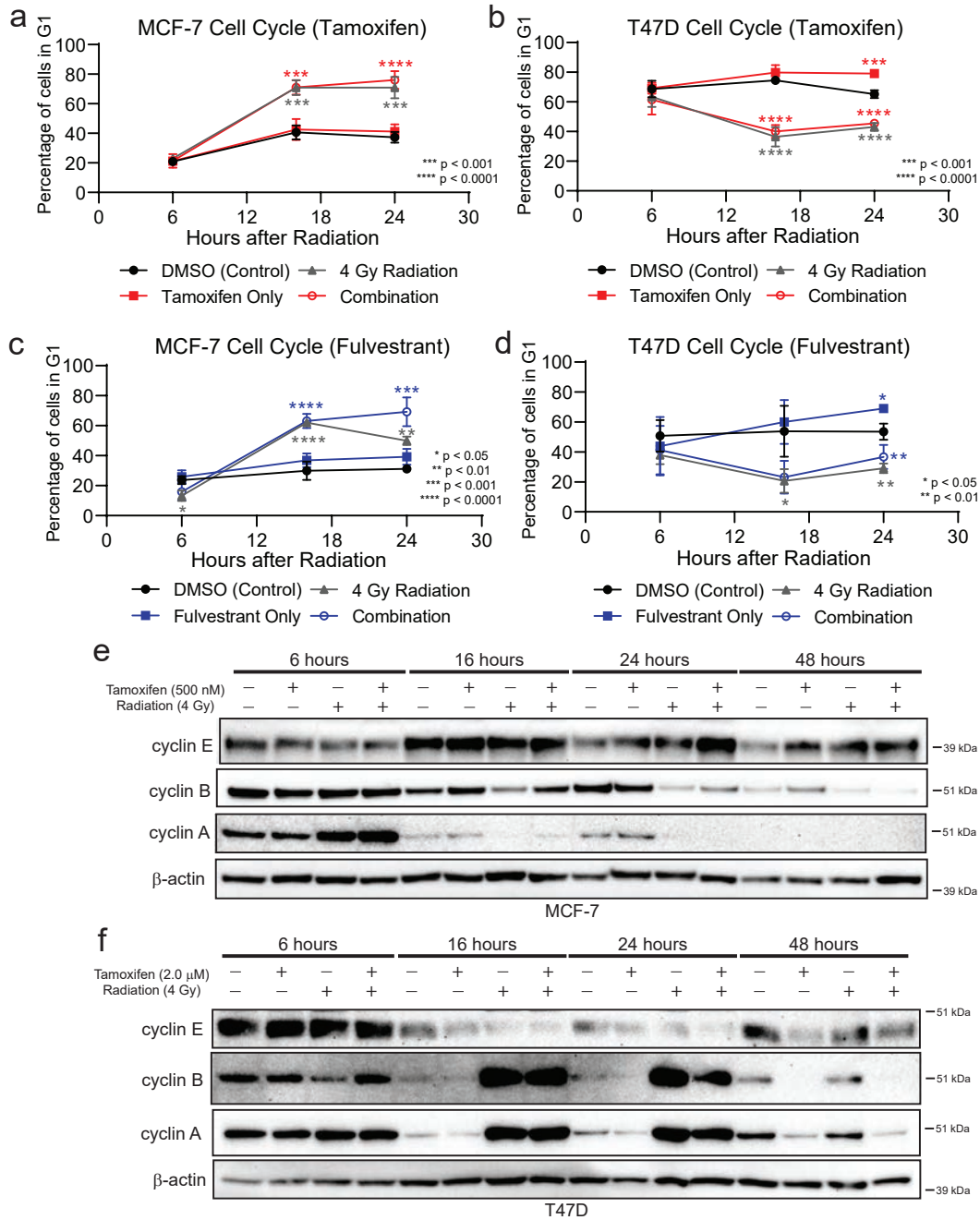


**Figure 4-7: Radiation treatment promotes cell cycle arrest in ER+ MCF-7 and T47D cells**

Cells were pretreated for one hour with tamoxifen or fulvestrant prior to radiotherapy, fixed at the indicated timepoints (6-, 16-, 24-hours after radiation), and stained with propidium iodide before flow cytometry analysis. MCF-7 cells were treated with radiation  $\pm$  tamoxifen (a). T47D cells were treated with radiation  $\pm$  tamoxifen (b). Similarly, MCF-7 (c) or T47D (d) cells were treated with radiation  $\pm$  fulvestrant. Expression of cyclins A, B, and E were assessed by western blot in MCF-7 (e) and T47D (f) cells treated with tamoxifen  $\pm$  radiation. Data from triplicate experiments are graphed as mean  $\pm$  SD. Western blots are representative of triplicate experiments. (\*  $p < 0.05$ ; \*\*  $p < 0.01$ ; \*\*\*  $p < 0.001$ ; \*\*\*\*  $p < 0.0001$ )

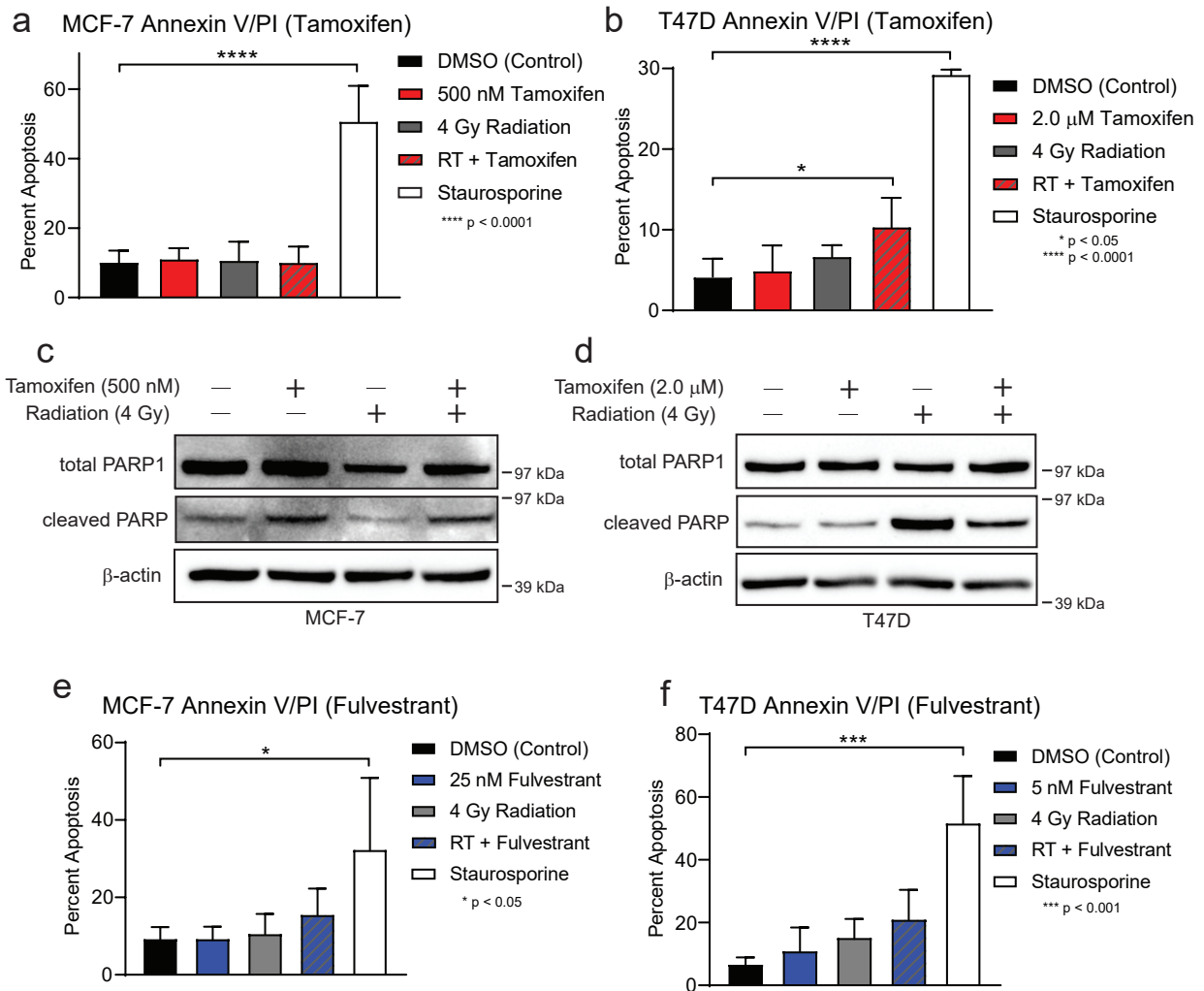


**Figure 4-8: Endocrine therapy treatment with radiation does not induce apoptosis in ER+ cells**

Annexin V/PI staining was measured via flow cytometry to assess apoptotic cells (total cells undergoing early and late apoptosis); staurosporine (500 nM) was used as a positive control. MCF-7 cells were treated with tamoxifen (500 nM), 4 Gy RT, or combination treatment (a). T47D cells were treated with tamoxifen (2  $\mu$ M), 4 Gy RT, or combination treatment (b). Levels of cleaved or total PARP1 were assessed by western blot in MCF-7 (c) and T47D (d) cells 48-hours after RT. Treatment with fulvestrant was also assessed by flow cytometry in MCF-7 (25 nM fulvestrant, e) and T47D (5 nM fulvestrant, f) cells. Data from triplicate experiments are graphed as mean  $\pm$  SD. (\*  $p < 0.01$ ; \*\*\*  $p < 0.001$ ; \*\*\*\*  $p < 0.0001$ )

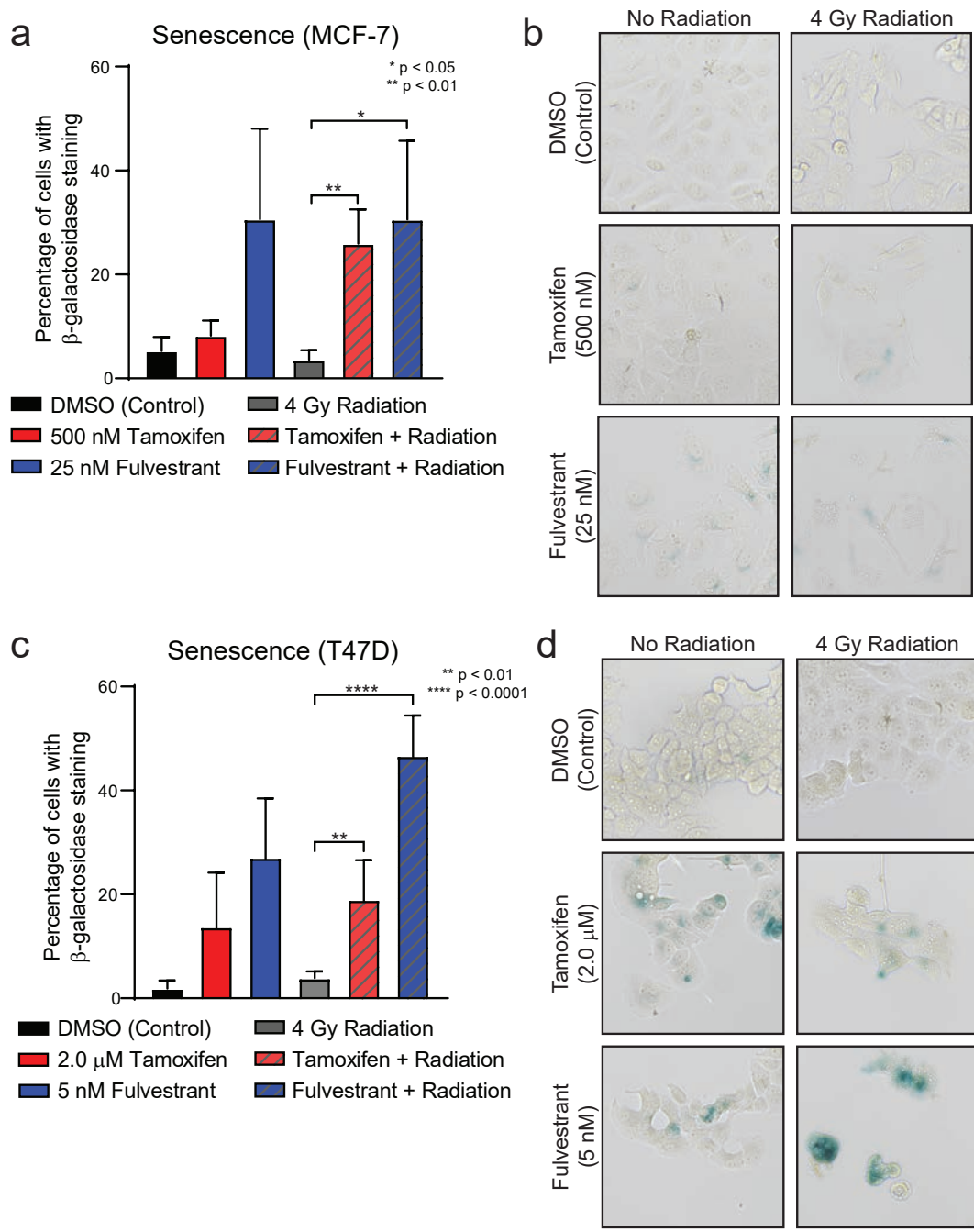


**Figure 4-9: Endocrine therapies in combination with radiation induce senescence**

MCF-7 cells were treated with 500 nM tamoxifen or 25 nM fulvestrant for one hour prior to 4 Gy radiation and stained for  $\beta$ -galactosidase at 14 days post-RT. Quantification of cells positive for  $\beta$ -galactosidase was performed for MCF-7 (a) and T47D (c) cells. Representative images of  $\beta$ -galactosidase staining are shown for each cell line (b, d). Data from three or four replicate experiments are graphed as mean  $\pm$  SD. (\*  $p < 0.05$ ; \*\*  $p < 0.01$ ; \*\*\*\*  $p < 0.0001$ )

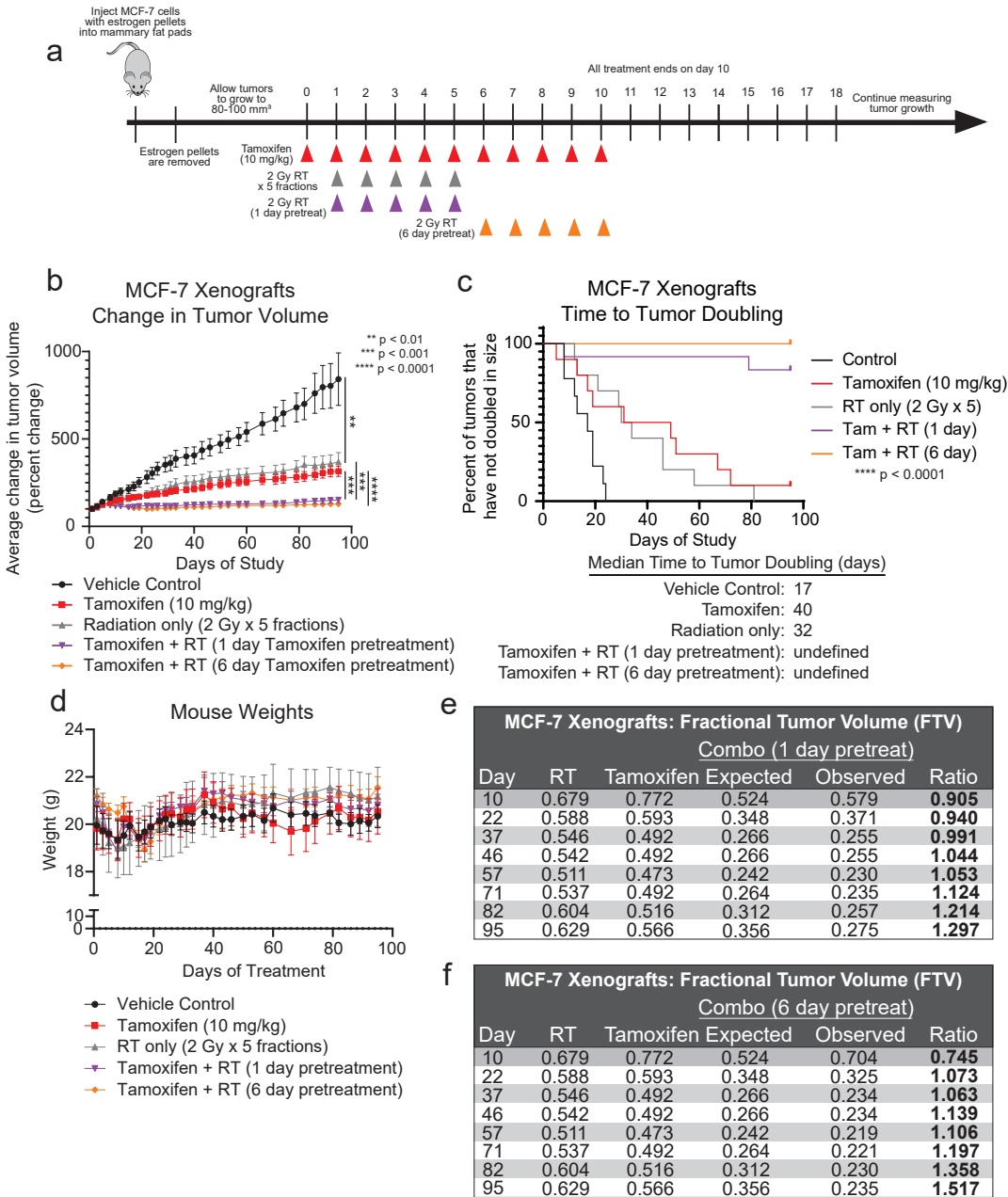


**Figure 4-10: Tamoxifen in combination with radiation is more effective than radiation alone in an MCF-7 xenograft model**

MCF-7 cells were injected into the mammary fat pads of CB17-SCID mice, and treatment was initiated when tumors were 80-100 mm<sup>3</sup>. Mice treated with the combination of tamoxifen and radiation received tamoxifen for one or six days prior to the start of radiotherapy (a). The average change in tumor volume was recorded for each treatment condition (b). Time to tumor doubling was assessed for each treatment (c). The combination treatment did not have significant toxicity as there were no changes in mouse weights (d). Tamoxifen with radiation was found to be synergistic using the fractional tumor volume method in which ratios >1 indicate synergy (e, f). Data are graphed as mean ± SEM. (\*\* p < 0.01, \*\*\* p < 0.001, \*\*\*\* p < 0.0001)

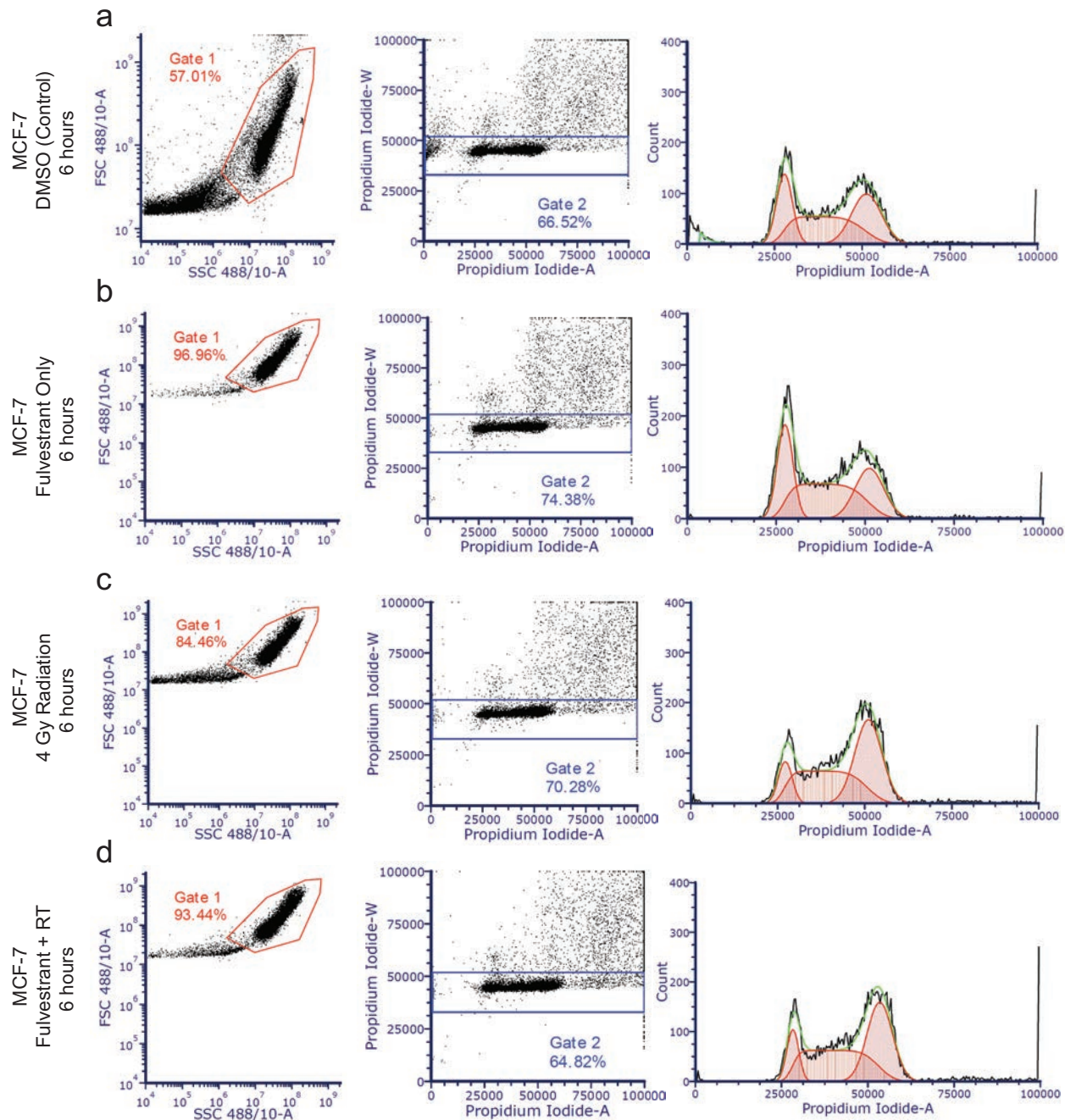


**Figure 4-11: Representative gating for PI staining of cell cycle by flow cytometry**

Gating of MCF-7 cells stained for PI after 6-hour treatment with (a) DMSO (Control), (b) fulvestrant, (c) radiation, or (d) fulvestrant + RT. Gates were used to select for live cells, and analysis software was used to determine the distribution of cells in each phase of the cell cycle. The percentage of cells in G1 phase is indicated over time (6-24 hours) in **Figure 4-7**.

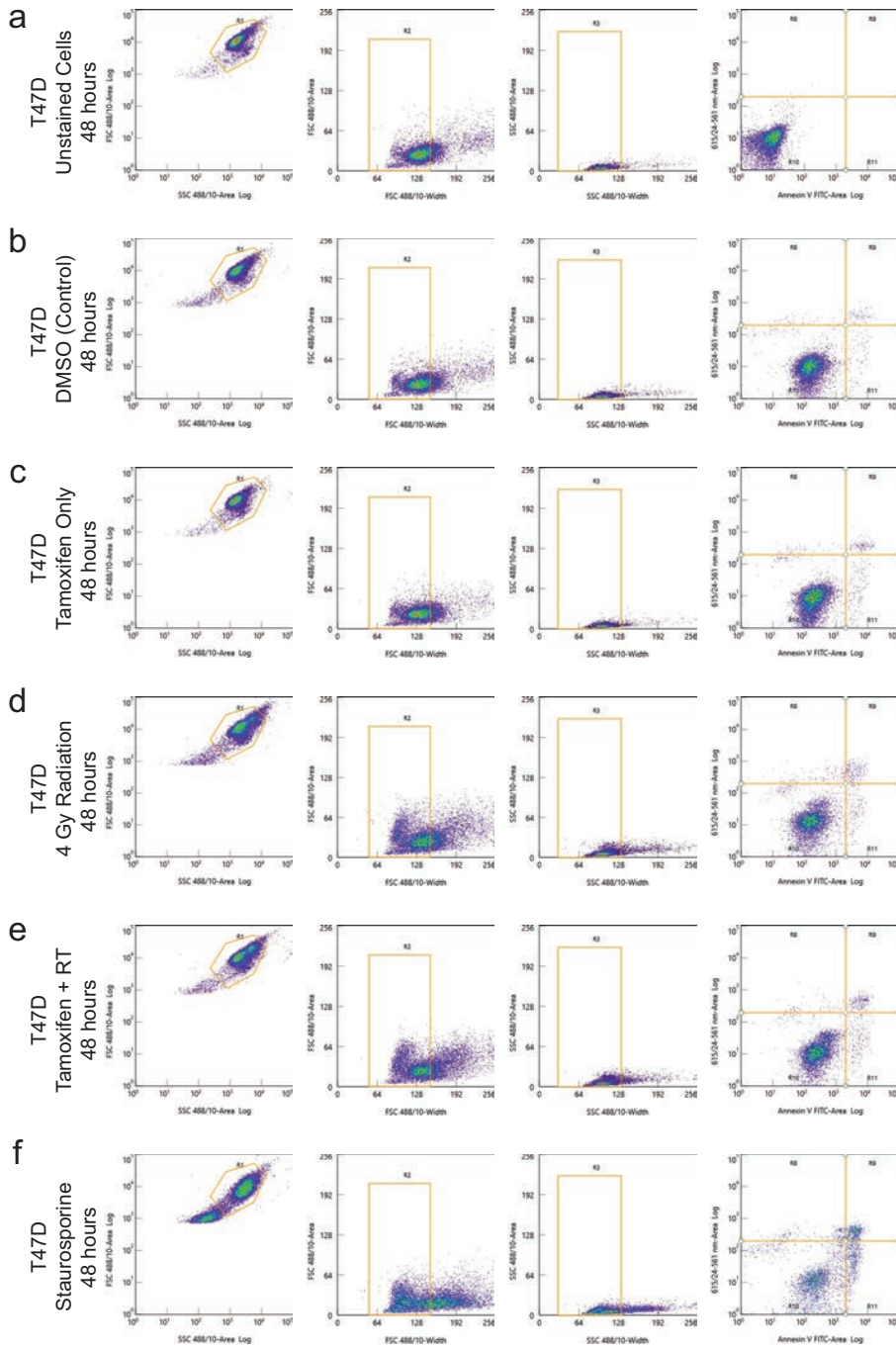


**Figure 4-12: Representative gating for AnnexinV/PI staining of apoptosis by flow cytometry**

Gating of (a) unstained T47D cells or T47D cells stained for AnnexinV/PI after 48-hour treatment with (b) DMSO (Control), (c) tamoxifen, (d) radiation, (e) tamoxifen + RT, or (f) staurosporine as a positive control, are shown. Gates were used to select for intact cells, and cells positive for Annexin V undergoing early apoptosis (quadrant R11) or late apoptosis (quadrant R9) were combined to indicate the total percentage of cells undergoing apoptosis as indicated in Figure 4-8.

## 4.8 References

1. Siegel, R. L., Miller, K. D. & Jemal, A. Cancer statistics, 2019. *CA. Cancer J. Clin.* **69**, 7–34 (2019).
2. Williams, C. & Lin, C.-Y. Oestrogen receptors in breast cancer: basic mechanisms and clinical implications. *ecancermedicalscience* **7**, (2013).
3. Early Breast Cancer Trialists' Collaborative Group (EBCTCG). Effects of chemotherapy and hormonal therapy for early breast cancer on recurrence and 15-year survival: an overview of the randomised trials. *Lancet Lond. Engl.* **365**, 1687–1717 (2005).
4. Martinkovich, S., Shah, D., Planey, S. L. & Arnott, J. A. Selective estrogen receptor modulators: tissue specificity and clinical utility. *Clin. Interv. Aging* **9**, 1437–1452 (2014).
5. Patel, H. K. & Bihani, T. Selective estrogen receptor modulators (SERMs) and selective estrogen receptor degraders (SERDs) in cancer treatment. *Pharmacol. Ther.* **186**, 1–24 (2018).
6. Lu, Y. & Liu, W. Selective Estrogen Receptor Degraders (SERDs): A Promising Strategy for Estrogen Receptor Positive Endocrine-Resistant Breast Cancer. *J. Med. Chem.* **63**, 15094–15114 (2020).
7. Brueggemeier, R. W., Hackett, J. C. & Diaz-Cruz, E. S. Aromatase Inhibitors in the Treatment of Breast Cancer. *Endocr. Rev.* **26**, 331–345 (2005).
8. Kyndi, M. *et al.* Estrogen Receptor, Progesterone Receptor, HER-2, and Response to Postmastectomy Radiotherapy in High-Risk Breast Cancer: The Danish Breast Cancer Cooperative Group. *J. Clin. Oncol.* **26**, 1419–1426 (2008).
9. Ahn, P. H. *et al.* Sequence of Radiotherapy With Tamoxifen in Conservatively Managed Breast Cancer Does Not Affect Local Relapse Rates. *J. Clin. Oncol.* **23**, 17–23 (2005).
10. Pierce, L. J. *et al.* Sequencing of Tamoxifen and Radiotherapy After Breast-Conserving Surgery in Early-Stage Breast Cancer. *J. Clin. Oncol.* **23**, 24–29 (2005).
11. Danova, M. *et al.* Cell Cycle Kinetic Effects of Tamoxifen on Human Breast Cancer Cells. *Ann. N. Y. Acad. Sci.* **698**, 174–181 (1993).
12. Dalberg, K., Johansson, H., Johansson, U. & Rutqvist, L. E. A randomized trial of long term adjuvant tamoxifen plus postoperative radiation therapy versus radiation therapy alone for patients with early stage breast carcinoma treated with breast-conserving surgery. *Cancer* **82**, 2204–2211 (1998).
13. Fisher, B. *et al.* Tamoxifen, Radiation Therapy, or Both for Prevention of Ipsilateral Breast Tumor Recurrence After Lumpectomy in Women With Invasive Breast Cancers of One Centimeter or Less. *J. Clin. Oncol.* **20**, 4141–4149 (2002).
14. Thompson, C. K., Lee, M. K., Baker, J. L., Attai, D. J. & DiNome, M. L. Taking a Second Look at Neoadjuvant Endocrine Therapy for the Treatment of Early Stage Estrogen Receptor Positive Breast Cancer During the COVID-19 Outbreak. *Ann. Surg.* **272**, e96–e97 (2020).



15. Pellicciaro, M. *et al.* Breast cancer patients with hormone neoadjuvant bridging therapy due to asymptomatic Corona virus infection. Case report, clinical and histopathologic findings. *Int. J. Surg. Case Rep.* **76**, 377–380 (2020).
16. Gasparri, M. L. *et al.* Changes in breast cancer management during the Corona Virus Disease 19 pandemic: An international survey of the European Breast Cancer Research Association of Surgical Trialists (EUBREAST). *Breast Edinb. Scotl.* **52**, 110–115 (2020).
17. Petroni, G. *et al.* Radiotherapy Delivered before CDK4/6 Inhibitors Mediates Superior Therapeutic Effects in ER+ Breast Cancer. *Clin. Cancer Res. Off. J. Am. Assoc. Cancer Res.* **27**, 1855–1863 (2021).
18. Santivasi, W. L. & Xia, F. Ionizing radiation-induced DNA damage, response, and repair. *Antioxid. Redox Signal.* **21**, 251–259 (2014).
19. Watts, C. K. *et al.* Antiestrogen inhibition of cell cycle progression in breast cancer cells in associated with inhibition of cyclin-dependent kinase activity and decreased retinoblastoma protein phosphorylation. *Mol. Endocrinol.* **9**, 1804–1813 (1995).
20. Mandlekar, S., Yu, R., Tan, T.-H. & Kong, A.-N. T. Activation of Caspase-3 and c-Jun NH2-terminal Kinase-1 Signaling Pathways in Tamoxifen-induced Apoptosis of Human Breast Cancer Cells. *Cancer Res.* **60**, 5995–6000 (2000).
21. Lewis-Wambi, J. S. & Jordan, V. C. Estrogen regulation of apoptosis: how can one hormone stimulate and inhibit? *Breast Cancer Res. BCR* **11**, 206 (2009).
22. Dowsett, M. *et al.* Proliferation and apoptosis as markers of benefit in neoadjuvant endocrine therapy of breast cancer. *Clin. Cancer Res. Off. J. Am. Assoc. Cancer Res.* **12**, 1024s–1030s (2006).
23. Lee, Y.-H., Kang, B. S. & Bae, Y.-S. Premature senescence in human breast cancer and colon cancer cells by tamoxifen-mediated reactive oxygen species generation. *Life Sci.* **97**, 116–122 (2014).
24. Liu, Z. *et al.* Estrogen receptor alpha inhibits senescence-like phenotype and facilitates transformation induced by oncogenic ras in human mammary epithelial cells. *Oncotarget* **7**, 39097–39107 (2016).
25. Wahl, D. R. *et al.* Glioblastoma Therapy Can Be Augmented by Targeting IDH1-Mediated NADPH Biosynthesis. *Cancer Res.* **77**, 960–970 (2017).
26. Alotaibi, M. *et al.* Radiosensitization by PARP Inhibition in DNA Repair Proficient and Deficient Tumor Cells: Proliferative Recovery in Senescent Cells. *Radiat. Res.* **185**, 229–245 (2016).
27. Chen, W.-S. *et al.* Depletion of securin induces senescence after irradiation and enhances radiosensitivity in human cancer cells regardless of functional p53 expression. *Int. J. Radiat. Oncol. Biol. Phys.* **77**, 566–574 (2010).
28. Li, M., You, L., Xue, J. & Lu, Y. Ionizing Radiation-Induced Cellular Senescence in Normal, Non-transformed Cells and the Involved DNA Damage Response: A Mini Review. *Front. Pharmacol.* **9**, 522 (2018).

29. Peng, X. *et al.* Cellular senescence contributes to radiation-induced hyposalivation by affecting the stem/progenitor cell niche. *Cell Death Dis.* **11**, 1–11 (2020).
30. Aratani, S. *et al.* Radiation-induced premature cellular senescence involved in glomerular diseases in rats. *Sci. Rep.* **8**, 16812 (2018).
31. Yokoyama, Y., Dhanabal, M., Griffioen, A. W., Sukhatme, V. P. & Ramakrishnan, S. Synergy between Angiostatin and Endostatin: Inhibition of Ovarian Cancer Growth. *Cancer Res.* **60**, 2190–2196 (2000).
32. Seluanov, A., Mittelman, D., Pereira-Smith, O. M., Wilson, J. H. & Gorbunova, V. DNA end joining becomes less efficient and more error-prone during cellular senescence. *Proc. Natl. Acad. Sci.* **101**, 7624–7629 (2004).
33. Speers, C. *et al.* Androgen receptor as a mediator and biomarker of radioresistance in triple-negative breast cancer. *Npj Breast Cancer* **3**, 29 (2017).
34. Michmerhuizen, A. R. *et al.* Seviteronel, a Novel CYP17 Lyase Inhibitor and Androgen Receptor Antagonist, Radiosensitizes AR-Positive Triple Negative Breast Cancer Cells. *Front. Endocrinol.* **11**, (2020).
35. Yard, B. D. *et al.* A genetic basis for the variation in the vulnerability of cancer to DNA damage. *Nat. Commun.* **7**, 11428 (2016).
36. Goodwin, J. F. *et al.* A hormone-DNA repair circuit governs the response to genotoxic insult. *Cancer Discov.* **3**, 1254–1271 (2013).
37. Polkinghorn, W. R. *et al.* Androgen receptor signaling regulates DNA repair in prostate cancers. *Cancer Discov.* **3**, 1245–1253 (2013).
38. Spratt, D. E. *et al.* Androgen Receptor Upregulation Mediates Radioresistance after Ionizing Radiation. *Cancer Res.* **75**, 4688–4696 (2015).
39. Kakouratos, C. *et al.* Apalutamide radio-sensitisation of prostate cancer. *Br. J. Cancer* 1–11 (2021) doi:10.1038/s41416-021-01528-1.
40. Kantorowitz, D. A., Thompson, H. J. & Furmanski, P. Effect of conjoint administration of tamoxifen and high-dose radiation on the development of mammary carcinoma. *Int. J. Radiat. Oncol.* **26**, 89–94 (1993).
41. Villalobos, M. *et al.* Interaction Between Ionizing Radiation, Estrogens and Antiestrogens in the Modification of Tumor Microenvironment in Estrogen Dependent Multicellular Spheroids. *Acta Oncol.* **34**, 413–417 (1995).
42. Azria, D. *et al.* Letrozole sensitizes breast cancer cells to ionizing radiation. *Breast Cancer Res.* **7**, R156–R163 (2005).
43. Wazer, D. E., Tercilla, O. F., Lin, P.-S. & Schmidt-Ullrich, R. Modulation in the radiosensitivity of MCF-7 human breast carcinoma cells by 17 $\beta$ -estradiol and tamoxifen. *Br. J. Radiol.* **62**, 1079–1083 (1989).
44. Wang, J., Yang, Q., Haffty, B. G., Li, X. & Moran, M. S. Fulvestrant radiosensitizes human estrogen receptor-positive breast cancer cells. *Biochem. Biophys. Res. Commun.* **431**, 146–151 (2013).

45. Wazer, D. E. *et al.* Factors influencing cosmetic outcome and complication risk after conservative surgery and radiotherapy for early-stage breast carcinoma. *J. Clin. Oncol. Off. J. Am. Soc. Clin. Oncol.* **10**, 356–363 (1992).
46. Wazer, D. E. *et al.* The effects of postradiation treatment with tamoxifen on local control and cosmetic outcome in the conservatively treated breast. *Cancer* **80**, 732–740 (1997).
47. Bentzen, S. M., Skoczylas, J. Z., Overgaard, M. & Overgaard, J. Radiotherapy-related lung fibrosis enhanced by tamoxifen. *J. Natl. Cancer Inst.* **88**, 918–922 (1996).
48. Speers, C. & Pierce, L. J. Molecular Signatures of Radiation Response in Breast Cancer: Towards Personalized Decision-Making in Radiation Treatment. *Int. J. Breast Cancer* **2017**, e4279724 (2017).
49. Chandler, B. C. *et al.* TTK inhibition radiosensitizes basal-like breast cancer through impaired homologous recombination. *J. Clin. Invest.* **130**, 958–973 (2020).
50. Mao, Z., Seluanov, A., Jiang, Y. & Gorbunova, V. TRF2 is required for repair of nontelomeric DNA double-strand breaks by homologous recombination. *Proc. Natl. Acad. Sci. U. S. A.* **104**, 13068–13073 (2007).
51. Pesch, A. M. *et al.* Short-term CDK4/6 Inhibition Radiosensitizes Estrogen Receptor–Positive Breast Cancers. *Clin. Cancer Res.* **26**, 6568–6580 (2020).
52. Speers, C. *et al.* Maternal Embryonic Leucine Zipper Kinase (MELK) as a Novel Mediator and Biomarker of Radioresistance in Human Breast Cancer. *Clin. Cancer Res.* **22**, 5864–5875 (2016).

## Chapter 5 : Androgen and Estrogen Receptor Co-Expression Determines Efficacy of Hormone Receptor-Mediated Radiosensitization in Breast Cancer<sup>5</sup>

### 5.1 Abstract

**Purpose:** Radiation therapy (RT) and hormone receptor (HR) inhibition are used for treatment of HR-positive breast cancers; however, little is known about the interaction of the androgen receptor (AR) and estrogen receptor (ER) in response to RT in AR-positive, ER-positive (AR+/ER+) breast cancers. Here we assessed radiosensitization of AR+/ER+ cell lines using pharmacologic or genetic inhibition/degradation of AR and/or ER.

**Methods:** Radiosensitization was assessed with AR antagonists (enzalutamide, apalutamide, darolutamide, seviteronel, ARD-61), ER antagonists (tamoxifen, fulvestrant), or using knockout of AR.

**Results:** Treatment with AR antagonists or ER antagonists in combination with RT did not result in radiosensitization changes (radiation enhancement ratios [rER]: 0.76-1.21). Fulvestrant treatment provided significant radiosensitization of CAMA-1 and BT-474 cells (rER: 1.06-2.0) but not ZR-75-1 cells (rER: 0.9-1.11). Combining tamoxifen with enzalutamide did not alter radiosensitivity using a 1-hour or 1-week pretreatment (rER: 0.95-1.14). Radiosensitivity was unchanged in AR knockout compared to Cas9 cells (rER:  $1.07 \pm 0.11$ ), and no additional radiosensitization was achieved with tamoxifen or fulvestrant compared to Cas9 cells (rER: 0.84-1.19).

**Conclusion:** While radiosensitizing in AR+ TNBC, AR inhibition does not modulate radiation sensitivity in AR+/ER+ breast cancer. Efficacy of ER antagonists in combination with RT may also be dependent on AR expression.

---

<sup>5</sup> This chapter was published in the *British Journal of Cancer* and completed in collaboration with the following authors: Lynn M. Lerner, Connor Ward, Andrea M. Pesch, Amanda Zhang, Rachel Schwartz, Kari Wilder-Romans, Joel R. Eisner, James M. Rae, Lori J. Pierce, and Corey W. Speers.

## 5.2 Introduction

Breast cancer is a heterogeneous disease, classified largely by the expression of the estrogen receptor (ER), progesterone receptor (PR), and by amplification of the human epidermal growth factor receptor 2 (HER2) (1). Over 80% of breast cancer patients have ER-positive (ER+) tumors that express ER (2), and the androgen receptor (AR) is co-expressed with the estrogen receptor in 70-95% of all ER+ breast cancers (3,4). AR expression is also found in 30-60% of non-ER expressing (ER-negative) tumors (5,6) where the role for AR in radiosensitization has previously been described (7,8). Functionally, both AR and ER have very similar roles as both are activated by hormone binding and act as transcription factors, binding to response elements in the nucleus (9). AR has been shown to compete with ER for binding to estrogen response elements (EREs) therefore acting as an antagonist to ER signaling in AR+/ER+ breast cancers (10). AR-targeting therapies have been investigated for their potential therapeutic use for the treatment of AR+ cancers. Multiple anti-androgen therapies have been developed first for use in patients with prostate cancer (11). The potential therapeutic use of these agents, including second-generation anti-androgens apalutamide (ARN-509) (12), darolutamide (ODM-201) (13), and enzalutamide (MDV3100) (14), has been explored in other AR+ cancers, including AR+ breast cancers. Enzalutamide is the most widely used AR-inhibitor and is currently being explored in multiple clinical trials in breast cancers (NCT04142060, NCT03207529, NCT02689427) (15). Similarly, darolutamide (NCT03383679) and seviteronel (NCT04947189) are also currently being explored in AR+ breast cancers. Previous work by our group and others has demonstrated that AR inhibition is an effective strategy for radiosensitization of triple negative breast cancers (TNBCs) (7,8,16). More recently, the role of the androgen receptor as a tumor suppressor in AR+/ER+ breast tumors *in vitro* and *in vivo* has been described, suggesting

that AR activation, not inhibition, may provide a therapeutic benefit (17), and this is currently being tested in ongoing clinical trials using AR agonists with encouraging findings (NCT01616758, NCT02463032). Thus, seemingly conflicting data support both AR antagonism and agonism as treatment strategies in AR+ breast cancer suggesting a context-dependent effect that is currently poorly understood. While ongoing work seeks to understand how these receptors may be influencing tumorigenesis, there is still a clinical need for the development of better biomarkers of response for AR-targeted therapies, including the use of both agonists and antagonists. In addition, although AR and ER belong to the same class of steroid hormone nuclear transcription factors (9), the overlapping functions of these hormone receptors (HR) in treatment response have not been well characterized.

Further, the roles of both AR and ER in the radiation response are not well understood. Previous studies indicate that TNBC patients with low AR expression have decreased rates of local recurrence following radiation therapy and that AR protein expression is a biomarker of response in AR+ TNBC models (8). Additional work has demonstrated that AR inhibition with the second-generation anti-androgen, enzalutamide, AR knockdown by siRNA, or treatment with the experimental dual AR and CYP17 lyase inhibitor, seviteronel, sensitizes AR+ TNBC cells to radiation therapy (7,8). Further, our group and others have shown that inhibition or degradation of ER with tamoxifen or fulvestrant, respectively, is sufficient to radiosensitize ER+ breast cancer models (18–22). Together these findings suggest a role for nuclear hormone receptors in the radiation response and warrant further investigation of AR and ER inhibition in AR+/ER+ breast cancer models.

Androgen receptor expression has also been investigated as a contributor to the radiation response in multiple types of cancer, including prostate cancer, breast cancer, and glioblastoma

(8–12). AR has been shown to be a mediator of radioresistance in prostate cancer (23), and inhibition of AR with apalutamide results in an increased radiosensitivity through a decrease in non-homologous end-joining (NHEJ) efficiency (24,25). Additionally, in AR+ glioblastoma cell lines and xenograft models, inhibition of AR with enzalutamide or seviteronel has been shown to provide sensitization to radiation therapy (26,27). These findings suggest that AR inhibition may be a generalizable strategy for the radiosensitization of cancers with high AR expression. Previous studies, however, do not address the role of AR when expressed in combination with other hormone receptors, including the estrogen receptor, and context-dependent biological effects have yet to be described.

Having previously demonstrated that ER-inhibition is an effective radiosensitization strategy in ER+, AR-low breast cancers (22), and AR inhibition is a potentially effective radiosensitization strategy in AR+/ER- breast cancer (8), the purpose of this study was to assess the effectiveness of AR inhibition as a radiosensitization strategy in AR+/ER+ breast cancer models. In contrast to findings in other AR+ diseases, including AR+ TNBC, here we demonstrate that AR inhibition with enzalutamide, apalutamide, darolutamide, and seviteronel, degradation of AR with the AR PROTAC degrader, ARD-61, or knockout of AR using CRISPR-Cas9, does not radiosensitize AR+/ER+ breast cancer cells *in vitro*. Additionally, dual inhibition or degradation of AR and ER is not sufficient, in most models, to radiosensitize AR+/ER+ breast cancer cells *in vitro* suggesting that these receptors may not be compensating for each other when co-expressed. Further, combination treatment of AR inhibition or knockout with ER inhibition or degradation does not have a synergistic effect on radiosensitization, suggesting that AR and ER are not directly and exclusively compensating for their role in the radiation response. While our previous data suggest that inhibition or degradation of ER results in radiosensitization

(22), here we demonstrate that ER inhibition is not uniformly sufficient to radiosensitize AR+/ER+ breast cancer models. Therefore, the prior observed radiosensitization was associated with AR-low/ER+ cell lines, further promoting the notion of an interaction between AR and ER in response to RT. Altogether these findings indicate a novel role for AR and ER signaling in AR+/ER+ breast cancer compared to the role of AR in TNBC or ER in AR-low/ER+ breast cancer models in response to radiation treatment with important clinical implications for this subset of patients.

## **5.3 Materials and Methods**

### ***5.3.1 Cell Culture***

Except where noted, all cells were grown at 37°C in a 5% CO<sub>2</sub> incubator. MCF-7 cells were grown in DMEM media (ThermoFisher 11965092) containing 1% penicillin/streptomycin (ThermoFisher 15070063) and 10% fetal bovine serum (FBS; Atlanta Biologicals S11550H). BT-474 and ZR-75-1 cells were grown in RPMI 1640 media (ThermoFisher 11875093) containing 1% penicillin/streptomycin and 10% FBS. CAMA-1 cells were grown in EMEM media (ThermoFisher 15070063) containing 1% penicillin/streptomycin and 10% FBS. ACC-422 cells were grown in MEM media (ThermoFisher 11095080) containing 1X Insulin-Transferrin-Selenium-Ethanolamine (ITS-X; Gibco 51500056), 1% penicillin/streptomycin, and 15% FBS. Charcoal stripped serum (CSS, Atlanta Biologicals S11650H) was used in multiple experiments in place of FBS to remove hormones and growth factors. When CSS was used, the base media was also free of phenol-red. DNA fingerprinting was performed using short tandem repeat (STR) profiling at the University of Michigan Advanced Genomics Core. The MycoAlert Mycoplasma Detection kit (Lonza LT07) was used to test cells routinely for mycoplasma.



### **5.3.2 Gene Expression Knockout**

CRISPR cell lines were generated using the lentiCRISPRv2 plasmid (Addgene #98291) and the AR guide sequence (5' CACCTCCAGCTTGATGCGAGCGTG 3'). As previously described (28), the lentiCRISPRv2 plasmid was digested with BsmB1 for 15 minutes at 55 degrees and gel-purified using the QIAquick Gel Extraction Kit (Qiagen #28706X4). Oligonucleotides were obtained from Integrated DNA Technologies and annealed at 95 degrees then cooled at 5 degrees/minute. The guide sequences were ligated into the CRISPR plasmid and transformed into Stbl3 bacteria. Lentivirus was prepared using HEK-293T cells transfected with 1.5µg PAX2 (Addgene #12260), 0.3µg MD2g (Addgene #12259), and 1.5µg plasmid in Opti-MEM media. DMEM media containing 30% FBS was used to produce virus and media containing virus was collected at 24- and 48-hours post-transfection. Virus-containing media was spun down and cleared through a 0.45-micron filter before adding to cells with 0.8µg/mL polybrene. Selection was performed with hygromycin (CAMA-1 or ZR-75-1: 500 µg/mL). CRISPR pools were used for all assays. Cas9 CRISPR control cells were made with a control guide targeting *AAVS1* (5' CACCGGGGGCCACTAGGGACAGGAT 3').

### **5.3.3 Proliferation Assays**

Cells were plated in a 96-well plate and allowed to fix overnight. Cells were treated with media containing 1.0 nM to 10 µM ARD-61. After growing for 72 hours cell viability was assessed with AlamarBlue (ThermoFisher DAL1100) at a concentration of 10% of the well volume. Viability was calculated using a plate reader by measuring the absorbance of each well with an excitation wavelength of 540 nm and an emission wavelength of 590 nm. GraphPad Prism 8.0 was used to calculate a dose-response curve and half-maximal inhibitor concentration

(IC50). Six technical replicates were used for each experiment, and the experiment was repeated three times (n=3).

#### **5.3.4 Clonogenic Survival Assays**

Cells were plated and allowed to fix overnight. Pretreatment (1-24 hours) with drug containing media was followed by radiation (0-6 Gy). After growth for 1-4 weeks, colonies were fixed with methanol/acetic acid and stained with crystal violet. Colonies with >50 cells were counted, and data was analyzed using the linear-quadratic model. All combination groups were normalized to the drug-only control (treated with 0 Gy RT). GraphPad Prism 8.0 was used to visualize the data. All experiments used three technical replicates and were repeated in triplicate (n=3).

#### **5.3.5 Western Blotting**

Cells were harvested at indicated time points. RIPA buffer (Thermo Fisher 89901) containing protease and phosphatase inhibitors (Sigma-Aldrich PHOSS-RO, CO-RO) was used to lyse cells. For nuclear fractionation experiments, the NE-PER Nuclear and Cytoplasmic Extraction Reagents (Thermo Scientific 78835) were used to separate the nuclear and cytoplasmic cellular fractions. All samples were sonicated then standardized using a BCA assay. Samples were run in a 4-12% NUPAGE Bis-Tris protein gel at 120V then transferred to a PVDF membrane, blocked in 5% milk in TBST, and primary antibody (AR: 1:1000, Millipore PG-21; ER $\alpha$ : 1:1000, Cell Signaling 8644;  $\beta$ -actin: 1:50,000, Cell Signaling 12262S; LaminB1: 1:1000, Cell Signaling 12586; GAPDH: 1:1000, Cell Signaling 2118L) was added overnight. Anti-rabbit secondary antibody (1:10,000, Cell Signaling 7074S) was then added and blots were visualized

using ECL Prime on a ChemiDoc Imaging System. ImageJ was used for quantification of western blots.

### **5.3.6 Reverse Transcription and qPCR**

To assess changes in mRNA levels, cells were first plated in complete media containing FBS. The next day, cells were pretreated with media without phenol red, containing CSS for 48 hours. Stimulation was then performed with  $\beta$ -estradiol or metribolone (R1881). After 24 hours of stimulation, RNA was extracted with TRIzol using the miRNeasy kit for RNA isolation (Qiagen 217004). Reverse transcription was performed using random primers (Thermo Fisher 48190011), dNTPs (Thermo Fisher 18427013), and the Superscript III enzyme (ThermoFisher 18080085). cDNA was then diluted 1:5 after completion of reverse transcription. Fast SYBR Green Master Mix (Thermo Fisher 4385612) reagents were used to perform a  $\Delta\Delta$ Ct comparison of expression of gene specific primers following hormone stripping with CSS, stimulation with E2, or stimulation with R1881 using the QuantStudio 6 Flex Real Time qPCR System. Primers for *AQP3* (F: 5' CCGTGACCTTTGCCATGTGCTT 3', R: 5' TTGTCGGCGAAGTGCCAGATTG 3'), *SEC14L2* (F: 5' CCTGAAGACCAAGATGGGAGAG 3', R: 5' GCTGTAGGTGTTGTCAAACCGC 3'), *PGR* (F: 5' AGGTCTACCCGCCCTATCTC 3', R: 5' AGTAGTTGTGCTGCCCTTCC 3'), *AR* (F: 5' CAGTGGATGGGCTGAAAAAT 3', R: 5' GGAGCTTGGTGAGCTGGTAG 3'), *GREB1* (F: 5' CAAAGAATAACCTGTTGGCCCTGC 3', R: 5' GACATGCCTGCGCTCTCATACTTA 3'), and *GAPDH* (F: 5' TGCACCACCAACTGCTTAGC 3', R: 5' GGCATGGACTGTGGTCATGAG 3') were obtained from Integrated DNA Technologies. The  $\Delta\Delta$ Ct comparison was calculated by comparing the genes of interested with GAPDH as an internal control, then comparing each condition to cells cultured in FBS as a control. The relative

expression of each gene was then assessed. All experiments used three technical replicates, and data is represented as relative expression  $\pm$  SEM from three independent experiments (n=3).

### **5.3.7 Drug Information**

Enzalutamide (MDV3100; HY-70002), apalutamide (ARN-509; HY-16060), darolutamide (ODM-201; HY-16985), tamoxifen (HY-13757A), fulvestrant (HY-13636), and  $\beta$ -estradiol (E2, HY-B0141) were obtained from MedChemExpress. Seviteronel (VT-464) was obtained from Innocrin Pharmaceuticals. ARD-61 was provided by the labs of Shaomeng Wang and Arul Chinnaiyan at the University of Michigan. R1881 was provided by the lab of Arul Chinnaiyan at the University of Michigan.

### **5.3.8 Irradiation**

A Kimtron IC-225 orthovoltage machine was used to provide X-ray radiation at the University of Michigan Experimental Irradiation Core. In keeping with previous work, a dose rate of 2 Gy/min was used (22,29–31).

### **5.3.9 Statistical Analyses**

GraphPad Prism 8.0 was used to perform all statistical analyses. For determination of IC50s, a dose-response curve was calculated. For all *in vitro* experiments, a one-way ANOVA with Dunnett's multiple comparisons or a one-way Student's *t*-test was used to compare treatment groups. All data meets the assumptions for the statistical tests that were used, and variance between comparison groups are similar.

## **5.4 Results**

### **5.4.1 Validation of AR+/ER+ breast cancer cell lines in vitro**

First, functional AR and ER activity was validated by western blot and through qPCR experiments in AR+/ER+ breast cancer cell lines (CAMA-1, ZR-75-1, BT-474; **Figure 1-1A**). To do this, nuclear fractionation experiments were performed to assess the cellular localization of AR and ER under hormone deplete (CSS) or stimulated conditions (E2 or R1881). While  $\beta$ -estradiol or R1881 stimulation was sufficient to induce nuclear translocation of ER $\alpha$  or AR respectively, there was little cross reactivity between the hormone receptors, further suggesting that estrogen or androgen stimulation is specific for the activation of each receptor (**Figure 1-1E**), and R1881 does not cross stimulate ER $\alpha$  nuclear translocation or vice versa.

To functionally evaluate AR and ER activity *in vitro*, we performed RT-qPCR experiments to assess transcription of ER $\alpha$  (*GREB1*, *PGR*) and AR (*SEC14L2*, *AQP3*, *AR*) target genes in CAMA-1, ZR-75-1, and BT-474 cells after stimulation of  $\beta$ -estradiol or R1881. First, *AR* transcript levels were assessed following CSS conditions or under stimulated conditions. While growth in CSS media was sufficient to induce an increase in levels of *AR* transcripts, stimulation with  $\beta$ -estradiol or R1881 resulted in a decrease in relative expression in CAMA-1 and BT-474 cells (**Figure 5-2A,K**). Treatment with  $\beta$ -estradiol in ZR-75-1 cells, however, increased the levels of *AR* transcript (**Figure 5-2F**). While R1881 stimulation was sufficient to significantly induce expression of *AQP3* in all three AR+/ER+ models (**Figure 5-2B,G,L**), expression of the AR target, *SEC14L2*, was induced in response to R1881 stimulation only in CAMA-1 and BT-474 (**Figure 5-2C,M**) but not ZR-75-1 cells (**Figure 5-2H**). Stimulation with  $\beta$ -estradiol was sufficient to induce transcription of ER $\alpha$  target genes (*GREB1*, *PGR*) in CAMA-1, BT-474, and ZR-75-1 cells (**Figure 5-2D,E,I,J,N,O**). Together, these findings suggest that, while functional in each AR+/ER+ *in vitro* model, AR may be playing a distinct role in ZR-75-1

cells compared to BT-474 and CAMA-1 due to the differences in *SEC14L2* and *AR* expression in response to androgen or estrogen stimulation.

#### ***5.4.2 AR inhibition with second generation anti-androgens does not radiosensitize AR+/ER+ breast cancer cell lines in vitro***

To determine whether AR is acting independently from ER signaling in ER+ breast cancers to promote radioresistance, clonogenic survival assays were performed with the second-generation AR antagonist, enzalutamide. To do this, AR+/ER+ cells were treated with DMSO or 500 nM to 2.5  $\mu$ M enzalutamide for one hour prior to radiation treatment. Enzalutamide treatment in combination with radiation therapy (RT) in AR+/ER+ CAMA-1 cells resulted in a significant increase in the surviving fraction of cells at 2Gy (SF-2Gy; **Figure 5-3A**). CAMA-1 cells treated with enzalutamide and RT had radiation enhancement ratios (rER) of 0.76-0.83 (**Figure 5-3A**). In comparison, well-characterized radiosensitization agents, like cisplatin, provide rER of 1.2 (32,33), while drugs used for radioprotection, like amifostine, have rER of 0.8 (34). In additional models, compared to treatment with DMSO, 0.5-2.5  $\mu$ M enzalutamide had little effect on radiosensitivity of ZR-75-1 cells (rER: 0.94-1.00, **Figure 5-3B**) or BT-474 cells (rER: 0.92-1.01, **Figure 5-3C**) with no change in SF-2Gy in either cell line. MCF-7 cells with high ER expression but low AR expression (AR-/ER+) were also treated with 0.5-2.0  $\mu$ M enzalutamide as a control. Enzalutamide had no effect on radiosensitivity of MCF-7 cells (rER: 0.95-1.05) with no change in SF-2Gy with treatment (**Figure 5-3D**). Therefore, enzalutamide treatment, at best, appears to have little effect on radiosensitivity of AR+/ER+ breast cancer cells, and at worst, enzalutamide may protect AR+/ER+ cells from RT-induced cell death.

To assess the effect of variable drug pretreatment time on cell survival, AR+/ER+ CAMA-1 cells were treated with enzalutamide (0.5-2.0  $\mu$ M) at 6 and 24 hours prior to RT, in

contrast to the one-hour pretreatment used in **Figure 5-3A-D**. Increased pretreatment time had no effect on the observed radiosensitization with rER of 0.92-0.95 for 6-hour enzalutamide pretreatment (**Figure 5-3E**) and rER of 1.05-1.10 when cells were pretreated for 24-hours prior to RT (**Figure 5-3F**). These data suggest that the longer pretreatment times are similarly insufficient at inducing radiosensitization in AR+/ER+ breast cancer cells, and prolonged AR inhibition does not affect radiosensitivity despite its known role in inducing G1 cell cycle arrest (35,36).

Next to further assess radiosensitivity using additional pharmacologic AR inhibitors, clonogenic survival assays were performed with apalutamide, darolutamide, or seviteronel. While apalutamide and darolutamide are both second-generation AR antagonists, apalutamide is structurally similar to enzalutamide. In contrast, darolutamide is structurally unique compared to enzalutamide and apalutamide and has less blood-brain barrier penetration, offering a unique clinical application as serum testosterone levels are not altered in CRPC patients with darolutamide treatment (13,37). Seviteronel, a dual CYP17 lyase and AR inhibitor with some antagonist activity against ER (38), has been shown to be effective in AR+ TNBC models (39). Similarly, use of apalutamide is effective as a radiosensitization strategy in AR+/ER- ACC-422 cells (rER: 1.08-1.33, **Figure 5-1B**). Using a one-hour pretreatment with apalutamide, darolutamide, or seviteronel, we further assessed radiosensitization in AR+/ER+ breast cancer cells. CAMA-1 cells had no change in radiosensitivity with 0.5-2.0  $\mu$ M apalutamide (rER: 0.95-1.01, **Figure 5-4A**), or 0.5-2.0  $\mu$ M darolutamide (rER: 0.92-0.93, **Figure 5-4E**). Similarly, ZR-75-1 cells treated with 0.5-2.0  $\mu$ M apalutamide (rER: 0.93-1.04, **Figure 5-4B**), 0.5-2.0  $\mu$ M darolutamide (rER: 0.92-1.1, **Figure 5-4F**), or 0.5-2.5  $\mu$ M seviteronel (rER: 0.97-1.08, **Figure 5-4I**) had no change in radiosensitization or SF 2Gy. BT-474 cells also had no change in

radiosensitization with 0.5-2.0  $\mu$ M apalutamide (rER: 0.96-0.98, **Figure 5-4C**), 0.5-2.0  $\mu$ M darolutamide (rER: 0.94-0.97, **Figure 5-4G**), or 0.5-2.5  $\mu$ M seviteronel (rER: 0.90-0.98, **Figure 5-4J**), further suggesting that though these inhibitors have structural and potential functional differences, each is insufficient under these conditions to induce radiosensitization of AR+/ER+ breast cancer cell lines *in vitro*.

As a control, clonogenic survival assays were also performed in AR-/ER+ MCF-7 cells, where treatment with 0.5-2.0  $\mu$ M apalutamide (rER: 0.85-0.98, **Figure 5-4D**), or 0.5-2.0  $\mu$ M darolutamide (rER: 1.02-1.10, **Figure 5-4H**) did not alter radiosensitization. In contrast to findings in AR+ TNBC (8), together these results suggest that one-hour pretreatment of apalutamide, or darolutamide, like enzalutamide, does not result in radiosensitization of AR+/ER+ breast cancer cells *in vitro*. Further, our results suggest that methods of targeting AR signaling using pharmacologic AR antagonists and/or blocking androgen production with CYP17 inhibitors are insufficient to alter the radiation response *in vitro* in AR+/ER+ breast cancer models.

#### ***5.4.3 PROTAC-mediated AR degradation in AR+/ER+ breast cancer cells***

Multiple studies have demonstrated that pharmacologic inhibition has different effects compared to protein depletion through genetic knockdown or use of pharmacologic degraders (40,41). Having observed no change in radiosensitization with pharmacologic inhibition of AR, we used a novel proteolysis targeting chimera (PROTAC) AR degrader, ARD-61, to assess radiosensitization (42,43). ARD-61 was effective at inhibiting cell viability in CAMA-1 cells with an IC<sub>50</sub> of 575 nM (**Figure 5-5A**). The kinetics of AR degradation in CAMA-1 cells was assessed by western blot and optimal degradation was found to occur from 12-36 hours post-ARD-61 treatment where  $\geq 90\%$  of AR protein is degraded with 250 nM treatment of ARD-61



(**Figure 5-5B**). Next, clonogenic survival assays were performed with 25-250 nM ARD-61 in AR+/ER+ breast cancer cells. 24-hour pretreatment with ARD-61 was used to achieve maximal AR degradation prior to RT. ARD-61-mediated AR degradation did not change radiosensitization of CAMA-1 cells with rER of 0.98-1.08 and no change in SF-2Gy (**Figure 5-5C**), suggesting that pharmacologic degradation of AR has a similar lack of effect on radiosensitization compared to pharmacologic inhibition in AR+/ER+ CAMA-1 cells.

#### ***5.4.4 Dual inhibition of AR and ER together does not radiosensitize AR+/ER+ cell lines***

Next, to understand whether there were overlapping roles for AR and ER in AR+/ER+ breast cancer models, clonogenic survival assays were performed with the selective estrogen receptor modulator (SERM), tamoxifen, or the selective estrogen receptor degrader (SERD), fulvestrant. While previous work has demonstrated a role for tamoxifen or fulvestrant in the radiosensitization of ER+ breast cancer models *in vitro* and *in vivo* (22), the role of AR and ER together and the impact on radiosensitization has not been assessed. ER inhibition with 0.5-2.0  $\mu$ M tamoxifen treatment alone in CAMA-1 cells resulted in only slight increases in radiosensitization with rER of 1.04-1.12 (**Figure 5-6A**). In ZR-75-1 cells, 0.5-2.0  $\mu$ M tamoxifen treatment resulted in slight radioprotection with rER of 0.79-0.91 (**Figure 5-6B**). These results suggest that inhibition of ER with tamoxifen was insufficient to alter radiosensitivity in AR+/ER+ breast cancer models *in vitro*. CAMA-1 cells were also pretreated with 1-10 nM fulvestrant for one hour before RT. Fulvestrant, unlike tamoxifen, did radiosensitize CAMA-1 (rER: 1.6-2.0, **Figure 5-6C**) and BT-474 (1-100 nM, rER: 1.06-1.50, **Figure 5-6D**) cells but not AR+/ER+ ZR-75-1 cells (1-10 nM, rER: 0.99-1.11, **Figure 5-6E**) or AR+/ER- ACC-422 cells (1-25 nM, rER: 1.03-1.17, **Figure 5-6F**). These data indicate that ER degradation with short-

term fulvestrant may be sufficient to sensitize select AR+/ER+ cell lines to ionizing radiation but is not sufficient to radiosensitize all AR+ breast cancer cell lines.

We next wanted to understand whether AR and ER may have an overlapping function allowing the hormone receptors to compensate in response to radiation treatment. To investigate this, clonogenic survival assays were performed in CAMA-1, ZR-75-1, and BT-474 cells pretreated for one-hour with 2.0  $\mu$ M tamoxifen and/or 2.0  $\mu$ M enzalutamide prior to RT. There was no significant change in radiosensitization in cells treated with tamoxifen alone (rER: 0.90-1.21), enzalutamide alone (rER: 0.89-1.00), or the combination of tamoxifen and enzalutamide (rER: 0.95-1.14, **Figure 5-6G-I**). These data suggest that short-term pretreatment with both ER and AR inhibitors is not sufficient to block a potential compensatory mechanism between AR and ER in response to ionizing radiation.

To determine whether extended pretreatment of AR+/ER+ cells with tamoxifen and/or enzalutamide treatment resulted in changes in radiosensitivity, cells were treated with drug once daily for seven days prior to RT. While ZR-75-1 cells had little change in radiosensitization with this extended pretreatment (rER with tamoxifen:  $1.00 \pm 0.24$ , rER with enzalutamide:  $1.16 \pm 0.3$ , rER with tamoxifen and enzalutamide:  $1.10 \pm 0.07$ , **Figure 5-7A**), CAMA-1 cells showed slight radiosensitization with tamoxifen alone (rER:  $1.26 \pm 0.11$ ) as well as with the combination treatment (rER:  $1.18 \pm 0.03$ , **Figure 5-7B**). There was also a decrease in the SF-2Gy of CAMA-1 cells with this extended duration of treatment prior to RT. This effect could be due to epigenetic changes that take place over the prolonged exposure to tamoxifen (44). Together these results suggest that antagonizing both AR and ER together is insufficient to radiosensitize AR+/ER+ breast cancer cells *in vitro* further suggesting that while AR and ER may have overlapping

functions, the receptors may not be working together to mediate radioresistance in models of breast cancer where they are co-expressed.

#### **5.4.5 *AR* knockout in combination with *ER* antagonists does not radiosensitize *AR*+/*ER*+ cells**

Having observed no radiosensitization when AR and ER were pharmacologically inhibited, we next tested whether genomic deletion of *AR* using CRISPR-Cas9 conferred radiosensitization. These experiments were used to further investigate the overlapping roles of AR and ER in these models. Isogenic cell line models with *AR* knockout (AR KO) or Cas9 control cells containing the Cas9 protein and a control guide (*AAVSI*) were generated in CAMA-1 or ZR-75-1 (**Figure 5-8A**) cells which endogenously express both AR and ER. Clonogenic survival assays were then performed using CAMA-1 and ZR-75-1 AR KO or Cas9 cells. To investigate whether ER antagonism was sufficient to radiosensitize CAMA-1 cells with genetic AR KO, CAMA-1 AR KO and Cas9 control cells were treated with tamoxifen or fulvestrant. In support of results observed with pharmacologic inhibition of AR in these cell lines, there was no change in radiosensitization in CAMA-1 Cas9 control cells compared to AR KO cells (**Figure 5-8B**). Treatment of Cas9 control cells with 2.0  $\mu$ M tamoxifen, however, provided slight radiosensitization (rER:  $1.21 \pm 0.24$ ). As observed in CAMA-1 parental cells, treatment of Cas9 control cells with 10 nM fulvestrant increased radiosensitivity (rER:  $2.1 \pm 0.5$ ). In CAMA-1 AR KO cells, however, there were similar levels of radiosensitization with tamoxifen (rER:  $1.00 \pm 0.2$ ) and fulvestrant (rER:  $1.8 \pm 0.3$ , **Figure 5-8B**) when compared to Cas9 control cells under similar treatment conditions. These results suggest that the presence or absence of AR in combination with treatment of tamoxifen or fulvestrant does not alter the observed radiosensitization. Radiosensitization of AR KO cells with ER antagonists was similar to observed radiosensitization in Cas9 cells further suggesting that genetic knockout of AR in

combination with ER inhibition was not sufficient to sensitize AR+/ER+ cells to ionizing radiation. There is no radiosensitization synergy observed between tamoxifen or fulvestrant treatment in CAMA-1 AR KO cells compared to Cas9 control.

Similar results were observed in ZR-75-1 AR KO or Cas9 control cells treated with tamoxifen or fulvestrant. In ZR-75-1 Cas9 control cells, no significant effects were observed as a result of treatment with 0.5-2.0  $\mu$ M tamoxifen (rER: 0.84-0.98, **Figure 5-8C**). This result was mirrored in ZR-75-1 AR KO cells with tamoxifen treatment (rER: 0.92-0.97, **Figure 5-8D**). Similar to results seen in ZR-75-1 parental cells, treating ZR-75-1 Cas9 control cells with fulvestrant did not result in significant radiosensitization with enhancement ratios of 1.02-1.10 (**Figure 5-8E**). In the same way, ZR-75-1 AR KO cells had enhancement ratios of 1.09-1.19 with 1-10 nM fulvestrant (**Figure 5-8F**). Together these results suggest that genetic knockout of AR protein in combination with ER inhibition or degradation is insufficient to radiosensitize AR+/ER+ CAMA-1 or ZR-75-1 cells, although there are cell specific differences in radiosensitization with tamoxifen or fulvestrant, respectively. Although AR inhibition in TNBC is radiosensitizing (7,8), as is ER inhibition in ER+ breast cancers with low AR expression (22), these findings further suggest that AR and ER signaling are not converging on a single pathway affecting the radiation response when AR and ER are co-expressed in models of breast cancer, or that there may be additional factors involved in the radiation response in AR+/ER+ breast cancer models.

## 5.5 Discussion

While previous studies have demonstrated that AR inhibitors can radiosensitize AR+ models of TNBC, prostate cancer, and glioblastoma (7,8,16,25,27,45,46), in this study we demonstrate that pharmacologic inhibition, degradation, or genetic knockout of AR using

CRISPR-Cas9, is not sufficient to radiosensitize AR+/ER+ breast cancer cell lines *in vitro* (**Figure 5-3, Figure 5-4, Figure 5-5, Figure 5-8**). While effective in ER+ MCF-7 and T47D cells (22), one-hour pretreatment with the ER inhibitors tamoxifen or fulvestrant results in minimal radiosensitization of AR+/ER+ cell lines (**Figure 5-6**). Further, the combination treatment of AR and ER inhibition via tamoxifen with enzalutamide is not sufficient to radiosensitize AR+/ER+ cells *in vitro* (**Figure 5-6, Figure 5-7**). Knockout of *AR* using CRISPR-Cas9 does not affect cell radiosensitivity relative to Cas9 control cells, and the addition of tamoxifen did not provide synergistic radiosensitization effects in CAMA-1 or ZR-75-1 cells (**Figure 5-8**). Conversely, treatment with fulvestrant, a selective estrogen receptor degrader (SERD) with some ability to degrade AR protein (47), was sufficient to radiosensitize CAMA-1 parental or Cas9 control cells; however, similar levels of radiosensitization were observed in CAMA-1 AR KO cells with fulvestrant treatment suggesting there is no additional synergistic effect of AR KO in combination with ER inhibition or degradation (**Figure 5-8**). Together these findings suggest that AR inhibition alone is not sufficient to radiosensitize AR+/ER+ breast cancer models. In addition, combined abrogation of AR and ER pharmacologically or through gene editing does not provide radiosensitization suggesting that AR and ER are not directly compensating in the radiation response.

Our findings here suggest an independent role for AR in AR+/ER+ breast cancer models in response to radiation compared to the previously established role for AR in the radiation response in AR+/ER- (TNBC) models and other AR+ cancers (15). In AR+/ER- breast cancer, AR is a biomarker of radioresistance and inhibition or knockout of AR results in radiosensitization, partially through the inhibition of a non-homologous end joining (NHEJ) repair-mediated response (7,8). Here, we demonstrate that in the presence of ER, AR may not be

functioning as a mediator of radioresistance, suggesting that AR inhibition is not an effective radiosensitization strategy in women with tumors expressing high levels of AR and ER. This is in contrast with previous work suggesting that AR inhibition, independent of ER status, results in radiosensitization in AR+ breast cancer models (16). This conflict may also be due to differences in treatment conditions and timing of treatment. For example, it should be noted that other studies used proliferation assays instead of clonogenic survival assays to assess radiation response, and much higher doses of enzalutamide (10-fold higher) and radiation (10 Gy) were used in these studies which may explain these differences in findings.

Further, our data indicate that anti-androgen or anti-estrogen therapies may be effective radiosensitization strategies in some, but not all AR+/ER+ breast tumors, suggesting a need for additional biomarkers of response for AR and/or ER antagonists. While an AR:ER positivity ratio of 78% has been demonstrated to have prognostic capacity in AR+/ER+ tumors (48), a more complete understanding of how signaling of androgen and estrogen receptors, along with signaling of other receptors and growth factors, is influencing the radiation response is needed to effectively identify reliable biomarkers of response. Our work also suggests that the use of anti-estrogen therapies may be an effective radiosensitization strategy in some, but not all, ER+ breast cancer models (22). Notably, while our study employs multiple AR+/ER+ cell lines, these cell lines have different molecular characteristics, including levels of AR and ER protein expression and functional downstream signaling as assessed by RT-qPCR (**Figure 5-1, Figure 5-2**). These molecular differences may also contribute to the differences observed in response to pharmacologic AR and ER inhibitors in combination with RT. While in this study we demonstrate that AR expression may be influencing the efficacy of ER inhibitors in modulating radiosensitization in AR+/ER+ breast cancer cells, future studies are necessary to understand

why ER-targeting therapies may be effective for the radiosensitization in some preclinical ER+ breast cancer models but not others. This may be due to expression of additional biomarkers that can impact on radiosensitivity including HER2 and EGFR (49–52), PI3K/mTOR (53,54), and PARP (55–57), among others. While preclinical studies are useful to start interrogating these questions using models that have been studied extensively, translation of these findings into the clinic brings additional variabilities including, but not limited to, individual patient characteristics, adherence to treatment, as well as other concurrent therapies. Therefore, biomarkers of response are also needed to understand how AR agonists and antagonists might be used in different patient populations in diverse biological contexts to increase tumor control.

Despite these findings, there are also a few limitations to the current study that are worth noting. These studies use tamoxifen instead of 4-hydroxytamoxifen (4-OHT), which is an active metabolite of tamoxifen, and 100x more potent than tamoxifen (58). As tamoxifen is a weaker anti-estrogen than 4-OHT and partial agonist of ER (59,60), the concentrations used may not be sufficient to induce radiosensitization in media containing FBS with supersaturated E2 levels. Future experiments will seek to expand these findings and investigate whether a more potent inhibitor like 4-OHT may be a more effective radiosensitization strategy in these tumors. Additionally, because all cell lines used in this study were cultured in media containing both phenol red and FBS, we cannot control for exogenous androgens and estrogens that exist within the media (61). While seviteronel is both a CYP17 and AR inhibitor, CYP17 is not commonly expressed in breast cancer cell lines, and the culture media used has supplemented cholesterol and steroid hormones, thus preventing cells from relying on CYP17 for androgen production. Together these limitations could also suggest that use of anti-androgens may be more effective when assessed in models containing more physiologically relevant levels of circulating

hormones. Future studies performed in xenograft models or using patient data from completed clinical trials should be performed to understand whether changes in estradiol and/or testosterone levels affect radiosensitivity with anti-androgen or anti-estrogen therapies. Finally, non-canonical ER functions including RNA binding (62) or non-genomic signaling (63) that may contribute to radiation response in the context of AR signaling cannot be excluded based on the data presented here and are also worth further exploration. Here we have investigated the role of AR and ER signaling using *in vitro* and immunocompromised models that eliminate any potential effects of the tumor microenvironment or immune infiltrates (64,65). Future studies may investigate these limitations by using immunocompetent *in vivo* models.

While AR-targeting therapies have become a mainstay for the treatment of prostate cancers, ongoing preclinical and clinical studies in AR+ tumors have demonstrated therapeutic potential for treatment of AR+ breast cancers using AR antagonists. In a phase II trial (NCT01889238), enzalutamide has been shown to provide clinical benefit to approximately 30% of AR+ TNBC patients (6). Additionally, a phase I trial is underway using darolutamide in breast cancer patients, including TNBC, HR+/HER2-, and HER2+ patients (NCT03004534). Recent data has also suggested that AR functions as a tumor suppressor in AR+/ER+ breast cancers (17), and ongoing trials are investigating the use of AR agonists (NCT01616758, NCT02463032). In addition, there are many ongoing clinical trials are investigating the concurrent use of anti-androgen and anti-estrogen therapies (including NCT02953860, NCT02955394, NCT02676986). The results from these trials will continue to shed light on the use of antagonists and agonists for the treatment of AR+ and/or ER+ breast tumors. Further, our work highlights the importance of understanding how AR and ER interact to influence tumorigenesis to appropriately direct clinical trial design and stratify patient populations most



effectively, as well as to inform the timing of radiation treatment in relation to AR inhibition as these studies suggest co-treatment may be tumor protective and thus undesirable.

## **5.6 Acknowledgements**

The authors thank Dr. Arul Chinnaiyan, Dr. Shaomeng Wang, and Dr. Steve Kregel for providing ARD-61. This work was supported a Breast Cancer Research Foundation (BCRF) Grant to L.J.P. (BCRF-21-128) and by a generous donation to C.W.S. by Susan and Richard Bayer. A.R.M. and A.M.P. are supported by National Institute of General Medical Sciences (NIGMS) training grants: T-32 GM113900 (A.R.M.), T32-GM007315 (A.R.M.), and T32-GM007767 (A.M.P.). A.R.M. is supported by the Rackham Predoctoral Fellowship Program and Rackham Graduate School Research Grants. A.M.P. is supported by a Ruth L. Kirschstein NRSA F31 award (F31CA254138).

## 5.7 Figures

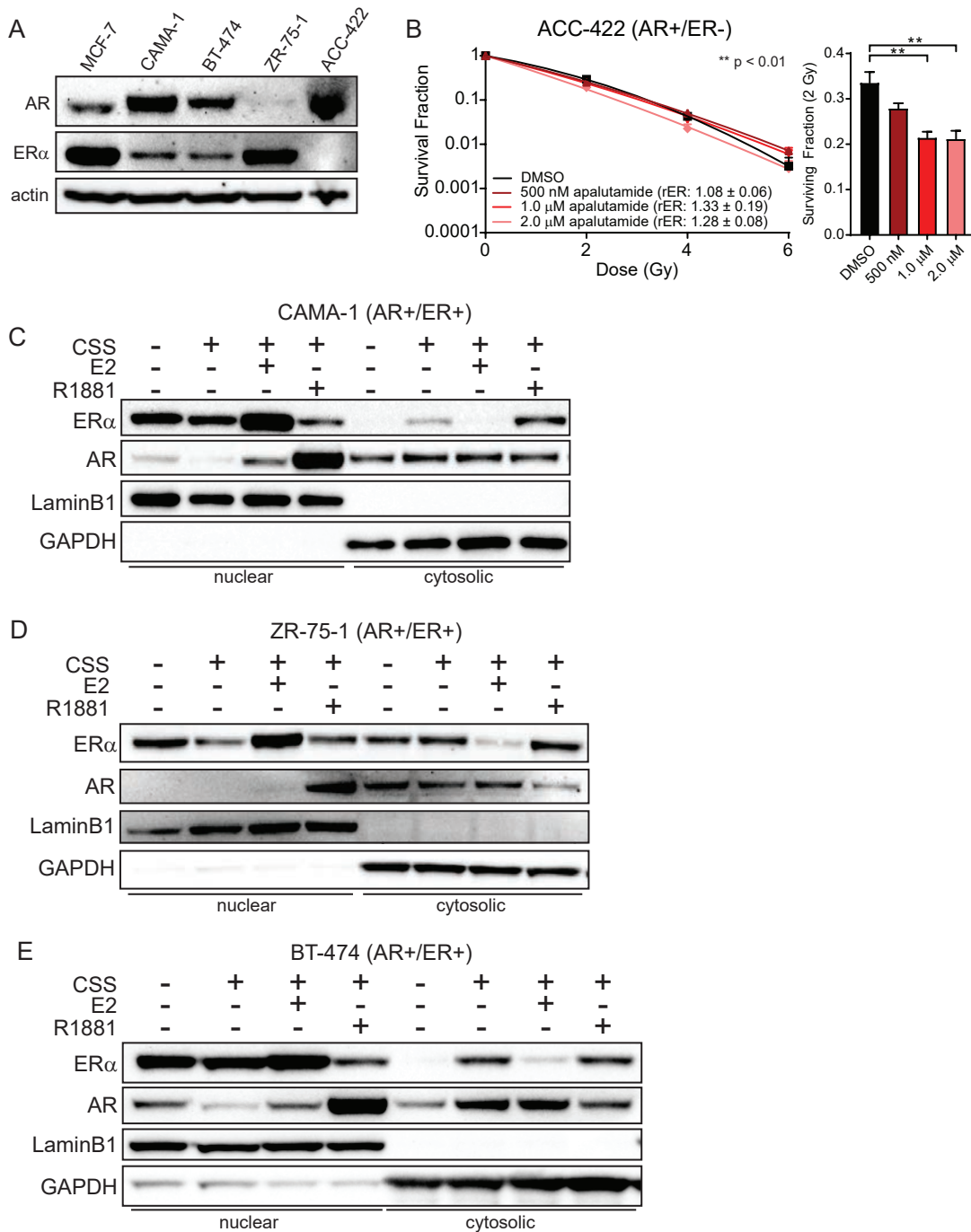


**Figure 5-1: Validation of AR function in AR+ breast cancer models**

Expression of AR and ER $\alpha$  was assessed by western blot (A) in a panel of breast cancer cell lines. Clonogenic survival assays were performed in (B) AR+/ER- ACC-422 cells treated with apalutamide for one hour prior to RT to assess radiosensitization. Western blots were performed in AR+/ER+ (C) CAMA-1, (D) ZR-75-1, and (E) BT-474 cells to assess cellular localization

(nucleus or cytosol) for AR or ER $\alpha$  following hormone depletion (CSS) or stimulation with 1 nM  $\beta$ -estradiol (E2) or R1881. A representative clonogenic survival assay is shown for the ACC-422 cells, and the SF-2Gy values are representative of three independent experiments (mean  $\pm$  SEM). Nuclear fractionation experiments were performed in duplicate or triplicate, and a representative blot is shown. \*\* p < 0.01

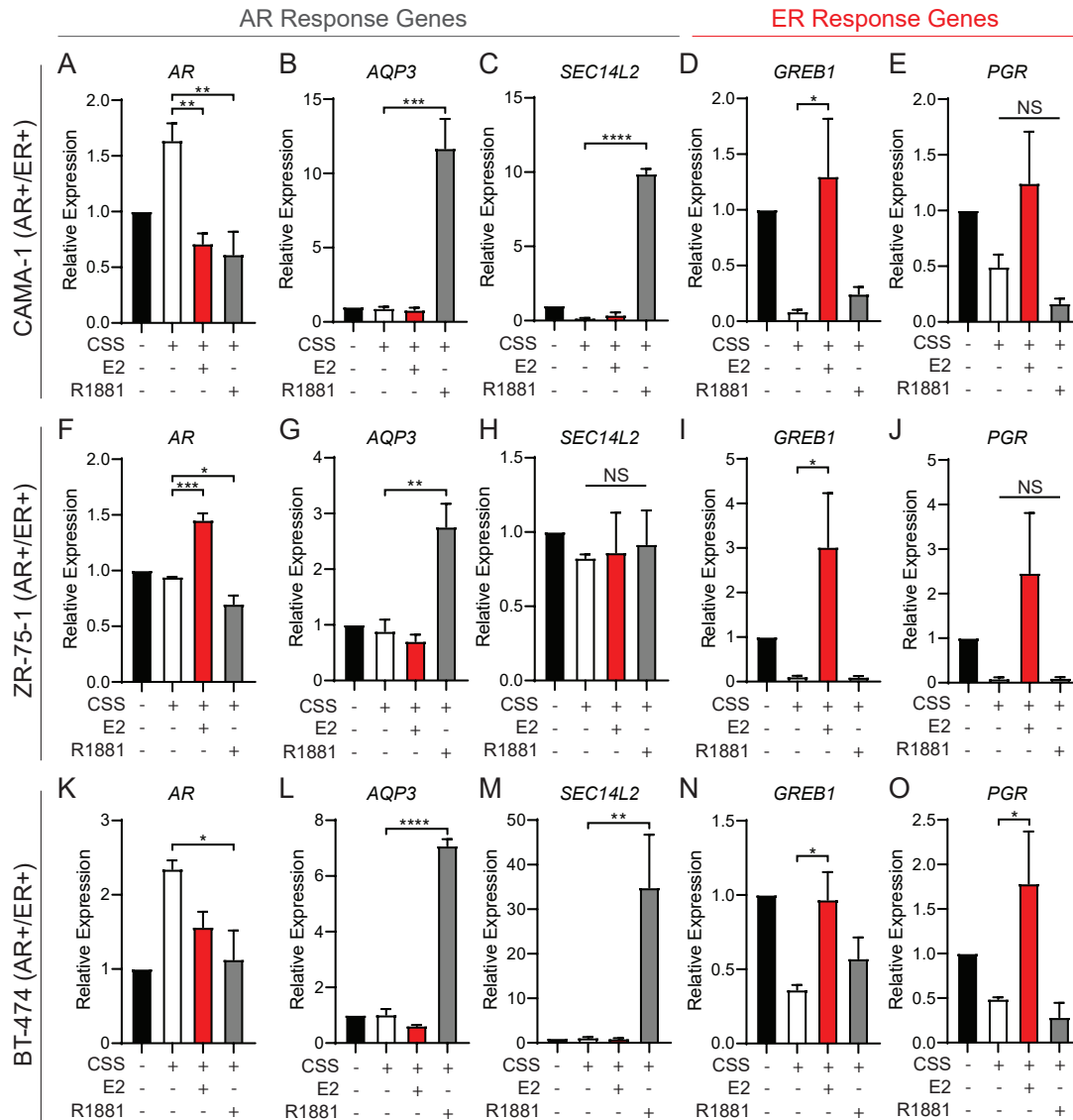


**Figure 5-2: Expression of AR and ER target genes was assessed in AR+/ER+ breast cancer cell lines**

qPCR experiments were performed to assess expression of AR target genes (*AR*, *AQP3*, *SEC14L2*) and ER target genes (*GREB1*, *PGR*) in AR+/ER+ (A-E) CAMA-1, (F-J) ZR-75-1, or (K-O) BT-474 cells grown in FBS or CSS, stimulated ± 1 nM β-estradiol or R1881. Data is shown as mean ± SEM for three independent experiments. \* p < 0.05; \*\* p < 0.01; \*\*\* p < 0.001; \*\*\*\* p < 0.0001; NS = not significant

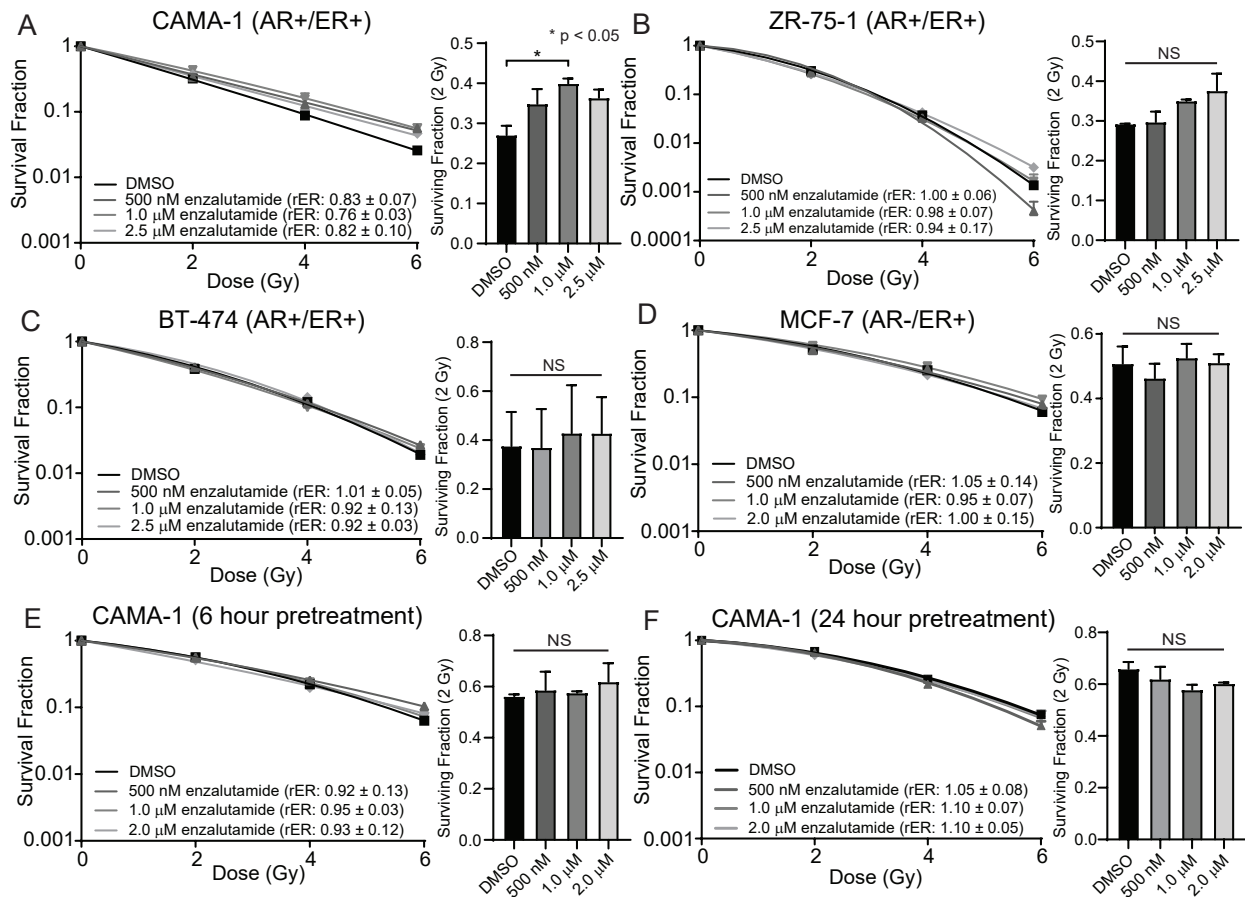


**Figure 5-3: AR inhibition with enzalutamide does not affect radiosensitivity of AR+/ER+ breast cancer cell lines in vitro**

Clonogenic survival assays were performed in AR+/ER+ (A) CAMA-1, (B) ZR-75-1, and (C) BT-474 cells to assess radiosensitization with a one-hour pretreatment of enzalutamide prior to radiation treatment. Assays were also performed in (D) MCF-7 cells which are ER+ with low AR expression. To assess the effects of a longer pretreatment with enzalutamide, clonogenic survival assays were performed in CAMA-1 cells with a (E) 6-hour or (F) 24-hour pretreatment with enzalutamide prior to radiation treatment. Representative clonogenic survival assays are shown for each cell line, and the surviving fraction of cells at 2 Gy (SF-2Gy) are representative of three independent experiments (mean  $\pm$  SEM). \*  $p < 0.05$ ; NS = not significant

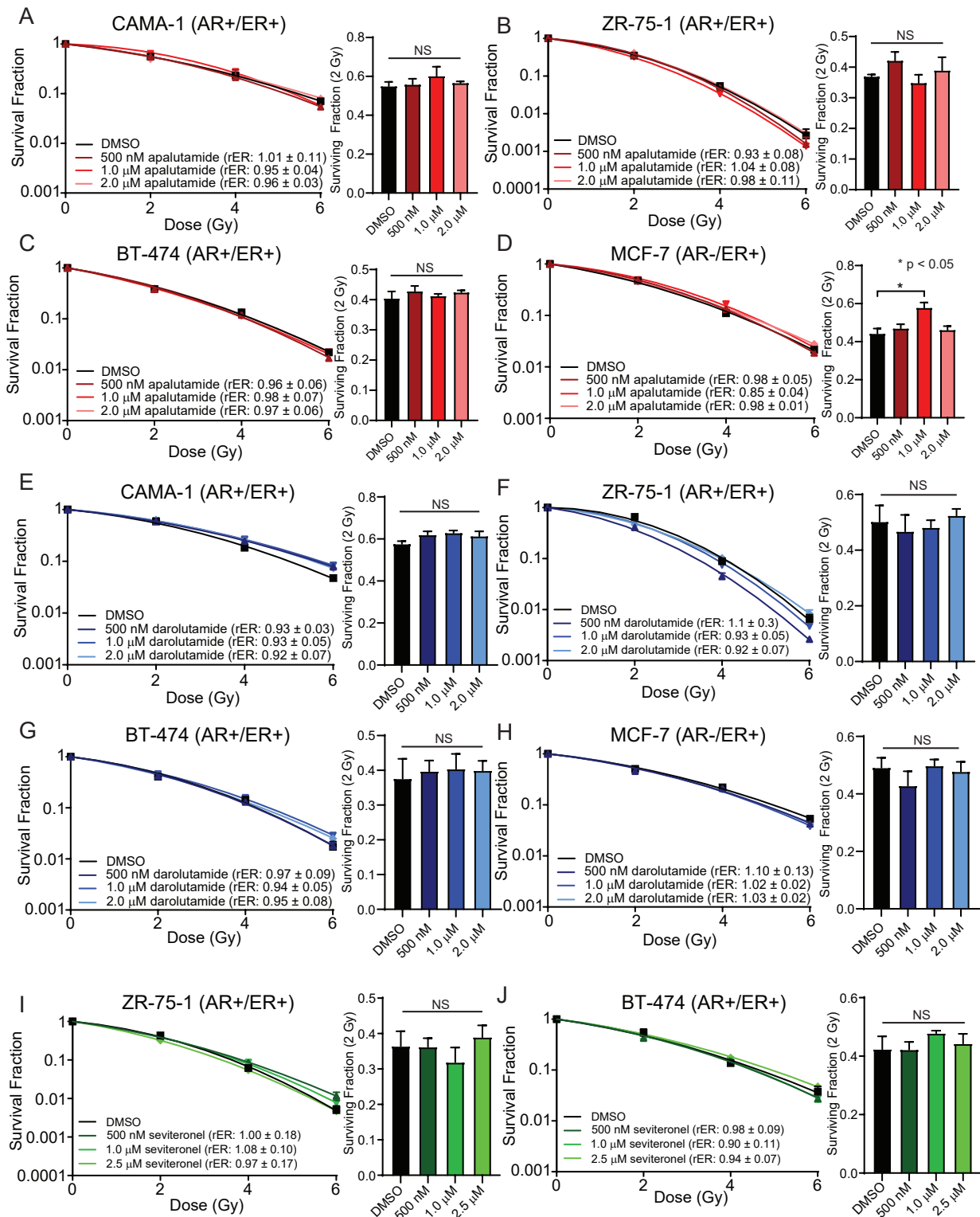


**Figure 5-4: Inhibition with apalutamide, darolutamide, or seviteronel does not affect radiosensitivity of AR+/ER+ breast cancer cell lines *in vitro***

Clonogenic survival assays were performed in AR+/ER+ (A) CAMA-1, (B) ZR-75-1, and (C) BT-474 cells to assess radiosensitization with a one-hour pretreatment of apalutamide prior to

radiation treatment. Assays were also performed in ER+ (**D**) MCF-7 cells with low AR expression. Similarly, clonogenic survival assays were performed in AR+/ER+ (**E**) CAMA-1, (**F**) ZR-75-1, and (**G**) BT-474 cells to assess radiosensitization with a one-hour pretreatment of darolutamide prior to radiation treatment. Assays were also performed in (**H**) MCF-7 cells. Next, clonogenic survival assays were performed in (**I**) ZR-75-1 and (**J**) BT-474 cells treated with seviteronel for one-hour prior to RT. Representative clonogenic survival assays are shown for each cell line, and the SF-2Gy are representative of three independent experiments (mean  $\pm$  SEM). \*  $p < 0.05$ ; NS = not significant

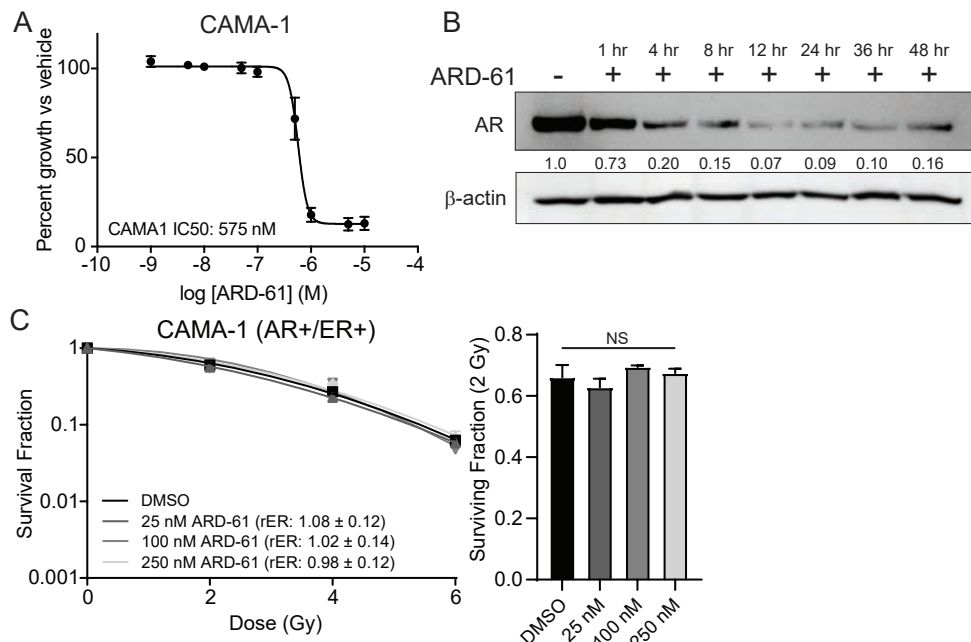


**Figure 5-5: AR degradation with ARD-61 decreases cell viability but does not sensitize CAMA-1 cells to ionizing radiation**

(A) Cellular viability of AR+/ER+ CAMA-1 cells was assessed at 72 hours with an IC<sub>50</sub> of 575 nM. (B) Degradation of AR protein levels was assessed by western blot after 1-48 hours treatment of ARD-61 with maximal degradation of AR occurring between 12-36 hours. (C) Radiosensitization of CAMA-1 cells with ARD-61 was assessed by clonogenic survival assay. Viability assays are the shown as the mean  $\pm$  SEM for three independent experiments. A representative western blot is shown with quantification of average AR protein from three independent experiments. A representative clonogenic survival assay is shown with the SF-2Gy from three independent experiments (mean  $\pm$  SEM). NS = not significant



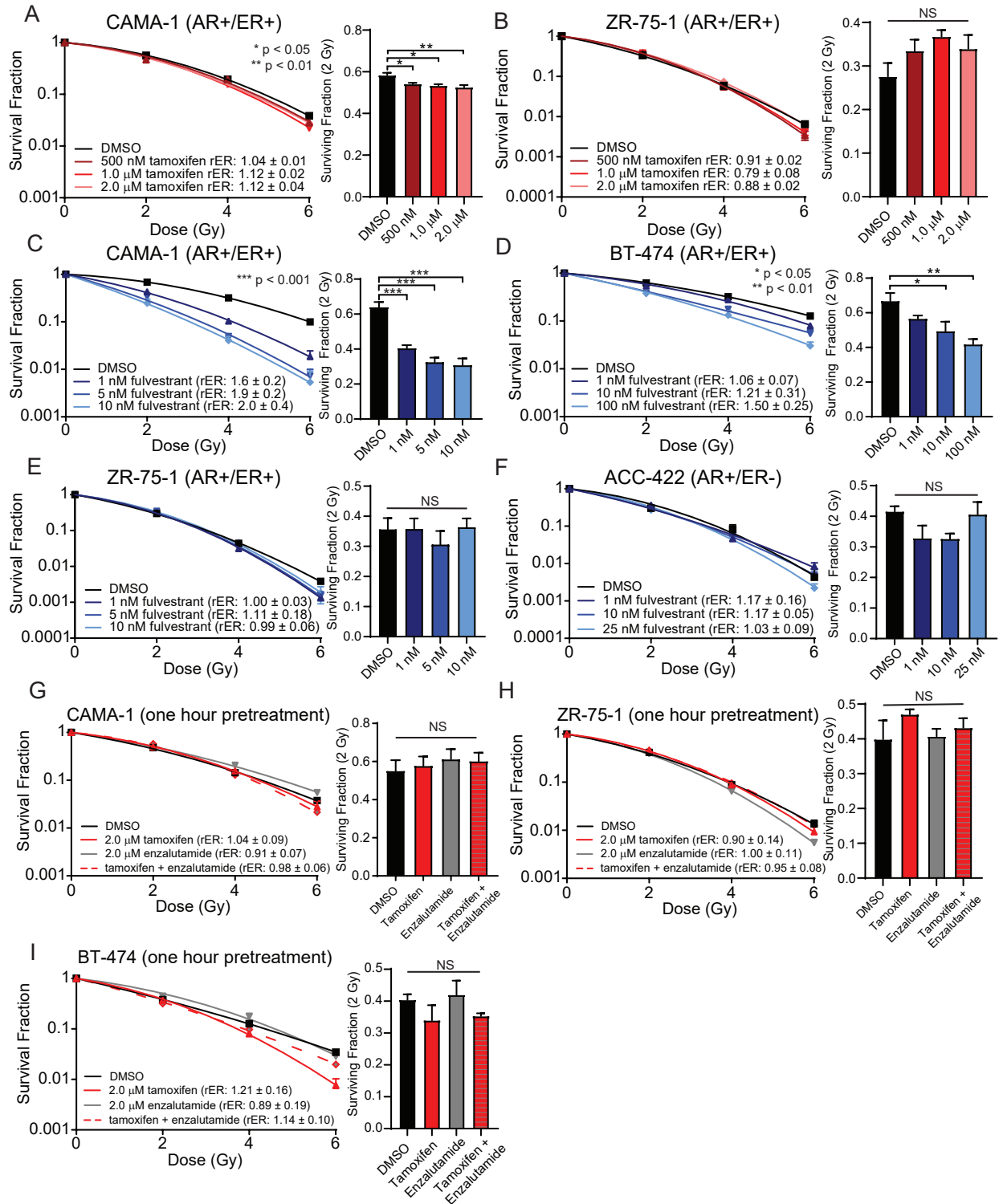


**Figure 5-6: ER inhibition ± AR inhibition with enzalutamide is not sufficient to radiosensitize AR+/ER+ breast cancer cells *in vitro***

Clonogenic survival assays were performed in (A) CAMA-1 or (B) ZR-75-1 cells with a one-hour pretreatment of tamoxifen prior to radiation treatment. Radiosensitization was assessed by

clonogenic survival assays in **(C)** CAMA-1, **(D)** BT-474, and **(E)** ZR-75-1 cells with treatment of fulvestrant, a known degrader of both ER and AR protein. Clonogenic survival assays were also performed in ACC-422 cells (AR+/ER-) with fulvestrant **(F)**. Additional clonogenic survival assays were performed in **(G)** CAMA-1, **(H)** ZR-75-1, or **(I)** BT-474 cells with a one-hour pretreatment of enzalutamide, tamoxifen, or enzalutamide and tamoxifen. Representative clonogenic survival assays are shown for each cell line, and the SF-2Gy are representative of three independent experiments (mean  $\pm$  SEM). \*  $p < 0.05$ ; \*\*  $p < 0.01$ ; \*\*\*  $p < 0.001$ ; NS = not significant

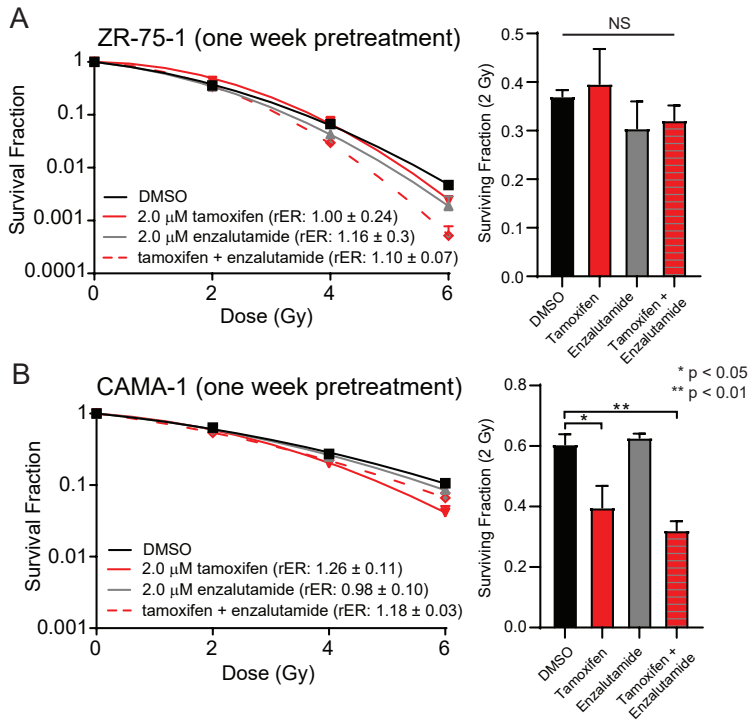


**Figure 5-7: Combined treatment of tamoxifen with enzalutamide does not radiosensitize AR+/ER+ breast cancer cell lines**

(A) Extended, one-week treatment with enzalutamide, tamoxifen, or enzalutamide and tamoxifen was delivered every 24 hours for 7 days prior to assessment of radiosensitization by clonogenic survival assays in (A) ZR-75-1 or (B) CAMA-1 cells. Representative clonogenic survival assays are shown for each cell line, and the SF-2Gy are representative of three independent experiments (mean  $\pm$  SEM). \*  $p < 0.05$ ; \*\*  $p < 0.01$ ; NS = not significant

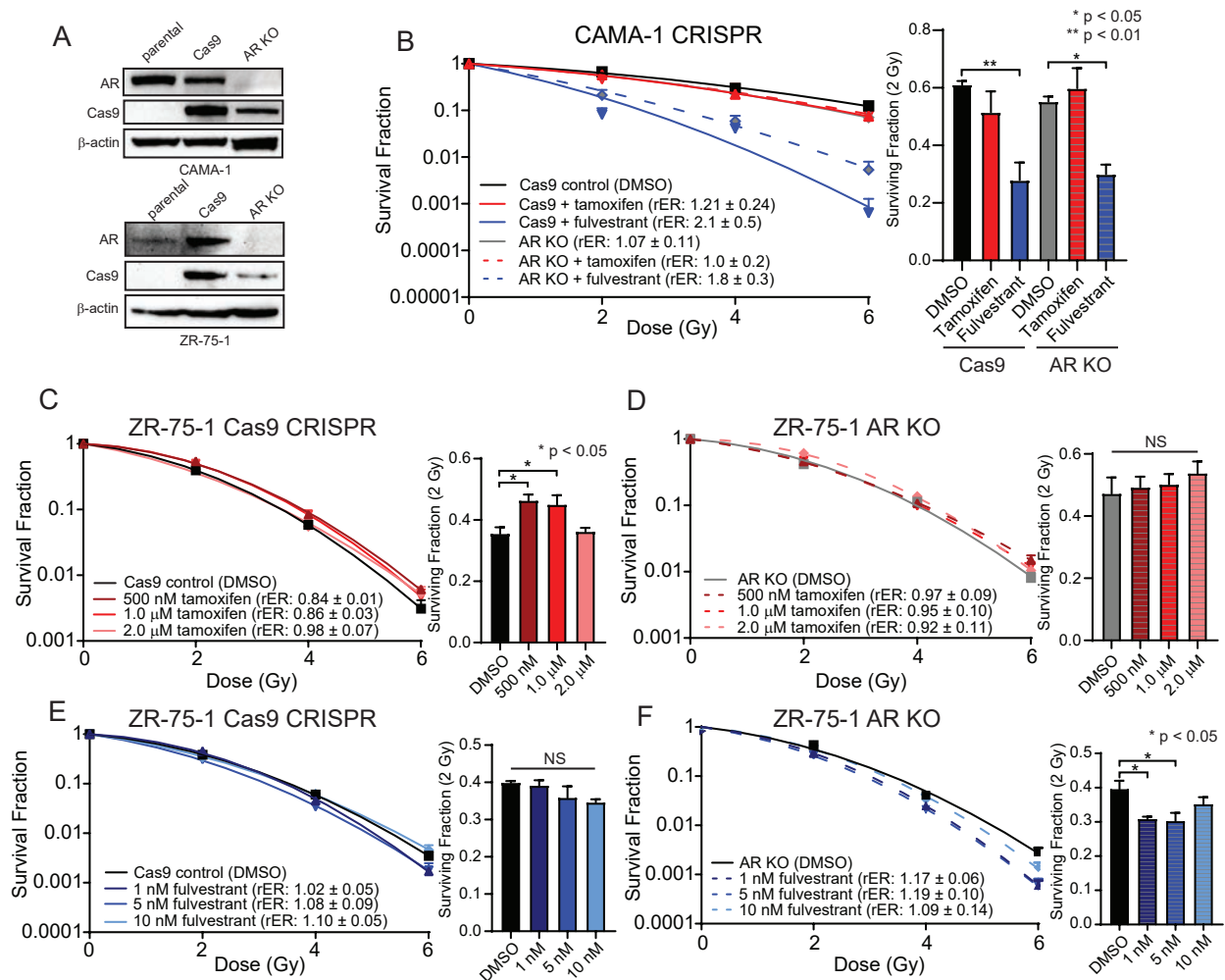


**Figure 5-8: Knockout of AR by CRISPR/Cas9 is not sufficient to provide radiosensitization to AR+/ER+ cells alone or in combination with ER inhibitors**

CRISPR/Cas9 mediated knockout of *AR* was confirmed by western blot (A) in CAMA-1 and ZR-75-1 cells. (B) Radiosensitization of CAMA-1 AR KO or Cas9 control cells was assessed by clonogenic survival assay alone or in combination with tamoxifen or fulvestrant treatment. Radiosensitization of ZR-75-1 (C) Cas9 control cells or (D) AR KO cells with tamoxifen was assessed by clonogenic survival assay. Similarly, radiosensitization with fulvestrant was assessed in ZR-75-1 (E) Cas9 control or (F) AR KO cells. Representative clonogenic survival assays are shown for each cell line, and the SF-2Gy are representative of three independent experiments (mean  $\pm$  SEM). \*  $p < 0.05$ , \*\*  $p < 0.01$ ; NS = not significant

## 5.8 References

1. Siegel RL, Miller KD, Jemal A. Cancer statistics, 2019. *CA Cancer J Clin*. 2019;69(1):7–34.
2. Howlader N, Altekruse SF, Li CI, Chen VW, Clarke CA, Ries LAG, et al. US Incidence of Breast Cancer Subtypes Defined by Joint Hormone Receptor and HER2 Status. *JNCI J Natl Cancer Inst*. 2014 Apr 28;106(5):dju055.
3. Proverbs-Singh T, Feldman JL, Morris MJ, Autio KA, Traina TA. Targeting the androgen receptor in prostate and breast cancer: several new agents in development. *Endocr Relat Cancer*. 2015 Jun;22(3):R87–106.
4. Niemeier LA, Dabbs DJ, Beriwal S, Striebel JM, Bhargava R. Androgen receptor in breast cancer: expression in estrogen receptor-positive tumors and in estrogen receptor-negative tumors with apocrine differentiation. *Mod Pathol*. 2010 Feb;23(2):205–12.
5. Gerratana L, Basile D, Buono G, De Placido S, Giuliano M, Minichillo S, et al. Androgen receptor in triple negative breast cancer: A potential target for the targetless subtype. *Cancer Treat Rev*. 2018 Jul 1;68:102–10.
6. Traina TA, Miller K, Yardley DA, Eakle J, Schwartzberg LS, O’Shaughnessy J, et al. Enzalutamide for the Treatment of Androgen Receptor-Expressing Triple-Negative Breast Cancer. *J Clin Oncol Off J Am Soc Clin Oncol*. 2018 20;36(9):884–90.
7. Michmerhuizen AR, Chandler B, Olsen E, Wilder-Romans K, Moubadder L, Liu M, et al. Seviteronel, a Novel CYP17 Lyase Inhibitor and Androgen Receptor Antagonist, Radiosensitizes AR-Positive Triple Negative Breast Cancer Cells. *Front Endocrinol [Internet]*. 2020 [cited 2020 Jan 17];11. Available from: <https://www.frontiersin.org/articles/10.3389/fendo.2020.00035/abstract>
8. Speers C, Zhao SG, Chandler B, Liu M, Wilder-Romans K, Olsen E, et al. Androgen receptor as a mediator and biomarker of radioresistance in triple-negative breast cancer. *Npj Breast Cancer*. 2017 Aug 18;3(1):29.
9. Fioretti FM, Sita-Lumsden A, Bevan CL, Brooke GN. Revising the role of the androgen receptor in breast cancer. *J Mol Endocrinol*. 2014 Jun;52(3):R257-265.
10. Karamouzis MV, Papavassiliou KA, Adamopoulos C, Papavassiliou AG. Targeting Androgen/Estrogen Receptors Crosstalk in Cancer. *Trends Cancer*. 2016 Jan 1;2(1):35–48.
11. Higano C. Enzalutamide, apalutamide, or darolutamide: are apples or bananas best for patients? *Nat Rev Urol*. 2019 Jun;16(6):335–6.
12. Clegg NJ, Wongvipat J, Joseph J, Tran C, Ouk S, Dilhas A, et al. ARN-509: a novel anti-androgen for prostate cancer treatment. *Cancer Res*. 2012 Mar 15;72(6):1494–503.
13. Moilanen AM, Riikonen R, Oksala R, Ravanti L, Aho E, Wohlfahrt G, et al. Discovery of ODM-201, a new-generation androgen receptor inhibitor targeting resistance mechanisms to androgen signaling-directed prostate cancer therapies. *Sci Rep*. 2015 Jul 3;5:12007.

14. Tran C, Ouk S, Clegg NJ, Chen Y, Watson PA, Arora V, et al. Development of a Second-Generation Antiandrogen for Treatment of Advanced Prostate Cancer. *Science*. 2009 May 8;324(5928):787–90.
15. Michmerhuizen AR, Spratt DE, Pierce LJ, Speers CW. ARE we there yet? Understanding androgen receptor signaling in breast cancer. *Npj Breast Cancer*. 2020 Sep 25;6(1):1–19.
16. Yard BD, Adams DJ, Chie EK, Tamayo P, Battaglia JS, Gopal P, et al. A genetic basis for the variation in the vulnerability of cancer to DNA damage. *Nat Commun*. 2016 Apr 25;7:11428.
17. Hickey TE, Selth LA, Chia KM, Laven-Law G, Milioli HH, Roden D, et al. The androgen receptor is a tumor suppressor in estrogen receptor–positive breast cancer. *Nat Med*. 2021 Feb;27(2):310–20.
18. Wazer DE, Tercilla OF, Lin PS, Schmidt-Ullrich R. Modulation in the radiosensitivity of MCF-7 human breast carcinoma cells by 17 $\beta$ -estradiol and tamoxifen. *Br J Radiol*. 1989 Dec 1;62(744):1079–83.
19. Azria D, Larbouret C, Cunat S, Ozsahin M, Gourgou S, Martineau P, et al. Letrozole sensitizes breast cancer cells to ionizing radiation. *Breast Cancer Res*. 2005;7(1):R156–63.
20. Villalobos M, Aranda M, Nunez MI, Becerra D, Olea N, Almodovar MR de, et al. Interaction Between Ionizing Radiation, Estrogens and Antiestrogens in the Modification of Tumor Microenvironment in Estrogen Dependent Multicellular Spheroids. *Acta Oncol*. 1995 Jan 1;34(3):413–7.
21. Wang J, Yang Q, Haffty BG, Li X, Moran MS. Fulvestrant radiosensitizes human estrogen receptor-positive breast cancer cells. *Biochem Biophys Res Commun*. 2013 Feb 8;431(2):146–51.
22. Michmerhuizen AR, Lerner LM, Pesch AM, Ward C, Schwartz R, Wilder-Romans K, et al. Estrogen receptor inhibition mediates radiosensitization of ER-positive breast cancer models. *Npj Breast Cancer*. 2022 Mar 10;8(1):1–12.
23. Spratt DE, Evans MJ, Davis BJ, Doran MG, Lee MX, Shah N, et al. Androgen Receptor Upregulation Mediates Radioresistance after Ionizing Radiation. *Cancer Res*. 2015 Nov 15;75(22):4688–96.
24. Polkinghorn WR, Parker JS, Lee MX, Kass EM, Spratt DE, Iaquinta PJ, et al. Androgen receptor signaling regulates DNA repair in prostate cancers. *Cancer Discov*. 2013 Nov;3(11):1245–53.
25. Kakouratos C, Kalamida D, Lamprou I, Xanthopoulou E, Nanos C, Giatromanolaki A, et al. Apalutamide radio-sensitisation of prostate cancer. *Br J Cancer*. 2021 Sep 1;1–11.
26. Sun H, Werner C, Dresser J, Wilder-Romans K, Baskin-Bey E, Eisner J, et al. Targeting androgen receptor signaling in glioblastoma (GBM) using seviteronel (sevi), a CYP17 lyase and androgen receptor inhibitor, alone and in combination with radiation (RT). *Neuro-Oncol*. 2018 Nov 5;20(suppl\_6):vi88–vi88.

27. Werner CK, Nna UJ, Sun H, Wilder-Romans K, Dresser J, Kothari AU, et al. Expression of the Androgen Receptor Governs Radiation Resistance in a Subset of Glioblastomas Vulnerable to Antiandrogen Therapy. *Mol Cancer Ther*. 2020 Oct 1;19(10):2163–74.
28. Pesch AM, Hirsh NH, Michmerhuizen AR, Jungles KM, Wilder-Romans K, Chandler BC, et al. RB expression confers sensitivity to CDK4/6 inhibitor–mediated radiosensitization across breast cancer subtypes. *JCI Insight* [Internet]. 2022 Feb 8 [cited 2022 Mar 29];7(3). Available from: <https://insight.jci.org/articles/view/154402>
29. Speers C, Zhao SG, Kothari V, Santola A, Liu M, Wilder-Romans K, et al. Maternal Embryonic Leucine Zipper Kinase (MELK) as a Novel Mediator and Biomarker of Radioresistance in Human Breast Cancer. *Clin Cancer Res*. 2016 Dec 1;22(23):5864–75.
30. Chandler BC, Moubadder L, Ritter CL, Liu M, Cameron M, Wilder-Romans K, et al. TTK inhibition radiosensitizes basal-like breast cancer through impaired homologous recombination. *J Clin Invest*. 2020 Feb 3;130(2):958–73.
31. Pesch AM, Hirsh NH, Chandler BC, Michmerhuizen AR, Ritter CL, Androsiglio MP, et al. Short-term CDK4/6 Inhibition Radiosensitizes Estrogen Receptor–Positive Breast Cancers. *Clin Cancer Res*. 2020 Sep 23;26(24):6568–80.
32. Skov K, Macphail S. Interaction of platinum drugs with clinically relevant X-ray doses in mammalian cells: A comparison of cisplatin, carboplatin, iproplatin, and tetraplatin. *Int J Radiat Oncol*. 1991 Feb 1;20(2):221–5.
33. Zhang X, Yang H, Gu K, Chen J, Rui M, Jiang GL. In vitro and in vivo study of a nanoliposomal cisplatin as a radiosensitizer [Internet]. *International Journal of Nanomedicine*. 2011 [cited 2018 Oct 24]. Available from: <https://www.dovepress.com/in-vitro-and-in-vivo-study-of-a-nanoliposomal-cisplatin-as-a-radiosens-peer-reviewed-article-IJN>
34. Koukourakis MI. Amifostine: is there evidence of tumor protection? *Semin Oncol*. 2003 Dec 1;30:18–30.
35. Balk SP, Knudsen KE. AR, the cell cycle, and prostate cancer. *Nucl Recept Signal* [Internet]. 2008 Feb 1;6. Available from: <https://www.ncbi.nlm.nih.gov/pmc/articles/PMC2254330/>
36. Knudsen KE, Arden KC, Cavenee WK. Multiple G1 Regulatory Elements Control the Androgen-dependent Proliferation of Prostatic Carcinoma Cells. *J Biol Chem*. 1998 Aug 7;273(32):20213–22.
37. Fizazi K, Massard C, Bono P, Jones R, Kataja V, James N, et al. Activity and safety of ODM-201 in patients with progressive metastatic castration-resistant prostate cancer (ARADES): an open-label phase 1 dose-escalation and randomised phase 2 dose expansion trial. *Lancet Oncol*. 2014 Aug 1;15(9):975–85.
38. Toren PJ, Kim S, Pham S, Mangalji A, Adomat H, Guns EST, et al. Anticancer Activity of a Novel Selective CYP17A1 Inhibitor in Preclinical Models of Castrate-Resistant Prostate Cancer. *Mol Cancer Ther*. 2015 Jan 1;14(1):59–69.
39. Christenson JL, O’Neill KI, Williams MM, Spoelstra NS, Jones KL, Trahan GD, et al. Activity of Combined Androgen Receptor Antagonism and Cell Cycle Inhibition in

- Androgen Receptor Positive Triple Negative Breast Cancer. *Mol Cancer Ther.* 2021 Jun 1;20(6):1062–71.
40. Chia K, Milioli H, Portman N, Laven-Law G, Coulson R, Yong A, et al. Non-canonical AR activity facilitates endocrine resistance in breast cancer. *Endocr Relat Cancer.* 2019 Feb 1;26(2):251–64.
  41. Shibata N, Shimokawa K, Nagai K, Ohoka N, Hattori T, Miyamoto N, et al. Pharmacological difference between degrader and inhibitor against oncogenic BCR-ABL kinase. *Sci Rep.* 2018 Sep 10;8(1):13549.
  42. Kregel S, Wang C, Han X, Xiao L, Fernandez-Salas E, Bawa P, et al. Androgen receptor degraders overcome common resistance mechanisms developed during prostate cancer treatment. *Neoplasia N Y N.* 2020 Jan 10;22(2):111–9.
  43. Han X, Zhao L, Xiang W, Qin C, Miao B, Xu T, et al. Discovery of Highly Potent and Efficient PROTAC Degradors of Androgen Receptor (AR) by Employing Weak Binding Affinity VHL E3 Ligase Ligands. *J Med Chem.* 2019 Dec 26;62(24):11218–31.
  44. Badia E, Oliva J, Balaguer P, Cavallès V. Tamoxifen resistance and epigenetic modifications in breast cancer cell lines. *Curr Med Chem.* 2007;14(28):3035–45.
  45. Werner CK, Nna UJ, Sun H, Wilder-Romans K, Dresser J, Kothari AU, et al. Expression of the of the androgen receptor governs radiation resistance in a subset of glioblastomas vulnerable to anti-androgen therapy. *Mol Cancer Ther [Internet].* 2020 Jan 1 [cited 2020 Aug 13]; Available from: <http://mct.aacrjournals.org/content/early/2020/08/11/1535-7163.MCT-20-0095>
  46. Goodwin JF, Schiewer MJ, Dean JL, Schrecengost RS, de Leeuw R, Han S, et al. A hormone-DNA repair circuit governs the response to genotoxic insult. *Cancer Discov.* 2013 Nov;3(11):1254–71.
  47. Bhattacharyya RS, Krishnan AV, Swami S, Feldman D. Fulvestrant (ICI 182,780) down-regulates androgen receptor expression and diminishes androgenic responses in LNCaP human prostate cancer cells. *Mol Cancer Ther.* 2006 Jun;5(6):1539–49.
  48. Ricciardelli C, Bianco-Miotto T, Jindal S, Butler LM, Leung S, McNeil CM, et al. The Magnitude of Androgen Receptor Positivity in Breast Cancer Is Critical for Reliable Prediction of Disease Outcome. *Clin Cancer Res.* 2018 May 15;24(10):2328–41.
  49. Pesch AM, Pierce LJ, Speers CW. Modulating the Radiation Response for Improved Outcomes in Breast Cancer. *JCO Precis Oncol.* 2021 Nov 1;(5):245–64.
  50. Duru N, Fan M, Candas D, Menea C, Liu HC, Nantajit D, et al. HER2-Associated Radioresistance of Breast Cancer Stem Cells Isolated from HER2-Negative Breast Cancer Cells. *Clin Cancer Res.* 2012 Dec 15;18(24):6634–47.
  51. Hou J, Zhou Z, Chen X, Zhao R, Yang Z, Wei N, et al. HER2 reduces breast cancer radiosensitivity by activating focal adhesion kinase in vitro and in vivo. *Oncotarget.* 2016 Jun 7;7(29):45186–98.
  52. Guo G, Wang T, Gao Q, Tamae D, Wong P, Chen T, et al. Expression of ErbB2 enhances radiation-induced NF- $\kappa$ B activation. *Oncogene.* 2004 Jan;23(2):535–45.



53. Liang K, Jin W, Knuefermann C, Schmidt M, Mills GB, Ang KK, et al. Targeting the Phosphatidylinositol 3-Kinase/Akt Pathway for Enhancing Breast Cancer Cells to Radiotherapy. *Mol Cancer Ther.* 2003 Apr 1;2(4):353–60.
54. Holler M, Grottke A, Mueck K, Manes J, Jücker M, Rodemann HP, et al. Dual Targeting of Akt and mTORC1 Impairs Repair of DNA Double-Strand Breaks and Increases Radiation Sensitivity of Human Tumor Cells. *PLOS ONE.* 2016 May 3;11(5):e0154745.
55. Michmerhuizen AR, Pesch AM, Moubadder L, Chandler BC, Wilder-Romans K, Cameron M, et al. PARP1 Inhibition Radiosensitizes Models of Inflammatory Breast Cancer to Ionizing Radiation. *Mol Cancer Ther.* 2019 Jan 1;molcanther.0520.2019.
56. Feng FY, Speers C, Liu M, Jackson WC, Moon D, Rinkinen J, et al. Targeted radiosensitization with PARP1 inhibition: optimization of therapy and identification of biomarkers of response in breast cancer. *Breast Cancer Res Treat.* 2014 Aug 1;147(1):81–94.
57. Jagsi R, Griffith KA, Bellon JR, Woodward WA, Horton JK, Ho AY, et al. TBCRC 024 Initial Results: A Multicenter Phase 1 Study of Veliparib Administered Concurrently With Chest Wall and Nodal Radiation Therapy in Patients With Inflammatory or Locoregionally Recurrent Breast Cancer. *Int J Radiat Oncol Biol Phys.* 2015 Nov 1;93(3):S137.
58. Katzenellenbogen BS, Norman MJ, Eckert RL, Peltz SW, Mangel WF. Bioactivities, Estrogen Receptor Interactions, and Plasminogen Activator-inducing Activities of Tamoxifen and Hydroxytamoxifen Isomers in MCF-7 Human Breast Cancer Cells. *Cancer Res.* 1984 Jan 1;44(1):112–9.
59. Martinkovich S, Shah D, Planey SL, Arnott JA. Selective estrogen receptor modulators: tissue specificity and clinical utility. *Clin Interv Aging.* 2014 Aug 28;9:1437–52.
60. Patel HK, Bihani T. Selective estrogen receptor modulators (SERMs) and selective estrogen receptor degraders (SERDs) in cancer treatment. *Pharmacol Ther.* 2018 Jun 1;186:1–24.
61. Berthois Y, Katzenellenbogen JA, Katzenellenbogen BS. Phenol red in tissue culture media is a weak estrogen: implications concerning the study of estrogen-responsive cells in culture. *Proc Natl Acad Sci U S A.* 1986 Apr;83(8):2496–500.
62. Xu Y, Huangyang P, Wang Y, Xue L, Devericks E, Nguyen HG, et al. ER $\alpha$  is an RNA-binding protein sustaining tumor cell survival and drug resistance. *Cell.* 2021 Sep 30;184(20):5215–5229.e17.
63. DeNardo DG, Cuba VL, Kim H, Wu K, Lee AV, Brown PH. Estrogen receptor DNA binding is not required for estrogen-induced breast cell growth. *Mol Cell Endocrinol.* 2007 Oct 15;277(1–2):13–25.
64. Wang T, Jin J, Qian C, Lou J, Lin J, Xu A, et al. Estrogen/ER in anti-tumor immunity regulation to tumor cell and tumor microenvironment. *Cancer Cell Int.* 2021 Jun 7;21(1):295.

65. Lai JJ, Lai KP, Zeng W, Chuang KH, Altuwaijri S, Chang C. Androgen Receptor Influences on Body Defense System via Modulation of Innate and Adaptive Immune Systems. *Am J Pathol.* 2012 Nov;181(5):1504–12.

## Chapter 6 : Summary and Perspectives

### 6.1 Summary

Standard of care therapies for patients with breast cancer are determined based on the presence and expression of molecular targets, including expression of the estrogen receptor (ER) and more recently, the androgen receptor (AR). While co-expressed in 70-90% of all ER+ breast cancers<sup>1-3</sup>, AR expression has been found to be a driver of disease progression in ER-negative breast tumors and therefore a target of treatment<sup>4</sup> (**Figure 6-1A**). Patients with breast cancer also receive radiotherapy (RT), which is effectively used in many patients to control local disease. Because previous studies have demonstrated that AR can be a mediator of radioresistance in AR-positive tumors (including breast<sup>5-7</sup>, prostate<sup>8-10</sup>, and glioblastoma<sup>11</sup>), our studies sought to understand how AR and ER may be influencing the radiation response by further investigating the mechanism of radioresistance due to expression of AR and/or ER in multiple hormone-receptor positive (HR+) breast cancer models (**Figure 6-1B**).

### 6.2 Future Directions

#### 6.2.1 AR+/ER- Breast Cancer

Initially we demonstrate that, though both enzalutamide, a second-generation anti-androgen, and seviteronel, a novel CYP17-lyase and AR inhibitor have limited effects on the viability of AR+ TNBC cells *in vitro* (**Figure 2-1, Figure 2-2**), both are sufficient to increase radiosensitivity when administered prior to RT. Treatment with seviteronel or knockdown of AR is sufficient to induce radiosensitization in AR+ TNBC (**Figure 2-3**). Similar to results seen with

enzalutamide<sup>5</sup>, this radiosensitization is due to a delay in the repair of dsDNA breaks following seviteronel treatment (**Figure 2-7**). We demonstrate, however, that seviteronel has differing effects *in vitro* compared to enzalutamide based on changes in gene expression (**Figure 2-4**, **Figure 2-5**, **Figure 2-6**) and chromatin immunoprecipitation (ChIP)-qPCR experiments assessing AR binding to dsDNA repair genes including (*XRCC2*, *XRCC3*, *PRKDC*, **Figure 2-9**). Our *in vitro* results suggest that AR inhibition is mediating radiosensitization by inhibiting dsDNA break repair, and previous work in breast and prostate cancer models indicate that AR inhibition also blocks non-homologous end joining (NHEJ) efficiency by inhibiting phosphorylation of DNAPKcs<sup>5,9</sup>. Radiosensitization with seviteronel was validated *in vivo* using the MDA-MB-453 cell line-based xenograft model where monotherapy with seviteronel or radiation alone was sufficient to delay tumor growth, but combination treatment with seviteronel and RT was found to be more effective and synergistic (**Figure 2-8**).

Having observed radiosensitization in AR+ TNBC cell lines with AR abrogation<sup>5</sup> (**Figure 2-3**, **Figure 5-1**), we next sought to characterize the canonical and noncanonical roles for AR in the radiation response *in vitro*. First, we validated that treatment with apalutamide, darolutamide, and enzalutamide was sufficient to block AR nuclear translocation by western blotting (**Figure 3-1**). Next, we demonstrated that AR is present in the nucleus following RT, further supporting a transcriptional role for AR in mediating the DNA damage response (**Figure 3-2**). We used transcriptomic and proteomic data to nominate the MAPK signaling pathway, and specifically p-ERK as a critical partner in AR-mediated radioresistance (**Figure 3-3**, **Figure 3-4**, **Figure 3-5**, **Figure 3-6**, **Figure 3-7**, **Figure 3-9**). We validated this model to demonstrate that stimulation with androgens results in an increase in p-ERK/total ERK levels (**Figure 3-10**). Together, our findings suggest that AR inhibition radiosensitizes AR+/ER- breast cancer models,

and this radiosensitization may be dependent upon a MAPK/ERK mediated mechanism to inhibit dsDNA break repair *in vitro* (**Figure 3-11**).

While AR has been identified as a mediator of radioresistance, and we have proposed a mechanism of radiosensitization using second generation anti-androgens including enzalutamide, additional studies are needed to identify biomarkers of response for treatment with AR inhibition alone or in combination with RT. As reviewed in chapter 1 (**Table 1-1, Table 1-2**), clinical trials for patients with AR+ TNBC or AR+/ER+ breast tumors are underway to assess the use of multiple AR inhibitors in different contexts<sup>12</sup>. Importantly, clinical studies demonstrate that enzalutamide is effective for the treatment of women who have AR+ TNBC, with a response rate of approximately 30%<sup>13</sup>. While effective in a subset of AR+ TNBC patients, there is a critical need for biomarkers of response for the use of AR inhibitors to understand which patients will benefit from treatment. When RT is added to the treatment paradigm, additional questions arise, including the optimal timing and sequence of therapies that provides the most benefit.

As we uncover the mechanistic underpinnings of AR-mediated radioresistance and radiosensitization mediated through AR-inhibition, additional opportunities have become available to investigate canonical and non-canonical roles for AR in response to ionizing RT. In particular, our studies have demonstrated a role for AR transcriptomically and proteomically in a MAPK-mediated response to RT. Additional experiments, however, are needed to understand how MAPK signaling may be affecting DNA repair, or how AR may be binding throughout the genome to promote direct expression of target genes, including those involved in DNA repair pathways. ChIP-qPCR or sequencing experiments could be used to assess AR's role in DNA binding in breast cancer models, and specifically in the context of ionizing radiation. Data from multiomics analyses including ChIP-seq, RNA-seq, and large-scale proteomics like Reverse

Phase Protein Arrays (RPPA), together could be used to profile the importance of AR expression following RT. This large-scale data would allow us to understand more completely the downstream signaling mediated by AR to promote radioresistance, thus exposing potential therapeutic targets or molecular vulnerabilities that may help determine biomarkers of response.

In addition to its canonical role as a transcription factor, AR also has non-canonical, non-genomic roles in prostate cancer<sup>14,15</sup> and breast cancer<sup>16-18</sup>. While our studies have investigated potential roles for AR in the transcriptional regulation of the DNA damage response, future studies are necessary to understand how AR may be functioning independent of its genomic role in the radiation response. Previous work has demonstrated that steroid receptors can interact with proteins in the cellular or plasma membranes resulting in nongenomic or extranuclear actions through associations with other proteins including growth factor receptors<sup>19</sup>. Therefore, future work could use multiple variations of AR constructs, including AR constructs that lack a nuclear localization signal or a DNA binding domain, which may be of interest to address extranuclear roles for AR. While AR-inhibitor mediated radiosensitization is likely a result of multiple intercellular changes, these proposed studies could begin to elucidate the non-genomic roles for AR in breast cancer, and specifically in response to RT *in vitro*.

### **6.2.2 AR-/ER+ Breast Cancer**

While endocrine therapies and RT are used for the treatment of women with ER+ breast cancers, the optimal timing and sequence of therapy is still debated. This is most notably due to the role of ER in regulating cell cycle progression and causing cell cycle arrest in G1 phase, the most radioresistant phase of the cell cycle. Our work, however, demonstrates that pretreatment with tamoxifen, fulvestrant, or the novel oral SERD, AZD-9496, is sufficient to radiosensitize AR-/ER+ breast cancer cell lines (MCF-7 and T47D, **Figure 4-1, Figure 4-2, Figure 4-3**).

Depletion of hormones results in radiosensitization that can be rescued with re-addition of  $\beta$ -estradiol (**Figure 4-1, Figure 4-3**). We demonstrated that this radiosensitization phenotype is due to a delay in dsDNA break repair as a result of impaired NHEJ efficiency with tamoxifen or fulvestrant treatment (**Figure 4-4**). In addition, there is an increase in cells becoming senescent following treatment with tamoxifen or fulvestrant and RT compared to treatment with RT alone (**Figure 4-9**). While cell cycle arrest was induced with endocrine therapies (**Figure 4-7**), G1 arrest was not found to be a major contributor to the observed radiosensitization, and there were no changes in apoptosis in cells treated with tamoxifen or fulvestrant with RT (**Figure 4-8**). These findings were validated in an *in vivo* xenograft model where tamoxifen was sufficient to radiosensitize and provide a synergistic effect when administered in combination with RT (**Figure 4-10**). Together our findings demonstrate that when administered concurrently, endocrine therapies can be effective radiosensitization strategies in ER+ breast cancer models.

Here we observed that treatment with tamoxifen or fulvestrant decreases NHEJ efficiency in ER+ breast cancer models using a transient NHEJ-reporter system; however, little is known about the specific ways in which ER may be regulating NHEJ protein machinery. While the role of estrogens and ER expression has been debated in the context of DNA damage and repair, some studies suggest that estrogens cause DNA damage<sup>20</sup>. Abrogation of ER has also been shown to inhibit dsDNA break repair through both the homologous recombination and NHEJ pathways<sup>21</sup>. The direct interactions between estrogens or ER with HR or NHEJ proteins, however, remain in question. Androgens and estrogens have been shown to induce NHEJ and DNAPK activity in prostate cancer and breast cancer, respectively<sup>22</sup>. In breast cancer specifically, DNAPK has also been shown to complex with ER, resulting in ER phosphorylation on Ser118 leading to increased stabilization and downstream transcriptional activity<sup>23</sup>. Therefore,

interactions between ER and DNAPK may be responsible, at least in part, for inhibition of NHEJ efficiency following treatment with ER inhibitors; however, these hypotheses require further experimental validation.

Additional studies are needed to fully understand the combined effects of endocrine therapies and RT both *in vitro* and *in vivo*. Previous work with aromatase inhibitors demonstrated combined treatment with letrozole and RT was radiosensitizing<sup>24</sup>. Novel orally bioavailable SERDs are of increasingly clinical interest<sup>25</sup> and are being investigated in clinical trials (including NCT03455270, NCT04711252, NCT04214288). Future work with aromatase inhibitors and novel oral SERDs will require additional studies to understand how these inhibitors, with unique structures, affect radiosensitivity of ER+ breast cancer models *in vitro* and *in vivo*. Further, if radiosensitization is observed with these novel compounds, mechanistic studies will be needed to determine whether radiosensitization is being mediated through the inhibition of NHEJ efficiency resulting in a delay in dsDNA break repair and an increase in senescence as was seen with tamoxifen or fulvestrant treatment (**Figure 4-4, Figure 4-9**). Phenotypic differences in radiosensitization and mechanistic differences could have implications for stratifying patient populations that would benefit most from combined treatment with ER-inhibitors in combination with radiotherapy.

While our work demonstrates a role for the estrogen receptor after RT in DNA repair and senescence, additional studies are needed to understand how ER interacts with DNA damage repair proteins or mediates a transcriptional program in response to ionizing radiation. To this end, future transcriptomic, proteomic, and ChIP studies are needed to identify the transcriptional cofactors, transcripts, and the estrogen response elements that are involved in an ER-mediated response to RT. While many preclinical studies have been performed to try to understand



whether ER inhibition will provide radiosensitization<sup>26-29</sup>, few studies offer a complete and robust explanation for the observed change or lack of change in radiosensitivity. One study has demonstrated a decrease in ER $\alpha$  mRNA and protein expression 72-96 hours after RT<sup>30</sup>; however, we observe radiosensitization with much shorter pretreatment times, most notably, administering drug one hour prior to RT. Therefore, future studies may benefit from querying earlier changes in ER $\alpha$  expression at the protein and transcript level that occur more acutely following treatment. Additional work has demonstrated a downregulation of estradiol synthesis in ER+ MCF-7 and T47D cells following RT<sup>31</sup>. Therefore, an important area of future study would include understanding how ER synthesis and aromatase activity may also be influenced by RT and in turn may influence the radiation response.

In addition, many groups have observed that ER, like AR, has noncanonical functions in cells that may be impacting the radiation response. Notably alternate receptors have been shown to activate alternate pathways including MAPK or GPCR resulting in cell growth independent from estrogen signaling<sup>32</sup>. Other studies have indicated an autophagy-related gene signature as a result of ER-mediated signaling<sup>33,34</sup>. These findings, along with the ongoing investigation between similarities between AR signaling in AR+ TNBC and ER signaling in ER+ breast cancers<sup>35</sup>, suggest that ER may be contributing to the radiation response, at least in part, through a noncanonical role in response to radiation-induced DNA damage.

### **6.2.3 AR+/ER+ Breast Cancer**

To further understand how AR may be contributing to radioresistance in AR+/ER+ breast cancer models, we assessed radiosensitivity of AR+/ER+ models *in vitro* with treatment of AR or ER inhibitors alone or in combination. When AR+/ER+ cells were treated with enzalutamide, apalutamide, darolutamide, an AR degrader (ARD-61), or genetic knockout using CRISPR-Cas9

there was no change in radiosensitivity (**Figure 5-3, Figure 5-4, Figure 5-5**). AR+/ER+ cells treated with tamoxifen or fulvestrant had limited radiosensitization with minor effects observed with tamoxifen treatment, but more pronounced radiosensitization with fulvestrant treatment in CAMA-1 and BT-474 cells, but not in ZR-75-1 cells (**Figure 5-6**). Combined inhibition or degradation of AR and ER *in vitro* did not induce a synergistic effect (**Figure 5-7, Figure 5-8**), suggesting that AR and ER may play distinct roles from one another and have a unique function in AR+/ER+ cells compared to AR+/ER- or AR-/ER+ breast cancer models.

Our findings need to be understood within the experimental context in which they were generated. All *in vitro* experiments were performed in the context of estrogens, and androgens as well as additional hormones and growth factors and phenol red which can act as a weak estrogen<sup>36</sup>. These conditions may alter our ability to assess efficacy of androgen or estrogen inhibitors due to culture conditions. While genetic knockout of *AR* may begin to address this question, additional studies and models are needed. In particular, the use of isogenic models with knockout of *AR* alone, *ER* alone, or combined knockout of *AR* and *ER* may be informative to understanding the independent or related roles for AR and ER in response to RT. In addition, future studies using cells cultured in hormone deplete conditions may investigate how removing all hormones from culture conditions may impact radiosensitivity in multiple contexts. Further, the use of *in vivo* animal models is needed to recapitulate the systemic effects of androgen and estrogen signaling more fully. In particular, questions still remain in our understanding of whether there are thresholds for estrogen or androgen receptor expression in AR+/ER+ tumors that may determine response to AR and/or ER inhibitors. As our previous work has demonstrated that when one receptor is more strongly expressed in AR+/ER- or AR-/ER+ models, AR inhibitors or ER inhibitors, respectively, can be effective radiosensitization agents.

Finally, the mechanistic underpinnings of radiosensitization induced with ER or AR inhibitors alone in AR+/ER- or AR-/ER+ breast cancer models, including our proposed role for MAPK signaling in AR-mediated radioresistance in AR+/ER- models, may be of interest in AR+/ER+ breast tumors as well. Hormones, including androgens, estrogens, and progestins, have been shown to activate members of the MAPK signaling pathway<sup>37-39</sup>. Further, a feedback loop has been identified for AR and ERK signaling in ER- breast cancer models<sup>40</sup>. Yet understanding of how AR, ER, and ERK or other MAPK signaling members may be interacting is still limited, and further investigation of these dynamics may uncover additional vulnerabilities that could be targeted to radiosensitize AR+/ER+ breast cancer models in the future.

### **6.3 Final Remarks**

In conclusion, the work described in this dissertation outlines the role of the androgen and estrogen receptors in response to ionizing radiation in breast cancer models. Specifically, here we identify context-specific roles for AR and ER in mediating radioresistance and demonstrate the importance of understanding the condition under which these receptors are studied. These findings should be taken in the larger context of how we understand roles of nuclear hormone receptors, including the androgen receptor, estrogen receptor, progesterone receptor (PR), and glucocorticoid receptor (GR) and others in breast cancer and other cancers that have been shown to be influenced by hormone expression, notably prostate cancer<sup>8,9</sup> and glioblastoma<sup>11</sup>. While our work has begun to understand the interplay between AR and ER in response to RT, this reflects a small subset of the interactions that may be taking place. These studies fail to account for PR or GR and the influence that these receptors may be having on the radiation response to promote radiosensitivity<sup>41-43</sup>. Notably, the use of high dose estrogens<sup>44,45</sup>,

androgens<sup>46,47</sup>, or progestins<sup>48</sup> has been used for the treatment of breast cancers with 20-30% remission rates.

While our current work seeks to understand the role for hormone receptor signaling in response to ionizing radiation, additional validation of our findings is needed using a diverse set of *in vivo* animal models. In particular, the use of immunotherapies in combination with AR or ER targeted therapies are of increasing interest and require the use of immunocompetent animal models. This is under investigation in prostate cancer where AR has been demonstrated to repress IFN $\gamma$  expression resulting in immunotherapy resistance<sup>49</sup>. Additional work has highlighted novel strategies for radiosensitization of breast cancers including the use of PARP1 inhibitors (Appendix A)<sup>50,51</sup>, TTK inhibition<sup>52</sup>, MELK inhibition<sup>53</sup>, CDK4/6 inhibition<sup>54,55</sup>, and inhibition of anti-apoptotic proteins including Bcl-xL and Mcl-1<sup>56</sup>. These radiosensitization strategies may also be investigated in the context of combinatorial therapies, with particular interest for the role of PARP1 or CDK4/6 inhibitors in potentiating DNA damage in response to ionizing radiation.

Therefore, additional studies are needed in breast cancer models to further investigate how AR or ER signaling may be impacting the immune response. Importantly, our work highlights the potential therapeutic use of AR or ER inhibitors as radiosensitization strategies in models where AR or ER are expressed alone and not co-expressed together. Our findings underscore the importance of deliberate clinical trial design to further address these questions in the patient populations that are most likely to benefit from concurrent administration of AR or ER inhibitors with radiotherapy. Biomarkers of response are also critically needed to help identify and stratify diverse patient populations that may benefit most from therapies. Together these studies provide preclinical data to help inform effective clinical trial design to validate our

findings and provide radiosensitization strategies for patients with breast cancer who are at high risk for locoregional recurrence.

## 6.4 Figure

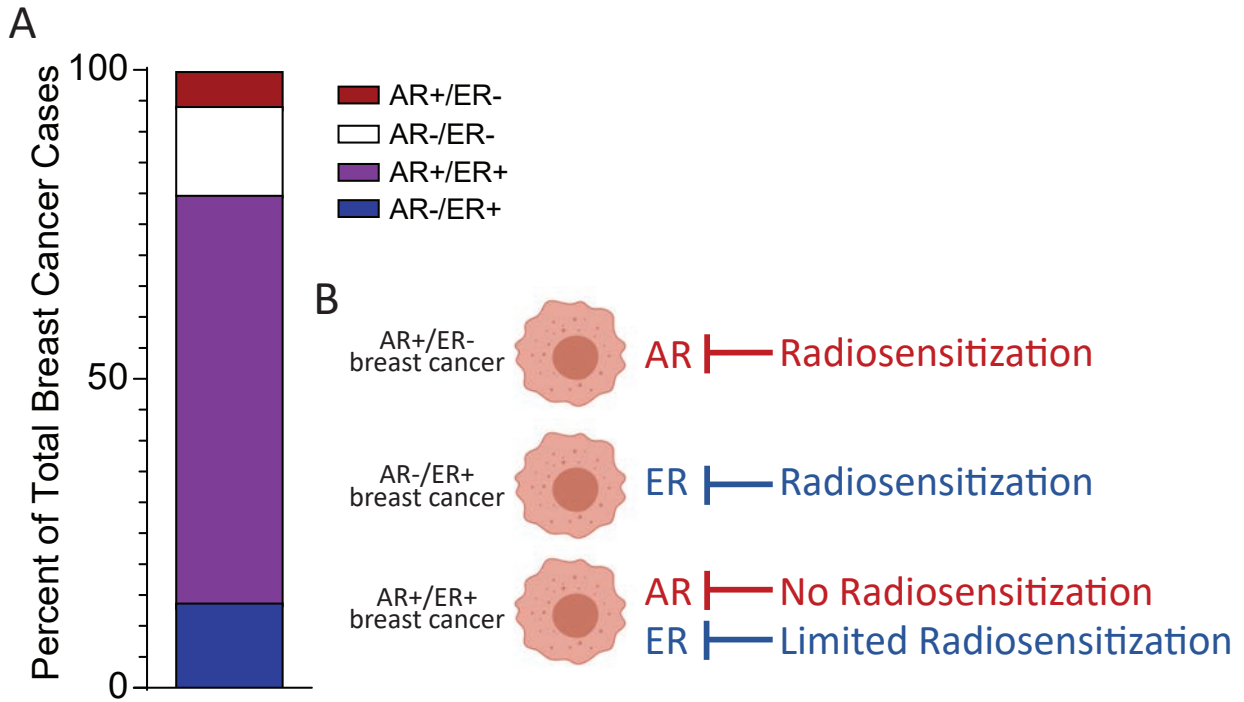


**Figure 6-1: Summary of hormone receptor expression and AR and ER mediated radiosensitization phenotypes in AR+ and ER+ breast cancers**

(A) Breakdown of androgen and estrogen receptor expression in breast tumors. (B) Graphical summary of radiosensitization phenotypes observed with AR and ER inhibitors in AR+/ER-, AR-/ER+, and AR+/ER+ breast cancers.

## 6.5 References

1. Hu, R. *et al.* Androgen Receptor Expression and Breast Cancer Survival in Postmenopausal Women. *Clinical Cancer Research* **17**, 1867–1874 (2011).
2. Kuenen-Boumeester, V. *et al.* The clinical significance of androgen receptors in breast cancer and their relation to histological and cell biological parameters. *European Journal of Cancer* **32**, 1560–1565 (1996).
3. Søreide, J. A., Lea, O. A., Varhaug, J. E., Skarstein, A. & Kvinnsland, S. Androgen receptors in operable breast cancer: relation to other steroid hormone receptors, correlations to prognostic factors and predictive value for effect of adjuvant tamoxifen treatment. *Eur J Surg Oncol* **18**, 112–118 (1992).
4. Lehmann, B. D. *et al.* Identification of human triple-negative breast cancer subtypes and preclinical models for selection of targeted therapies. *J Clin Invest* **121**, 2750–2767 (2011).
5. Speers, C. *et al.* Androgen receptor as a mediator and biomarker of radioresistance in triple-negative breast cancer. *npj Breast Cancer* **3**, 29 (2017).
6. Michmerhuizen, A. R. *et al.* Seviteronel, a Novel CYP17 Lyase Inhibitor and Androgen Receptor Antagonist, Radiosensitizes AR-Positive Triple Negative Breast Cancer Cells. *Front. Endocrinol.* **11**, (2020).
7. Yard, B. D. *et al.* A genetic basis for the variation in the vulnerability of cancer to DNA damage. *Nature Communications* **7**, 11428 (2016).
8. Kakouratos, C. *et al.* Apalutamide radio-sensitisation of prostate cancer. *Br J Cancer* 1–11 (2021) doi:10.1038/s41416-021-01528-1.
9. Goodwin, J. F. *et al.* A hormone-DNA repair circuit governs the response to genotoxic insult. *Cancer Discov* **3**, 1254–1271 (2013).
10. Schweizer, M. T. & Yu, E. Y. AR-Signaling in Human Malignancies: Prostate Cancer and Beyond. *Cancers (Basel)* **9**, (2017).
11. Werner, C. K. *et al.* Expression of the Androgen Receptor Governs Radiation Resistance in a Subset of Glioblastomas Vulnerable to Antiandrogen Therapy. *Mol Cancer Ther* **19**, 2163–2174 (2020).
12. Michmerhuizen, A. R., Spratt, D. E., Pierce, L. J. & Speers, C. W. ARe we there yet? Understanding androgen receptor signaling in breast cancer. *npj Breast Cancer* **6**, 1–19 (2020).
13. Traina, T. A. *et al.* Enzalutamide for the Treatment of Androgen Receptor-Expressing Triple-Negative Breast Cancer. *JCO* **36**, 884–890 (2018).
14. Liao, R. S. *et al.* Androgen receptor-mediated non-genomic regulation of prostate cancer cell proliferation. *Transl Androl Urol* **2**, 187–196 (2013).
15. He, Y. *et al.* A noncanonical AR addiction drives enzalutamide resistance in prostate cancer. *Nat Commun* **12**, 1521 (2021).

16. Chia, K. *et al.* Non-canonical AR activity facilitates endocrine resistance in breast cancer. *Endocrine-Related Cancer* **26**, 251–264 (2019).
17. Khatun, A. *et al.* Transcriptional Repression and Protein Degradation of the Ca<sup>2+</sup>-Activated K<sup>+</sup> Channel KCa1.1 by Androgen Receptor Inhibition in Human Breast Cancer Cells. *Front Physiol* **9**, (2018).
18. Ren, Q. *et al.* Expression of androgen receptor and its phosphorylated forms in breast cancer progression. *Cancer* **119**, 2532–2540 (2013).
19. Kampa, M., Pelekanou, V. & Castanas, E. Membrane-initiated steroid action in breast and prostate cancer. *Steroids* **73**, 953–960 (2008).
20. Caldon, C. E. Estrogen Signaling and the DNA Damage Response in Hormone Dependent Breast Cancers. *Frontiers in Oncology* **4**, (2014).
21. Wang, J., Yang, Q., Haffty, B. G., Li, X. & Moran, M. S. Fulvestrant radiosensitizes human estrogen receptor-positive breast cancer cells. *Biochemical and Biophysical Research Communications* **431**, 146–151 (2013).
22. Schiewer, M. J. & Knudsen, K. E. Linking DNA Damage and Hormone Signaling Pathways in Cancer. *Trends in Endocrinology & Metabolism* **27**, 216–225 (2016).
23. Jiménez-Salazar, J. E., Damian-Ferrara, R., Arteaga, M., Batina, N. & Damián-Matsumura, P. Non-Genomic Actions of Estrogens on the DNA Repair Pathways Are Associated With Chemotherapy Resistance in Breast Cancer. *Frontiers in Oncology* **11**, (2021).
24. Azria, D. *et al.* Letrozole sensitizes breast cancer cells to ionizing radiation. *Breast Cancer Res* **7**, R156–R163 (2005).
25. Hernando, C. *et al.* Oral Selective Estrogen Receptor Degraders (SERDs) as a Novel Breast Cancer Therapy: Present and Future from a Clinical Perspective. *International Journal of Molecular Sciences* **22**, 7812 (2021).
26. Wazer, D. E., Tercilla, O. F., Lin, P.-S. & Schmidt-Ullrich, R. Modulation in the radiosensitivity of MCF-7 human breast carcinoma cells by 17 $\beta$ -estradiol and tamoxifen. *BJR* **62**, 1079–1083 (1989).
27. Villalobos, M. *et al.* Interaction Between Ionizing Radiation, Estrogens and Antiestrogens in the Modification of Tumor Microenvironment in Estrogen Dependent Multicellular Spheroids. *Acta Oncologica* **34**, 413–417 (1995).
28. Moral, R. del *et al.* Interactions between radiotherapy and endocrine therapy in breast cancer. *Endocrine-Related Cancer* **9**, 197–205 (2002).
29. Marthinsen, A., Strickert, T., Paulsen, G., Dybdahl, A. & Abdulkadir, S. Hormonal agents and ionizing radiation may modulate... *Cancer Detec Prev* **22**, (1998).
30. Toillon, R. A. *et al.* Interaction between estrogen receptor alpha, ionizing radiation and (anti-) estrogens in breast cancer cells. *Breast Cancer Res Treat* **93**, 207–215 (2005).
31. Yang, P. *et al.* Ionizing radiation downregulates estradiol synthesis via endoplasmic reticulum stress and inhibits the proliferation of estrogen receptor-positive breast cancer cells. *Cell Death Dis* **12**, 1–10 (2021).



32. Ranganathan, P., Nadig, N. & Nambiar, S. Non-canonical Estrogen Signaling in Endocrine Resistance. *Frontiers in Endocrinology* **10**, (2019).
33. Felzen, V. *et al.* Estrogen receptor  $\alpha$  regulates non-canonical autophagy that provides stress resistance to neuroblastoma and breast cancer cells and involves BAG3 function. *Cell Death Dis* **6**, e1812–e1812 (2015).
34. Fan, D. *et al.* Estrogen Receptor  $\alpha$  Induces Prosurvival Autophagy in Papillary Thyroid Cancer via Stimulating Reactive Oxygen Species and Extracellular Signal Regulated Kinases. *The Journal of Clinical Endocrinology & Metabolism* **100**, E561–E571 (2015).
35. Ni, M. *et al.* Targeting Androgen Receptor in Estrogen Receptor-Negative Breast Cancer. *Cancer Cell* **20**, 119–131 (2011).
36. Berthois, Y., Katzenellenbogen, J. A. & Katzenellenbogen, B. S. Phenol red in tissue culture media is a weak estrogen: implications concerning the study of estrogen-responsive cells in culture. *Proc Natl Acad Sci U S A* **83**, 2496–2500 (1986).
37. Peterziel, H. *et al.* Rapid signalling by androgen receptor in prostate cancer cells. *Oncogene* **18**, 6322–6329 (1999).
38. Di Domenico, M., Castoria, G., Bilancio, A., Migliaccio, A. & Auricchio, F. Estradiol activation of human colon carcinoma-derived Caco-2 cell growth. *Cancer Res* **56**, 4516–4521 (1996).
39. Migliaccio, A. *et al.* Activation of the Src/p21ras/Erk pathway by progesterone receptor via cross-talk with estrogen receptor. *EMBO J* **17**, 2008–2018 (1998).
40. Chia, K. M., Liu, J., Francis, G. D. & Naderi, A. A Feedback Loop between Androgen Receptor and ERK Signaling in Estrogen Receptor-Negative Breast Cancer. *Neoplasia* **13**, 154–166 (2011).
41. Crockart, N. *et al.* Glucocorticoids modulate tumor radiation response through a decrease in tumor oxygen consumption. *Clin Cancer Res* **13**, 630–635 (2007).
42. Vares, G. *et al.* Progesterone prevents radiation-induced apoptosis in breast cancer cells. *Oncogene* **23**, 4603–4613 (2004).
43. Suzuki, Y. *et al.* Progesterone receptor is a favorable prognostic factor of radiation therapy for adenocarcinoma of the uterine cervix. *Int J Radiat Oncol Biol Phys* **47**, 1229–1234 (2000).
44. Coelingh Bennink, H. J. T., Verhoeven, C., Dutman, A. E. & Thijssen, J. The use of high-dose estrogens for the treatment of breast cancer. *Maturitas* **95**, 11–23 (2017).
45. Lønning, P. E. *et al.* High-dose estrogen treatment in postmenopausal breast cancer patients heavily exposed to endocrine therapy. *Breast Cancer Res Treat* **67**, 111–116 (2001).
46. Talley, R. W. *et al.* A dose-response evaluation of androgens in the treatment of metastatic breast cancer. *Cancer* **32**, 315–320 (1973).
47. Goldenberg, I. S. Testosterone Propionate Therapy in Breast Cancer. *JAMA* **188**, 1069–1072 (1964).

48. Hortobagyi, G. N. *et al.* Oral medroxyprogesterone acetate in the treatment of metastatic breast cancer. *Breast Cancer Res Tr* **5**, 321–326 (1985).
49. Guan, X. *et al.* Androgen receptor activity in T cells limits checkpoint blockade efficacy. *Nature* 1–6 (2022) doi:10.1038/s41586-022-04522-6.
50. Feng, F. Y. *et al.* Targeted radiosensitization with PARP1 inhibition: optimization of therapy and identification of biomarkers of response in breast cancer. *Breast Cancer Res Treat* **147**, 81–94 (2014).
51. Michmerhuizen, A. R. *et al.* PARP1 Inhibition Radiosensitizes Models of Inflammatory Breast Cancer to Ionizing Radiation. *Molecular Cancer Therapeutics* **18**, 2063–2073 (2019).
52. Chandler, B. C. *et al.* TTK inhibition radiosensitizes basal-like breast cancer through impaired homologous recombination. *J Clin Invest* **130**, 958–973 (2020).
53. Speers, C. *et al.* Maternal Embryonic Leucine Zipper Kinase (MELK) as a Novel Mediator and Biomarker of Radioresistance in Human Breast Cancer. *Clin Cancer Res* **22**, 5864–5875 (2016).
54. Pesch, A. M. *et al.* Short-term CDK4/6 Inhibition Radiosensitizes Estrogen Receptor–Positive Breast Cancers. *Clin Cancer Res* **26**, 6568–6580 (2020).
55. Pesch, A. M. *et al.* RB expression confers sensitivity to CDK4/6 inhibitor–mediated radiosensitization across breast cancer subtypes. *JCI Insight* **7**, (2022).
56. Pesch, A. M. *et al.* Abstract 1943: Radiosensitization of PIK3CA wild type triple negative breast cancers with Bcl-family inhibition. *Cancer Research* **81**, 1943 (2021).

## Appendix A : PARP1 Inhibition Radiosensitizes Models of Inflammatory Breast Cancer to Ionizing Radiation<sup>6</sup>

### A.1 Abstract:

Sustained locoregional control of disease is a significant issue in patients with inflammatory breast cancer (IBC), with local control rates of 80% or less at 5 years. Given the unsatisfactory outcomes for these patients, there is a clear need for intensification of local therapy, including radiation. Inhibition of the DNA repair protein poly adenosine diphosphate-ribose polymerase 1 (PARP1) has had little efficacy as a single agent in breast cancer outside of studies restricted to patients with BRCA mutations; however, PARP1 inhibition (PARPi) may lead to the radiosensitization of aggressive tumor types. Thus, this study investigates inhibition of PARP1 as a novel and promising radiosensitization strategy in IBC. In all existing IBC models (SUM-149, SUM-190, MDA-IBC-3), PARPi (AZD2281-olaparib and ABT-888-veliparib) had limited single agent efficacy (IC<sub>50</sub> > 10 μM) in proliferation assays. Despite limited single agent efficacy, sub-micromolar concentrations of AZD2281 in combination with RT led to significant radiosensitization (rER 1.12-1.76). This effect was partially dependent on *BRCAl* mutational status. Radiosensitization was due, at least in part, to delayed resolution of double strand DNA breaks as measured by multiple assays. Using a SUM-190 xenograft model *in vivo*, the combination of PARPi and RT

---

<sup>6</sup>This chapter was published in *Molecular Cancer Therapeutics* and completed in collaboration with the following authors: Andrea M. Pesch\*, Leah Moubadder, Benjamin C. Chandler, Kari Wilder-Romans, Meleah Cameron, Eric Olsen, Dafydd G. Thomas, Amanda Zhang, Nicole Hirsh, Cassandra L. Ritter, Meilan Liu, Shyam Nyati, Lori J. Pierce, Reshma Jagsi, and Corey Speers. \*denotes co-first author and equal contribution

significantly delays tumor doubling and tripling times compared to PARPi or RT alone with limited toxicity. This study demonstrates that PARPi improves the effectiveness of radiotherapy in IBC models and provides the preclinical rationale for the opening phase II randomized trial of RT +/- PARPi in women with IBC (SWOG 1706, NCT03598257).

## **A.2 Introduction**

Inflammatory breast cancer (IBC) diagnoses represent well under 5% of new breast cancer cases but account for a disproportionate share of breast cancer mortality<sup>1</sup>. Despite aggressive, multimodal therapy, patients have high rates of locoregional recurrence and distant metastases<sup>1</sup>. Treatment strategies for many breast cancer subtypes are largely directed against the protein drivers of each molecular subtype, including targeted therapies against the estrogen receptor (ER) or the human epidermal growth factor receptor 2 (HER2). IBC, however, represents a heterogeneous population that includes tumors across all of the molecular subtypes<sup>2</sup>. Current treatment guidelines for IBC patients take into consideration the molecular subtype of the tumor and include anti-HER2 or anti-estrogen therapy when appropriate, but more effective and targeted therapeutic options for patients with IBC are extremely limited. Without more effective alternatives, IBC patients typically receive neoadjuvant chemotherapy followed by mastectomy and adjuvant radiation (RT) to the chest wall and regional lymphatics<sup>1</sup>. The key molecular drivers of IBC are currently unknown, and this uncertainty manifests as ineffective clinical therapeutic strategies. In IBC, there is a critical need to identify more effective treatment strategies to decrease rates of locoregional recurrence.

In an attempt to understand the heterogeneity of IBC, a recent study of 53 IBC tumors demonstrated that over 90% of tumors studied contained actionable mutations in genes such as

*PIK3CA* and *BRCA1/2* that could be targeted using therapies that are either FDA-approved or currently in clinical trial<sup>3</sup>. In line with this finding, there are a number of phase I and phase II clinical trials seeking to repurpose other FDA-approved drugs for indication in IBC<sup>1</sup>. Targeted therapies in these trials include agents against PD-1 (pembrolizumab), VEGF-A (bevacizumab)<sup>4,5</sup>, JAK1/2 (ruxolitinib), and the viral agent T-VEC (talimogene laherparepvec)<sup>1</sup>. Many different chemotherapy and radiation therapy regimens have been explored in IBC, but rates of recurrence and overall survival have not significantly improved<sup>6</sup>. However, the ability to sensitize IBC tumors to current treatments such as radiation represents a promising treatment strategy for patients with IBC.

Inhibition of poly adenosine diphosphate-ribose polymerase 1 (PARP1) has been explored in clinical trials for many cancer types. PARP1 inhibition (PARPi) does not demonstrate significant single agent efficacy in the treatment of most breast cancers<sup>7,8</sup>; however, PARPi is an effective targeted therapy in subsets of patients harboring *BRCA1/2* mutations<sup>9</sup>. In addition to the use of PARP1 inhibitors as monotherapy, our group has shown previously that PARPi can effectively radiosensitize a large range of breast cancer cell lines, including those with functional BRCA1 and BRCA2<sup>10</sup>. PARP1, through the addition of poly-ADP ribose (PAR) moieties to sites of single strand DNA (ssDNA) damage, plays a critical role in recognition and recruitment of DNA repair machinery for a variety of different DNA repair processes. If ssDNA lesions go unrepaired, double strand DNA (dsDNA) breaks form.

For cells with intact repair pathways, non-homologous end joining (NHEJ) or homologous recombination (HR) allows the cell to repair DNA. In the case of cancers with *BRCA1/2* mutations, where BRCA-mediated homologous recombination is already deficient, the use of PARP1 inhibitors alone can promote the lethal accumulation of dsDNA breaks, leading to

selective death of tumor cells – a concept referred to as synthetic lethality. In cells with wild type BRCA, other deficiencies in DNA repair pathways – and the addition of PARPi – may predispose tumor cells to higher levels of DNA damage caused by therapeutic radiation<sup>10</sup>. To that end, the present study aimed to determine the effect and efficacy of combining PARP1 inhibition and radiation in multiple preclinical models of IBC.

### **A.3 Methods**

#### ***A.3.1 Cell Culture***

All IBC cell lines were grown in HAMS F12 media (Gibco 11765-054) in a 5% CO<sub>2</sub> incubator. Media for SUM-149 cells was supplemented with 5% FBS (Atlanta Biologicals), 10mM HEPES (Thermo Fisher 15630080), 1x antibiotic-antimycotic (anti-anti, Thermo Fisher 15240062), 1µg/mL hydrocortisone (Sigma H4001), and 5µg/mL insulin (Sigma I9278). SUM-190 media was supplemented with 1% FBS, 1µg/mL hydrocortisone, 5µg/mL insulin (Sigma I0516), 50nM sodium selenite (Sigma S9133), 5µg/mL apo-Transferrin (Sigma T-8158), 10nM triiodo thyronine (T3, Sigma T5516), 10mM HEPES, and 0.03% ethanolamine (Sigma 411000). MDA-IBC-3 cells were grown with 10% FBS, 1µg/mL hydrocortisone, 1x anti-anti, and 5µg/mL insulin (Sigma I0516). SUM cell lines were obtained from Stephen Ethier at the Medical University of South Carolina, and MDA-IBC-3 cells were obtained directly from Wendy Woodward at the University of Texas MD Anderson Cancer Center. All cell lines were routinely tested for mycoplasma contamination (Lonza LT07-418) and were authenticated using fragment analysis at the University of Michigan DNA sequencing core. Olaparib (MedChem Express HY-10162) and veliparib (MedChem Express HY-10129) were reconstituted in 100% DMSO for cellular assays.

### ***A.3.2 Proliferation Assays***

SUM-190 and SUM-149 cells were plated in 96 well plates overnight and treated the next morning with either olaparib or veliparib using a dose range of 1pM to 10 $\mu$ M. After 72 hours, AlamarBlue (Thermo Fisher DAL1025) was added up to 10% of the final volume and read on a microplate reader after incubation at 37°C for 3 hours. MDA-IBC-3 cells were plated in 6-well plates and treated with a dose range of 1nM to 10 $\mu$ M of either olaparib or veliparib. After 72 hours, cells were trypsinized and counted with a hemocytometer.

### ***A.3.3 Clonogenic Survival Assays***

SUM-149 and SUM-190 cells were plated at various densities from single cell suspension in 6-well plates and radiated the following day after a one-hour pretreatment with olaparib. Cells were grown for up to three weeks, then fixed with methanol/acetic acid and stained with 1% crystal violet. Colonies with a minimum of 50 cells were counted for each treatment condition. Plating efficiency was determined and used to calculate toxicity. Cell survival curves were calculated as described previously<sup>10</sup>. MDA-IBC-3 cells were grown in soft agar (Thermo Fisher 214050) with a base layer of 0.5% agar solution and a top layer of 0.4% agar containing the cell suspension. Drug treatments in supernatant media were added fresh each week. Colonies were grown for up to four weeks before staining with 0.005% crystal violet.

### ***A.3.4 Immunofluorescence***

Cells were plated on 18 mm coverslips in 12-well plates and allowed to adhere to coverslips overnight. The following day, cells were treated with media containing either olaparib or vehicle one hour before radiation (2 Gy), and coverslips were fixed at predetermined time points after radiation.  $\gamma$ H2AX foci were detected using anti-phospho-histone H2AX (ser139) monoclonal

antibody (Millipore 05-636), with a goat anti-mouse fluorescent secondary antibody (Invitrogen A11005). At least 100 cells were scored visually for  $\gamma$ H2AX foci in three independent experiments. Cells containing  $\geq 15$   $\gamma$ H2AX foci were scored positive and were pooled for statistical analysis.

### ***A.3.5 Immunoblotting***

Cells were plated overnight and pre-treated the next morning with olaparib. Plates were irradiated one hour after pretreatment, and cells were harvested at 6 and 24 hours after radiation. Lysates were extracted using RIPA buffer (Thermo Fisher 89901) containing protease and phosphatase inhibitors (Sigma-Aldrich PHOSS-RO, CO-RO). Proteins were detected using the anti-PAR antibody (LS-B12794, 1:5000), the anti-PARP1 antibody (ab6079, 1:1000), and anti- $\beta$ -Actin (8H10D10, Cell Signaling 12262S, 1:50,000).

### ***A.3.6 Xenograft Models***

Bilateral subcutaneous flank injections were performed on 4-6 week old CB17-SCID female mice with  $1 \times 10^6$  SUM-190 cells resuspended in 100 $\mu$ L PBS with 50% Matrigel (Thermo Fisher CB-40234). Tumors were allowed to grow until reaching approximately 80mm<sup>3</sup>. Olaparib treatment was given by intraperitoneal injection 24 hours prior to the first radiation treatment. For long term studies, mice were treated with vehicle (10% 2-hydroxypropyl-beta-cyclodextrin in phosphate buffered saline, Thermo Fisher 10010-023), olaparib (50mg/kg) alone, radiation alone (2 Gy x 8 fractions) or the combination of olaparib + RT, with 16-20 tumors per treatment group. Tumor growth was measured three times a week using digital calipers, and mice were weighed on the same days. Tumor volume was calculated using the equation  $V=(L*W^2)*\pi/6$ . For short term studies, mice were treated with vehicle control, olaparib, or radiation for 48 hours



before the tumors were harvested. Mice treated with both olaparib and radiation received olaparib treatment 24 hours before radiation treatment. The tumors were then harvested 48 hours after radiation. Immunohistochemical staining was performed on tumors for all four conditions. All procedures involving mice were approved by the Institutional Animal Care & Use Committee (IACUC) at the University of Michigan and conform to their relevant regulatory standards.

### ***A.3.7 Irradiation***

Irradiation was carried out using a Philips RT250 (Kimtron Medical) at a dose rate of approximately 2 Gy/min in the University of Michigan Experimental Irradiation Core as previously described<sup>10</sup>. Irradiation of mouse tumors was carried out as described previously<sup>11</sup>.

### ***A.3.8 Immunohistochemistry***

Immunohistochemical staining was performed on the DAKO Autostainer (Agilent, Carpinteria, CA) using Envision+ or liquid streptavidin-biotin and diaminobenzadine (DAB) as the chromogen. De-paraffinized sections were labeled with the antibodies listed in **Table A-1** for 30 minutes at ambient temperature. Microwave epitope retrieval, as specified in **Table A-1**, was used prior to staining for all antibodies. Appropriate negative (no primary antibody) and positive controls (as listed in **Table A-1**) were stained in parallel with each set of slides studied. Whole-slide digital images were generated using an Aperio AT2 scanner (Leica Biosystems Imaging, Vista, CA, USA) at 20X magnification, with a resolution of 0.5  $\mu\text{m}$  per pixel. The scanner uses a 20x / 0.75 NA objective and an LED light source. The same instrument and settings were used throughout the study for all whole-slide images generated. The images were checked for quality before use, and scans were repeated as necessary. Digital slides were analyzed using the

Visopharm image analysis software suite (DK-2970 Hoersholm, Denmark, v2019.2) to count stained and unstained nuclei.

#### ***A.3.9 Comet Assay***

Cells were plated in 6 well plates and allowed to adhere overnight. Cells were pretreated with olaparib for one hour before radiation and collected at designated time points after radiation.

Cells were mixed with low melting point agarose (Thermo Fisher 15-455-200) and spread on CometSlides (Trevigen 4250-050-03). The cells were lysed with lysis solution (Trevigen 4250-050-01), and DNA was separated by electrophoresis. Propidium iodide (Thermo Fisher P3566) was used to stain DNA. A fluorescent microscope was used to take images of at least 50 cells/treatment. Images were analyzed using Comet Assay IV Software Version 4.3 to calculate the Olive tail moment. Results were pooled for statistical analyses.

#### ***A.3.10 Statistical Analyses***

GraphPad Prism 7.0 was used to perform statistical tests. *In vitro* statistical analyses were performed using the two-tailed student's t-test or a one-way ANOVA in the case of multiple comparisons. For *in vivo* studies, a two-way ANOVA was used to compare tumor growth, and the fractional tumor volume (FTV) method for assessing synergy *in vivo* was used as previously described<sup>12,13</sup>.

### **A.4 Results**

#### ***A.4.1 Single agent PARPi does not significantly affect proliferation of IBC cell lines in vitro***

First, we sought to characterize the effect of two PARP1 inhibitors, olaparib (AZD2281) and veliparib (ABT-888)<sup>14</sup>, on the proliferation of IBC cell lines. In SUM-190 and MDA-IBC-3

cells, single agent PARPi with olaparib or veliparib does not cause a significant decrease in proliferation at concentrations up to 10 $\mu$ M (**Figure A-1A-D**). While veliparib does not appear to impact proliferation of SUM-149 cells (IC<sub>50</sub> > 10 $\mu$ M, **Figure A-1E**), olaparib does have a modest effect as a single agent in SUM-149 cells (IC<sub>50</sub> = 2.2 $\mu$ M, **Figure A-1F**). All models tested were isolated from patients with IBC; however, SUM-149 cells are unique as they harbor a BRCA1 2288delT mutation as well as allelic loss of the wild type BRCA1 gene, rendering them BRCA1 deficient<sup>15</sup>. Thus, SUM-149 cells may be especially sensitive to additional inhibition of DNA repair pathways<sup>15</sup>.

#### ***A.4.2 PARPi leads to radiosensitization of IBC cell lines in vitro***

While single agent PARPi with either olaparib or veliparib did not inhibit cell proliferation, we sought to determine the effect of PARP1 inhibition on the radiosensitivity of IBC cell lines. Clonogenic survival assays were performed with olaparib in each of the three IBC cell lines, as olaparib is a more potent PARP1 inhibitor compared to veliparib, with both PARP1 enzymatic inhibition efficacy and PARP trapping function. All IBC cell lines displayed significant radiosensitization as a result of pretreatment with olaparib. In SUM-190 cells, a dose-dependent radiosensitization was observed, with average radiation enhancement ratios (rER) of  $1.45 \pm 0.03$  and  $1.64 \pm 0.21$  at concentrations of 1 $\mu$ M and 2 $\mu$ M olaparib, respectively (**Figure A-2A, Table A-2A**). A similar trend was observed in MDA-IBC-3 cells, with enhancement ratios of  $1.12 \pm 0.08$  and  $1.28 \pm 0.06$  under the same treatment conditions (**Figure A-2C, Table A-2B**). Because SUM-149 cells express a truncated form of the BRCA1 protein, treatment with olaparib leads to marked radiosensitization at much lower doses. At 10nM and 20nM, the average enhancement ratios for SUM-149 cells were approximately  $1.42 \pm 0.01$  and  $1.76 \pm 0.11$  (**Figure A-2E, Table A-2C**). The enhancement ratios observed here are similar to or greater than

that of cisplatin (rER=1.2-1.3), a compound well-characterized for its ability to act as a radiosensitizing agent<sup>16,17</sup>. Furthermore, the surviving fraction of cells at 6 Gy (**Figure A-2B, D, F**) was significantly lower across all three inflammatory cell lines with the addition of olaparib. The radiation enhancement ratios demonstrated a marked dose-dependent increase, while toxicity from each treatment was minimal (**Table A-2**).

#### ***A.4.3 PARP1 inhibition and radiation leads to delayed repair of DNA double strand breaks compared to radiation alone***

In cancer cells, ionizing radiation induces both single strand and double strand DNA breaks. In situations where DNA repair is inhibited and single strand breaks go unrepaired, the collapse of replication forks can propagate chromosomal damage and lead to the accumulation of lethal dsDNA breaks. Because PARP1 is involved in the recruitment of DNA repair proteins to DNA strand breaks, we sought to understand the effect of PARP1 inhibition and radiation on the accumulation of DNA damage in IBC cell lines. In SUM-190 and SUM-149 cells, radiation treatment alone (2 Gy) induces  $\gamma$ H2AX foci in greater than 75% of cells (**Figure A-3A, B**). In both cell lines, dsDNA breaks are retained at significantly higher levels at 12 and 16 hours after treatment with olaparib and radiation compared to treatment with radiation alone (**Figure A-3C, D**). Furthermore, a similar difference in dsDNA breaks was observed between RT alone and combination treatment in SUM-190 cells at 4 hours after radiation. In short, the presence of olaparib leads to the accumulation and persistence of dsDNA breaks in the combination treatment compared to the radiation treatment alone in both SUM-190 and SUM-149 cells. In order to independently confirm these findings, we performed the neutral comet assay to assess for dsDNA breaks (**Figure A-4A**). In SUM-190 cells, the combination of PARPi and RT in SUM-190 cells lead to a significantly longer tail moment, indicating increased dsDNA breaks

compared to treatment with RT alone ( $p = 0.029$ ). The tail moment was also significantly higher compared to cells treated with vehicle or olaparib as a single agent (**Figure A-4A**).

Representative images for each treatment condition are shown (**Figure A-4A**).

#### ***A.4.4 Olaparib effectively inhibits PAR formation in IBC cell lines***

In order to determine if inhibition of PARP1 enzymatic activity occurs at concentrations of olaparib that are sufficient to induce radiosensitization, we treated cells with olaparib  $\pm$  4 Gy radiation and measured the total PAR and PARP1 levels in IBC cell lines. In SUM-190 and MDA-IBC-3 cells, PAR formation is significantly inhibited with 1  $\mu$ M of olaparib (**Figure A-4B, C**). Inhibition of PAR formation, however, can also be achieved at the same level in SUM-149 cells with 20nM of olaparib (**Figure A-4D**). Therefore, inhibition of PAR formation with olaparib occurs at low concentrations (20nM) that are sufficient to confer radiosensitization in SUM-149 cells. Though olaparib effectively inhibits PARylation at these concentrations, the amount of PARP1 in the cell lines remains relatively constant in all models (**Figure A-4B-D**).

#### ***A.4.5 PARP1 inhibition significantly inhibits growth of SUM-190 xenografts in vivo***

Having demonstrated that PARP1 inhibition can effectively radiosensitize IBC cell lines *in vitro*, we next sought to validate these findings in an *in vivo* xenograft model. For *in vivo* studies, subcutaneous tumors were allowed to reach  $\sim 80$  mm<sup>3</sup> in CB-17 SCID mice whereupon treatment was initiated with one of the following: vehicle, 50 mg/kg olaparib alone daily, radiation alone (8 fractions of 2 Gy), or the combination (olaparib 50 mg/kg + 2 Gy RT daily for 8 fractions) (**Figure A-5A**). To truly assess the radiosensitizing effects of PARP1 inhibition, olaparib treatment was started one day before initiation of radiation and discontinued after the last fraction of radiation.

Consistent with the *in vitro* proliferation assays, treatment with olaparib alone did not significantly delay tumor growth or doubling time of xenograft tumors. As expected, radiation alone did lead to a decrease in tumor size initially, but tumors continued to grow after the completion of fractionated radiation (**Figure A-5B**). Mice receiving both radiation and olaparib treatment had significantly smaller tumors after completion of the study compared to those receiving radiation alone ( $p < 0.0001$ ). There was a significant delay in the time to tumor doubling ( $p < 0.0001$ , **Figure A-5C**) and tripling ( $p < 0.0001$ , **Figure A-5D**) in the animals treated with combination olaparib and RT. In addition, time to tumor doubling and tripling was not reached in the combination treated group after 35 days. Weights of the mice (**Figure A-5E**) remained relatively constant throughout the experiment, indicating there was limited toxicity observed with combination treatment. Interestingly, the effects of the combination treatment with olaparib and radiation were found to be synergistic using the fractional tumor volume (FTV) method as previously described (**Figure A-5F**)<sup>12</sup>. Immunohistochemistry studies in tumors harvested from the mice at the end of the experiment demonstrated that levels of Ki67, a marker of cell proliferation, were significantly decreased in all treatment groups compared to control mice, with the most significant decrease in the combination treated animals ( $p = 0.0004$ , **Figure A-6A, B**). There was also a decrease in p16 staining levels in the mice treated with radiation alone ( $p = 0.0072$ ) and the combination treated group ( $p = 0.0385$ ) in the long-term experiments (**Figure A-6C, D**), suggesting a decrease in cellular senescence in these tumors<sup>18</sup>. The on-target effects of olaparib were confirmed in the short-term studies (48 hours of PARPi treatment alone or 24 hours of PARPi pretreatment before radiation). As expected, total levels of PARP1 were unaffected by treatment with olaparib, radiation, or the combination treatment (**Figure A-7A, B**), while PAR levels were significantly lower in the PARPi treated animals (**Figure A-7C, D**).

## A.5 Discussion

In this study, we demonstrate that PARP1 inhibition alone is insufficient in delaying IBC cell line growth and proliferation (**Figure A-1**). Combination treatment with PARP1 inhibition and ionizing radiation, however, results in significant radiosensitization of IBC models *in vitro* (**Figure A-2**), and the combination treatment results in delayed tumor growth *in vivo* (**Figure A-5**). Additionally, we demonstrate that PARP1 inhibition in combination with radiation significantly delays resolution of dsDNA breaks using *in vitro* models of IBC (**Figure A-3**, **Figure A-4**). Taken together, these results suggest that PARP1 inhibition with radiation therapy may be a promising strategy for the treatment of inflammatory breast cancer.

Although these studies suggest that PARP1 inhibition may be an effective radiosensitization strategy for the treatment of IBC, other potential targets for treatment have also been identified. Several groups have identified molecular alterations in IBC tumors and *in vitro* models that may help to describe the aggressive phenotype associated with IBC<sup>1</sup>. Owing to the inflammatory nature of these cancers, the use of lipid lowering agents such as statins has been met with some success<sup>19,20</sup>. Preclinical data using statins in IBC show statin treatment can lead to increased apoptosis and radiosensitivity, inhibition of proliferation and invasion, and decreased metastatic dissemination of tumors<sup>21</sup>. In a population-based cohort study in patients with IBC, statin use was associated with improved progression-free survival in IBC patients<sup>21</sup>. Recent studies have sought to better define this inflammatory microenvironment, and many have noted that macrophages may be important in mediating the radiosensitivity and metastatic potential of IBC tumors<sup>22-25</sup>. Immune regulating agents have also been implicated in the aggressiveness of IBC. In addition to the role that cytokines such as INF $\alpha$  and TNF $\alpha$  may play in pathogenesis<sup>26</sup>, many studies have reported that PD-L1 is consistently overexpressed in IBC

tumors<sup>27,28</sup>. Upregulation of downstream signaling proteins including mTOR and JAK2/STAT3 have also been observed<sup>28,29</sup>. The role of RhoC in IBC has also been reported, but recent evidence suggests that downstream signaling may lead to unique metabolic regulation<sup>30</sup> and changes in lipid raft formation<sup>31</sup>. Transcriptional reprogramming of IBC cells is also common, including C/EBP $\delta$ -mediated upregulation of VEGF-A<sup>32</sup> and upregulation of the redox-sensitive transcription factor NF $\kappa$ B and the E3 ubiquitin ligase XIAP<sup>33-36</sup>. These promising studies suggest that more effective treatment strategies are on the horizon.

Although we have demonstrated the radiosensitizing effects of olaparib in our models, these studies highlight the challenges of studying IBC. This study uses most of the available preclinical models of IBC but also highlights that there are a limited number of available models in which to study IBC. Thus, the need for additional model systems is critical to gaining a better understanding of the heterogeneity and pathogenesis of inflammatory breast cancers. While our studies were conducted in IBC cell lines, an important future direction of this work will involve the use of patient-derived xenograft (PDX) models of IBC. In addition, this study primarily utilized the more potent PARPi olaparib, though our previous studies also evaluated the efficacy of radiosensitization using veliparib<sup>10</sup>. Olaparib may be more potent given its dual functionality as a PARP enzymatic inhibitor and PARP trapper, whereas veliparib only has functions as an enzymatic inhibitor of PARP1 at the doses used for these studies<sup>37</sup>. Although more potent, toxicity in clinical trials to date does not appear worse with olaparib and clinical data suggests that olaparib is well tolerated *in vivo*<sup>8</sup>.

The dual functionality of some PARP inhibitors (such as olaparib) to both inhibit enzymatic activity of the PARP1 protein as well as induce PARP trapping has been well documented<sup>37-40</sup>. Recent literature also suggests that PARPi may cause an increase in replication



fork acceleration, resulting in replicative stress that ultimately leads to cell death<sup>41</sup>. Though the study reported here does not directly address the relative contributions of enzymatic PARP1 inhibition versus PARP trapping on radiosensitization, studies are underway to determine how these functions may differentially contribute to the compounds' radiosensitizing effects. In addition to olaparib, PARP inhibitors such as talazoparib and rucaparib are used to treat other types of breast cancer<sup>42,43</sup>. These inhibitors may also be valuable in the treatment of IBC in combination with radiation and are currently being investigated.

While we have shown that PARP1 inhibition can be used for the radiosensitization of inflammatory breast cancer, olaparib and other PARP1 inhibitors are currently being investigated as radiosensitization agents for the treatment of triple negative breast cancer (RadioPARP/ NCT03109080), head and neck cancer<sup>44</sup>, pancreatic cancer<sup>45</sup>, prostate cancer<sup>46</sup>, and ovarian cancer<sup>47</sup>. More recent trials are testing whether PARP1 inhibition is effective in combination with radiation in squamous cell carcinoma<sup>48</sup> (NCT02229656), locally advanced rectal cancer (NCT02921256 and NCT01589419), high grade gliomas (NCT03212742), non-small cell lung cancer (NCT01386385 and NCT02412371), and soft tissue sarcoma<sup>49</sup> (NCT02787642). Thus, while this study is the first to report that PARP inhibition may be an effective strategy in patients with IBC, the concept of PARP inhibitor-mediated radiosensitization is being explored in many other cancer contexts.

IBC is a subset of breast cancer with limited treatment options and the lowest 5-year survival rates of any breast cancer type<sup>1</sup>. Despite the limitations of the model systems, these data have provided the preclinical rationale for further clinical investigation. In a phase I trial, our group previously demonstrated that PARP1 inhibition in combination with radiation may be a safe and effective strategy for women with IBC (and in women with locoregionally recurrent

breast cancer)<sup>50</sup>. To that end, a randomized phase II trial (SWOG 1706, NCT03598257) comparing the effects of olaparib and radiation therapy to radiation therapy alone in patients with IBC is now underway. Patients in the combination arm begin treatment with olaparib one day prior to the initiation of radiation therapy, and olaparib is administered until the final day of radiation treatment. Invasive disease-free survival of women receiving treatment with olaparib and radiation will be compared to that of the group receiving radiation alone. Secondary endpoints, such as local disease control, distant relapse-free survival and overall survival will also be assessed. In addition, correlative studies from this trial will be used to see if biomarkers of treatment response and efficacy can be identified. These correlative studies will also define the genomic and transcriptomic landscape of IBC in a large patient population and will assess how circulating tumor DNA (ctDNA) levels are affected by combination and single agent treatment.

Though it is evident from our study that PARP1 inhibition with olaparib leads to radiosensitization of IBC cell lines, further studies are needed to determine the exact mechanism of olaparib-induced radiosensitization in IBC. Future transcriptomic and proteomic analysis of current model systems across multiple platforms may provide some insight as to the mechanism of this radiosensitization, and such studies are currently underway. Finally, correlative studies from SWOG 1706 will help inform future mechanistic studies and will provide a platform in which to evaluate potential predictive or prognostic biomarkers that may be able to help more effectively guide selection of IBC patients for this approach to treatment intensification.

## **A.6 Acknowledgements**

The authors would like to thank the Breast Cancer Research Foundation (through a grant to L. Pierce), The Komen for the Cure Foundation (through a grant to R. Jagsi), and the University of Michigan Rogel Cancer Center (through a grant to C. Speers). A. Michmerhuizen, A. Pesch, and B. Chandler are supported by the following training grants: T32-GM007315, T32-GM007767, T32-CA140044. The authors would also like to thank Wendy Woodward at MD Anderson Cancer Center for providing MDA-IBC-3 cells, and Stephen Ethier at the Medical University of South Carolina for providing SUM-149 and SUM-190 cells.

## A.7 Figures

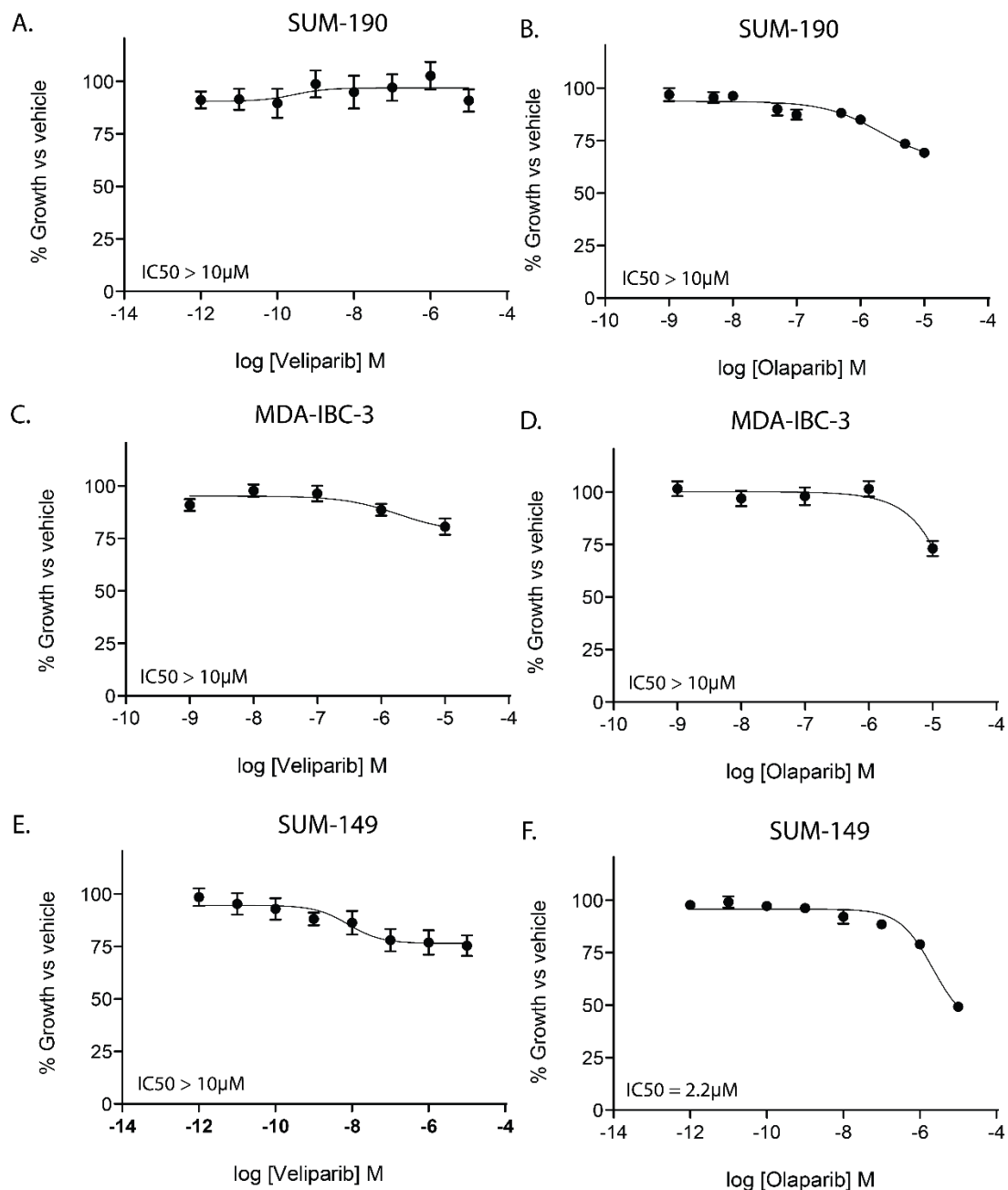


**Figure A-1: PARP1 inhibition does not affect proliferation of IBC cell lines**

IBC cell lines were treated with either olaparib or veliparib and cell viability was measured 72 hours after treatment. In SUM-190 (A,B) and MDA-IBC-3 (C,D) cells, neither veliparib or olaparib showed significant effects on proliferation at doses up to 10 μM. In SUM-149 cells (E,F), olaparib, but not veliparib, can inhibit proliferation at high doses (2.2 μM). Graphs are shown as the average of three independent experiments ± SEM.

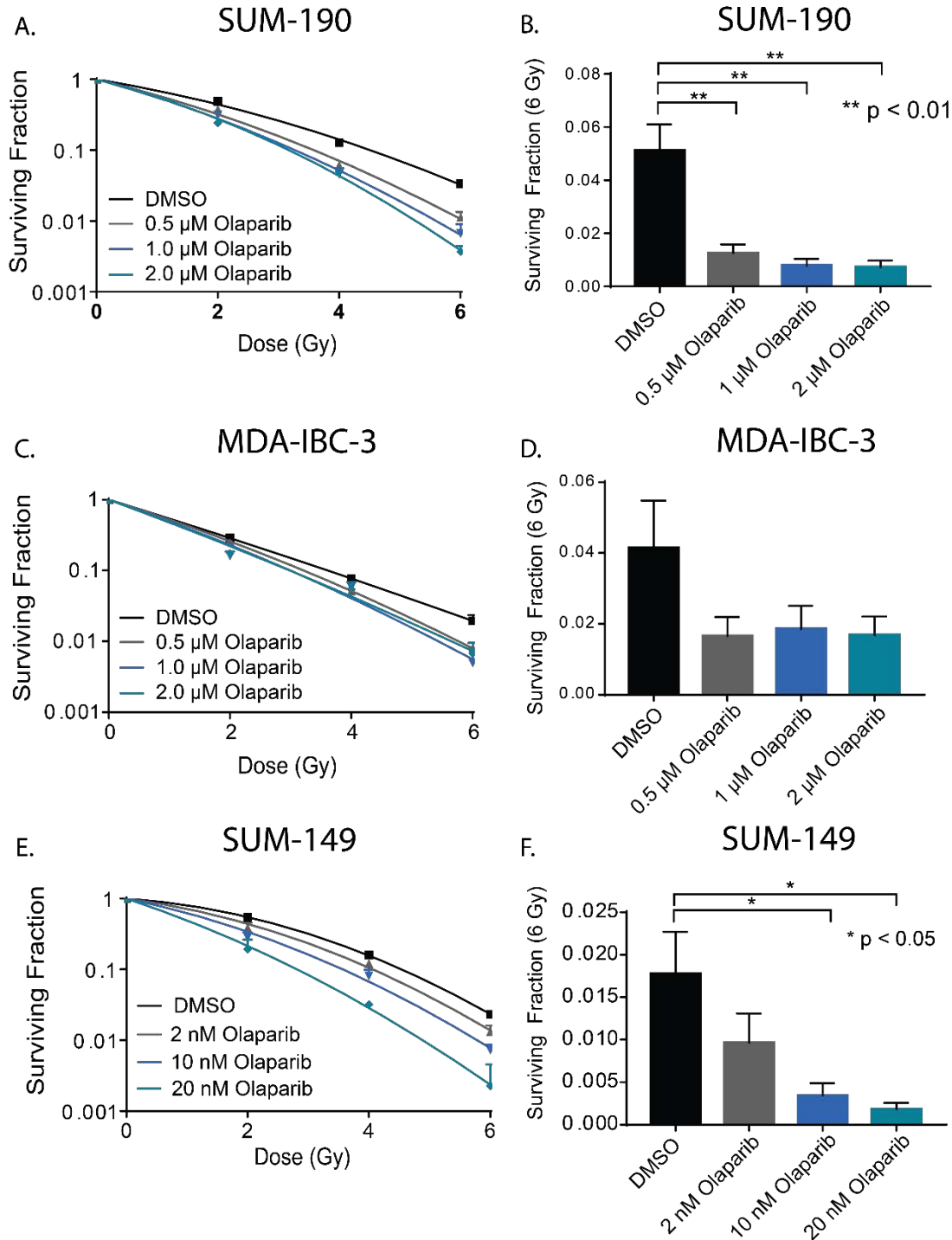


**Figure A-2: Clonogenic survival of IBC cell lines decreases with olaparib treatment**

Olaparib treatment results in a dose-dependent reduction in survival fraction of SUM-190 (A), MDA-IBC-3 (C), and SUM-149 (E) cell lines. Representative data from single experiments are shown for each cell line. The surviving fraction of cells after 6 Gy (B, D, F) was calculated as the mean of three independent experiments and depicted  $\pm$  SEM for each cell line. ( $p < 0.05 = *$ ,  $p < 0.01 = **$ )

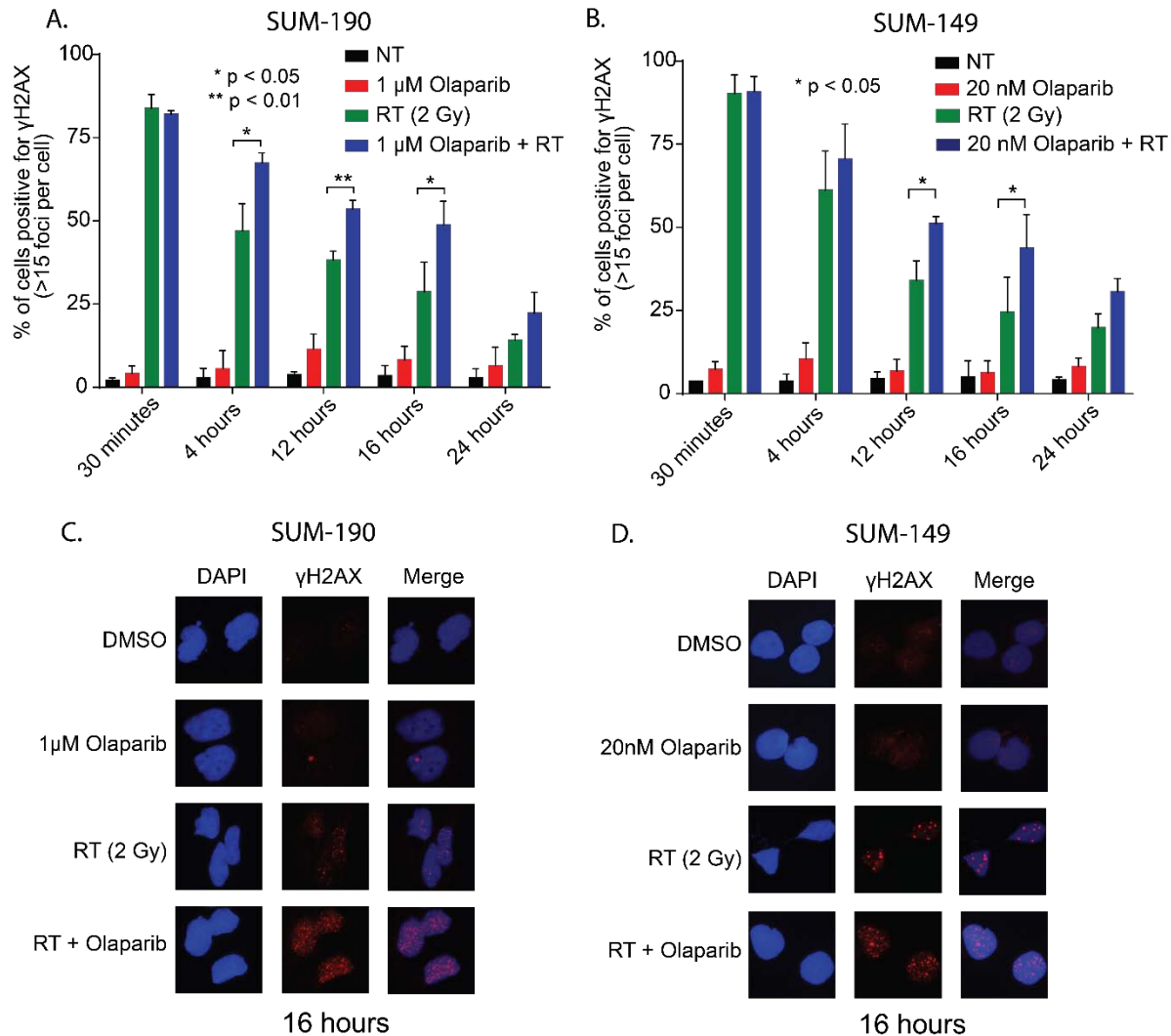


**Figure A-3: Radiation in combination with the PARP1 inhibition leads to persistence of DNA damage in IBC cell lines**

Immunofluorescence microscopy was used to measure  $\gamma$ H2AX foci in SUM-190 (A) and SUM-149 (B) cells. Cells were pretreated for one hour with olaparib and fixed at 0.5, 4, 12, 16, and 24 hours after radiation, then stained for DAPI and  $\gamma$ H2AX. Cells containing  $\geq 15$  foci were scored as positive. In SUM-190 cells at 4, 12, and 16 hours, there were significantly higher levels of cells positive for  $\gamma$ H2AX for those treated with the combination of 2 Gy radiation and 1  $\mu$ M olaparib compared to cells treated with 2 Gy radiation alone. In SUM-149 cells, 20 nM olaparib and 2 Gy radiation results in a higher percentage of  $\gamma$ H2AX positive cells compared to cells treated with radiation alone at both 12 and 16 hours. Representative images of  $\gamma$ H2AX foci in SUM-190 (C) and SUM-149 (D) cells at 16 hours are shown for all treatment groups. Graphs represent the average of three independent experiments  $\pm$  SD. ( $p < 0.05 = *$ )

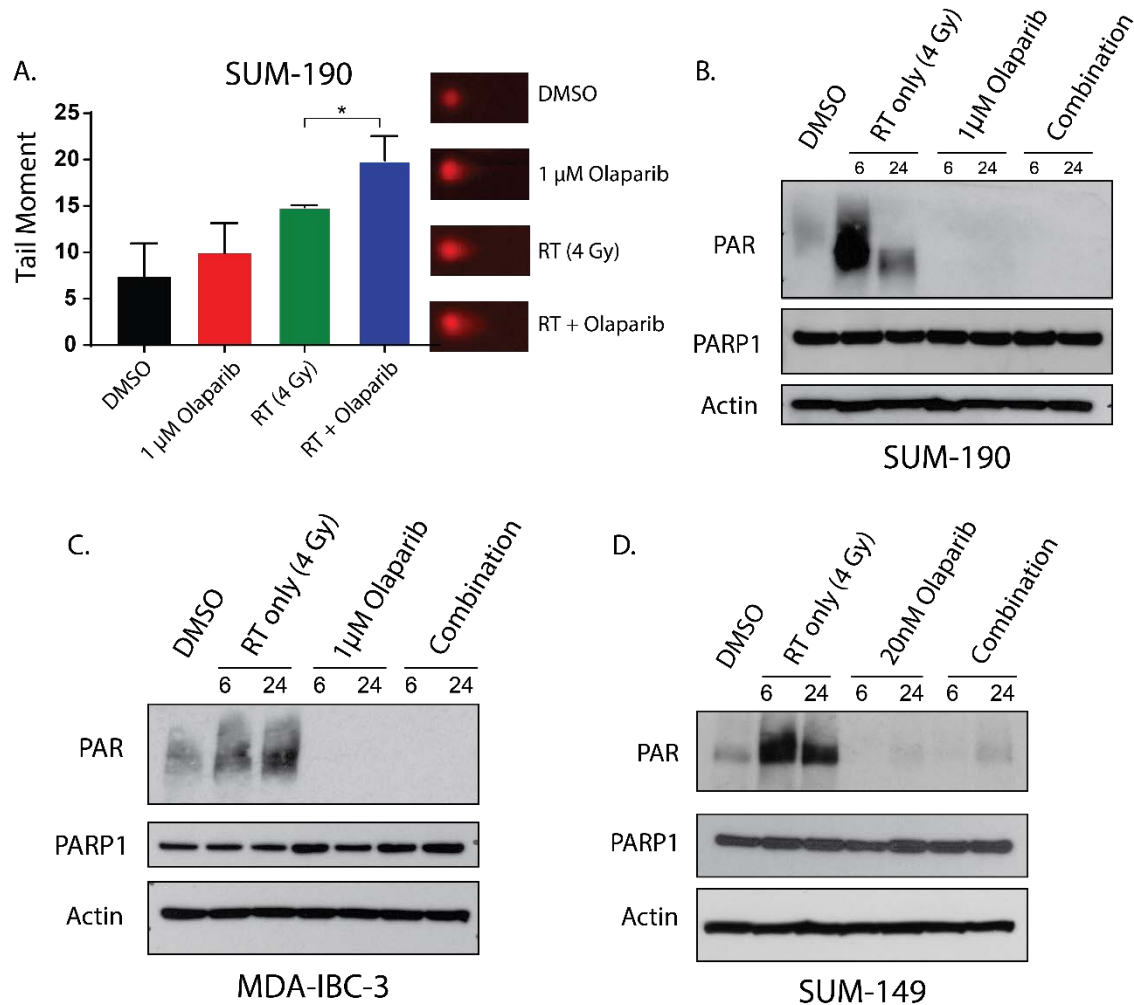


**Figure A-4: PARP1 inhibition increases dsDNA breaks and significantly decreases PAR formation in IBC cell lines**

Neutral comet assay in SUM-190 cells (A) shows higher levels of dsDNA damage at 4 hours in cells treated with radiation and olaparib compared to untreated cells, or cells treated with RT or olaparib alone ( $p < 0.05 = *$ ). Graphs represent the average of three independent experiments  $\pm$  SD and representative images for each treatment are shown. In SUM-190 (B) and MDA-IBC-3 (C) cells, radiation induced DNA damage causes an increase in PAR formation at both 6 and 24 hours after 4 Gy radiation. In the combination group that receives a one-hour pretreatment of 1  $\mu$ M olaparib before radiation, PAR formation is significantly lower at 6 and 24 hours after RT. In SUM-149 (D) cells, this same trend can be observed at a much lower dose of olaparib (20nM). Though the enzymatic activity of PARP1 is efficiently inhibited at these doses, total levels of PARP are not significantly different across the treatment conditions.

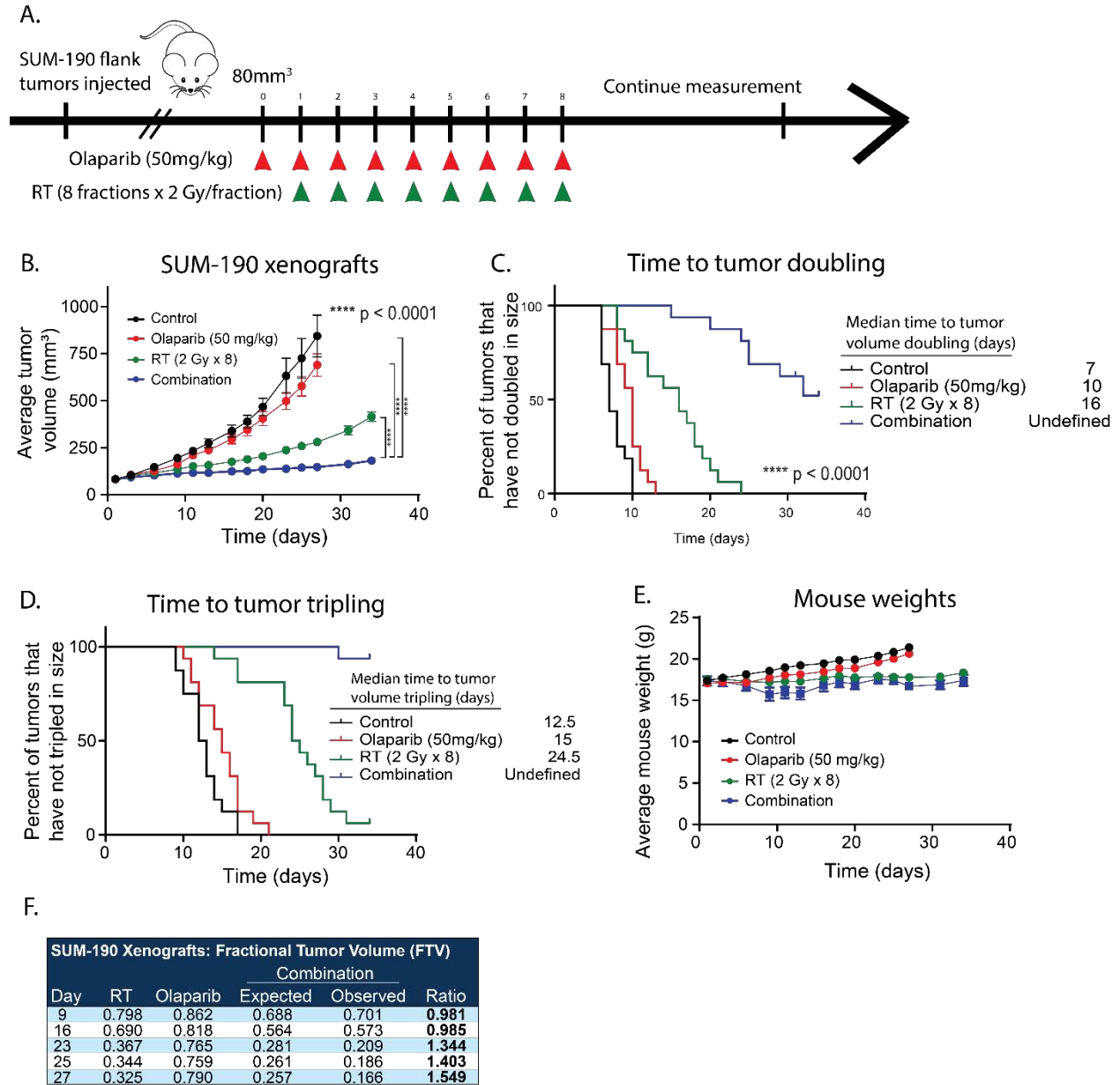


**Figure A-5: PARP1 inhibition with radiation is more effective than radiation alone in a SUM-190 xenograft model**

SUM-190 cells were subcutaneously injected into CB17-SCID mice, and treatment was started when tumors reached approximately 80 mm<sup>3</sup> (A). Olaparib treatment began one day before the initiation of radiation treatment and ended on the same day as the last fraction of radiation. With this paradigm, the combination treatment leads to delayed growth of tumors (B) and an increased time to tumor doubling (C) and tumor tripling (D) (p < 0.0001 = \*\*\*\*). The treatment did not display significant toxicities, and animal weights were not significantly different between the treatment groups (E). Using the FTV method, there was a synergistic effect with olaparib and RT treatment to antagonize tumor growth (ratios >1 indicate synergism) (F). A two-way ANOVA was performed to compare tumor volume between experimental groups.



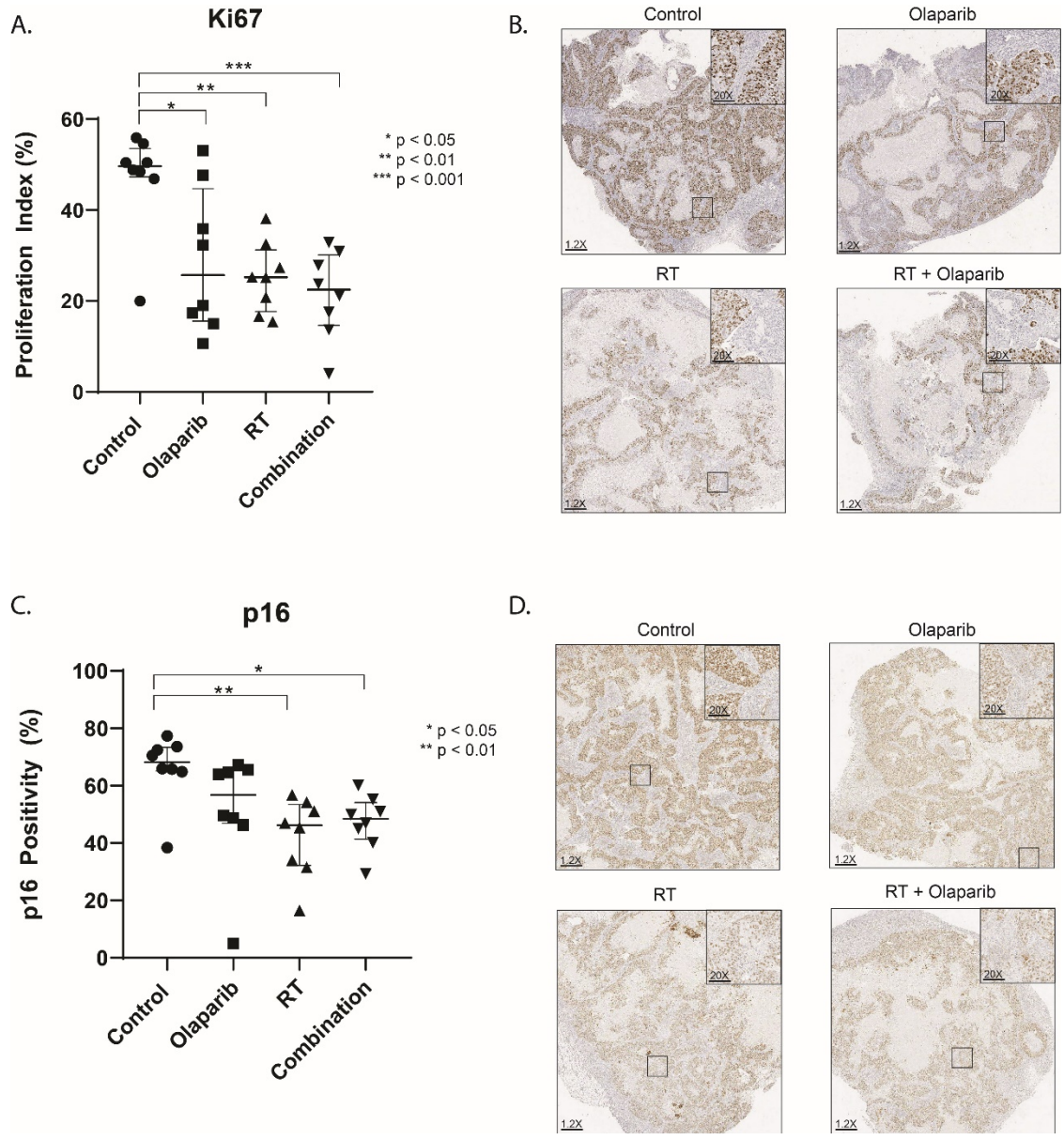


**Figure A-6: Ki67 and p16 levels are decreased in tumors from animals treated with radiation and combination PARP-inhibitor and radiation**

SUM-190 xenograft tumors that were harvested from mice at the completion of the long-term *in vivo* study. Protein expression levels were assessed by immunohistochemical staining. Levels of Ki67, a marker of proliferation, are significantly decreased in all treatment groups (A), and p16 levels are significantly decreased in the RT-alone and combination treated groups (B). Representative images from each group are shown (C,D). (p < 0.05 = \*, p < 0.01 = \*\*, p < 0.001 = \*\*\*)

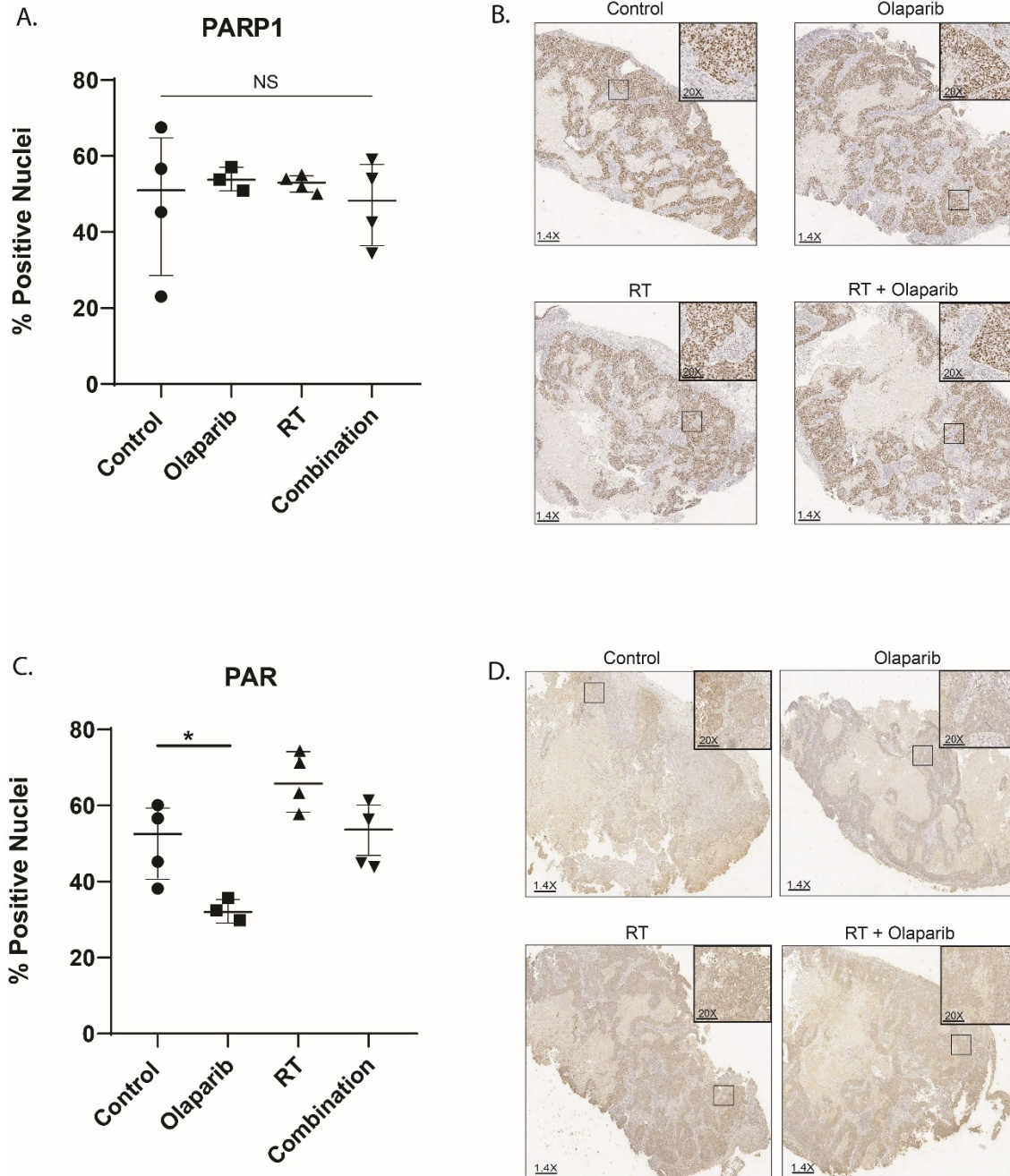


**Figure A-7: Total PARP1 levels do not change with treatment but PAR levels are decreased by PARPi**

Total levels of PARP1 were assessed in tumors from mice treated with olaparib. Olaparib treatment did not affect PARP1 protein expression by IHC in olaparib alone, RT alone, or combination treated animals (A). Representative images of PARP1 staining are shown for all treatment conditions (B). PAR levels were, however, significantly decreased in the animals treated with olaparib alone (C). Representative images of PAR staining are shown for all treatment conditions (D). (NS = not significant,  $p < 0.05 = *$ )

## A.8 Tables

**Table A-1: Extended methods for immunohistochemistry**

Antibodies used in all of the immunohistochemistry experiments are listed with each of the corresponding dilutions, retrieval techniques, and positive controls.

Ab	Company	Cat #	Source	Clone	Dilution	Epitope retrieval	Detection	Control Tissue
Ki67	AbCam	Ab16667	Rabbit MonoAb	SP-6	1:250	pH6 HIER	Env+	Tonsil
p16 (INK4a)	AbCam	Ab108349	Rabbit MonoAb	EPR1473	1:2000	pH6 HIER	Env+	Kidney
PARP1	AbCam	Ab191217	Rabbit MonoAb	EPR18461	1:1000	pH6 HIER	Env+	HeLa cell pellet
PAR	AbCam	Ab14460	Chicken		1:500	pH6 HIER	LSAB+	Pancreas

HIER: Heat induced epitope retrieval

LSAB+: Liquid streptavidin Biotin

Env+: Envision+ Polymer IIRP Second antibody

**Table A-2: Enhancement ratios and toxicity for IBC clonogenic survival assays**

A.

SUM-190 Clonogenic Survival Assay		
Treatment	Enhancement Ratio	Cytotoxicity
DMSO	1.0	1.0
0.5 $\mu$ M	1.25 $\pm$ 0.06	0.77 $\pm$ 0.02
1 $\mu$ M	1.45 $\pm$ 0.03	0.62 $\pm$ 0.13
2 $\mu$ M	1.64 $\pm$ 0.21	0.63 $\pm$ 0.10

B.

MDA-IBC-3 Clonogenic Survival Assay		
Treatment	Enhancement Ratio	Cytotoxicity
DMSO	1.0	1.0
0.5 $\mu$ M	1.20 $\pm$ 0.39	0.61 $\pm$ 0.39
1 $\mu$ M	1.12 $\pm$ 0.08	0.46 $\pm$ 0.27
2 $\mu$ M	1.28 $\pm$ 0.06	0.43 $\pm$ 0.31

C.

SUM-149 Clonogenic Survival Assay		
Treatment	Enhancement Ratio	Cytotoxicity
DMSO	1.0	1.0
2 nM	1.22 $\pm$ 0.05	0.82 $\pm$ 0.23
10 nM	1.42 $\pm$ 0.01	0.49 $\pm$ 0.24
20 nM	1.76 $\pm$ 0.11	0.39 $\pm$ 0.23

## A.9 References

1. Menta, A. *et al.* Inflammatory Breast Cancer: What to know about this Unique Aggressive Breast Cancer. *The Surgical Clinics of North America* **98**, 787–800 (2018).
2. Li, J. *et al.* Outcomes of patients with inflammatory breast cancer by hormone receptor- and HER2-defined molecular subtypes: A population-based study from the SEER program. *Oncotarget* **8**, 49370–49379 (2017).
3. Ross, J. S. *et al.* Comprehensive genomic profiling of inflammatory breast cancer cases reveals a high frequency of clinically relevant genomic alterations. *Breast Cancer Res Treat* **154**, 155–162 (2015).
4. Wedam, S. B. *et al.* Antiangiogenic and antitumor effects of bevacizumab in patients with inflammatory and locally advanced breast cancer. *J Clin Oncol* **24**, 769–777 (2006).
5. Yang, S. X. *et al.* Gene expression profile and angiogenic marker correlates with response to neoadjuvant bevacizumab followed by bevacizumab plus chemotherapy in breast cancer. *Clin Cancer Res* **14**, 5893–5899 (2008).
6. Bourgier, C. *et al.* Exclusive alternating chemotherapy and radiotherapy in nonmetastatic inflammatory breast cancer: 20 years of follow-up. *Int J Radiat Oncol Biol Phys* **82**, 690–695 (2012).
7. Gelmon, K. A. *et al.* Olaparib in patients with recurrent high-grade serous or poorly differentiated ovarian carcinoma or triple-negative breast cancer: a phase 2, multicentre, open-label, non-randomised study. *Lancet Oncol* **12**, 852–861 (2011).
8. Dent, R. A. *et al.* Phase I trial of the oral PARP inhibitor olaparib in combination with paclitaxel for first- or second-line treatment of patients with metastatic triple-negative breast cancer. *Breast Cancer Res* **15**, R88 (2013).
9. Comen, E. & Robson, M. Poly(ADP-Ribose) Polymerase Inhibitors in Triple-Negative Breast Cancer. *The Cancer Journal* **16**, 48–52 (2010).
10. Feng, F. Y. *et al.* Targeted radiosensitization with PARP1 inhibition: optimization of therapy and identification of biomarkers of response in breast cancer. *Breast Cancer Res Treat* **147**, 81–94 (2014).
11. Speers, C. *et al.* Maternal Embryonic Leucine Zipper Kinase (MELK) as a Novel Mediator and Biomarker of Radioresistance in Human Breast Cancer. *Clin Cancer Res* **22**, 5864–5875 (2016).
12. Matar, P. *et al.* Combined Epidermal Growth Factor Receptor Targeting with the Tyrosine Kinase Inhibitor Gefitinib (ZD1839) and the Monoclonal Antibody Cetuximab (IMC-C225): Superiority Over Single-Agent Receptor Targeting. *Clin Cancer Res* **10**, 6487–6501 (2004).
13. Yokoyama, Y., Dhanabal, M., Griffioen, A. W., Sukhatme, V. P. & Ramakrishnan, S. Synergy between Angiostatin and Endostatin: Inhibition of Ovarian Cancer Growth. *Cancer Res* **60**, 2190–2196 (2000).

14. Donawho, C. K. *et al.* ABT-888, an Orally Active Poly(ADP-Ribose) Polymerase Inhibitor that Potentiates DNA-Damaging Agents in Preclinical Tumor Models. *Clinical Cancer Research* **13**, 2728–2737 (2007).
15. Elstrodt, F. *et al.* BRCA1 mutation analysis of 41 human breast cancer cell lines reveals three new deleterious mutants. *Cancer Res* **66**, 41–45 (2006).
16. Skov, K. & Macphail, S. Interaction of platinum drugs with clinically relevant X-ray doses in mammalian cells: A comparison of cisplatin, carboplatin, iproplatin, and tetraplatin. *International Journal of Radiation Oncology\*Biophysics* **20**, 221–225 (1991).
17. Zhang, X. *et al.* In vitro and in vivo study of a nanoliposomal cisplatin as a radiosensitizer. *International Journal of Nanomedicine* <https://www.dovepress.com/in-vitro-and-in-vivo-study-of-a-nanoliposomal-cisplatin-as-a-radiosens-peer-reviewed-article-IJN> (2011) doi:10.2147/IJN.S15997.
18. Althubiti, M. *et al.* Characterization of novel markers of senescence and their prognostic potential in cancer. *Cell Death Dis* **5**, e1528–e1528 (2014).
19. Wolfe, A. R. *et al.* Simvastatin prevents triple-negative breast cancer metastasis in pre-clinical models through regulation of FOXO3a. *Breast Cancer Res Treat* **154**, 495–508 (2015).
20. Van Wyhe, R. D., Rahal, O. M. & Woodward, W. A. Effect of statins on breast cancer recurrence and mortality: a review. *Breast Cancer (Dove Med Press)* **9**, 559–565 (2017).
21. Brewer, T. M. *et al.* Statin use in primary inflammatory breast cancer: a cohort study. *Br J Cancer* **109**, 318–324 (2013).
22. Reddy, J. P. *et al.* Mammary stem cell and macrophage markers are enriched in normal tissue adjacent to inflammatory breast cancer. *Breast Cancer Res Treat* **171**, 283–293 (2018).
23. Allen, S. G. *et al.* Macrophages Enhance Migration in Inflammatory Breast Cancer Cells via RhoC GTPase Signaling. *Sci Rep* **6**, 39190 (2016).
24. Rahal, O. M. *et al.* Blocking Interleukin (IL)4- and IL13-Mediated Phosphorylation of STAT6 (Tyr641) Decreases M2 Polarization of Macrophages and Protects Against Macrophage-Mediated Radioresistance of Inflammatory Breast Cancer. *Int J Radiat Oncol Biol Phys* **100**, 1034–1043 (2018).
25. Wolfe, A. R. *et al.* Mesenchymal stem cells and macrophages interact through IL-6 to promote inflammatory breast cancer in pre-clinical models. *Oncotarget* **7**, 82482–82492 (2016).
26. Bertucci, F. *et al.* Genomic profiling of inflammatory breast cancer: A review. *The Breast* **23**, 538–545 (2014).
27. Bertucci, F. *et al.* PDL1 expression in inflammatory breast cancer is frequent and predicts for the pathological response to chemotherapy. *Oncotarget* **6**, 13506–13519 (2015).

28. Hamm, C. A. *et al.* Genomic and Immunological Tumor Profiling Identifies Targetable Pathways and Extensive CD8+/PDL1+ Immune Infiltration in Inflammatory Breast Cancer Tumors. *Mol Cancer Ther* **15**, 1746–1756 (2016).
29. Jhaveri, K. *et al.* Hyperactivated mTOR and JAK2/STAT3 Pathways: Molecular Drivers and Potential Therapeutic Targets of Inflammatory and Invasive Ductal Breast Cancers After Neoadjuvant Chemotherapy. *Clin Breast Cancer* **16**, 113-122.e1 (2016).
30. Wynn, M. L. *et al.* RhoC GTPase Is a Potent Regulator of Glutamine Metabolism and N-Acetylaspartate Production in Inflammatory Breast Cancer Cells. *J Biol Chem* **291**, 13715–13729 (2016).
31. Joglekar, M., Elbazanti, W. O., Weitzman, M. D., Lehman, H. L. & van Golen, K. L. Caveolin-1 Mediates Inflammatory Breast Cancer Cell Invasion via the Akt1 Pathway and RhoC GTPase. *Journal of Cellular Biochemistry* **116**, 923–933 (2015).
32. Balamurugan, K. & Sterneck, E. The Many Faces of C/EBP $\delta$  and their Relevance for Inflammation and Cancer. *Int J Biol Sci* **9**, 917–933 (2013).
33. Allensworth, J. L. *et al.* Disulfiram (DSF) acts as a copper ionophore to induce copper-dependent oxidative stress and mediate anti-tumor efficacy in inflammatory breast cancer. *Mol Oncol* **9**, 1155–1168 (2015).
34. Arora, J. *et al.* Inflammatory breast cancer tumor emboli express high levels of anti-apoptotic proteins: use of a quantitative high content and high-throughput 3D IBC spheroid assay to identify targeting strategies. *Oncotarget* **8**, 25848–25863 (2017).
35. Lerebours, F. *et al.* NF-kappa B genes have a major role in Inflammatory Breast Cancer. *BMC Cancer* **8**, 41 (2008).
36. Van Laere, S. J. *et al.* NF- $\kappa$ B activation in inflammatory breast cancer is associated with oestrogen receptor downregulation, secondary to EGFR and/or ErbB2 overexpression and MAPK hyperactivation. *Br J Cancer* **97**, 659–669 (2007).
37. Murai, J. *et al.* Differential trapping of PARP1 and PARP2 by clinical PARP inhibitors. *Cancer Res* **72**, 5588–5599 (2012).
38. Menear, K. A. *et al.* 4-[3-(4-cyclopropanecarbonylpiperazine-1-carbonyl)-4-fluorobenzyl]-2H-phthalazin-1-one: a novel bioavailable inhibitor of poly(ADP-ribose) polymerase-1. *J Med Chem* **51**, 6581–6591 (2008).
39. Parsels, L. A. *et al.* PARP1 Trapping and DNA Replication Stress Enhance Radiosensitization with Combined WEE1 and PARP Inhibitors. *Mol Cancer Res* **16**, 222–232 (2018).
40. Murai, J. *et al.* Rationale for poly(ADP-ribose) polymerase (PARP) inhibitors in combination therapy with camptothecins or temozolomide based on PARP trapping versus catalytic inhibition. *J Pharmacol Exp Ther* **349**, 408–416 (2014).
41. Maya-Mendoza, A. *et al.* High speed of fork progression induces DNA replication stress and genomic instability. *Nature* **559**, 279–284 (2018).
42. Drew, Y. *et al.* Phase 2 multicentre trial investigating intermittent and continuous dosing schedules of the poly(ADP-ribose) polymerase inhibitor rucaparib in germline BRCA

mutation carriers with advanced ovarian and breast cancer. *Br J Cancer* **114**, 723–730 (2016).

43. Litton, J. K. *et al.* Talazoparib in Patients with Advanced Breast Cancer and a Germline BRCA Mutation. *New England Journal of Medicine* **379**, 753–763 (2018).
44. Karam, S. D. *et al.* Final Report of a Phase I Trial of Olaparib with Cetuximab and Radiation for Heavy Smoker Patients with Locally Advanced Head and Neck Cancer. *Clin Cancer Res* **24**, 4949–4959 (2018).
45. Vance, S. *et al.* Selective radiosensitization of p53 mutant pancreatic cancer cells by combined inhibition of Chk1 and PARP1. *Cell Cycle* **10**, 4321–4329 (2011).
46. Han, S. *et al.* Targeted radiosensitization of ETS fusion-positive prostate cancer through PARP1 inhibition. *Neoplasia* **15**, 1207–1217 (2013).
47. Bi, Y. *et al.* Radiosensitization by the PARP inhibitor olaparib in BRCA1-proficient and deficient high-grade serous ovarian carcinomas. *Gynecol Oncol* **150**, 534–544 (2018).
48. Wurster, S. *et al.* PARP1 inhibition radiosensitizes HNSCC cells deficient in homologous recombination by disabling the DNA replication fork elongation response. *Oncotarget* **7**, 9732–9741 (2016).
49. Mangoni, M. *et al.* Enhancement of Soft Tissue Sarcoma Cell Radiosensitivity by Poly(ADP-ribose) Polymerase-1 Inhibitors. *Radiat Res* **190**, 464–472 (2018).
50. Jagsi, R. *et al.* TBCRC 024 Initial Results: A Multicenter Phase 1 Study of Veliparib Administered Concurrently With Chest Wall and Nodal Radiation Therapy in Patients With Inflammatory or Locoregionally Recurrent Breast Cancer. *International Journal of Radiation Oncology, Biology, Physics* **93**, S137 (2015).